frontiers | Research Topics

Coastal environmental quality and marine biodiversity assessment, volume II

Edited by
Dilip Kumar Jha, Ganesh Thiruchitrambalam, Meilin Wu and Prashanthi Devi Marimuthu

Published in
Frontiers in Marine Science

ISSN 1664-8714
ISBN 978-2-8325-5257-5
DOI 10.3389/978-2-8325-5257-5

About Frontiers

Frontiers is more than just an open access publisher of scholarly articles: it is a pioneering approach to the world of academia, radically improving the way scholarly research is managed. The grand vision of Frontiers is a world where all people have an equal opportunity to seek, share and generate knowledge. Frontiers provides immediate and permanent online open access to all its publications, but this alone is not enough to realize our grand goals.

Frontiers journal series

The Frontiers journal series is a multi-tier and interdisciplinary set of open-access, online journals, promising a paradigm shift from the current review, selection and dissemination processes in academic publishing. All Frontiers journals are driven by researchers for researchers; therefore, they constitute a service to the scholarly community. At the same time, the *Frontiers journal series* operates on a revolutionary invention, the tiered publishing system, initially addressing specific communities of scholars, and gradually climbing up to broader public understanding, thus serving the interests of the lay society, too.

Dedication to quality

Each Frontiers article is a landmark of the highest quality, thanks to genuinely collaborative interactions between authors and review editors, who include some of the world's best academicians. Research must be certified by peers before entering a stream of knowledge that may eventually reach the public - and shape society; therefore, Frontiers only applies the most rigorous and unbiased reviews. Frontiers revolutionizes research publishing by freely delivering the most outstanding research, evaluated with no bias from both the academic and social point of view. By applying the most advanced information technologies, Frontiers is catapulting scholarly publishing into a new generation.

What are Frontiers Research Topics?

Frontiers Research Topics are very popular trademarks of the *Frontiers journals series*: they are collections of at least ten articles, all centered on a particular subject. With their unique mix of varied contributions from Original Research to Review Articles, Frontiers Research Topics unify the most influential researchers, the latest key findings and historical advances in a hot research area.

Find out more on how to host your own Frontiers Research Topic or contribute to one as an author by contacting the Frontiers editorial office: frontiersin.org/about/contact

Coastal environmental quality and marine biodiversity assessment, volume II

Topic editors

Dilip Kumar Jha — National Institute of Ocean Technology, India

Ganesh Thiruchitrambalam — Pondicherry University, Port Blair Campus, India

Meilin Wu — South China Sea Institute of Oceanology, Chinese Academy of Sciences (CAS), China

Prashanthi Devi Marimuthu — Bharathidasan University, India

Citation

Jha, D. K., Thiruchitrambalam, G., Wu, M., Marimuthu, P. D., eds. (2024). *Coastal environmental quality and marine biodiversity assessment, volume II*. Lausanne: Frontiers Media SA. doi: 10.3389/978-2-8325-5257-5

Table of contents

frontiers | Frontiers in Marine Science

TYPE Editorial
PUBLISHED 24 July 2024
DOI 10.3389/fmars.2024.1456175

OPEN ACCESS

EDITED AND REVIEWED BY
Hans Uwe Dahms,
Kaohsiung Medical University, Taiwan

*CORRESPONDENCE
Dilip Kumar Jha
dilipjhaniot@gmail.com

RECEIVED 28 June 2024
ACCEPTED 08 July 2024
PUBLISHED 24 July 2024

CITATION
Jha DK, Thiruchitrambalam G, Wu M and Marimuthu PD (2024) Editorial: Coastal environmental quality and marine biodiversity assessment, volume II. *Front. Mar. Sci.* 11:1456175. doi: 10.3389/fmars.2024.1456175

Editorial: Coastal environmental quality and marine biodiversity assessment, volume II

Dilip Kumar Jha[1]*, Ganesh Thiruchitrambalam[2], Meilin Wu[3] and Prashanthi Devi Marimuthu[4]

[1]National Institute of Ocean Technology (NIOT), Ministry of Earth Sciences, Govt. of India, Chennai, India, [2]Department of Ocean Studies and Marine Biology, Pondicherry University, Port Blair, India, [3]State Key Laboratory of Tropical Oceanography, South China Sea Institute of Oceanology, Chinese Academy of Sciences (CAS), Guangzhou, China, [4]Department of Environmental Science and Management, Bharathidasan University, Tiruchirappalli, India

KEYWORDS

phytoplankton, seawater quality, microbial community, anthropogenic, metal

Editorial on the Research Topic
Coastal environmental quality and marine biodiversity assessment, volume II

The biological productivity and ecological sustainability of coastal and marine ecosystems are greatly associated with abiotic and biotic factors in the surrounding coastal ecosystem (Yuvaraj et al., 2018). Large volumes of contaminants are being released from anthropogenic sources like industry, agriculture, and urban areas which result in the deterioration of seawater and sediment quality in coastal areas. The bulk of marine pollution comes from above-mentioned sources, accounting more than 80% of its sources on land. Offshore oil & gas extraction and maritime oil transportation are also one of the major sources of pollution in the coastal and marine environments. Consequently, the issue of coastal pollution has spread throughout the world and requires proper mitigation planning for sustainable ecosystem management.

Anthropogenic discharges of pollutants into the coastal zone have led to increased concentrations of nutrients, metals, and microorganisms, which are negatively affecting the world's estuaries and coastal environment. To help understand geographical and temporal changes in coastal environment ecology, it is crucial to prevent and control coastal and marine pollution and develop better monitoring systems. Recent technological advances in monitoring the seawater quality of coastal and marine environments and ecology, such as automated data collecting, real-time data gathering, and periodic monitoring of these ecosystems, are crucial to comprehending real-time data and its environmental implications.

Physicochemical characteristics of water, nutrients, microorganisms, metal toxicity, phytoplankton, and sediment quality are significant variables that require monitoring (Jha et al., 2021; Ratnam et al., 2022; Sathish Kumar et al., 2022). Good water and sediment quality are very important for the sustainable fishery, especially for the small lobsters (Scyllarinids) which do not form a prominent fishery, but they form an important link in the benthic and pelagic biodiversity in nearshore waters (Sekiguchi et al., 2007; Kumar

et al., 2009). Regular monitoring of coastal and marine environment is required to estimate the physicochemical and biological characteristics of seawater and sediment to develop a mitigation plan for promoting healthy habitats for flora and fauna, and contribute to coastal conservation and fisheries management (Vijayakumaran et al., 2005; Jha et al., 2017, 2018). The study examines the scientific strategies, including a recently developed statistical model, or a mix of methods in the coastal and marine environment, emphasizing ecological and environmental degradation and suggesting mitigation management.

Seawater quality and its impact on coastal and marine ecosystem

Trace metals are released into the coastal and marine environment by a variety of natural and anthropogenic activities, including dust deposition, volcanic eruptions, mineral weathering, mining, fossil fuel combustion, agriculture, industry, maritime traffic, urbanization, & sewage discharge, and thus enter the food web (Koduvayur et al., 2022). Naik et al. revealed that Cadmium and Arsenic concentrations are considered prime contributors to ecological risk along the estuarine and coastal regions of Tamil Nadu. Further, the findings also revealed the level of metals (Cr, Cu, Pb, Cd, Co, Mn, Ni, Zn, As), would increase over time as a result of emerging industries such as ceramic, painting, glass, pesticides, herbicides, and battery manufacturing in the surrounding vicinity. Water environments may purify themselves to some extent, but when wastewater discharge loads exceed a threshold, a natural equilibrium is upset, resulting decline in water quality. Chen et al. reported that the total nitrogen, total phosphorus, and chemical oxygen demand in Zhanjiang Bay's upstream discharge outlets exceed the permissible limits. However, since Zhanjiang Bay has been largely nitrogen-restricted over the past decade, the impact of nitrogen discharges on eutrophication in the bay may also be insignificant. He et al. reported that chemical oxygen demand significantly and positively correlated with dissolved inorganic nitrogen (DIN) and dissolved inorganic phosphate (DIP) in all the seasons at Guangdong coastal water. Further, DIN/DIP exhibited a significant positive correlation with Chl-a in all seasons, indicating that high Chl-a concentrations could be due to the nutrient supply in marine ecosystems and hence, it is imperative to strengthen the integrated management of land and sea and effectively combat the eutrophication of coastal and estuary waters to prevent algal blooms.

Planktons, which are divided into two groups: zooplankton (animals) and phytoplankton (plants), are a diverse group of aquatic organisms that are unable to swim against the water current (Jha et al., 2023). Small plants known as phytoplankton are considered to be the primary energy source in aquatic environments and constitute the majority of the plankton population. The manmade activities that contribute pollutants and nutrients to coastal waters make them dynamic and these modifications may affect primary production patterns and, consequently, pelagic food webs of the coastal and marine ecosystem (Sathish Kumar et al., 2023). Eutrophication in coastal and marine ecosystems is a serious global issue due to the regular input of nutrients from land-based sources (Ratnam et al., 2022). There is a need for innovative tools to assess eutrophication and hence Zhou et al. applied two comprehensive methods the Assessment of Estuarine Trophic Status (ASSETS) and the Northwest Pacific Action Plan Common Procedure (NOWPAP CP) to better understand the health of the Guangdong coastal waters. Further, it was proposed that the NOWPAP CP approach could provide information about the long-term changes in the biological effects of nutrient enrichment, while the modified ASSETS method could more comprehensively and precisely demonstrate the eutrophication conditions in the coastal waters of Guangdong. Wang et al. revealed that supplementing with B vitamins, specifically B1, B12, and to a lesser extent B2 and B6, caused notable changes in the composition of phytoplankton communities, further, it was observed that some phytoplankton species, such as diatoms and Prymnesiales, may be auxotrophic for B vitamins and that they would become more abundant when given extra B vitamins. The resulting changes in phytoplankton communities reduced Copepoda populations, leading to a decrease in their relative abundance. Sathish Kumar et al. studied several stations scattered across Tamil Nadu's five coastal districts and observed the spatial variation of the phytoplankton community and its response to shifting environmental conditions. They reported 85 species of phytoplankton, including diatoms (64), dinoflagellates (18), silicoflagellates (1), and Cyanophyceae (2) showed that the south coast of Tamil Nadu had a progressive decline in phytoplankton abundance, which was highest in the Thanjavur coast and could be related to the high nutrient in the coastal waters. Wang et al. revealed that there is no clear evidence of diatom and dinoflagellate succession with N:P ratio across seasons in the East China Sea. They demonstrated that the bulk of the study region was mid-eutrophic with severe organic pollution, and that eutrophication and organic pollution had a considerable impact on phytoplankton abundances. Furthermore, faster warming caused by coastal nuclear power plants, as well as nitrogen regime changes, have a substantial impact on the phytoplankton community's temporal shift. These findings provide important insights into how eutrophic conditions affect the structure of phytoplankton communities in coastal aquatic systems.

The ecological function of microbes

It is important to study the microbial load in the seawater to find out the possible rise of infectious diseases and gastrointestinal infections in people linked with the seafood chain (Fleisher et al., 2010; Dheenan et al., 2014) residing in the coastal vicinity. Verma et al. discovered microorganisms in deep water have a major influence on a variety of biogeochemical processes and exhibit a remarkable adaption feature to low temperatures and high pressure. They investigated how changes in the physicochemical conditions

and heavy metal concentrations in the Bay of Bengal impacted the composition of deep-sea bacterial communities at three different depths. The structural and metabolic diversity of deep-sea sediment microbial communities was examined using ectoenzymatic experiments, physiological profiling of populations at the community level, and culture-based sequencing of 16S rRNA genes. The genera Fictibacillus, Lysinibacillus, Salinicola, Robertmurraya, and Blastococcus include five potentially new species that have been identified. A high degree of metabolic diversity was seen in the carbon substrate utilization profiles, suggesting that deep-sea microbial communities actively participate in biogeochemical cycles. Thangaraj et al. revealed that how varying water masses affected the prokaryotic communities' composition and metabolic potential for samples taken and analyzed in the autumn of 2018 and 2019 from different layers of the Korea Strait. They also demonstrated that the temperature and salinity of the water masses were significant in controlling the prokaryotic population and metabolic alterations, particularly in the Bottom and Upper Layers in 2019, which were different from those in 2018 because of the water masses' varied composition. Further, compared to the relatively steady variable of temperature in 2018, it was observed that the Freshwater input from the East China Sea into the 2019 Upper Layer significantly affected the prokaryotic population shift from high density in 2018 to high diversity in 2019 than the relatively stable variable of temperature in 2018. Furthermore, to predict the biogeochemical pattern, these findings offer a baseline understanding in this little-studied region and emphasize the need for thorough research that takes into account not only the various water masses from the Upper to the Bottom Layers but also the effects of climate change, such as global warming and ocean acidification.

Author contributions

DJ: Conceptualization, Writing – original draft. TG: Writing – original draft. MW: Writing – review & editing. MD: Writing – review & editing.

Acknowledgments

Authors are grateful to Rui Fernandes, Charlie Chen, Alice Lickley, and Talitha Gray for their support in organizing the Research Topic, the submission process of articles, and completing the review process. We want to thank the chief editors for the necessary approval and final acceptance of the peer-reviewed articles. We also thank all the reviewers for their excellent contribution for the successful completion of this issue.

Conflict of interest

The authors declare that the research was conducted in the absence of any commercial or financial relationships that could be construed as a potential conflict of interest.

Publisher's note

References

Dheenan, P. S., Jha, D. K., Vinithkumar, N. V., Ponmalar, A. A., Venkateshwaran, P., and Kirubagaran, R. (2014). Spatial variation of physicochemical and bacteriological parameters elucidation with GIS in Rangat Bay, middle Andaman. *India. J. Sea Res.* 85, 534–541. doi: 10.1016/j.seares.2013.09.001

Fleisher, J. M., Fleming, L. E., Solo-Gabriele, H. M., Kish, J. K., Sinigalliano, C. D., Plano, L., et al. (2010). The BEACHES study: health effects and exposures from non-point source microbial contaminants in subtropical recreational marine waters. *Int. J. Epidemiol.* 39, 1291–1298. doi: 10.1093/ije/dyq084

Jha, D. K., Dharani, G., Verma., P., Ratnam, K., Senthil Kumar., R., and Rajaguru, S. (2021). Evaluation of factors influencing the trace metals in Puducherry and Diu coasts of India through multivariate techniques. *Mar. Pollut. Bull.* 167, 2021. doi: 10.1016/j.marpolbul.2021.112342

Jha, D. K., Kirubagaran, R., Vinithkumar, N. V., Dharani, G., and Madeswaran, P. (2018). "The andaman and nicobar islands," in *World seas: An environmental evaluation* (Charles Sheppard (Academic press, UK and USA), 185–209.

Jha, D. K., Rajaprabhu, G., Kirubagaran, R., Sendhil Kumar, R., Dharani, G., and Das, A. K. (2017). Estimation of potential zones for offshore mariculture in the Indian Sea using geographical information system as a management tool. *J. Coast. Conserv.* 21, 893–902. doi: 10.1007/s11852-017-0556-y

Jha, D. K., Wu, M., Thiruchitrambalam, G., and Marimuthu, P. D. (2023). Editorial: Coastal and marine environmental quality assessments. *Front. Mar. Sci.* 10. doi: 10.3389/fmars.2023.1141278

Koduvayur, M. V., Vasudevan, S., Pandey, V., Santhanakumar, J., Jha, D. K., and Dharani, G. (2022). Comparative evaluation of heavy metal concentration in different organs of the asian seabass: A multivariate approach. *Front. Mar. Sci.* 9. doi: 10.3389/fmars.2022.1012541

Kumar, T. S., Vijayakumaran, M., Murugan, T. S., Jha, D. K., Sreeraj, G., and Muthukumar, S. (2009). Captive breeding and larval development of the scyllarine lobster petrarctusrugosus. *New Zealand. J. Mar. Freshw. Res.* 43, 101–112. doi: 10.1080/00288330909509985

Ratnam, K., Jha, D. K., Prashanthi Devi, M., and Dharani, G. (2022). Evaluation of physicochemical characteristics of coastal waters of nellore, southeast coast of India, by a multivariate statistical approach. *Front. Mar. Sci.* 9, 857957. doi: 10.3389/fmars.2022.857957

Sathish Kumar, P., Dharani, G., Santhanakumar, J., Jha, D. K., Pandey, V., Venkatnarayanan, S., et al. (2023). Assessment of phytoplankton diversity, distribution, and environmental variables along the southeast coast of India. *Front. Mar. Sci.* 10. doi: 10.3389/fmars.2023.1215627

Sathish Kumar, P., Venkatnarayanan, S., Pandey, V., Ratnam, K., Jha, D. K., Rajaguru, S., et al. (2022). Multivariate approach to evaluate the factors controlling the phytoplankton abundance and diversity along the coastal waters of Diu, northeastern Arabian Sea. *Oceanologia* 64, 267–275. doi: 10.1016/j.oceano.2021.11.005

Sekiguchi, H., Booth, J. D., and Webber, W. R. (2007). "Early life histories of slipper lobsters," in *The biology and fisheries of the slipper lobster*. Eds. K. L. Lavalli and E. Spannier (New York, CRC Press, Boca Raton, London), 69–90.

Vijayakumaran, M., Murugan, T. S., Remany, M. C., Mary Leema, T., Jha, D. K., Santhanakumar, J., et al. (2005). Captive breeding of the spiny lobster, panulirus homarus. *New Zealand. J. Mar. Freshw. Res.* 39, 325–334. doi: 10.1080/00288330.2005.9517313

Yuvaraj, P., Satheeswaran, T., Damotharan, P., Karthikeyan, V., Jha, D. K., Dharani, G., et al. (2018). Evaluation of the environmental quality of Parangipettai, southeast coast of India, by using multivariate and geospatial tool. *Mar. Pollut. Bull.* 131, 239–247. doi: 10.1016/j.marpolbul.2018.04.022

frontiers | Frontiers in Marine Science

TYPE Original Research
PUBLISHED 21 July 2023
DOI 10.3389/fmars.2023.1215251

OPEN ACCESS

EDITED BY
Dilip Kumar Jha,
National Institute of Ocean Technology, India

REVIEWED BY
Gopalakrishnan Thilagam,
Pachaiyappa's College for Men, India
Karnan C,
Council of Scientific and Industrial Research (CSIR), India
Shrikant D. Khandare,
National Institute of Ocean Technology, India

*CORRESPONDENCE
Il-Nam Kim
ilnamkim@inu.ac.kr

RECEIVED 01 May 2023
ACCEPTED 03 July 2023
PUBLISHED 21 July 2023

CITATION
Thangaraj S, Kim H-R, Kim S-Y, Jung H-K, Kim J-H and Kim I-N (2023) Water mass structure determine the prokaryotic community and metabolic pattern in the Korea Strait during fall 2018 and 2019. *Front. Mar. Sci.* 10:1215251. doi: 10.3389/fmars.2023.1215251

Water mass structure determine the prokaryotic community and metabolic pattern in the Korea Strait during fall 2018 and 2019

Satheeswaran Thangaraj[1,2,3,4], Hyo-Ryeon Kim[1], Seo-Young Kim[1], Hae-Kun Jung[5], Ju-Hyoung Kim[6] and Il-Nam Kim[1]*

[1]Department of Marine Science, Incheon National University, Incheon, Republic of Korea, [2]Freddy and Nadine Herrmann Institute of Earth Sciences, Hebrew University of Jerusalem, Jerusalem, Israel, [3]Interuniversity Institute for Marine Sciences, Eilat, Israel, [4]Department of Physiology, Saveetha Dental College and Hospital, Saveetha Institute of Medical & Technical Sciences, Saveetha University, Chennai, India, [5]Fisheries Resources and Environment Research Division, East Sea Fisheries Research Institute, National Institute of Fisheries Science, Gangneung, Republic of Korea, [6]Department of Aquaculture and Aquatic Science, Kunsan National University, Gunsan, Republic of Korea

The Korea Strait (KS) is a crucial marine passage for transporting heat, salt, and materials from the South Sea to the East Sea. The Tsushima Warm Water (TWW) and Korea Strait Bottom Cold Water (KSBCW) are major water masses that flow across the strait, but their effects on prokaryotic communities have been unclear. We used high-throughput sequencing to study the impact of TWW and KSBCW on prokaryotic composition and metabolic changes in the upper (0–50m; UL), middle (50–75m; ML), and bottom (75–150m; BL) layers during the fall of 2018 and 2019. The results showed that the UL had a freshwater influence from Changjiang Diluted Water in 2019, altering prokaryotic compositions and metabolic potentials. The KSBCW in the BL transported new bacterial communities with unique metabolic characteristics. Key genes involved in carbon metabolism had water mass impacts, preferring lower saline and temperature environments, and carbon fixation potential shifted from phototrophs in 2018 to chemotrophs in 2019. Temperature changes induced acclimation processes producing heat- and cold-shock genes/proteins. Our findings indicate that the freshwater influence and KSBCW modified the prokaryotic composition and metabolic function differentially. These results are important in understanding the relationship between water masses and ongoing environmental changes in this understudied region.

KEYWORDS

prokaryotes, bacteria, water mass, carbon metabolism, stress genes, Korea Strait, Tsushima Warm Water, Korea Strait Bottom Cold Water

Abbreviations: KS, Korea Strait; TWW, Tsushima Warm Water; TSW, Tsushima Surface Water; TMW, Tsushima Mid Water; KSBCW, Korea Strait Bottom Cold Water; UL, Upper Layer; ML, Middle Layer; BL, Bottom Layer; T, Temperature; S, Salinity; FW, Fresh Water; CDW, Changjiang Diluted Water; ECS, East China Sea.

1 Introduction

Prokaryotes are critical components of the ocean ecosystem, accounting for 70% of the total biomass on the ocean surface and 75% of the total biomass in the deep ocean (Fuhrman et al., 1989; Arístegui et al., 2009). They significantly contribute to ocean biogeochemical cycles *via* energy transmission and organic matter remineralization (Mason et al., 2003). Previous studies have found that prokaryotic abundance on the surface differs from that in the deep ocean (Tseng et al., 2015; Zorz et al., 2019; references therein). For example, Flavobacteria, Cyanobacteria, and Alphaproteobacteria are the dominant groups in the upper layer, whereas Alpha, Gamma, and Deltaproteobacteria dominate the middle layer (Walsh et al., 2016). Increased data have demonstrated that the richness of prokaryotes also varies with depth, that is, some research on bacteria describes increasing richness with depth (Walsh et al., 2016), whereas other studies detect declines (Bryant et al., 2016). This is because depth is closely related to the physical and biogeochemical properties of the water columns under unique conditions (Stocker, 2012). Thus, in-depth research on prokaryotic organisms is valuable (Wang et al., 2021a), as knowledge of their metabolic processes allows us to build ecological and biogeochemical models (Ducklow, 2000; Del Giorgio and Williams, 2005).

Physical mixing among different water masses is a crucial factor that influences the prokaryotic composition in the ocean (Venkatachalam et al., 2017). Several studies have revealed that the dynamics of different water masses, each with its physicochemical properties, produce differences in prokaryotic physiology and composition (Shade et al., 2008; Varela et al., 2008; Celussi et al., 2010; Galand et al., 2010; Laque et al., 2010). Physical properties such as temperature (T) and salinity (S) gradients in water masses are important driving factors in determining the prokaryotic population due to their biological mediation within cells. These properties affect prokaryotic photosynthetic activity, carbon, nitrogen, and sulfur metabolism, and other functional processes in various regions including the Western Sub-Arctic (Li et al., 2018), North Atlantic (Agogué et al., 2008), Eastern North Atlantic (Varela et al., 2008), Arctic Ocean (Galand et al., 2009), and Beaufort Sea (Fu et al., 2019). Water masses at the same location can be vertically classified into different types based on their T-S relationship. In the Southern Ocean, for example, the upper layer occupied by the Antarctic Surface Water that features warmer and less S conditions, while the middle layer occupied by the Winter Water with colder and less-S characteristics, and the deep layer occupied by the Circumpolar Deep Water that has warmer and high-S conditions (Randall-Goodwin et al., 2014).

The Korea Strait (KS) is a shallow channel (bottom depth <~200m) with a length of around 330 km and a breadth of approximately 140 km (Teague et al., 2006). It is situated between Korea and Japan and is separated into western and eastern channels by Tsushima Island. It serves as the sole pathway for transporting heat, salt, and materials from the South Sea to the East Sea (Figure 1A). Comprehending the inflow mechanism of the Korea Strait (KS) is vital in assessing and predicting alterations in the circulation of the East Sea (Teague et al., 2006). The major water masses flowing across the KS are Tsushima Warm Water (TWW) and Korea Strait Bottom Cold Water (KSBCW). The TWW, a branch of the Kuroshio Current, is the primary surface to mid-layer current (Teague et al., 2006) flowing northward from the Pacific Ocean to the East Sea (Lee et al., 2010), with an annual mean transport of ~2.5 Sv [1 Sv:10^6 m^3 s^{-1}] (Na et al., 2009). TWW is distinguished into two water types based on T-S relationship: Tsushima Surface Water (TSW; T>20°C and S<34.0 PSU) and Tsushima Middle Water (TMW; T:12–17°C and S>34.2 PSU) (Chang and Isobe, 2003; Moon et al., 2009). The KSBCW (T<10° C and S>34.0 PSU) is inhabited by a cold underwater running beneath the TMW in the western channel (Kim and Lee, 2004) originating from the East Sea and flowing southward along the Korean coast (Lee et al., 2010), with a monthly mean transport of approximately 0.35 Sv (Kim et al., 2006). In KS, approximately half of the transport was contained in the upper 50m and 10% occur below 100m, while the remaining was transported between ~50–100m (Teague et al., 2006).

Previous research has revealed that KS is the most dynamic environment due to its topography, water mass, and river discharge (i.e., from Changjiang River) (Lee et al., 2010). The annual freshwater (FW) discharge from the Changjiang River to the KS has been estimated to be 9.25×10^{11} m^3 yr^{-1} (Tian et al., 1993), which alters the hydrographic conditions (low S and high T) and modifies biological processes in the receiving region (Liu et al., 2003; Jiao et al., 2007; Onitsuka et al., 2007; Yoon et al., 2022). Yang et al. (2000) demonstrated that the phytoplankton ecosystem changes along the KS because of the influence of T variation by TWW and excessive nutrient loading by FW. Regarding bacterial dynamics in KS, there have been few studies on organic matter production as a result of changes in hydrographic conditions (Chung and Kang, 1995; Kang and Kang, 2002). Lee and Choi (2021) and Kim et al. (2022) showed that the composition of distinct water masses in the East Sea's Ulleung basin, i.e., TWW, has a major impact on bacterial production and diversity. Similarly, Ichinomiya et al. (2019) found that fluctuations in T and S of the TWW in the northern Japan basin significantly influence microbial abundance and diversity. Given that over 90% of the world's ocean floor has a temperature of less than approximately 4°C (Levitus and Boyer, 1994), microorganisms inhabiting this environment must have adapted to the cold conditions. This has resulted in unique metabolic activity and species diversity compared to those found in the upper layers of the ocean (Knoblauch and Jørgensen, 1999). Similarly, the bottom cold water mass from the Yellow Sea with higher S and lower T (similar to the KSBCW characteristics) exhibited different prokaryotic dominance in the bottom layer compared to that observed in the surface layer (Wang et al., 2021a).

Despite the distinct characteristics of warm water mass (i.e., TWW) in the surface layer and cold-water mass (i.e., KSBCW) in the bottom layers of KS, no studies have been conducted to define these water mass impacts on prokaryotic composition and distribution (surface to bottom) that change over time. Furthermore, the absence of genomic information in KS hampered our knowledge of the impact of different water masses on prokaryotic metabolic processes to build a biogeochemical

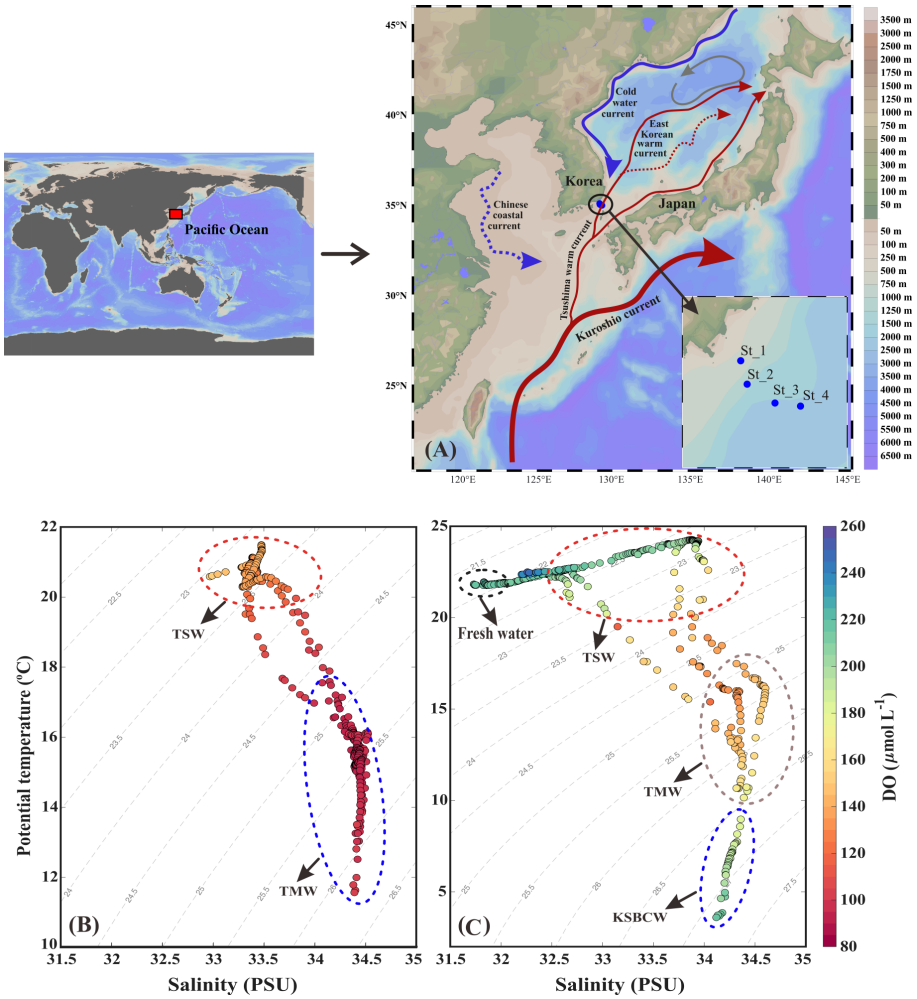

FIGURE 1
(A) Sample collecting points from the Korea Strait. **(B)** The potential temperature and salinity distribution during fall 2018; **(C)** the potential temperature and salinity distribution during fall 2019. Tsushima Surface Water (TSW; T>20°C and S<34.0 PSU), Tsushima Middle Water (TMW; T: 12–17°C and S>34.2 PSU), and Korea Strait Bottom Cold Water (KSBCW; T<10°C and S>34 PSU).

model of this important location. In this study, therefore, we aimed to (1) identify and characterize the different water masses from the surface to bottom layers during the fall of 2018 and 2019, (2) find their unique driving factors in determining the prokaryotic composition and distribution, and (3) investigate the response of metabolic potential according to the composition of different water masses.

2 Materials and methods

2.1 Sampling and measurements of physical and biogeochemical parameters

Seawater samples from 0 to 150 m were collected at four stations for physicochemical and sequencing analyses using R/V *Nara* in October 2018 and 2019 from KS. Seawater was collected in Niskin bottles on a rosette sampler. At all stations, the T, S, and dissolved oxygen (DO) profiles were determined using an SBE 911 Plus (CTD; Sea-Bird Electronics, USA) sensor system attached to a rosette sampler. The accuracies of T, conductivity, and DO sensors were ± 0.001°C, ± 0.0003 S m^{-1}, and ± 2% of the full-scale range, respectively. To determine the nutrient concentrations of nitrite (NO_2^-) and nitrate (NO_3^-), seawater samples were collected in 15 ml pre-acid rinsed plastic bottles and placed at –20°C until further analysis. Nitrite (NO_2^-) and nitrate (NO_3^-) were analyzed in the laboratory using a continuous flow auto-analyzer (QuAAtro 39, Seal Analytical, UK). The analytical precision of the nutrients was greater than 1%. Nutrient measurements were performed using the same method as that used by Hydes et al. (2010) in the GO-SHIP protocol, and reference materials (Kanso RMNS) were used to track the performance of the system and the consistency of the nutrient data. The sum of nitrite and nitrate measured in this study was defined as dissolved inorganic nitrogen (DIN). For DNA extraction, 2 L of seawater was filtered through 0.22 μm

cellulose ester membrane filters (Millipore, Ireland) to capture bacterial cells. The filtered samples were immediately frozen and stored at −80°C until DNA extraction. A total of 24 samples for sequencing analysis were obtained during the study period (4 stations × 3 depths × 2 years) across the upper layer (UL; <50m), middle layer (ML; ~50-75m), and bottom layer (BL; >75m).

2.2 DNA extraction library preparation and sequencing analysis

DNA was extracted from 24 genome samples using a DNA isolation kit (Qiagen, Germany) and cross-checked using a NanoDrop (Thermo Scientific, USA). After the quality check (Phred > = 20) (Bokulich et al., 2013), a 16S rRNA library was prepared to target the V3 and V4 hypervariable regions (Co. 3BIGS, South Korea, https://3bigs.com) based on RNA genes in chromosomes. In brief, 50 ng of genomic DNA was used to amplify the 16S rRNA gene v3 region for 26 cycles using a PCR kit. The forward and reverse primer concertation was kept at 0.2 μm each. The PCR was validated using positive control and non-template control samples. The Illumina adapted sequences were: forward, 5′- TCGTCGGCAGCGTCAGATGTGTATAAGAGACAGTCGTCGGCAGCGTCAGATGTGTATAAGAGACAGCCTACGGGNGGCWGCAG, and reverse, 5′- GTCTCGTGGGCTCGGAGATGTGTATAAGAGACAGGTCTCGTGGGCTCGGAGATGTGTATAAGAGACAGGACTACHVGGGTATCTAATCC-3. The 16s rRNA sequencing aimed to cover the high coverage diversity in this study following the protocol described by (Chakravorty et al., 2007; Klindworth et al., 2013). The extracted samples were analyzed and amplified using Illumina MiSeq (MiSeq control software v2.4.1.3) and real-time analysis (v1.18.54.0). 16S rRNA targeting was performed using a quantitative kit for the DNA samples. Primers were prepared for all DNA fragments and subjected to quality checks using a Bioanalyzer trace system, followed by clustering. The paired-end reads were demultiplexed, trimmed, and quality-filtered before assembling the reads using QIIME1.9.1. (Price et al., 2009) and USEARCH7 was used to detect or filter OTUs. The National Center for Biotechnology Information (NCBI), and SILVA 138.1 databases were used to determine the similarity (97%) of OTUs using UCLUST and close reference analyses. The OTU table was normalized to the 16S copy number abundance by dividing each OTU. After filtration, the generated OTU table using the Biological Observation Matrix format was clustered into OTU based on ≥97% similarity threshold using the Python Nearest Alignment Space Termination method (PyNAST) (Caporaso et al., 2010). We performed comparative OTU assignments with the database in terms of phylum, class, order, family, and genus separately, using RDP classifiers. Permutational multivariate analysis of variance (PERMANOVA) was used to observe significant differences among groups. The relative abundances of individual taxonomic classifications were estimated using STAMP (V2.1.3). The generated 16S rRNA data were submitted to the NCBI Sequence Read Archive (accession no. PRJNA898851).

2.3 Functional analysis

The predictive functional genes/potential of the prokaryotic communities was obtained using the Silva-Tax4Fun (Aßhauer et al., 2015). The SILVA-labeled OTU tables were used as an input file in Tax4Fun, which is an open-source R package. The SILVA-labeled OTUs are transformed into prokaryotic KEGG organisms in Tax4Fun, and the 16S rRNA copy number from the NCBI genome annotation is used to further standardize the data. The prokaryotic communities were assigned to their predictive functions by linearly combining the normalized taxonomic abundances into the precomputed association matrix of KEGG Ortholog reference profiles to Silva-defined microorganisms constructed by Tax4Fun (Wemheuer et al., 2020). The difference in the abundance of functional genes among the samples was tested with the Tukey-Kramer test (STAMP V2.1.3.) following the protocol described by (Parks et al., 2014).

2.4 Data visualization and statistical analysis

The surface S data used in this study for October 2018 and 2019 were obtained from Ocean Color, NASA (https://oceancolor.gsfc.nasa.gov/). The physiochemical parameters were drawn using Ocean Data View (v 5.6.3) and correlation analysis was performed using R software (v1.3.109).

3 Results and discussion

3.1 Water mass distribution and hydrographic condition

We used a T-S diagram to determine the physiochemical characteristics for water mass analysis during the fall of 2018 and 2019 (Figures 1B, C). Based on T-S diagram, two different water masses (i.e., TSW and TMW) in fall 2018 (Figure 1B) and four different water masses (i.e., FW, TSW, TMW, and KSBCW) in fall 2019 (Figure 1C) were likely to have participated in the physical mixing process in the western channel of KS. In particular, TSW with high T and low S (T>20°C and S<34.0 PSU) and TMW with low T and high S (~12<T<17°C and S>34.0 PSU) were observed in both years. However, compared to the fall of 2018, the BL of 2019 showed unique KSBCW characteristics with lower T and higher S (T<10°C and S>34.0 PSU), and the UL of 2019 showed lower S (<32.0 PSU) due to FW input. These results collectively suggest that during the fall of 2018, TSW influences across the UL (<50m), and TMW extends from ML to BL (~50m–140m), whereas during the fall of 2019, the UL was dominated by TSW with FW influence, ML by TMW, and BL (>75m) by the KSBCW.

In detail, during the fall of 2018, the UL showed a warmer T range of 20.40–21.42°C and a S range of 32.99–33.46 PSU (Figures 2A, B), while compared to the UL, the ML (~40–70m) T was reduced (12.11–20.42°C) and the S was elevated (33.31–34.46

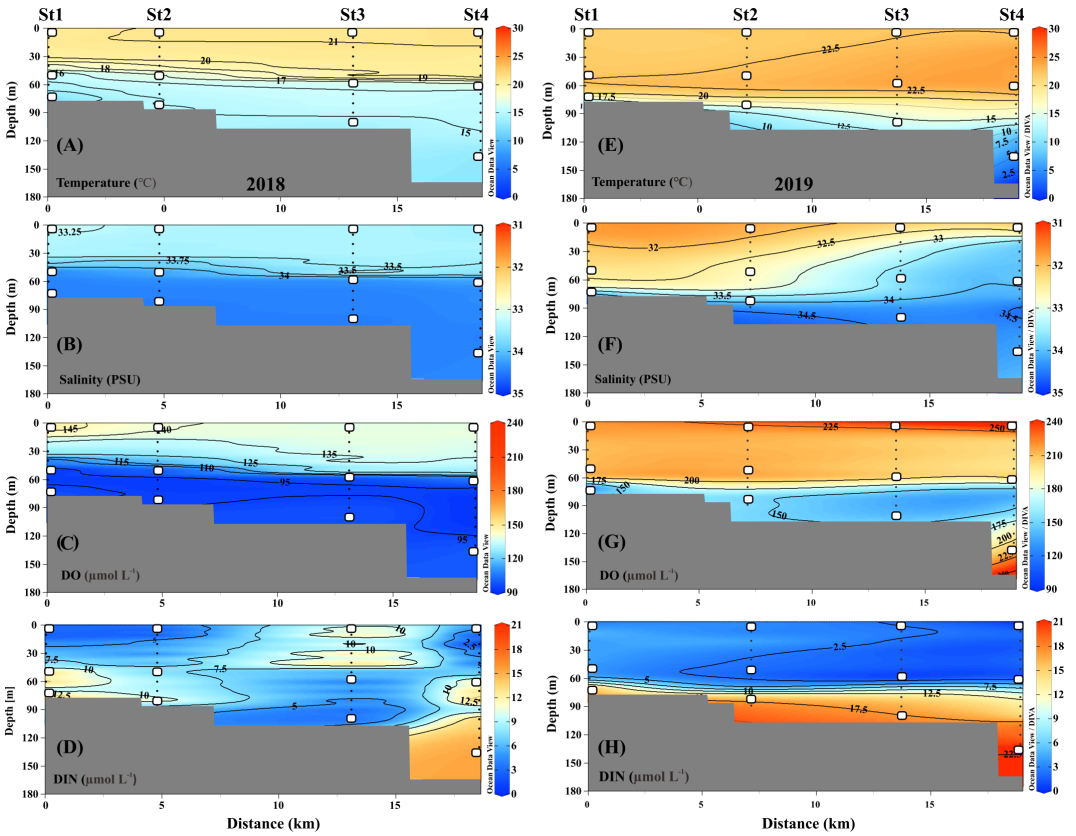

FIGURE 2
Distribution of temperature, salinity, dissolved oxygen (DO), and dissolved inorganic nitrogen (DIN) from sampled depths at different layers. **(A–D)** samples collected from 2018; **(E–H)** samples collected from 2019. While squares indicate the samples obtained for genomic analysis.

PSU). This suggests that the higher T and lower S in the UL of 2018 were influenced by the TSW. Unlike in 2018, stations 1 and 2 in the UL of 2019 showed the different temperature (Figure 2E) and lower range of S (<32 PSU) than those observed at the same stations in 2018 (>33 PSU) (Figures 2B, F). This low-S water indicates FW influence from the Changjiang Diluted Water (CDW) from the East China Sea (ECS) (Figure S1) (Chang and Isobe, 2003; Gomes et al., 2018; Kim et al., 2022; Yoon et al., 2022). Similar to the S variation, the UL T in the fall of 2019 was higher (21.76–24.26°C) than that observed in the fall of 2018. The T in the BL (70–140 m) also varied between 2018 and 2019. Specifically, the T in BL ranged from 11.71 to 16.01°C in 2018, while the T in 2019 ranged from 4.97 to 18.22°C. In particular, the low-cold water of the KSBCW (T<10°C) was dominant in the BL during the fall of 2019. The DO profile also differed between the fall of 2018 and 2019 (Figures 2C, G). For example, in the fall of 2018, the UL DO was influenced by TSW with a range of 126.88–150.89 µmol L^{-1}, while in the fall of 2019, TSW along with FW influences increased DO ranges from 203.61–248.61 µmol L^{-1}. Similarly, the ML DO in the fall of 2018 ranged from 91.08–139.43 µmol L^{-1}, whereas the DO in the fall of 2019 was higher with a range of 119.21–215.71 µmol L^{-1}. DIN distribution in UL ranged from 1.28–13.57 µmol L^{-1} in the fall of 2018 (Figure 2D), while in the fall of 2019, it showed a reduction ranging from 0.88–4.93 µmol L^{-1} (Figure 2H). On the opposite, the BL in fall 2019 detected with higher DIN (11.80–21.45 µmol L^{-1}) than those in fall 2018 BL (2.28–15.92 µmol L^{-1}), indicating that KSBCW transported higher nutrients to the KS from the East Sea during fall 2019. Taken together, during the fall of 2018, the UL was occupied by TSW (i.e., low-S and high-T characteristics), and the ML/BL was dominated by TMW (i.e., high-S characteristics). The UL was influenced by a mixture of FW (Sts. 1–2) and TSW (Sts. 3–4), the ML was dominated by TMW, and the BL was occupied by the KSBCW (i.e., low-T characteristics) during the fall of 2019 (Table 1).

3.2 Water mass structure determines the prokaryotic composition

After assembly, 251,120 OTUs were identified from samples collected in the fall of 2018, whereas 2,211,501 OTUs were identified in samples collected in the fall of 2019 (Supplementary Table 1). From the 2018 samples, 46 classes, 93 orders, 173 families, and 389 genera were identified, while 39 classes, 85 orders, 148 families, and 350 genera were identified in the 2019 samples. This shows that while there were more OTUs in the fall of 2019 (i.e., high diversity), the prokaryotic abundance was greater (i.e., high density) in the fall of 2018. In particular, the phylum Proteobacteria accounted for 57% of total species in fall 2018 and 52% in fall 2019. However, Bacteroidetes accounted for 12% in the fall of 2018 and 27% in the fall of 2019, and Actinobacteria accounted for 7% in

TABLE 1 Characteristics of water masses identified during the fall of 2018 and 2019 in the Korea Strait.

Cruise	Layer	Water Mass	T (°C)	S (PSU)	Characteristics	References
Fall 2018	UL	TSW	>20	>33.0	high T and low S	Moon et al. (1996); Chang and Isobe (2003); Kim and Lee (2004); Moon et al. (2009); Jeong and Cho (2018)
	ML	TMW	~12-19	>34.3	high S (max)	
	BL					
Fall 2019	UL	FW	>20	<32.0	low S (min)	
		TSW	>20	>33.0	high T and low S	
	ML	TMW	~12-19	>34.3	high S (max)	
	BL	KSBCW	<10	<34.3	low T (min)	

U/M/BL, upper/middle/bottom layer.
TS(M)W, Tsushima Surface (Middle) Water; FW, Freshwater; KSBCW, Korea Strait Bottom Cold Water.

the fall of 2018 and 8% in the fall of 2019. Notably, cyanobacteria accounted for 6.5% of the total abundance in the fall of 2018, nearly twice compared to the fall of 2019 (3.65%).

The dominant 25 orders (92% of total abundance) revealed that relative abundance (i.e., specific abundance is divided by total abundance) varied among each layer, representing the different water mass influences (Figure 3). In UL 2018, for example, the Flavobacteriales showed 16.04% total abundance, which increased to 33.28% in 2019 UL with FW region (i.e., Sts. 1–2) and to 47.03% at high T region (i.e., Sts. 3–4) (Figure 3A). Similarly, Rhodobacterales in UL showed an increasing trend from 9.69% in 2018 to 18.41% in the FW region and 13.95% with a high T region in 2019. In contrast, the Pelagibacterales decreased from 14.63% during the fall of 2018 to 13.54% in the FW region and 6.64% in the high T region during the fall of 2019; Synechococcales decreased from 9.35% during the fall of 2018 to 2.10% in FW region and 5.23% in high T region during the fall of 2019. These variations might be the cause of environmental changes caused by the distribution of distinct water masses. The main orders (15 most abundant) were correlated with the environmental parameters (Figure 4). In the fall of 2018 UL, dominant communities such as Pelagibacterials, Flavobacteriales, and Synechococcales were positively correlated with T and DIN. In the fall of 2019, Pelagibacterials and Synechococcales were positive, while Flavobacteriales and Rhodobacterales were negatively correlated with S (at Sts. 1–2). However, under high T conditions (at Sts. 3–4) these Pelagibacterials and Synechococcus showed negative correlations, while other communities showed positive correlations with T. Together, this suggests that the UL prokaryotic composition is mainly driven by the T and DIN in fall 2018, and S and T in fall 2019.

The shallow shelf region is a transitional zone with significant anthropogenic runoff and strong impacts from diverse water masses (Agardi et al., 2005). Several variables, including S (Zäncker et al., 2018), T (Bachmann et al., 2018), nutrients (Raes et al., 2018), and DO availability (Aldunate et al., 2018), have been shown to have a major influence on bacterial populations in such regions. In this study, we found that T and S variables have a substantial influence on all layers (Figure 4), suggesting that water mass is the primary determinant of bacterial composition. Specifically, FW has a significant impact on the physical properties of seawater, causing changes in the bacterial population (Fu et al., 2019). Compared to UL 2018, the UL 2019 (Sts. 1–2) exhibited low-S waters (S<32.0 PSU), indicating a FW effect from the CDW from the ECS (Chang and Isobe, 2003; Gomes et al., 2018; Kim et al., 2022). The Changjiang River has the world's third largest and the fifth-largest in FW discharge (Beardsley et al., 1985). According to previous studies, 70% of CDW is transferred annually *via* KS to the East Sea (Chang and Isobe, 2003; Senjyu et al., 2006; Moon et al., 2019). As a result, CDW influence plays a significant role in the large biological effects on the ECS and Korean coastal environment (Son and Choi, 2022) and alters phytoplankton composition (Yoon et al., 2022). Within the past ten years, the CDW has had the largest FW discharge in 2019-2020 followed by 2016 and 2017, but there was no significant FW discharge in 2018 (Son and Choi, 2022). Following this, the satellite observations of sea surface S show that the CDW influence from the ECS to the KS was significantly larger in fall 2019 than in fall 2018 (Figure S1). The contrasting T and S characteristics observed in the 2018 and 2019 UL samples were indicative of differences in the composition of the bacterial communities. Specifically, changes in Pelagibacterials and Synechococcales in the UL demonstrated how FW discharge distinguishes their distribution patterns and responds to environmental conditions. The populations of Pelagibacterials and Synechococcales showed a positive correlation with S in the fall of 2019 UL and a positive association with T in the fall of 2018 UL. When the S decreased in the fall of 2019 (Sts. 1–2), Flavobacteriales increased (33.28%) nearly double compared to the fall of 2018 (16.04%), and Synechococcales decreased almost four times (2.10%) in 2019 compared to the fall of 2018 (9.35%) UL. This suggests that S and T were the key factors in determining the dominant communities in the UL of KS, specifically T alone in the fall of 2018 and T and FW (S reduction mainly) in the fall of 2019.

Unlike UL, several communities in ML did not show much variation, i.e., the relative abundance of Pelagibacterales in the fall of 2018 showed 18.90%, which is similar to the fall of 2019 (16.26%), and those of Oceanospirillales showed 4.28% in 2018 and 5.08% in 2019, respectively. However, few communities in ML showed exceptional variation, such as Flavobacteriales and Synechococcales, which showed approximately four-fold elevation in fall 2019 compared to fall 2018. Although several community abundances were similar in both years of ML, they were

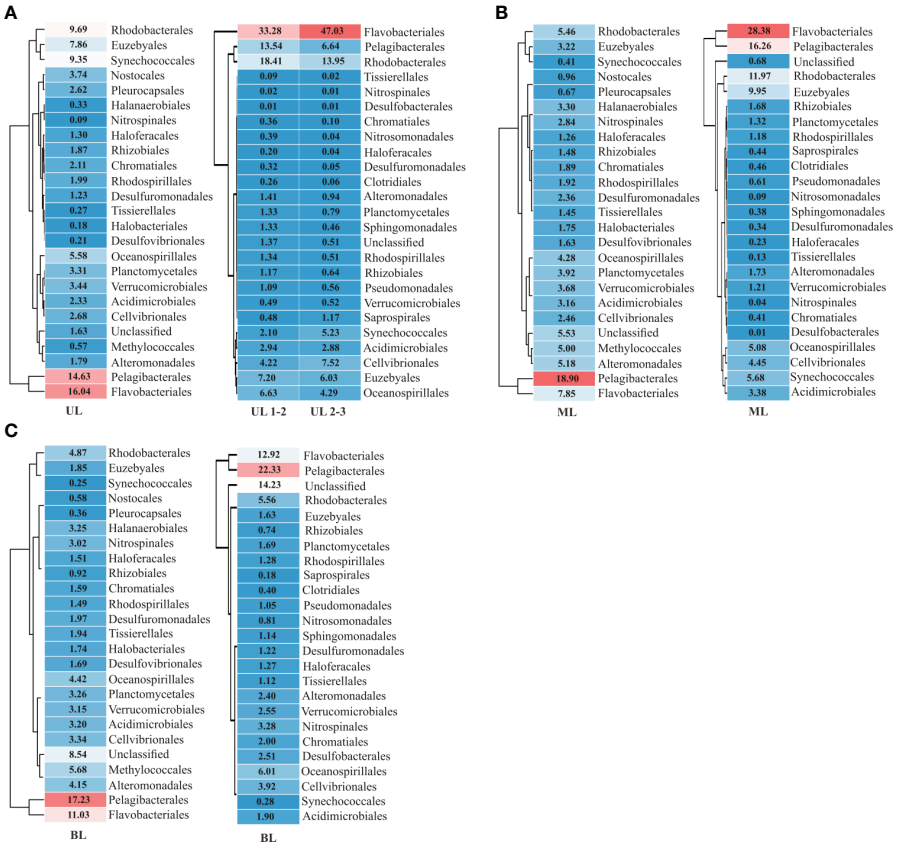

FIGURE 3
Prokaryotic diversity and density in order level. The dominant orders encompass 92% of the total abundances are listed here. **(A)** Results obtained from 2018 and 2019 UL (upper layer); **(B)** results obtained from 2018 and 2019 ML (middle layer), and **(C)** results obtained from 2018 and 2019 BL (bottom layer). UL 1-2 represents FWI fresh water influence (Sts. 1–2), and (Sts. 2–4), represents high temperature condition. The description of abundance in order are shown in Supplementary Table 2.

differentially correlated with T variation (Figure 4). In BL, although dominant communities such as Pelagibacterales, Synechococcales, and Flavobacteriales showed similar abundances between the falls of 2018 and 2019, several new communities (i.e., Saprospirales, Clostridiales, Pseudomonadales, Nitrosomodales, Sphingomonadales, and Desulfomonadales) were detected in the fall of 2019 as high abundance; interestingly, all these communities were negatively correlated with T (<10°C), which is a unique feature of KSBCW.

The vertical structure of water masses has been considered another factor for microbial dispersal due to various hydrological qualities that function as barriers to mixing among distinct water masses (Matsuoka et al., 2012). The same bacterial groups respond differentially to different water masses vertically (Fu et al., 2019), and thus were isolated from each other due to their limited mobility (Spencer-Cervato and Thierstein, 1997). A time series study in Southern California found that when vertical stratification was weak during the winter, the bacterial composition was homogenized but became divergent vertically when surface water warmed up and stratified (Chow et al., 2013). In this study, the vertical structure of different water masses is caused not only by the T and S properties, which produce a mixing barrier but also by the diverse origins of the water mass at different depths. The TWW (TSW+TMW) originated in the warm equatorial Pacific area and flowed from the surface to the middle layer (Teague et al., 2006), whereas the cold bottom KSBCW originated in the East Sea (Lee et al., 2010). According to the "barrier to dispersal" theory (Spencer-Cervato and Thierstein, 1997), water masses from different origins would transport their source bacterial populations and organic materials to a new place, where they are modified by changes in environmental conditions but retain unique signatures in the absence of homogenization with other water sources. This is also supported by a previous study in the western channel of KS, where the vertical water-column structure of the TMW and KSBCW showed changes in phytoplankton composition due to vertically different T and S properties (Shon et al., 2008). Furthermore, the bacterial composition in TWW showed a horizontal similarity, but not in its vertical distribution in the East Sea (Lee and Choi, 2021). All these findings support our assumption that the observed several new communities and higher DIN in BL during the fall of 2019 might be brought along with the KSBCW and suggest that T and DIN were the primary factors. Taken together, it is observed that in UL compared to 2018, FW in 2019 modified the prokaryotic composition, whereas no significant change was observed in ML, but several new communities were brought to BL in 2019 along with KSBCW compared to 2018 without KSBCW. To better understand

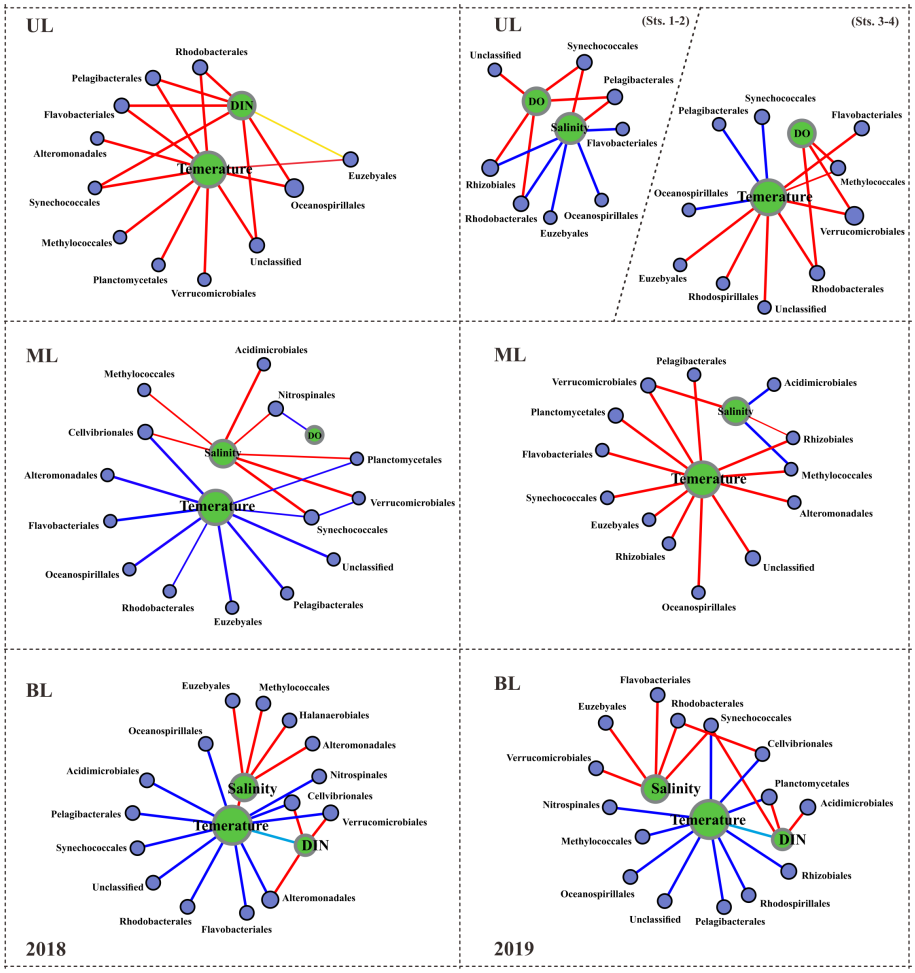

FIGURE 4
Spearman correlation between the environmental parameters and the prokaryotic families. This correlation analysis was conducted with the major abundant 15 families, but, correlations with R values greater than or equal to 0.3 are displayed here. Red lines indicate positive correlations; dark blue lines indicate negative correlations; sky blue lines indicate negative correlations with environmental factors; the thicker the lines, the stronger the correlations. UL (upper layer), ML (middle layer), and BL (bottom layer).

the metabolic potential of distinct prokaryotic communities driven by different water masses, we further explored their metabolic potential/functional characteristics in the following section.

3.3 Prokaryotic metabolic potential in response to the difference in the composition of water masses

Water mass intrusion, such as prokaryotic composition, affects photosynthetic characteristics (Figure S2). During the fall of 2018 and 2019, 46 genes from four sub-divisions were found, including 11 genes of photosystem I (PSI), 24 genes of photosystem II (PSII), 7 genes of the light-harvesting complex, and 4 genes of a reaction center. In comparison with ML and BL, the UL showed high relative abundances of photosynthesis genes; specifically, compared with the UL in the fall of 2019, the UL samples obtained in the fall of 2018 showed high gene abundance. In general, photosynthesis occurs mostly in the surface ocean than in deep environments, owing to light availability. Global ocean Synechococcus data suggest that high T have a vital influence on UL, where the majority of their population resides as a primary photosynthetic community (Zinser et al., 2007; Flombaum et al., 2013; Kent et al., 2016). In this study, we observed high Synechococcales abundance in the UL compared to ML and BL (Figure 3), which were similar to sequencing data from the Indian Ocean (Wang et al., 2021b) and Western Subarctic Pacific Ocean (Li et al., 2018). Similar to photosynthesis, compared to the 2019 UL samples, the 2018 UL samples showed high Synechococcales abundance (Figure 3A).

Different variables influence cyanobacteria in the upper ocean (Wang et al., 2021b), with the T being the greatest driver, followed by DIN, on their metabolic adaptability (Thompson et al., 2017). In this study, the T in 2019 UL (21.77–24.27°C) showed elevation compared to the T in 2018 UL (20.40–21.42°C), but we found that DIN was greater in 2018 UL (1.28-13.57 μmol L^{-1}) than in 2019 UL (0.88-4.93 μmol L^{-1}) and that our correlation analysis (Figure 4) revealed a positive interaction between DIN and Synechococcales in 2018 UL, which was not seen in 2019 UL. This suggests that

although the T is a vital factor for Synechococcales, DIN has a greater influence on their composition because it tends to synthesize more sugar (Li et al., 2019) to create more proteins for phytoplankton adaption (Thangaraj and Sun, 2021) in the ocean environment (Zubkov et al., 2003). Shim and Yoon (2021) recently studied the long-term (20-year; 1999-2018) nitrate fluctuation in the East Sea and concluded that the TWW from the CDW, coupled with the input of other rivers (e.g., Changjiang, Nakdong, Taehwa, and Hyungsan), influences the nutrient concentration in the Kuroshio Current extension and Korean coastal environment (Asanuma et al., 2014; Yoon et al., 2022). Based on these earlier findings and our results, we hypothesized that although TSW influenced T more than photosynthetic properties in 2018 and 2019, DIN availability was a significant parameter from the surrounding rivers to determine the high photosynthetic potential in the UL of 2018.

Several genes encoding various carbon-fixing pathways were identified during the study period (Figures 5, 6). Among these, certain Calvin cycle genes had similar abundances between fall 2018 and 2019 from UL to BL (Figures 5), and did not show significant variation regardless of different water mass compositions, that is, ribulose 1,5-bisphosphate (RuBisCO), a key carbon fixation gene, phosphoribulokinase (PRK), which catalyzes ATP-dependent phosphorylation, phosphoglycerate kinase (PK) involved in carbohydrate degradation, and glycerol-3-phosphate dehydrogenase (GPDH) associated with redox conversion. However, fewer genes showed a notable variation only in the UL, such as the aldolase enzyme, which helps in sugar breakdown and energy generation, revealing that a high abundance was in the UL (34%; occupied by TSW) in the fall of 2018 than those compared its abundances in the fall of 2019 UL (30%; occupied by FW and TSW). Similarly, the ribose 5-P isomerase, involved in energy conversion, was abundant in UL (34% in 2019) and (27% in 2018). We analyzed these specific gene abundances in the fall of 2019 to understand FW influence (Figure S3) and noticed that the Sts. 1–2 influenced from the FW increased aldolase levels compared to the Sts. 3–4 under high-T conditions by TSW influence. In contrast, FW region decreased ribose 5-P isomerase activity compared to that observed at higher T. In addition, several other key genes were differentially modified by FW, either by increasing fructose bisphosphate (FBP) and transketolase (TKT) or decreasing sedoheptulose bisphosphates (SBPase) and ribose 5-p isomerase. We observed that the relative abundance of these key genes in Sts. 3–4 (with TSW) was similar in the fall of 2018 and 2019, regardless of T variation. This suggests that, although the UL T (Sts. 3–4) driven by TSW in the fall of 2019 is higher than that in the fall of 2018, it does not have a significant impact on Calvin cycle genes; however, the FW (Sts. 1–2) significantly altered the abundance of these genes.

In addition to the Calvin cycle, various alternative carbon fixation mechanisms that can efficiently fix carbon instead of the Calvin cycle were identified (Figure 6). These alternative pathways are similar in that they insert inorganic carbon into existing carbon backbones and fix carbon through succinyl-CoA/acetyl-CoA cycles, and the enzymes involved in these alternative cycles largely overlap. The need for energy (ATP) and reducing equivalents to fix a carbon

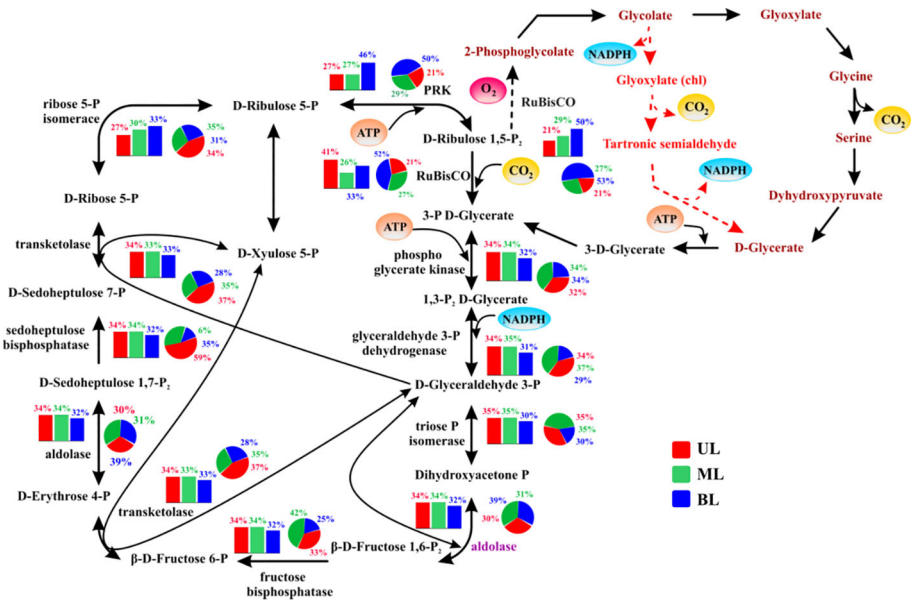

FIGURE 5
The relative abundance of genes/enzymes involved in the Calvin cycle (the reductive pentose phosphate pathway). The bar chart represents samples obtained from 2018; the pie chart represents samples obtained from 2019. UL (upper layer), ML (middle layer), and BL (bottom layer). The description, of abundance and function of each gene shown here, are given in Supplementary Table 3. The carboxylation steps involving (RuBisCO) Ribulose 1,5-bisphosphate carboxylase oxygenase is highlighted in the red bubble with inorganic carbon as the source of carbon dioxide (CO_2) in yellow. Known/suspected enzymes control or limiting over Calvin cycle activity are shown in purple text. Oxygenation of RuBisCO is shown as a dashed arrow and canonical phosphoglycerate-process photorespiratory pathways are shown as brown text. Reactions generating or requiring ATP or NADPH are highlighted in a circle, although NADH may be substituted for NADPH in some organisms in some reactions. The entry and exit are shown in yellow circles and oxygen is shown in red. Major points for the intermediate existence of the Calvin cycle are shown in red arrows.

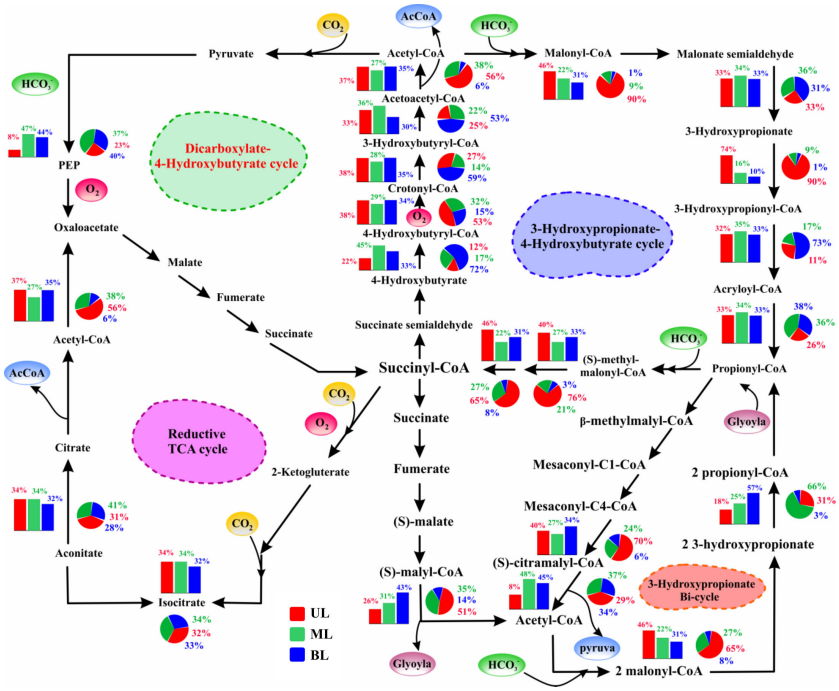

FIGURE 6
The relative abundance of genes/enzymes involved in multiple/alternative carbon fixation pathways. The bar chart represents samples obtained from 2018; the pie chart represents samples obtained from 2019. UL (upper layer), ML (middle layer), and BL (bottom layer). Schematic of intermediates and enzymes of four of the five (non-Calvin cycle) alternative pathways utilized by chemolithotroph and autotrophic microorganisms. All pathways use the common strategy of cycling between acetyl-CoA (circumference) and succinyl-CoA (center) to form the C2 and C3 carbon products that exit the cycle (acetyl-CoA and pyruvate; shown in blue). These metabolic pathways overlap partially one another concerning enzymes and intermediate usage, which allows them to represent spoked on a circle, with centered on succinyl-CoA. The incorporation of carboxylation steps is indicated by yellow circles (carbon dioxide) and green circles (bicarbonate). The enzymes requiring reactions or co-factors with complete or partial oxygen sensitivity are indicated in red, although some oxygen-resistant alternative enzymes exist for some of these reactions. The description of the abundance and function of each gene shown here are given in Supplementary Table 3.

molecule are the primary techniques used to determine the variations in these carbon cycle differentiations. These alternative carbon fixation pathways have two features: i) lower ATP required for carbon fixation than the Calvin cycle, and ii) carboxylation enzymes that use bicarbonate rather than dissolved CO_2 (Bar-Even et al., 2012; Boyle and Morgan, 2011).

The 3-hydroxy propionate (3-HOP) cycle has a carboxylation enzyme, acetyl-CoA carboxylase, which uses bicarbonate as a substrate. In the UL, this enzyme revealed significant change from the fall of 2018 (8%) to the fall of 2019 (29%). This enzyme is oxygen-insensitive and does not catalyze oxygenation processes, such as RuBisCO (Zarzycki et al., 2009), allowing for high primary productivity (Boyle and Morgan, 2011; Bar-Even et al., 2012). According to Könneke et al. (2014), the chemoautotrophic carbon fixation pathway (for archaea:3-HP/4-HB) is more energy-efficient than the Calvin cycle. In this study, the hydroxy-propionate (involved in the protein interaction) gene in the UL was more prevalent in the fall of 2019 (90%) compared to the fall of 2018 (74%). Furthermore, in UL 2019, methyl malonyl-CoA epimerase (converts succinate to propionate) (65%) and methyl malonyl-CoA mutase (pyruvate to propanoate) (76%), were more abundant than those in 2018 (46% and 40%, respectively). Because these genes were superficially abundant in the fall of 2019, we aimed to explore the role of FW influence (Figure S4) and noticed that S reduction (Sts. 1–2) increased in abundance compared with high T conditions (Sts. 3–4), suggesting that the increased abundance of all these enzymes in the fall of 2019 was mainly modified by S variation rather than T.

Unlike UL, most gene abundances in ML 2018 and 2019 did not show significant changes. However, certain functional genes, such as 4-hydroxybutyryl-CoA synthetase and 3-hydroxybutyryl-Coa, were abundant in 2019 BL samples, which had a lower T (<5°C) than the T range of >12°C in 2018. We also noticed that RuBisCO was more abundant in the BL in 2019 than in the BL in 2018. This implies that these enzymes are susceptible to cooler T in prokaryotic metabolism. Variations in these carbon fixation pathways (Calvin and others) revealed that carbon fixation by phototrophs and chemotrophs was not completely different between 2018 and 2019. However, the S and T sensitivity of certain key genes indicated differing water mass influences: preference for lower S/higher T (UL) and lower T conditions (BL).

The T is a vital physicochemical parameter that influences all biological processes through enzymatic reactions (Franks et al., 1990). T changes can cause prokaryotes to respond in multiple ways to a new environment to maintain consistent metabolic activity and trigger several adaptive modifications (Jaenicke and Sterner, 2006). The maintenance of overall metabolic rates with the fewest changes in molecular composition would activate a less energy-demanding mechanism (Rabus et al., 2002). This might explain why various

carbon metabolisms were observed in this study because these multiple carbon pathways have lower energy needs and rely on available bicarbonate raters rather than CO_2, such as 3-HP/4-HB, which is a more energy-efficient metabolism than the Calvin cycle. A recent study spanning over 1000 km in the Baltic Sea demonstrated that microbial communities and associated functional gene abundances can be altered not only by T but also by S variation (Broman et al., 2022). They revealed that S was the primary driver of functional gene modifications related to the carbon and nitrogen cycles. Their findings support our hypothesis that S reduction through FW input would greatly modify the functional capabilities of prokaryotic communities in the fall of 2019 UL compared to that in the fall of 2018. Our assumption is also in agreement with studies that have found that S influences the gene abundance of microbial communities in systems such as lakes and estuarine environments (Dai et al., 2018; Yang et al., 2023). For example, a study conducted in the Hangzhou Bay estuary identified S as one of the most influential variables for amino acid catabolism related to gene abundances in nitrogen, sulfur, and phosphorus pathways in prokaryotes (Dai et al., 2018). In our study, the major carbon pathways that changed gene abundance were seemingly controlled by the S variation in the UL of the fall of 2019 compared to that of the fall of 2018. Additionally, S variation has been shown to promote key genes in carbon metabolism (Figures S3, S4), which were more prevalent in the fall of 2019 (Sts. 1–2). Taken together, our results indicate that S variation *via* FW input has a larger impact on the UL of fall 2019 than relatively stable parameters, such as T, which is similar to earlier observations between S and other environmental parameters (Seidel et al., 2021; Broman et al., 2022).

RuBisCO possesses less sensitivity and higher velocity, which favors a CO_2-rich environment, such as rising CO_2 levels (Zhu et al., 2010). The RuBisCO gene in the deep ocean was recently identified in high abundance in the Synechococcus community with oxygen-rich surface water exposed to high light conditions (Han et al., 2022). Notably, with lower oxygen levels in the deep ocean, there are numerous Calvin cycle genes, including that abundant RuBisCO in chemoautotrophs, such as Nitrosomonas, Nitrosospira, and Acidomicrobium found (Han et al., 2022). Although large amounts of RuBisCO were found in the UL, they were found in higher abundances in the BL, which had lower oxygen levels than the UL in both years (Figures 3C, G). In particular, high abundances of RuBisCO were noticed in the 2019 BL, which had a lower T and higher DO compared to the 2018 BL. This pattern illustrates that, regardless of the DO reduction in BL lower T >10°C in 2019, which is a unique feature of the KSBCW in this region, the carbon fixation shifted from photoautotrophs to chemoautotrophs compared to that in 2018. In particular, archaeal communities are sensitive to high oxygen concentrations and can maintain higher enzyme activity under low DO and T conditions (Demirci et al., 2020). These large abundances of chemotrophic carbon-fixing genes in BL in 2019 reduced oxygen conditions and could explain the deoxygenated habitat of this archaeal colony. Furthermore, in this study, most enzymes in the archaeal carbon fixation pathway were shown to be T sensitive and so prevalent in BL (specifically in 2019), which could be the reason for their preference for cooler environments (Danovaro et al., 2017). Our results are consistent with those of recent Bohai Sea metagenome and metatranscriptome studies, which found 6 to 33-fold increases in these genes with decreased oxygen concentration (Han et al., 2022). The abundance of Synechococcales and numerous genes in the Calvin cycle in the UL indicates that photoautotrophic carbon fixation at the UL and chemoautotrophic carbon fixation at the BL were more prevalent during this study. In particular, compared to 2018, the UL 2019 was relatively different due to FW influence, and compared to 2018, the BL in 2019 was different (promoting chemoautotroph carbon fixation) primarily driven by lower T.

This study revealed key genes involved in nitrogen fixation (*nifH*), ammonium assimilation (*glnA*) ammonium oxidation (*amoA*), hydroxylamine oxidation (*hao*), and nitrite oxidation (*nxrAB*) (Figure 7), and showed that *nifH, amoA, hao, and nxrB* in UL of both years had significant changes. Specifically, *nifH* gene abundance in the 2019 UL was greater than that in 2018. Similarly, *hao*, *nxrB* genes showed a slight elevation in the UL in 2019 compared to the 2018 UL. In contrast, *amoA* and *glnA* in the UL were highly abundant in 2018 compared to 2019. This suggests that compared to the UL in 2018, the metabolic potential related to nitrogen fixation (*nifH*) and nitrification (*hao* + *nxrB*) was greater in 2019, whereas ammonium oxidation (*amoA*) and assimilation (*glnA*) were lower. As these gene abundances varied in UL 2019 compared to UL 2018, we estimated their individual abundances based on water mass differentiation and found that FW influence (at Sts. 1–2) in 2019 increased nitrogen fixation and nitrification (i.e., hydroxylamine oxidation and nitrite oxidation) potentials and decreased ammonia oxidation and assimilation potential (Figure S5). This suggests that the metabolic potential of the nitrogen cycle in the fall of 2019 was significantly modified by FW input compared to 2018. Our results are similar to those of a recent proteome investigation by Ilgrande et al. (2018) on nitrifying communities and their metabolic potential for S variation. They found that S changes could reduce ammonium and nitrite oxidation potential to 42%, and other metabolic processes related to the nitrogen cycle were positively influenced. Liu et al. (2022) showed that S changes in response to different nutrient-cycling genes and found that decreasing S can modify nitrogen metabolic genes in aquatic environments.

Sulfur oxidation and reduction were identified (Figure S6), with oxidation genes (*Sox A, B,X,Y,Z*) being the most abundant in the UL in both years. Compared to 2018, the 2019 samples had slightly higher UL abundances and lower BL abundances. However, unlike nitrogen metabolism, the Sts. 1–2 (i.e., the region of FW influence) did not show the individual genes involved in sulfur metabolism; however, the Sts. 3–4 showing high T by TSW increased in abundance (Figure S7). This variation demonstrates the effect of T on the sulfur oxidation potential. For example, the UL T values in 2019 were higher than those in 2018. Similar to sulfur oxidation, T fluctuations influenced the sulfur reduction genes between 2018 and 2019. Interestingly, the *dsrA,B* genes were abundant in both years BL, specifically in 2019 BL, showing that these functional genes were dominant in the KSBCW and were susceptible to warmer environments driven by TWW.

These findings are in line with those from the Okhotsk Sea (near our study area) (Li et al., 2018) and the South Atlantic Subtropical gyre (Murillo et al., 2014). An incubation experiment in the Arctic

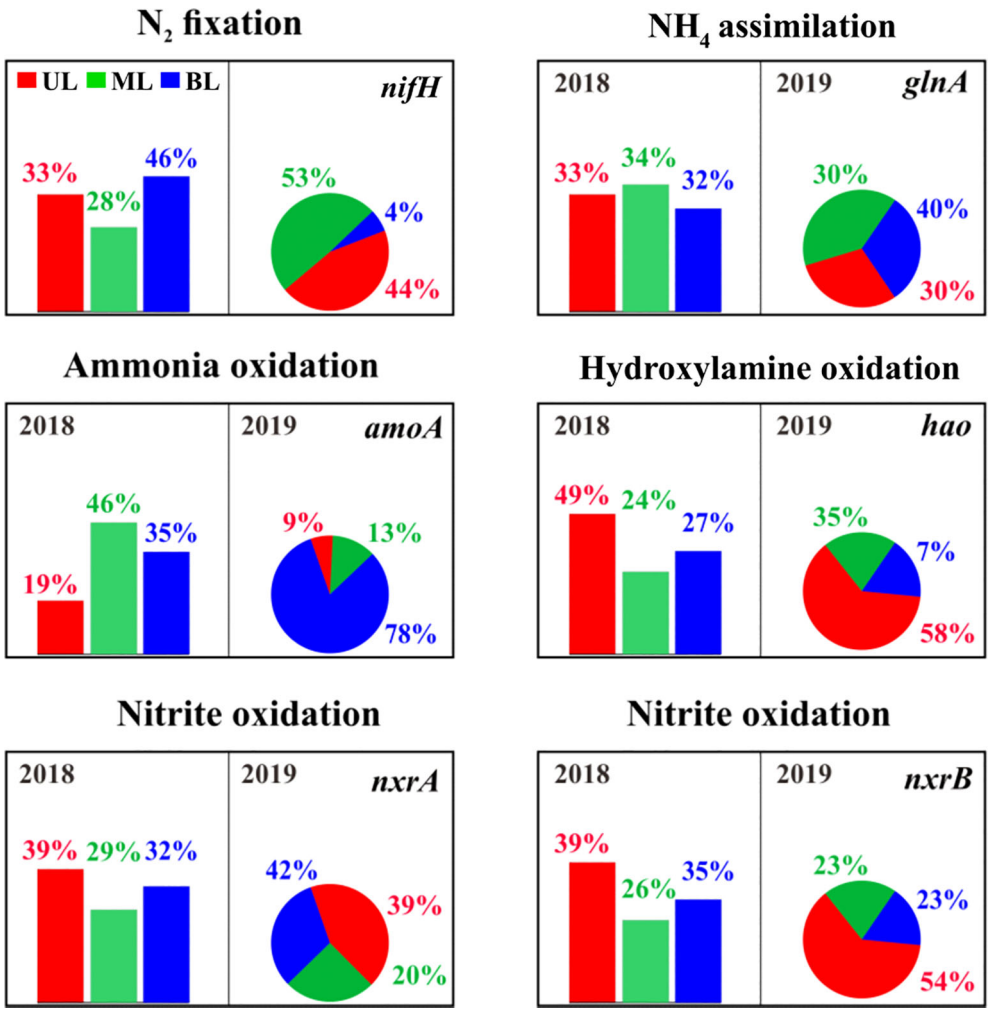

FIGURE 7
The relative abundance of genes/enzymes involved in the nitrification process. The bar chart represents samples from 2018, and the pie chart represents samples from 2019. The description of the abundance and function of each gene represents shown here are given in Supplementary Table 3.

seawater (0°C, 10°C, and 20°C) revealed unique T responses for sulfate oxidation and reduction potential, implying differing characterization of sulfur-oriented bacterial populations (Robador et al., 2009). This shows that the respiration rates of sulfur-oriented bacteria increased significantly at lower T, which might explain the high abundance of *dsrA,B* genes found in this study. Comparative investigations between psychrophilic and mesophilic bacteria have revealed that under cold T, bacteria have a high enzymatic level for a long time to adapt (Feller and Gerday, 2003). Other studies have demonstrated that electron transfer coupling is less effective at lower T (Rabus et al., 2002), which is consistent with the current findings, with most oxidation and reduction gene abundance. Alphaproteobacteria play an important role in sulfur metabolism and have abundant sulfur oxidation and reduction genes (Li et al., 2018). Alphaproteobacteria were more abundant in the UL samples in this investigation (Supplemental Table 2), which might explain the increased abundance of sulfur reduction and oxidation. Our findings agree with a previous study that discovered sulfur-oxidizing Alphaproteobacteria with chemolithotroph lifestyles in surface water at higher T (Meyer and Kuever, 2007). Acclimation to low T does not fully compensate for the thermodynamic restrictions imposed on complex biochemical processes, such as respiratory energy generation.

This study found both heat and cold shock genes/proteins in response to T fluctuations driven by the difference in the composition of water masses (Figure 8). In this study, heat shock proteins were more abundant in the UL in both 2018 and 2019 compared to the other layers. However, compared to 2018, samples from 2019 showed higher abundance, with T ranges in the UL of 2019 being higher than those in 2018. Similar to other results, we estimated the FW influence of these heat shock protein abundances in the fall of 2019 and found no evidence that S variation may alter these gene abundances (Figure S8). Increasing T in the bacterial environment has been reported to harm protein synthesis in cellular processes (Maleki et al., 2016). In bacteria, heat shock proteins increase protein synthesis mechanisms (De Maio, 1999) to adjust to T changes (Maleki et al., 2016). In particular, when bacteria are exposed to higher T, the *DnaK* gene, which plays a role in repairing

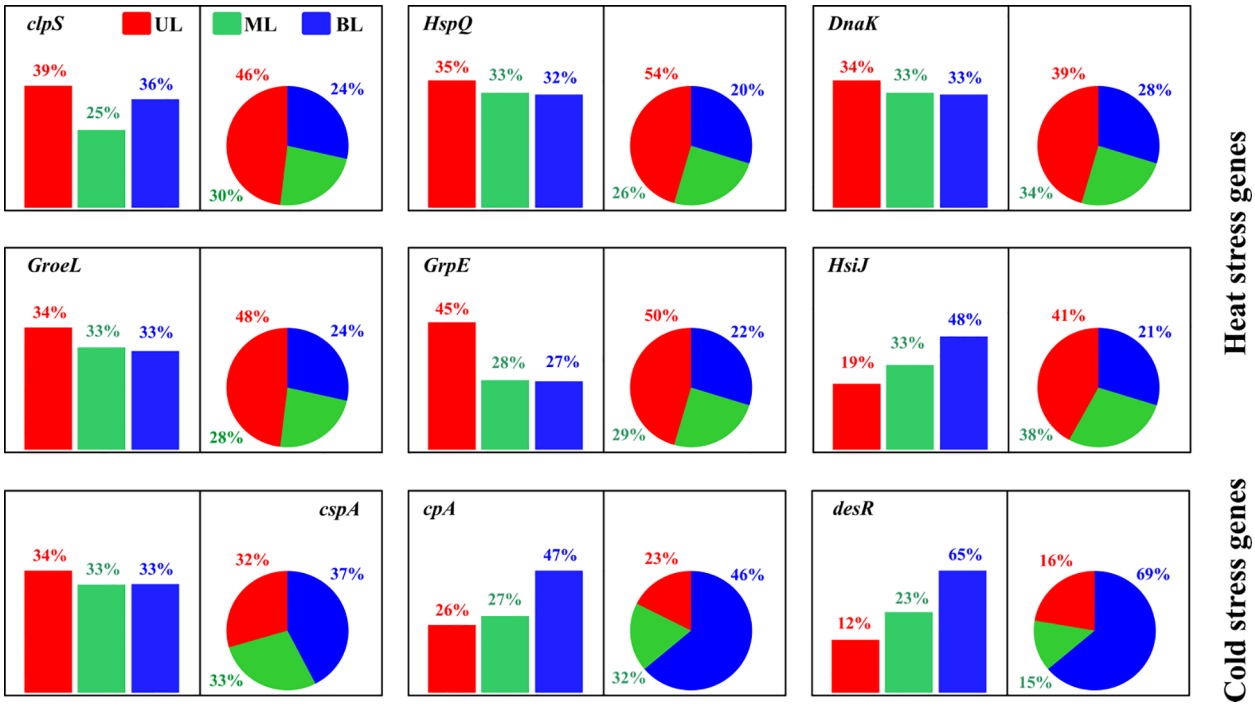

FIGURE 8
The relative abundance of cold and heat shock genes/proteins in bacterial metabolism. The bar chart represents samples from 2018, and the pie chart represents samples from 2019. UL (upper layer), ML (middle layer), and BL (bottom layer). The description of the abundance and function of each gene represents showed here are given in Supplementary Table 3.

thermally damaged proteins for cell survival, increases (Yusof et al., 2022). Our *DnaK* gene was found to be highly prevalent in the UL in both years of this study. More specifically, as compared with the 2018 UL, this gene was shown to be higher (14% higher) in 2019. Similarly, other heat shock genes (*clpS* and *HspQ*) found in this study were shown to be greater (11%-115%) in 2019 compared to 2018. This implies that in comparison to 2018, prokaryotes created more heat shock proteins (in abundance) in 2019 to repair their damaged proteins to survive. Our results also demonstrate that when the T in the study area is high, these heat shock proteins increase in prokaryotes, which could be considered biomarkers of this region to increase surface ocean T. Cold shock genes are generated in cold environments in response to T changes to preserve bacteria's optimal growth conditions (Keto-Timonen et al., 2016). Bacterial enzymatic activity is reduced under these conditions, which affects transcription and translation mechanisms (Phadtare and Inouye, 2004). Cold shock genes assist cells in overcoming these alterations by altering their nucleic acid components (Phadtare and Severinov, 2010). After cold shock genes are created, enzymatic activity in bacteria accelerates, allowing cells to develop at a lower T and even at a slower phase (Ermolenko & Makhatadze, 2002). We found that the high abundance of the *cspA, cpA*, and *desR* cold genes in the BL was evident in fall 2019 compared to fall 2018, owing to the intrusion of KSBCW (<10°C), which could be considered as biomarkers of this specific water mass in this region.

The Changjiang River is known as a hotspot with a yearly T increase of approximately 3.5°C and an anticipated 30% increase in annual precipitation (Gu et al., 2015) due to climate change, which is expected to boost FW flow to ECS *via* CDW (Liu et al., 2021). Previous investigations found that approximately 70% of the ECS FW is transferred annually through KS (Senjyu et al., 2006; Moon et al., 2019; Yoon et al., 2022) which might change the environmental conditions of KS in the future. According to a recent study, the Kuroshio current extension is sensitive to global climate change and has the potential to warm significantly in the future (Lam et al., 2021), in addition to increasing warming TWW into the East Sea *via* the KS. Collectively, we anticipate large physical and biogeochemical changes in future KS based on significant increases in FW input from the Changjiang River and surface warming from the TWW. The results of this study, describing FW influence and T variation in prokaryotic composition, and their functional capabilities from genome abundances to biomarkers potential to different water masses from UL to BL, could be used as a reference for future investigations.

4 Summary and conclusion

In this study, we compared the prokaryotic communities from different layers of the KS between the fall of 2018 and 2019 to investigate how different water masses influenced their composition and metabolic potential. Our results showed that the S and T of the water masses played an important role in regulating the prokaryotic population and metabolic modifications, especially in the UL and BL in 2019, which differed from those in 2018 due to the difference in the composition of water masses. We observed that the FW input

from the ECS into the 2019 UL had a significant impact on altering the prokaryotic population from high density in 2018 to high diversity in 2019 than the relatively stable variable of T in 2018. In the 2019 BL, the lower T driven by the KSBCW brought several new communities from its origin to the KS, which was different from the BL in 2018. We also investigated the functional genes and found that they were influenced by different water mass conditions, including a preference for lower S and lower/higher T. Specifically, compared to 2018, the UL in 2019 promoted phototroph carbon fixation, whereas the BL in 2019 promoted chemoautotroph carbon fixation driven by KSBCW (T<10°C). We identified several biomarker genes based on the T variation in different water mass compositions from the UL to the BL in the study region. This study is the first attempt to demonstrate the effect of different water masses on the prokaryotic composition and metabolic/functional potential in the KS. Our findings provide a baseline understanding of the biogeochemical pattern in this understudied region and highlight the need for more comprehensive studies that consider not only the distinct water masses from the UL to the BL but also the effects of climate change, such as warming and acidification, to predict the biogeochemical pattern in the future.

Data availability statement

The datasets presented in this study can be found in online repositories. The names of the repository/repositories and accession number(s) can be found in the article/Supplementary Material.

Author contributions

ST and I-NK developed the concept and design of the article. H-RK and I-NK conducted sampling. I-NK, ST and H-RK conducted measurements and analysis. ST, and I-NK wrote the manuscript. S-YK, H-KJ, and J-HK discussed the results and commented on the article.

Funding

This research was supported by the National Institute of Fisheries Science, Ministry of Oceans and Fisheries, Korea (R2023008) and the National Research Foundation of Korea (NRF) funded by the Korean government (MSIT) (NRF-2022R1A2C1008475). This study was also supported by a grant from the Korea Institute of Ocean Science and Technology (KIOST) (PEA008A) and Korea Institute of Marine Science and Technology Promotion (KIMST) funded by the Ministry of Oceans and Fisheries (MOF), Korea, titled "Development of Risk Managing Technology Tackling Ocean and Fisheries Crisis around Korean Peninsula by Kuroshio Current" (RS-2023-00256330).

Acknowledgments

We would like to thank the captain and crew members of the R/V *Nara* for their endless support during the fall 2018 and 2019 cruises. We express our gratitude to Dr. Dae-Hyun Kim for his valuable assistance with the processing of CTD data.

Conflict of interest

The authors declare no conflicts of interest and the research was conducted in the absence of any commercial or financial relationships that could be construed as a potential conflict of interest.

Publisher's note

All claims expressed in this article are solely those of the authors and do not necessarily represent those of their affiliated organizations, or those of the publisher, the editors and the reviewers. Any product that may be evaluated in this article, or claim that may be made by its manufacturer, is not guaranteed or endorsed by the publisher.

Supplementary material

The Supplementary Material for this article can be found online at: https://www.frontiersin.org/articles/10.3389/fmars.2023.1215251/full#supplementary-material

References

Aßhauer, K. P., Wemheuer, B., Daniel, R., and Meinicke, P. J. B. (2015). Tax4Fun: predicting functional profiles from metagenomic 16S rRNA data. *Bioinformatics* 31, 2882–2884. doi: 10.1093/bioinformatics/btv287

Agardi, T., Alder, J., Dayton, P., Curran, S., Kitchingman, A., Wilson, M., et al. *Millennium ecosystem assessment: ecosystems and human well-being* (2005) (Washington, DC: Current State and Trends Island Press).

Agogué, H., Brink, M., Dinasquet, J., and Herndl, G. J. (2008). Major gradients in putatively nitrifying and non-nitrifying archaea in the deep north Atlantic. *Nature* 456, 788–791. doi: 10.1038/nature07535

Aldunate, M., de la Iglesia, R., Bertagnolli, A. D., and Ulloa, O. (2018). Oxygen modulates bacterial community composition in the coastal upwelling waters off central Chile. *Deep Sea Res. Part II: Topical Stud. Oceanography* 156, 68–79. doi: 10.1016/j.dsr2.2018.02.001

Arístegui, J., Gasol, J. M., Duarte, C. M., and Herndld, G. (2009). Microbial oceanography of the dark ocean's pelagic realm. *Limnology Oceanography* 54, 1501–1529. doi: 10.4319/lo.2009.54.5.1501

Asanuma, I., Zhang, X.-G., Zhao, C., Huang, B., and Hasegawa, D. (2014). Nutrients distribution in the coastal water of East Asia relative to the kuroshio. *Landscape Ecol. Eng.* 10, 191–199. doi: 10.1007/s11355-013-0242-7

Bachmann, J., Heimbach, T., Hassenrück, C., Kopprio, G. A., Iversen, M. H., Grossart, H. P., et al. (2018). Environmental drivers of free-living vs. particle-attached bacterial community composition in the Mauritania upwelling system. *Front. Microbiol.* 9, 2836. doi: 10.3389/fmicb.2018.02836

Bar-Even, A., Noor, E., and Milo, R. (2012). A survey of carbon fixation pathways through a quantitative lens. *J. Exp. Bot.* 63, 2325–2342. doi: 10.1093/jxb/err417

Beardsley, R., Limeburner, R., Yu, H., and Cannon, G. (1985). Discharge of the changjiang (Yangtze river) into the East China sea. *Continental Shelf Res.* 4, 57–76. doi: 10.1016/0278-4343(85)90022-6

Bokulich, N. A., Subramanian, S., Faith, J. J., Gevers, D., Gordon, J. I., Knight, R., et al. (2013). Quality-filtering vastly improves diversity estimates from illumina amplicon sequencing. *Nat. Methods* 10, 57–59. doi: 10.1038/nmeth.2276

Boyle, N. R., and Morgan, J. A. (2011). Computation of metabolic fluxes and efficiencies for biological carbon dioxide fixation. *Metab. Eng.* 13, 150–158. doi: 10.1016/j.ymben.2011.01.005

Broman, E., Izabel-Shen, D., Rodríguez-Gijón, A., Bonaglia, S., Garcia, S. L., and Nascimento, F. J. (2022). Microbial functional genes are driven by gradients in sediment stoichiometry, oxygen, and salinity across the Baltic benthic ecosystem. *Microbiome* 10 (1), 1–17. doi: 10.1186/s40168-022-01321-z

Bryant, J. A., Clemente, T. M., Viviani, D. A., Fong, A. A., Thomas, K. A., Kemp, P., et al. (2016). Diversity and activity of communities inhabiting plastic debris in the north pacific gyre. *MSystems* 1, e00024–e00016. doi: 10.1128/mSystems.00024-16

Caporaso, J. G., Kuczynski, J., Stombaugh, J., Bittinger, K., Bushman, F. D., Costello, E. K., et al. (2010). QIIME allows analysis of high-throughput community sequencing data. *Nat. Methods* 7, 335–336. doi: 10.1038/nmeth.f.303

Celussi, M., Bergamasco, A., Cataletto, B., Umani, S. F., and Del Negro, P. (2010). Water masses' bacterial community structure and microbial activities in the Ross Sea, Antarctica. *Antarctic Sci.* 22, 361–370. doi: 10.1017/S0954102010000192

Chakravorty, S., Helb, D., Burday, M., Connell, N., and Alland, D. (2007). A detailed analysis of 16S ribosomal RNA gene segments for the diagnosis of pathogenic bacteria. *J. microbiological Methods* 69, 330–339. doi: 10.1016/j.mimet.2007.02.005

Chang, P. H., and Isobe, A. (2003). A numerical study on the changjiang diluted water in the yellow and East China seas. *J. Geophysical Research: Oceans* 108, (C9). doi: 10.1029/2002JC001749

Chow, C.-E. T., Sachdeva, R., Cram, J. A., Steele, J. A., Needham, D. M., Patel, A., et al. (2013). Temporal variability and coherence of euphotic zone bacterial communities over a decade in the southern California bight. *ISME J.* 7, 2259–2273. doi: 10.1038/ismej.2013.122

Chung, I.-K., and Kang, Y.-H. (1995). The ultrastructure of the chlorococcalean picoplankton isolated from the western channel of the Korea strait. *J. Korean Soceity Oceanography* 30, 529–536.

Dai, T., Zhang, Y., Ning, D., Su, Z., Tang, Y., Huang, B., et al. (2018). Dynamics of sediment microbial functional capacity and community interaction networks in an urbanized coastal estuary. *Front. Microbiol.* 9, 2731. doi: 10.3389/fmicb.2018.02731

Danovaro, R., Corinaldesi, C., Dell'Anno, A., and Snelgrove, P. V. (2017). *The deep-sea under global change* Vol. 27 (Curr. Biol), R461–R465. doi: 10.1016/j.cub.2017.02.046

Del Giorgio, P. A., and Williams, P. L. B. (2005). The global significance of respiration in aquatic ecosystems: from single cells to the biosphere. *Respiration Aquat. Ecosyst.* 1. doi: 10.1093/acprof:oso/9780198527084.003.0014

De Maio, A. J. S. (1999). Heat shock proteins: facts, thoughts, and dreams. *Shock* 11, 1–12. doi: 10.1097/00024382-199901000-00001

Demirci, H., Tolar, B. B., Doukov, T., Petriceks, A., Pal, A., Yoshikuni, Y., et al. (2020). Structural adaptation of oxygen tolerance in 4-hydroxybutyrl-CoA dehydratase, a key enzyme of archaeal carbon fixation. *bioRxiv*, 2020-02. doi: 10.1101/2020.02.05.935528

Ducklow, H. (2000). Bacterial production and biomass in the oceans. *Microbial Ecol. oceans* 1, 85–120.

Ermolenko, D., and Makhatadze, G. (2002). Bacterial cold-shock proteins. *Cell. Mol. Life Sci. CMLS* 59, 1902–1913. doi: 10.1007/PL00012513

Feller, G., and Gerday, C. (2003). Psychrophilic enzymes: hot topics in cold adaptation. *Nat. Rev. Microbiol.* 1, 200–208. doi: 10.1038/nrmicro773

Flombaum, P., Gallegos, J. L., Gordillo, R. A., Rincón, J., Zabala, L. L., Jiao, N., et al. (2013). Present and future global distributions of the marine cyanobacteria prochlorococcus and synechococcus. *Proc. Natl. Acad. Sci.* 110, 9824–9829. doi: 10.1073/pnas.1307701110

Franks, F., Mathias, S., and Hatley, R. (1990). Water, temperature and life. *Philos. Trans. R. Soc. London. B Biol. Sci.* 326 (1237), 517–533. doi: 10.1098/rstb.1990.0029

Fu, Y., Rivkin, R. B., and Lang, A. S. (2019). Effects of vertical water mass segregation on bacterial community structure in the Beaufort Sea. *Microorganisms* 7, 385. doi: 10.3390/microorganisms7100385

Fuhrman, J. A., Sleeter, T. D., Carlson, C. A., and Proctor, L. M. (1989). Dominance of bacterial biomass in the Sargasso Sea and its ecological implications. *Mar. Ecol. Prog. Ser.*, 207–217. doi: 10.3354/meps057207

Galand, P. E., Casamayor, E. O., Kirchman, D. L., and Lovejoy, C. (2009). Ecology of the rare microbial biosphere of the Arctic ocean. *Proc. Nat. Acad. Sci.* 106 (52), 22427–22432. doi: 10.1073/pnas.0908284106

Galand, P. E., Potvin, M., Casamayor, E. O., and Lovejoy, C. (2010). Hydrography shapes bacterial biogeography of the deep Arctic ocean. *ISME J.* 4, 564–576. doi: 10.1038/ismej.2009.134

Gomes, H. D. R., Xu, Q., Ishizaka, J., Carpenter, E. J., Yager, P. L., and Goes, J. I. (2018). The influence of riverine nutrients in niche partitioning of phytoplankton communities–a contrast between the Amazon river plume and the ChangJiang (Yangtze) river diluted water of the East China Sea. *Front. Mar. Sci.* 5, 343. doi: 10.3389/fmars.2018.00343

Gu, H., Yu, Z., Wang, G., Wang, J., Ju, Q., Yang, C., et al. (2015). Impact of climate change on hydrological extremes in the Yangtze river basin, China. *Stochastic Environ. Res. Risk Assess.* 29, 693–707. doi: 10.1007/s00477-014-0957-5

Han, Y., Zhang, M., Chen, X., Zhai, W., Tan,, E., and Tang, K., and (2022). Transcriptomic evidences for microbial carbon and nitrogen cycles in the deoxygenated seawaters of bohai Sea. *Environ. Int.* 158, 106889. doi: 10.1016/j.envint.2021.106889

Hydes, D., Aoyama, M., Aminot, A., Bakker, K., Becker, S., Coverly, S., et al. (2010). *Recommendations for the determination of nutrients in seawater to high levels of precision and inter-comparability using continuous flow analysers* (GO-SHIP (Unesco/IOC).

Ichinomiya, M., Yamada, K., Nakagawa, Y., Nishino, Y., Kasai, H., and Kuwata, A. (2019). Parmales abundance and species composition in the waters surrounding Hokkaido, north Japan. *Polar Sci.* 19, 130–136. doi: 10.1016/j.polar.2018.08.001

Ilgrande, C., Leroy, B., Wattiez, R., Vlaeminck, S. E., Boon, N., and Clauwaert, P. (2018). Metabolic and proteomic responses to salinity in synthetic nitrifying communities of nitrosomonas spp. and nitrobacter spp. *Front. Microbiol.* 9, 2914. doi: 10.3389/fmicb.2018.02914

Jaenicke, R., and Sterner, R. (2006). Life at high temperatures. *prokaryotes*, 167–209. doi: 10.1007/0-387-30742-7_7

Jeong, W. G., and Cho, S. M. (2018). Estimation of primary production of the waters around rack oyster farm at wando, Korea. *Fisheries Aquat. Sci.* 21 (1), 1–7. doi: 10.1186/s41240-018-0086-z

Jiao, N., Zhang, Y., Zeng, Y., Gardner, W. D., Mishonov, A. V., Richardson, M. J., et al. (2007). Ecological anomalies in the East China Sea: impacts of the three gorges dam? *Water Res.* 41, 1287–1293. doi: 10.1016/j.watres.2006.11.053

Kang, H., and Kang, D.-S. (2002). Contribution of marine microbes to particulate organic matter in the Korea strait. *J. korean Soc. oceanography* 37, 35–44.

Kent, A. G., Dupont, C. L., Yooseph, S., and Martiny, A. C. (2016). Global biogeography of prochlorococcus genome diversity in the surface ocean. *ISME J.* 10, 1856–1865. doi: 10.1038/ismej.2015.265

Keto-Timonen, R., Hietala, N., Palonen, E., Hakakorpi, A., Lindström, M., and Korkeala, H. (2016). Cold shock proteins: a minireview with special emphasis on csp-family of enteropathogenic yersinia. *Front. Microbiol.* 7, 1151. doi: 10.3389/fmicb.2016.01151

Kim, I.-N., and Lee, T.-S. (2004). Physicochemical properties and the origin of summer bottom cold waters in the Korea strait. *Ocean Polar Res.* 26, 595–606. doi: 10.4217/OPR.2004.26.4.595

Kim, H.-R., Lim, J.-H., Kim, J.-H., Thangaraj, S., and Kim, I.-N. (2022). Physical process controlling the surface bacterial community composition in the ulleung basin of East Sea. *Front. Mar. Sci.* 9, 841492. doi: 10.3389/fmars.2022.841492

Kim, Y. H., Kim, Y. B., Kim, K., Chang, K. I., Lyu, S. J., Cho, Y. K., et al. (2006). Seasonal variation of the Korea strait bottom cold water and its relation to the bottom current. *Geophys. Res. Lett.* 33 (24). doi: 10.1029/2006GL027625

Klindworth, A., Pruesse, E., Schweer, T., Peplies, J., Quast, C., Horn, M., et al. (2013). Evaluation of general 16S ribosomal RNA gene PCR primers for classical and next-generation sequencing-based diversity studies. *Nucleic Acids Res.* 41, e1–e1. doi: 10.1093/nar/gks808

Knoblauch, C., and Jørgensen, B. B. (1999). Effect of temperature on sulphate reduction, growth rate and growth yield in five psychrophilic sulphate-reducing bacteria from Arctic sediments. *Environ. Microbiol.* 1, 457–467. doi: 10.1046/j.1462-2920.1999.00061.x

Könneke, M., Schubert, D. M., Brown, P. C., Hügler, M., Standfest, S., Schwander, T., et al. (2014). Ammonia-oxidizing archaea use the most energy-efficient aerobic pathway for CO2 fixation. *Proc. Natl. Acad. Sci.* 111, 8239–8244. doi: 10.1073/pnas.1402028111

Lam, A. R., Macleod, K. G., Schilling, S. H., Leckie, R. M., Fraass, A. J., Patterson, M. O., et al. (2021). Pliocene to earliest pleistocene (5–2.5 ma) reconstruction of the kuroshio current extension reveals a dynamic current. *Paleoceanography Paleoclimatology* 36, e2021PA004318. doi: 10.1029/2021PA004318

Laque, T., Farjalla, V. F., Rosado, A. S., and Esteves, F. A. (2010). Spatiotemporal variation of bacterial community composition and possible controlling factors in tropical shallow lagoons. *Microbial Ecol.* 59, 819–829. doi: 10.1007/s00248-010-9642-5

Lee, J.-K., and Choi, K.-H. (2021). Bacterial communities from the water column and the surface sediments along a transect in the East Sea. *J. Mar. Life Sci.* 6, 9–22.

Lee, Y.-W., Park, H.-J., Choy, E.-J., Kim, Y.-S., and Kang, C.-K. (2010). Temporal variation of phytoplankton community related to water column structure in the Korea strait. *Ocean Polar Res.* 32, 321–329. doi: 10.4217/OPR.2010.32.3.321

Levitus, S., and Boyer, T. (1994). *World ocean atlas 1994 volume 4: temperature* Vol. 4 (Washington: DC, US Department of Commerce, NOAA Atlas NESDIS).

Li, Y., Jing, H., Xia, X., Cheung, S., Suzuki, K., and Liu, H. (2018). Metagenomic insights into the microbial community and nutrient cycling in the western subarctic pacific ocean. *Front. Microbiol.* 9, 623. doi: 10.3389/fmicb.2018.00623

Li, Y.-Y., Chen, X.-H., Xue, C., Zhang, H., Sun, G., Xie, Z.-X., et al. (2019). Proteomic response to rising temperature in the marine cyanobacterium synechococcus grown in different nitrogen sources. *Front. Microbiol.* 10, 1976 doi: 10.3389/fmicb.2019.01976

Liu, Z., Gan, J., Wu, H., Hu, J., Cai, Z., and Deng, Y. (2021). Advances on coastal and estuarine circulations around the changjiang estuary in the recent decades 2000–2020). *Front. Mar. Sci.* 8, 615929. doi: 10.3389/fmars.2021.615929

Liu, Q., Yang, J., Wang, B., Liu, W., Hua, Z., and Jiang, H. (2022). Influence of salinity on the diversity and composition of carbohydrate metabolism, nitrogen and sulfur cycling genes in lake surface sediments. *Front. Microbiol.* 13, 1019010. doi: 10.3389/fmicb.2022.1019010

Liu, S. M., Zhang, J., Chen, H., Wu, Y., Xiong, H., and Zhang, Z. (2003). Nutrients in the changjiang and its tributaries. *Biogeochemistry* 62, 1–18. doi: 10.1023/A:1021162214304

Matsuoka, A., Bricaud, A., Benner, R., Para, J., Sempéré, R., Prieur, L., et al. (2012). Tracing the transport of colored dissolved organic matter in water masses of the southern Beaufort Sea: relationship with hydrographic characteristics. *Biogeosciences* 9 (3), 925–940. doi: 10.5194/bg-9-925-2012

Maleki, F., Khosravi, A., Nasser, A., Taghinejad, H., and Azizian, M. (2016). Bacterial heat shock protein activity. *J. Clin. Diagn. research: JCDR* 10, BE01. doi: 10.7860/JCDR/2016/14568.7444

Mason, R. L., Gunst, R. F., and Hess, J. L. (2003). *Statistical design and analysis of experiments: with applications to engineering and science* (John Wiley & Sons).

Meyer, B., and Kuever, J. (2007). Molecular analysis of the diversity of sulfate-reducing and sulfur-oxidizing prokaryotes in the environment, using aprA as functional marker gene. *Appl. Environ. Microbiol.* 73, 7664–7679. doi: 10.1128/AEM.01272-07

Moon, J. H., Hirose, N., Yoon, J. H., and Pang, I. C. (2009). Effect of the along-strait wind on the volume transport through the Tsushima/Korea strait in September. *J. oceanography* 65, 17–29. doi: 10.1007/s10872-009-0002-3

Moon, J.-H., Kim, T., Son, Y. B., Hong, J.-S., Lee, J.-H., Chang, P.-H., et al. (2019). Contribution of low-salinity water to sea surface warming of the East China Sea in the summer of 2016. *Prog. oceanography* 175, 68–80. doi: 10.1016/j.pocean.2019.03.012

Moon, C. H., Yang, H. S., and Lee, K. W. (1996). Regeneration processes of nutrients in the polar front area of the East Sea 1. relationships between water mass and nutrient distribution pattern in autumn. *Korean J. Fisheries Aquat. Sci.* 29 (4), 503–526.

Murillo, A. A., Ramírez-Flandes, S., Delong, E. F., and Ulloa, O. (2014). Enhanced metabolic versatility of planktonic sulfur-oxidizing γ-proteobacteria in an oxygen-deficient coastal ecosystem. *Front. Mar. Sci.* 1, 18. doi: 10.3389/fmars.2014.00018

Na, H., Isoda, Y., Kim, K., Kim, Y. H., and Lyu, S. J. (2009). Recent observations in the straits of the East/Japan Sea: a review of hydrography, currents and volume transports. *J. Mar. Syst.* 78, 200–205. doi: 10.1016/j.jmarsys.2009.02.018

Onitsuka, G., Yanagi, T., and Yoon, J. H. (2007). A numerical study on nutrient sources in the surface layer of the Japan Sea using a coupled physical-ecosystem model. *J. Geophysical Research: Oceans* 112, (C5). doi: 10.1029/2006JC003981

Parks, D. H., Tyson, G. W., Hugenholtz, P., and Beiko, R. G. (2014). STAMP: statistical analysis of taxonomic and functional profiles. *Bioinformatics* 30, 3123–3124. doi: 10.1093/bioinformatics/btu494

Phadtare, S., and Inouye, M. (2004). Genome-wide transcriptional analysis of the cold shock response in wild-type and cold-sensitive, quadruple-csp-deletion strains of escherichia coli. *J. bacteriology* 186, 7007–7014. doi: 10.1128/JB.186.20.7007-7014.2004

Phadtare, S., and Severinov, K. (2010). RNA Remodeling and gene regulation by cold shock proteins. *RNA Biol.* 7, 788–795. doi: 10.4161/rna.7.6.13482

Price, M. N., Dehal, P. S., and Arkin, A. P. (2009). FastTree: computing large minimum evolution trees with profiles instead of a distance matrix. *Mol. Biol. Evol.* 26, 1641–1650. doi: 10.1093/molbev/msp077

Rabus, R., Brüchert, V., Amann, J., and Könneke, M. (2002). Physiological response to temperature changes of the marine, sulfate-reducing bacterium desulfobacterium autotrophicum. *FEMS Microbiol. Ecol.* 42, 409–417. doi: 10.1111/j.1574-6941.2002.tb01030.x

Raes, E. J., Bodrossy, L., Van De Kamp, J., Bissett, A., Ostrowski, M., Brown, M. V., et al. (2018). Oceanographic boundaries constrain microbial diversity gradients in the south pacific ocean. *Proc. Natl. Acad. Sci.* 115, E8266–E8275. doi: 10.1073/pnas.1719335115

Randall-Goodwin, E., Meredith, M., Jenkins, A., Sherrell, R., and Abrahamsen, E. (2014). Water mass structure and freshwater distributions in the amundsen Sea polynya, Antarctica. *Elem Sci. Anth*. doi: 10.12952/journal.elementa.000065

Robador, A., Brüchert, V., and Jørgensen, B. B. (2009). The impact of temperature change on the activity and community composition of sulfate-reducing bacteria in arctic versus temperate marine sediments. *Environ. Microbiol.* 11, 1692–1703. doi: 10.1111/j.1462-2920.2009.01896.x

Seidel, L., Broman, E., Turner, S., Ståhle, M., and Dopson, M. (2021). Interplay between eutrophication and climate warming on bacterial communities in coastal sediments differs depending on water depth and oxygen history. *Sci. Rep.* 11 (1), 23384. doi: 10.1038/s41598-021-02725-x

Senjyu, T., Enomoto, H., Matsuno, T., and Matsui, S. (2006). Interannual salinity variations in the tsushima strait and its relation to the changjiang discharge. *J. Oceanography* 62, 681–692. doi: 10.1007/s10872-006-0086-y

Shade, A., Jones, S. E., and Mcmahon, K. D. (2008). The influence of habitat heterogeneity on freshwater bacterial community composition and dynamics. *Environ. Microbiol.* 10, 1057–1067. doi: 10.1111/j.1462-2920.2007.01527.x

Shim, M. J., and Yoon, Y. Y. (2021). Long-term variation of nitrate in the East Sea, Korea. *Environ. Monit. Assess.* 193, 1–13. doi: 10.1007/s10661-021-09425-z

Shon, D.-H., Shin, K.-S., Jang, P.-G., Kim, Y.-O., Chang, M., and Kim, W.-S. (2008). Effect of thermal stratification and mixing on phytoplankton community structure in the western channel of the Korea strait. *Ocean Polar Res.* 30, 261–275. doi: 10.4217/OPR.2008.30.3.261

Son, Y. B., and Choi, J. (2022). Mapping the changjiang diluted water in the East China Sea during summer over the a 10-year period summer season using GOCI satellite sensor data. *Front. Mar. Sci.* 9, 1024306.

Spencer-Cervato, C., and Thierstein, H. R. (1997). First appearance of globorotalia truncatulinoides: cladogenesis and immigration. *Mar. Micropaleontology* 30, 267–291. doi: 10.1016/S0377-8398(97)00004-2

Stocker, R. (2012). Marine microbes see a sea of gradients. *Science* 338, 628–633. doi: 10.1126/science.1208929

Teague, W. J., Ko, D. S., Jacobs, G. A., Perkins, H. T., Book, J. W., Smith, S. R., et al. (2006). Currents through the Korea/Tsushima strait: a review of LINKS observations. *Oceanography* 19 (3), 50. doi: 10.5670/oceanog.2006.43

Thangaraj, S., and Sun, J. (2021). Transcriptomic reprogramming of the oceanic diatom skeletonema dohrnii under warming ocean and acidification. *Environ. Microbiol.* 23, 980–995. doi: 10.1111/1462-2920.15248

Thompson, L. R., Williams, G. J., Haroon, M. F., Shibl, A., Larsen, P., Shorenstein, J., et al. (2017). Metagenomic covariation along densely sampled environmental gradients in the red Sea. *ISME J.* 11, 138–151. doi: 10.1038/ismej.2016.99

Tian, R., Hu, F., and Martin, J. (1993). Summer nutrient fronts in the changjiang (Yantze river) estuary. *Estuarine Coast. Shelf Sci.* 37, 27–41. doi: 10.1006/ecss.1993.1039

Tseng, C.-H., Chiang, P.-W., Lai, H.-C., Shiah, F.-K., Hsu, T.-C., Chen, Y.-L., et al. (2015). Prokaryotic assemblages and metagenomes in pelagic zones of the south China Sea. *BMC Genomics* 16, 1–16. doi: 10.1186/s12864-015-1434-3

Varela, M. M., Van Aken, H. M., Sintes, E., and Herndl, G. J. (2008). Latitudinal trends of crenarchaeota and bacteria in the meso-and bathypelagic water masses of the Eastern north Atlantic. *Environ. Microbiol.* 10, 110–124. doi: 10.1111/j.1462-2920.2007.01437.x

Venkatachalam, S., Ansorge, I. J., Mendes, A., Melato, L. I., Matcher, G. F., and Dorrington, R. A. (2017). A pivotal role for ocean eddies in the distribution of microbial communities across the Antarctic circumpolar current. *PloS One* 12, e0183400. doi: 10.1371/journal.pone.0183400

Walsh, E. A., Kirkpatrick, J. B., Rutherford, S. D., Smith, D. C., Sogin, M., and D'hondt, S. (2016). Bacterial diversity and community composition from seasurface to subseafloor. *ISME J.* 10, 979–989. doi: 10.1038/ismej.2015.175

Wang, Y., Hu, X., Sun, Y., and Wang, C. (2021a). Influence of the cold bottom water on taxonomic and functional composition and complexity of microbial communities in the southern yellow Sea during the summer. *Sci. Total Environ.* 759, 143496. doi: 10.1016/j.scitotenv.2020.143496

Wang, Y., Liao, S., Gai, Y., Liu, G., Jin, T., Liu, H., et al. (2021b). Metagenomic analysis reveals microbial community structure and metabolic potential for nitrogen acquisition in the oligotrophic surface water of the Indian ocean. *Front. Microbiol.* 12, 518865. doi: 10.3389/fmicb.2021.518865

Wemheuer, F., Taylor, J. A., Daniel, R., Johnston, E., Meinicke, P., Thomas, T., et al. (2020). Tax4Fun2: prediction of habitat-specific functional profiles and functional redundancy based on 16S rRNA gene sequences. *Environ. Microbiol.* 15 (1), 1–12. doi: 10.1186/s40793-020-00358-7

Yang, J.-S., Choi, H.-Y., Jeong, H.-J., Jeong, J.-Y., and Park, J.-K. (2000). The outbreak of red tides in the coastal waters off kohung, chonnam, Korea: 1. physical and chemical characteristics in 1997. *J. Of Korean Soc. Of Oceanography* 5, 16–26.

Yang, C., Yang, S., and Vigier, N. (2023). Li Isotopic variations of particulate non-silicate phases during estuarine water mixing. *Geochimica Cosmochimica Acta* 354, 229–239. doi: 10.1016/j.gca.2023.06.020

Yoon, J. N., Lee, M., Jin, H., Lim, Y. K., Ro, H., Park, Y. G., et al. (2022). Summer distributional characteristics of surface phytoplankton related with multiple environmental variables in the Korean coastal waters. *J. Mar. Sci. Eng.* 10 (7), 850. doi: 10.3390/jmse10070850

Yusof, N. A., Masnoddin, M., Charles, J., Thien, Y. Q., Nasib, F. N., Wong, C. M. V. L., et al. (2022). Can heat shock protein 70 (HSP70) serve as biomarkers in Antarctica for future ocean acidification, warming and salinity stress? *Polar Biol.* 45 (3), 371–394. doi: 10.1007/s00300-022-03006-7

Zäncker, B., Cunliffe, M., and Engel, A. (2018). Bacterial community composition in the sea surface microlayer off the Peruvian coast. *Front. Microbiol.* 9, 2699. doi: 10.3389/fmicb.2018.02699

Zarzycki, J., Brecht, V., Müller, M., and Fuchs, G. (2009). Identifying the missing steps of the autotrophic 3-hydroxypropionate CO2 fixation cycle in chloroflexus aurantiacus. *Proc. Natl. Acad. Sci.* 106, 21317–21322. doi: 10.1073/pnas.0908356106

Zhu, X.-G., Long, S. P., and Ort, D. R. (2010). Improving photosynthetic efficiency for greater yield. *Annu. Rev. Plant Biol.* 61, 235–261. doi: 10.1146/annurev-arplant-042809-112206

Zinser, E. R., Johnson, Z. I., Coe, A., Karaca, E., Veneziano, D., and Chisholm, S. W. J. (2007). Influence of light and temperature on prochlorococcus ecotype distributions in the Atlantic ocean. *Limnology Oceanography* 52, 2205–2220. doi: 10.4319/lo.2007.52.5.2205

Zorz, J., Willis, C., Comeau, A. M., Langille, M. G., Johnson, C. L., Li, W. K., et al. (2019). Drivers of regional bacterial community structure and diversity in the Northwest Atlantic ocean. *Front. Microbiol.* 10, 281. doi: 10.3389/fmicb.2019.00281

Zubkov, M. V., Fuchs, B. M., Tarran, G. A., Burkill, P. H., Amann, R. J. A., and Microbiology, E. (2003). High rate of uptake of organic nitrogen compounds by prochlorococcus cyanobacteria as a key to their dominance in oligotrophic oceanic waters. *Appl. Environ. Microbiol.* 69, 1299–1304. doi: 10.1128/AEM.69.2.1299-1304.2003

frontiers | Frontiers in Marine Science

TYPE Original Research
PUBLISHED 10 August 2023
DOI 10.3389/fmars.2023.1236609

OPEN ACCESS

EDITED BY
Meilin WU,
South China Sea Institute of Oceanology (CAS), China

REVIEWED BY
Xianbiao Lin,
Ocean University of China, China
Bin Yang,
Jiangsu Ocean University, China

*CORRESPONDENCE
Peng Zhang
zhangpeng@gdou.edu.cn

RECEIVED 08 June 2023
ACCEPTED 19 July 2023
PUBLISHED 10 August 2023

CITATION
He Y, Zhang P, Xu F, Zhao L and Zhang J (2023) Seasonal nutrients variation, eutrophication pattern, and Chlorophyll *a* response adjacent to Guangdong coastal water, China.
Front. Mar. Sci. 10:1236609.
doi: 10.3389/fmars.2023.1236609

Seasonal nutrients variation, eutrophication pattern, and Chlorophyll *a* response adjacent to Guangdong coastal water, China

Yingxian He, Peng Zhang*, Fang Xu, Lirong Zhao and Jibiao Zhang

College of Chemistry and Environmental Science, Guangdong Ocean University, Zhanjiang, Guangdong, China

Nutrients were the key biogenic elements for the primary production in coastal water, and the increase of nutrient concentration led to eutrophication and frequent occurrence of harmful algal blooms. However, the seasonal nutrients variation, eutrophication pattern, and Chlorophyll *a* (Chl-*a*) response adjacent to Guangdong coastal water were still scarcely. In this study, to clarity the seasonal nutrients variation, eutrophication pattern, and Chl-*a*, response adjacent to coastal water, the spatiotemporal dissolved inorganic nitrogen (DIN) and phosphorus (DIP) patterns and Chl-*a* were explored by field observation using 52 stations in the coastal waters of Guangdong Province during the dry (April and May), wet (July and August) and normal (October and November) seasons in 2020. The results showed that the variability of Chl-*a*, DIN and DIP were significantly different in seasons ($P<0.01$), and the mean concentrations of Chl-*a*, DIN and DIP were 11.97 ± 28.12 μg/L, 25.84 ± 35.72 μmol/L and 0.59 ± 0.71 μmol/L.Among them, the mean value of Chl-*a* increased significantly from 9.99 ± 9.84 μg/L in the dry season to 18.28 ± 38.07 μg/L in the wet season, and then decreased significantly to 7.65 ± 27.64 μg/L in the normal season.The mean DIN value decreased significantly from 30.68 ± 43.58 μmol/L in the dry season to 21.91 ± 35.45 μmol/L in the wet season, and then increased to 24.91 ± 26.12 μmol/L in the normal season. the mean DIP value decreased from 0.58 ± 0.73 μmol/L in the dry season to 0.48 ± 0.65 μmol/L in the wet season and then increased significantly to 0.70 ± 0.73μmol/L in the normal season. In addition, the DIN and DIP concentrations at most monitoring stations met the Grade II national seawater quality standards, and only a few monitoring stations fail to meet the Grade IV national seawater quality standard. The DIN/DIP ratios ranged from 2.05 to 259.47, with an average of 43.77 ± 41.01, far exceeding the Redfield ratio, indicating the presence of P limitation in the nearshore waters of Guangdong Province. Besides, the EI values in the coastal waters of Guangdong Province are higher at 0.00 and 82.51, with an average of 4.16 ± 10.90. DIN and DIP were significantly and positively correlated with COD in each season ($P<0.05$). Moreover, DIN/DIP showed significantly positive correlations with Chl-*a* in all

seasons (P<0.01), indicating that high Chl-*a* concentrations could be sustained by the nutrients supply in marine ecosystems. Therefore, it is necessary to strengthen the integrated management of land and sea and effectively mitigate regional estuarine and coastal water eutrophication and harmful algal blooms.

KEYWORDS

nutrients, eutrophication pattern, chlorophyll *a*, coastal water, Guangdong

1 Introduction

The oceans cover 71% of the Earth's surface area, and marine primary productivity is an important foundation of marine ecosystems. Phytoplankton in the ocean are one of the primary producers of the ocean. They use light energy to absorb nutrients from seawater and convert inorganic carbon into organic carbon, while releasing oxygen, thus directly or indirectly providing the material base on which other organisms in the ocean depend. Chlorophyll *a* (Chl-*a*) in phytoplankton is an important indicator to monitor changes in phytoplankton abundance and also an important indicator of the degree of nutrient pollution of seawater. Therefore, accurate analysis and study of the variation of Chl-*a* in seawater plays a crucial role in exploring the phenomenon of eutrophication in the ocean. (Field et al., 1998; Falkowski et al., 2008; Lie et al., 2011; Aranguren-Gassis et al., 2019).

Nitrogen and phosphorus from seawater are essential nutrients for marine phytoplankton in coastal waters. At the same time, they are also the basis of marine primary productivity and the food chain.(Howarth, 2009; Butusov et al., 2013). Meanwhile, nitrogen and phosphorus in seawater are limiting nutrients for phytoplankton, and their concentration and composition directly affect the species, quantity and disteibution of phytoplankton. (Abell et al., 2010; Paerl et al., 2011; Paerl et al., 2016; Schindler et al., 2016; Smith et al., 2017; Yuan et al., 2018). The distribution and transformation of nitrogen and phosphorus elements in the ocean have been the main sources of nutrients in the ocean, including rivers, atmospheric deposition, and sediment release, and play a very important role in nutrient balance and dynamics (Liu J, et al., 2022). The growth of phytoplankton is closely related to the nutrient salts in seawater, and the concentration of Chl-*a* also changes with the nutrient salt concentration in seawater. Insufficient nutrient salts will limit the production of phytoplankton, leading to a subsequent decrease in the Chl-*a* concentration in seawater, which affects the primary productivity of the ocean; while too high a level of nutrient salt concentration tends to increase the Chl-*a* concentration, thus causing eutrophication and serious harm to the marine ecosystem.(Justi et al., 1995). At the same time, the nutrient ratio also has an effect on the concentration of Chl-*a* in seawater (Wang et al., 2015; Wang et al., 2017; Zou et al., 2022).With the development of human life science and technology production, the input of land-based sources of pollutants has an increasing impact on the marine environment, and one of the most serious problems facing mankind at present is the eutrophication of coastal waters (Philippart et al., 2007; Beusekom et al., 2019; Ibáñez and penuelas, 2019). Eutrophication of water resources refers to the phenomenon that under the influence of human activities, a large amount of nitrogen, phosphorus and other nutrients required by organisms enter slow-flowing water bodies such as lakes, rivers and bays, causing rapid reproduction of algae and other planktonic organisms, a decrease in dissolved oxygen in water bodies, deterioration of water quality, and the death of fish and other organisms in large quantities (Conley et al., 2009; Li et al., 2022). It is usually associated with an increase in nutrient concentrations in the water column (Hoyer et al., 2002; Mourão et al., 2020). Regionally, oceans with different characteristics also exhibit different nutrient distribution characteristics due to current current movements and biological activities (Pan et al., 2003). Meanwhile, Chl-*a* production and primary productivity of phytoplankton can directly reflect the degree of eutrophication in water bodies (Qin et al., 2013; Li et al., 2016).

Currently, eutrophication was one of the main issues in worldwide coastal waters. (Yu et al., 2018; Zhang C, et al., 2020). In addition, harmful algal blooms will persist in Chinese coastal waters because the water bodies are disturbed by nutrient imbalance (Zhen et al., 2017; Huang et al., 2018; Wu et al., 2022). It has been shown that, based on historical observations, eutrophication has led to a dramatic increase in microalgal biomass and a decrease in diatom-methanotrophic ratios in the East China Sea, especially in the spring; and that eutrophication has played an important role in multiple harmful algal bloom events in the Bohai Sea, both in the bays and near the estuaries (Zhou et al., 2022; Li et al., 2023; Wang et al., 2023). Thus, eutrophication is one of the most prominent environmental problems in China's coastal waters (Vaquer-Sunyer and Duarte, 2008; Li et al., 2013). The input of pollutants from land-based sources to offshore waters is increasing day by day (Niu et al., 2020). For example, the water quality of offshore waters in Bohai Bay in Tianjin is polluted, and the increase of land-based pollutants entering offshore waters along with surface runoff is the main reason (Guo et al., 2005; Liu et al., 2019); the water quality near the estuary in shallow waters of Liaodong Bay is poor (Pei et al., 2019); the distribution of pollutants in offshore waters in Shandong is increasing from the far shore to the near shore, and eutrophication is serious(Yang et al., 2020); the water quality

condition of offshore seawater in Lianyungang, Jiangsu shows that the water quality condition in the region is seriously affected by human activities (Wang et al., 2011; Wang et al., 2022). The Yangtze estuary is not only the locomotive of economic development affecting China, but also a key area of coastal pollution (Cui and Xian, 2018). Although the problems caused by pollution of sediment, heavy metals, ecological environment, red tide and other major chemical pollutants in the nearshore coastal seawater of Guangdong Province have been widely reported in the literature (Zhang L, et al., 2020; Liu Y, et al., 2022), the eutrophication studies in Guangdong Province are mainly focused on the coastal waters of the Pearl River Estuary. (Huang et al., 2003; Shi et al., 2017; Chen et al., 2023), and the spatial and temporal distribution of nutrients and eutrophication of water bodies in the whole Guangdong Province coastal water are scarcely understood.

With the rapid social and economic development, human activities such as land-based pollutant discharge and marine aquaculture in coastal areas of Guangdong Province are expanding. The ecological and environmental problems associated with eutrophication are (Ke et al., 2023) still to be solved. In this paper, we analyze the survey data of Guangdong near-shore coastal areas in 2020 to understand the water quality of Guangdong near-shore waters by analyzing the observation data of three water seasons: normal season, wet season and dry season. Therefore, the objectives of this study are (1) to elucidate the spatial and temporal patterns of nutrients and Chl-*a* response associated with coastal waters of Guangdong Province, (2) to determine the degree of eutrophication by eutrophication index (EI), and (3) to identify the relationships between dissolved inorganic nitrogen (DIN), phosphorus (DIP), and EI and control factors in different seasons, (4) to explore the effect of seasonal changes in nutrients on Chl-*a*.The results of the study can provide basic data accumulation for the effective control of eutrophication marine environmental problems in local nearshore seawater in Guangdong Province, and provide scientific basis for the comprehensive management of nearshore coastal environment in Guangdong Province in the future.

2 Materials and methods

2.1 Study areas

Guangdong Province is located in the southern Nanling Mountains, along the South China Sea coast, bordering Guangxi, Hunan, Jiangxi, Fujian, Hong Kong, and Macau, and facing Hainan across the Qiongzhou Strait (Song et al., 2022). Meanwhile, Guangdong Province is located in the southeastern part of the coastal economic zone, south of the South China Sea, with a sea area of 419,300 square kilometers, making it a large marine economic province in China (Figure 1A). Located between latitude 20°09′~25°31′ North and longitude 109°45′~117°20′ East, it has a vast land

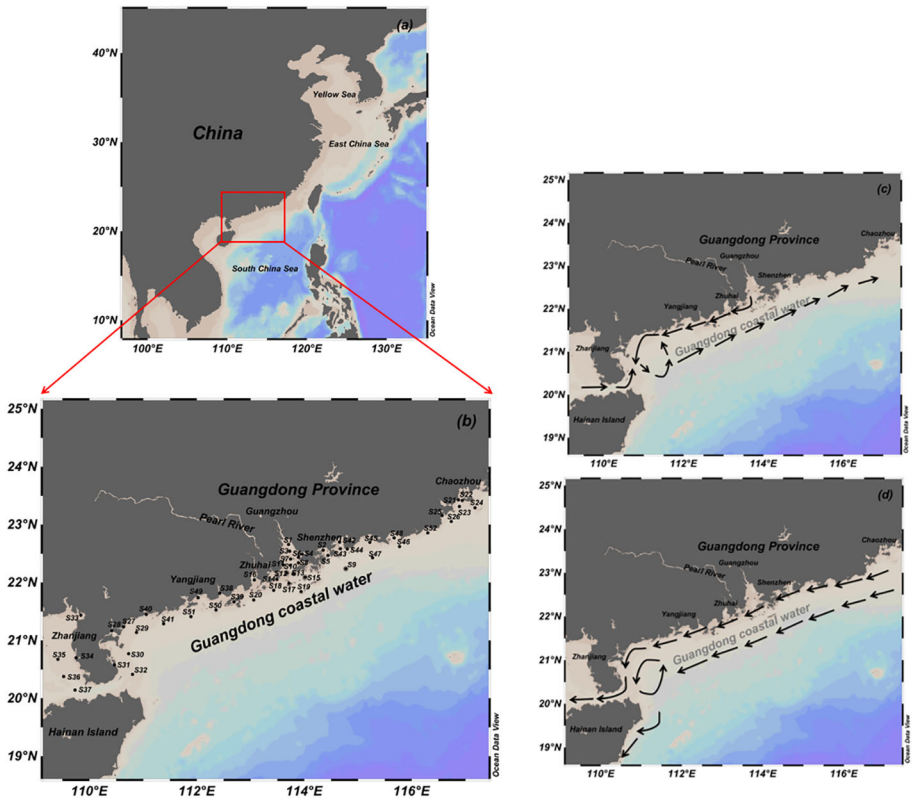

FIGURE 1
Research areas **(A)** and monitoring stations **(B)** in coastal waters of Guangdong Province, and the direction of ocean currents in summer **(C)** and winter **(D)**. (Wei et al., 2020).

area of 179,800km^2. The climate of the offshore waters of Guangdong Province belongs to the subtropical monsoon climate. The direction of the sea currents in the coastal waters of Guangdong Province changes in different seasons. Generally speaking, in summer, due to the influence of the monsoon, the currents mainly flow from south to north, while in winter, the monsoon is reversed, resulting in a corresponding change in the direction of the currents, which mainly blow from the north to the South China Sea (Figures 1C, D). In the spring and fall seasons, the alternation of the northeast monsoon and southwest monsoon brings about changes in the direction and strength of the currents, which may show a more complex distribution of flow direction and speed. However, the currents may also be affected by other factors, such as typhoons, tides, land runoff and so on (Qian et al., 2014; Wei et al., 2020). The total length of the mainland coastline is 4114km, and the marine resources are abundant. According to the Guangdong Yearbook, there are 714 species of marine organisms in Guangdong waters, including 187 species of phytoplankton, 319 species of zooplankton, 175 species of benthic and intertidal organisms, 24 species of reef-building stony corals, and 9 species of coral reef fish. Zhuhai, Guangdong Province, has 147 islands, one of the cities with more islands in China. since the 1970s, with the high economic development and population density of Guangdong, the degree of pollution of Guangdong's offshore waters has been increasing. Among them, the Pearl River estuary is the most polluted sea area, the rising trend of pollution is more obvious, and the seawater eutrophication is serious (Ke et al., 2022).

2.2 Data sources and laboratory analysis

Monitoring data from the Guangdong Provincial Department of Ecological and Environmental Protection (http://gdee.gd.gov.cn/) in 2020 for the offshore waters of Guangdong Province were the source of data for the analysis and study in this paper. Water flow seasons were sampled during the dry, wet and normal seasons in 2020 according to seasonal hydrological changes (Ministry of Environmental Protection of the People's Republic of China, 2002). April and May during the monitoring period represent the dry season, July and August represent the wet season, and October and November are the normal seasons. In order to ensure the comparability of data among the three water seasons, monitoring data from 52 common station monitoring stations were used in this paper (Figure 1B).

After the sample were collected, they were first filtered through acetate filter membrane with a pore size of 0.45 μm. The filters need to be rinsed with pure water before use (China National Standardization Management Committee, 2007). Water samples were frozen at - 20°C prior to chemical analysis. In this study, DIN included NO_3^-N, NO_2^-N, NH_4^+N, and PO_4^{3}–P was considered as DIP (Sun et al., 2021). In the laboratory analysis, where Chl-*a*, NO_3^-N, NO_2^-N, NH_4^+N, and DIP were analyzed by Spectrophotometric method (Chen et al., 2016), sodium hypobromite oxidation method, diazo-diazo method, respectively. zinc- cadmium reduction method (Wang et al., 2022; Lu et al., 2023), and phosphorus-molybdenum blue method (Murphy and Riley, 1962; Mariko et al., 2018). The detection limit of Chl-*a* was 0.04 mg/L; the detection limit of NO_3^-N, NO_2^-N and PO_4^{3}–P was 0.02 μmol/L; the detection limit of NH_4^+N was 0.03 μmol/L.The relative standard deviations of the selected samples were determined by the standard colorimetric method described in the Specifications for Marine Investigations (China National Standardization Administration, 2007). The relative standard deviations (RSDs) of the selected samples were< 5% for repeated determinations (China National Standardization Administration, 2007). Details of the analytical methods, procedures and instrumentation in this study have been described in the Specifications for Marine Investigations (China National Standardization Administration Committee, 2007).

2.3 Data processing and statistical analysis

2.3.1 Water quality and eutrophication evaluation methods

According to the evaluation method of seawater quality, DIN and DIP pollution evaluation usually uses the single factor pollution index (P_i) method (Zhou and Cai, 1998; Ming et al., 2010). And its calculation formula is as follows:

$$P_i = C_i / S_i \tag{1}$$

Where (1): C_i and S_i are DIN and DIP measured data and Chinese national seawater quality standard values based on marine functional zoning, respectively. When P_i>1, it is regarded as exceeding the standard water quality, and the water body has been polluted; when P_i<1, it indicates that the water body is not polluted, and the degree of pollution of the water body increases with the increase of P_i value.

In addition, to determine the number of monitoring stations with higher DIN and DIP pollution patterns in coastal waters in each season, the exceedance rate (%) was introduced, which is expressed as:

$$Over - standard\ rate\text{-}\ \%\ \text{-} = \frac{N_i}{\sum N_i} \times 100\ \% \tag{2}$$

Where (2): N_i and ΣN_i are the number of coastal water monitoring stations with high DIN and DIP concentrations in coastal waters of Guangdong (P_i > 1) and the total number of monitoring stations by season, respectively (Ministry of Environmental Protection of the People's Republic of China, 2009).

In order to comprehensively evaluate the degree of eutrophication in the near-shore waters of Guangdong Province, this paper applies the integrated index method to calculate the eutrophication index (EI) of the surveyed waters based on DIN, DIP and COD survey data (Quan et al., 2005; Zou et al.,1983; Chen et al., 2016). And its calculation formula is as follows:

$$EI = \frac{C_{COD} \times C_{DIN} \times C_{DIP}}{4500} \times 10^6 \tag{3}$$

Where (3): C_{COD}, C_{DIN} and C_{DIP} are the concentrations of COD, DIN and DIP respectively (unit is mg/L). When the index

EI≥1, it means that the sea water body is eutrophic, and the larger the EI value is, the more serious the eutrophication is.

2.3.2 Data processing and analysis

This paper uses the geographic information system ArcGIS (10.2) to draw a schematic diagram of monitoring stations in Guangdong Province; uses Excel software to process data, and Ocean Data View (4.0) software to draw spatial distribution maps of Chl-*a*, DIN, DIP concentration, nitrogen/phosphorus ratio N/P and eutrophication index EI; and uses Origin (2021) software to draw coastal Guangdong Province monitoring stations of the water quality exceedance rate, and the correlation heat map of the relationship between DIN, DIP and EI and control factors; The data were first tested for normal distribution in SPSS software, ($P<0.05$) and the results obtained clearly did not conform to normal distribution, and then non-parametric tests (Kruskal-Wallis test) were used to assess the significant differences in seasonal variations, as well as Spearman's correlation significance test for the impact factors of nutrients to test the statistical differences in the data.The data in this paper are expressed using the arithmetic mean ± standard deviation (Mean ± SD).

3 Results

3.1 Seasonal Chl-*a* variation in coastal waters of Guangdong Province

There were significant seasonal differences in Chl-*a* concentrations in coastal waters of Guangdong Province ($P<0.01$). During the survey period, the average concentration of Chl-*a* in the coastal waters of Guangdong Province was 11.97 ± 28.12 μg/L, with a concentration range of 0.18-218.40 μg/L.From a temporal perspective, the average concentration of Chl-*a* in the three water seasons was 9.99 ± 9.84 μg/L in the dry season, with a concentration range of 1.22-36.04 μg/L; The average concentration of Chl-*a* in the wet season was 18.28 ± 38.07 μg/L, with a concentration range of 0.18-218.40 μg/L; The average concentration of Chl-*a* in the normal season was 7.65 ± 27.64μg/L, and the concentration range was 0.22-202.80μg/L.Upon comparison, the average Chl-*a* concentration was the highest in the nearshore waters of Guangdong Province during the wet season, and its Chl-*a* concentration showed a trend of increasing and then decreasing from the dry season to the normal season. In terms of spatial distribution, during the dry season, the highest Chl-*a* concentration was found in the waters near Zhanjiang City, at Station 33, at 36.04 μg/L. This was followed by the waters near Zhuhai City (Figure 2A). During the wet season, Chl-*a* concentrations were higher in Zhanjiang City, Yangjiang City and the outer locations of the Pearl River Estuary, which highest Chl-*a* concentrations were found at Station 8 near Shenzhen City with up to 218.40 μg/L (Figure 2B). During the normal season, the waters with high Chl-*a* concentrations were mainly concentrated near Yangjiang City, where the highest recorded in the season occurred at Station 49. While all other areas were at low levels (Figure 2C).

3.2 Spatiotemporal variation of DIN concentration in coastal waters of Guangdong Province

There were significantly seasonal differences in DIN concentrations in coastal waters of Guangdong Province ($P<0.01$). During the survey period, the average concentration of dissolved inorganic nitrogen DIN in the coastal waters of Guangdong Province was 25.84 ± 35.72μmol/L, with a concentration range of 0.29-231.21μmol/L. From the perspective of time, in the three water seasons, the average concentration of DIN in the dry season was 30.68 ± 43.58μmol/L, and the concentration range was 0.29-231.21μmol/L; the average concentration of DIN in the wet season was 21.91 ± 35.45μmol/L, and the concentration range was 0.35-127.30μmol/L; the average concentration of DIN in the normal season was 24.91 ± 26.12μmol/L, and the concentration range was 2.11-99.21μmol/L. By comparison, the average concentration of DIN in the dry season was higher in the coastal waters of Guangdong Province. However, the distribution of DIN concentration from the dry season to the normal season showed a trend of first decreasing and then increasing. From the perspective of spatial distribution, the horizontal distribution of DIN concentration in all three seasons showed decreasing near-shore to far-shore, with the Pearl River port as the center and decreasing outward concentration (Figure 3). During the dry period, the high DIN concentration was mainly concentrated in the location of the Pearl River estuary, and the highest level was recorded at the Station 1 in its nearby waters (Figure 3A); while in the wet season, the DIN concentration at each station was generally lower than that in the dry season. During the period of wet water, in addition to the high DIN pollution concentration in the Pearl River Estuary, the DIN concentration in the sea near Zhuhai, Jiangmen, Yangjiang and Zhanjiang is also high compared to other stations (Figure 3B). In the normal season, the distribution of DIN concentration is basically the same as that in the wet season, but the distribution range of high DIN concentration is much smaller than that in the wet season (Figure 3C).

3.3 Spatial and temporal variation of DIP concentration in coastal waters of Guangdong Province

There were significantly seasonal differences in DIP concentrations in coastal waters of Guangdong Province ($P<0.01$). During the survey period, the average concentration of dissolved inorganic phosphorus DIP in the coastal waters of Guangdong Province was 0.59 ± 0.71μmol/L, with a concentration range of 0.01-3.65μmol/L. From a temporal perspective, in the three water seasons, the average concentration of DIP in the dry season was 0.58 ± 0.73μmol/L, with a concentration range of 0.09-3.23μmol/L; The average concentration of DIP during the wet season was 0.48 ± 0.65μmol/L, with the concentration range of 0.06-3.10μmol/L; the average concentration of DIP during the normal season was 0.70 ± 0.73μmol/L, with the concentration range of 0.01-3.65μmol/L. By comparison, the average concentration of DIP during the normal season was the highest in the coastal waters of Guangdong Province, and the concentration of DIP from the dry season to the normal

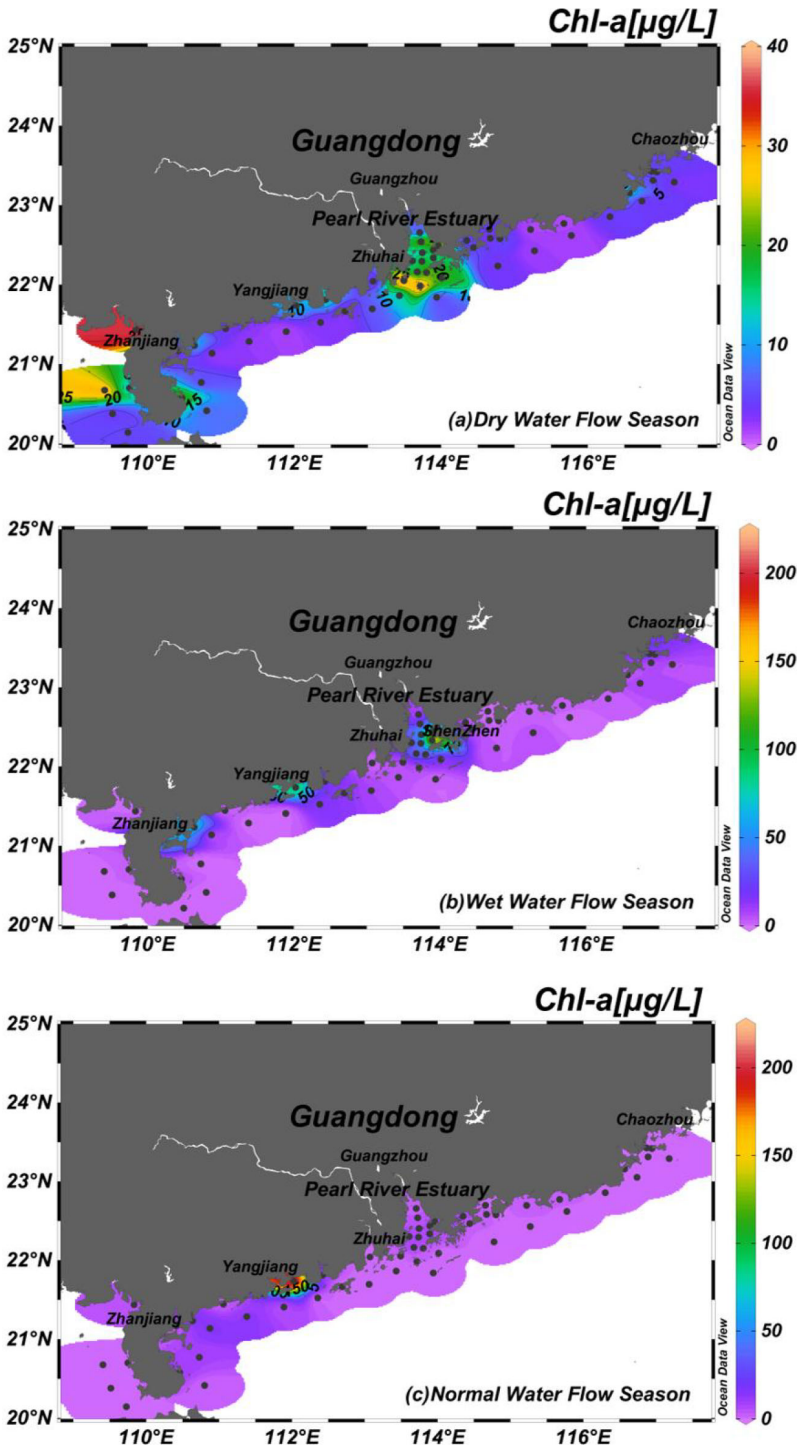

FIGURE 2
Spatiotemporal variation of Chl-*a* concentration during the dry season **(A)**, wet season **(B)**, and normal season **(C)** in the Guangdong coastal water.

season showed a first decrease and then increase. The DIP concentration from the dry season to the normal season showed a trend of decreasing and then increasing, and the DIP concentration in the normal was higher than the DIP concentration in the dry season. In the dry season, the high DIP concentrations were mainly concentrated in the waters near the Pearl River Estuary and Zhanjiang City (Figure 4A); while in the wet season, the DIP concentrations at all stations were generally lower than those in the dry season (Figure 4B). During the normal period, the highest value of DIP concentration appeared in the sea near Zhanjiang City, where the highest record was obtained at Station 28, up to 3.65 μmol/L, followed by the location of the Pearl River Estuary (Figure 4C).

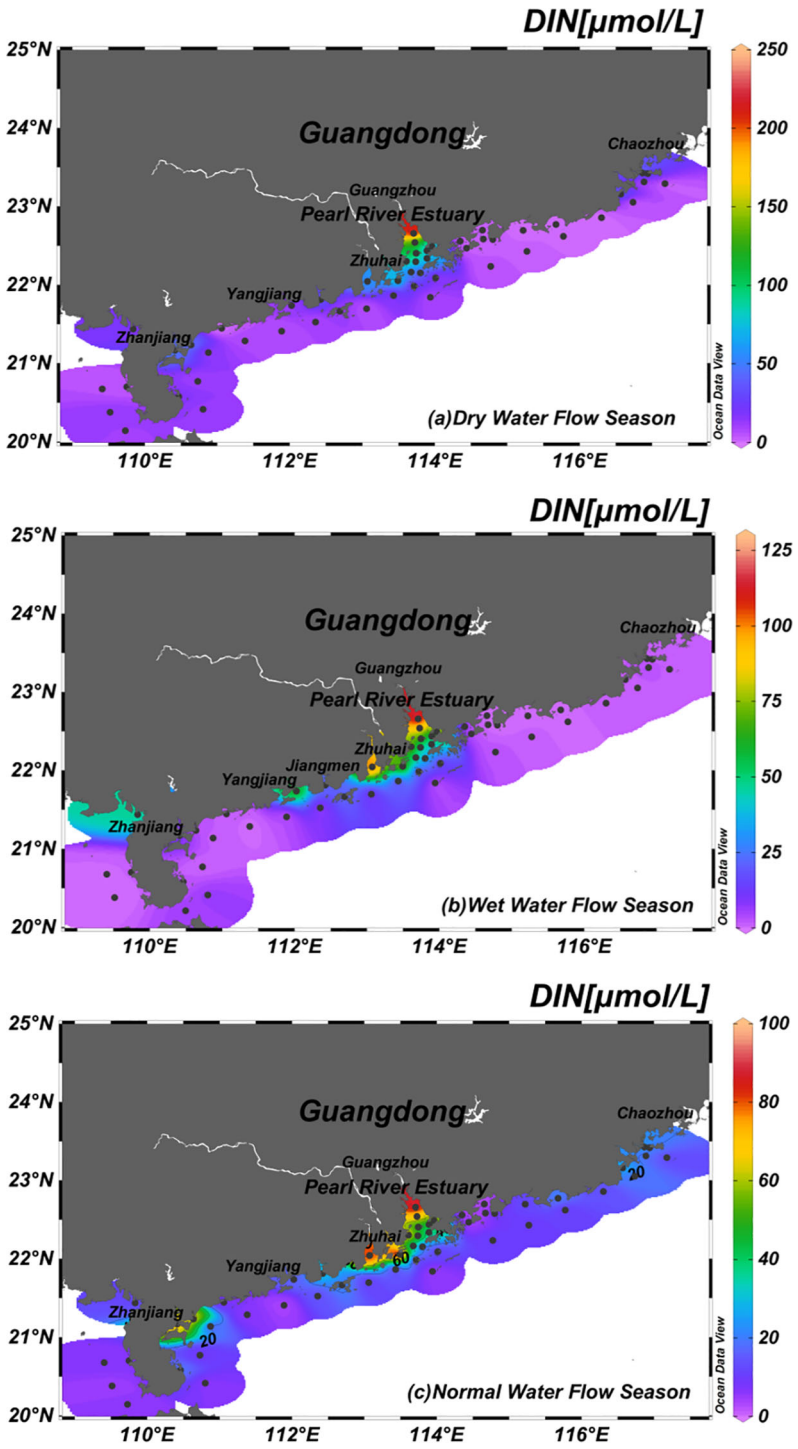

FIGURE 3
Spatiotemporal variation of DIN concentration during the dry season **(A)**, wet season **(B)**, and normal season **(C)** in the Guangdong coastal water.

3.4 Spatial and temporal variation of DIN/DIP in coastal waters of Guangdong Province

There was a significant difference in DIN/DIP in seasonal coastal waters of Guangdong Province ($P<0.05$). During the survey period, the DIN/DIP in the nearshore waters of Guangdong Province fluctuated between 2.05 and 259.47 with a mean value of 43.77 ± 41.01. The mean value of DIN/DIP in the coastal waters of Guangdong Province decreased from 49.52 ± 41.50 in the dry season to 37.13 ± 42.38 in the wet season, and then increased significantly to 44.65 ± 38.91 in the normal season. The DIN/DIP ranged from 3.05 to 259.47 during the dry season. The DIN/DIP ranged from 2.05 to 231.02 during the wet season and from 15.73 to

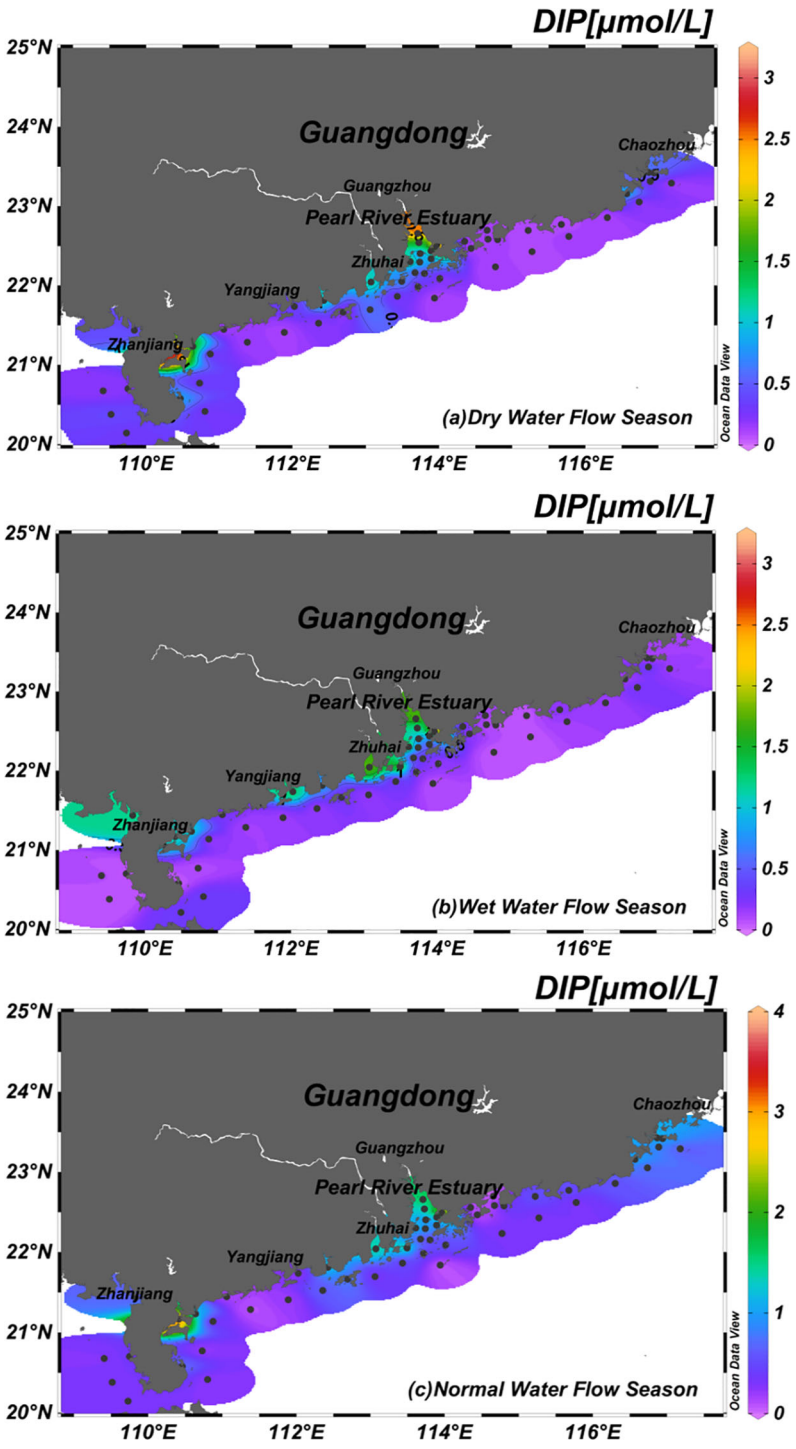

FIGURE 4
Spatiotemporal variation of DIP concentration during the dry season **(A)**, wet season **(B)**, and normal season **(C)** in the Guangdong coastal water.

238.04 during the normal season. Spatially, there were some differences in DIN/DIP in the nearshore waters of Guangdong (Figure 5). During the dry season, the proportion of DIN/DIP distribution was larger near the Pearl River Estuary and smaller away from the estuary. The highest value of DIN/DIP was found at the monitoring station near Shenzhen, which was Station 7, with a high value of 259.47. (Figure 5A). During the period of wet water, the range with higher DIN/DIP ratio was the sea area near Zhuhai city (Figure 5B). During the normal season, the range of higher DIN/DIP ratio is different from the dry and wet seasons, it occurs far from the Pearl River Estuary, and the highest record occurs near Shenzhen, specifically at Station 2, where the DIN/DIP is 238. 04. (Figure 5C).

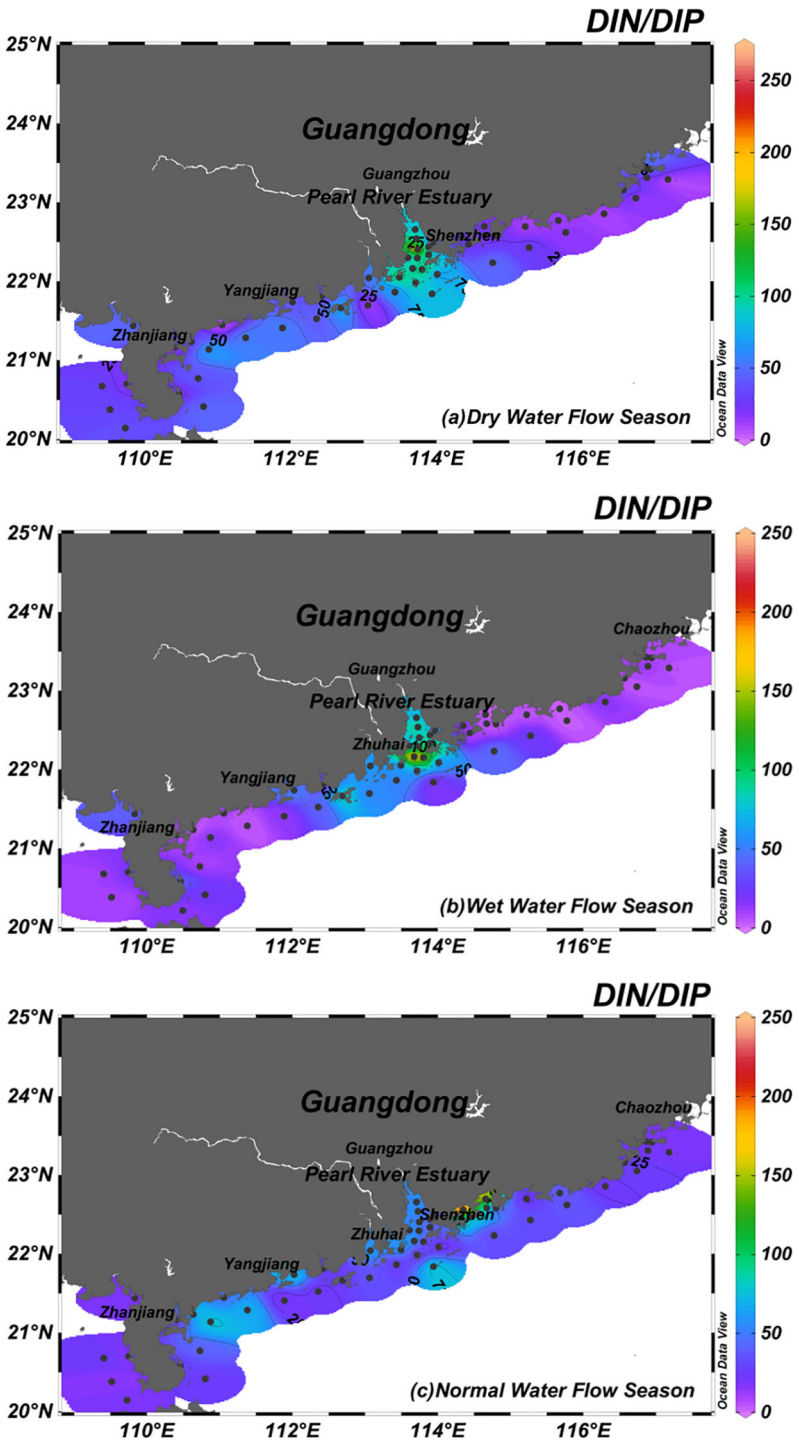

FIGURE 5
Spatiotemporal variation of DIN/DIP during the dry season **(A)**, wet season **(B)**, and normal season **(C)** in the Guangdong coastal water.

3.5 Spatial and temporal variation of EI in coastal waters of Guangdong Province

There were significantly seasonal differences in EI in coastal waters of Guangdong Province ($P<0.05$). During the survey period, the average EI of the three water periods in the nearshore waters of Guangdong was 4.16 ± 10.90, and the minimum and maximum values of EI were 0.00 and 82.51, respectively. The EI of the nearshore waters of Guangdong showed a decreasing trend from the dry season to the normal season. During the dry season, the range of EI in the coastal waters of Guangdong was 0.00-82.51, with a mean value of 5.93 ± 15.44; During the wet season, the range of EI in the coastal waters of Guangdong was 0.00-34.77, with a mean value of 3.93 ± 8.93; During the normal season, the range of EI in the coastal waters of Guangdong was 0.00-31.87, with a mean value of 2.63 ± 6.09; spatially, the EI in the offshore waters of Guangdong

showed significant differences (Figure 6). During the dry season, the EI was higher near the Pearl River Estuary, and the further away from the Pearl River Estuary, the lower the EI was (Figure 6A). During the wet season, its EI is smaller than that in the dry season. Except for the stations near the Pearl River Estuary, the EI of the waters near Zhanjiang City, Yangjiang City, Zhongshan City, Shenzhen City and Zhuhai City is relatively large (Figure 6B). Normal water period, its highest EI value appeared in the sea near Zhanjiang City, which is the Station 28 to obtain the highest record of this water period, up to 31.87, followed by higher EI in the sea near Zhongshan City and Zhuhai City (Figure 6C).

3.6 Seasonal relationships between DIN, DIP, EI and environmental factors

The Spearman correlation coefficients showed that the influencing factors of DIN, DIP and EI showed some seasonal variations in the

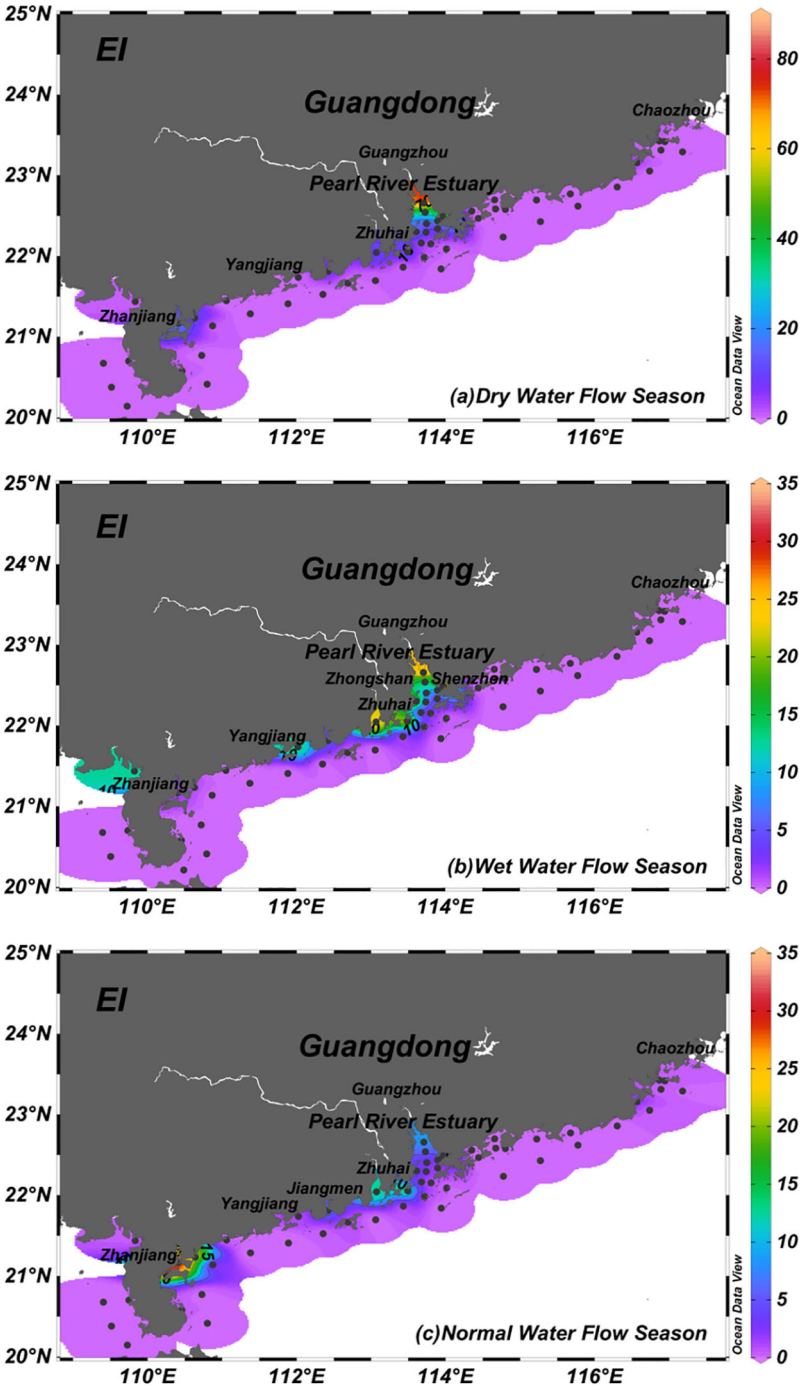

FIGURE 6
Spatiotemporal variation of EI during the dry season **(A)**, wet season **(B)**, and normal season **(C)** in the Guangdong coastal water.

nearshore waters of Guangdong Province (Figure 7). In the dry and wet water periods, DIN, DIP, EI and Chl-*a* were significantly positively correlated (P<0.01); while in the normal season (Figure 7C), EI and Chl-*a* were positively (Figures 7A, B) correlated (P<0.05), but DIN, DIP and Chl-*a* were not significantly correlated. In the three water periods, DIN, DIP, and EI were significantly negatively correlated with pH (P<0.01). In the wet season, DIN was significantly positively correlated with DO (P<0.05), except for the other water periods, the concentrations of DIN and DO were not correlated. Meanwhile, there was no significant correlation between DIP, EI and DO. DIN, DIP and EI were positively correlated with COD in all three water periods (P<0.05). The concentrations of DIN, DIP and EI were significantly positively correlated in all three water periods (P<0.01). In addition (Figure 7D), DIN, DIP and EI were significantly and positively correlated with suspended matter in all three water periods (P<0.01). DIN, DIP, and EI were positively correlated with petroleum during the

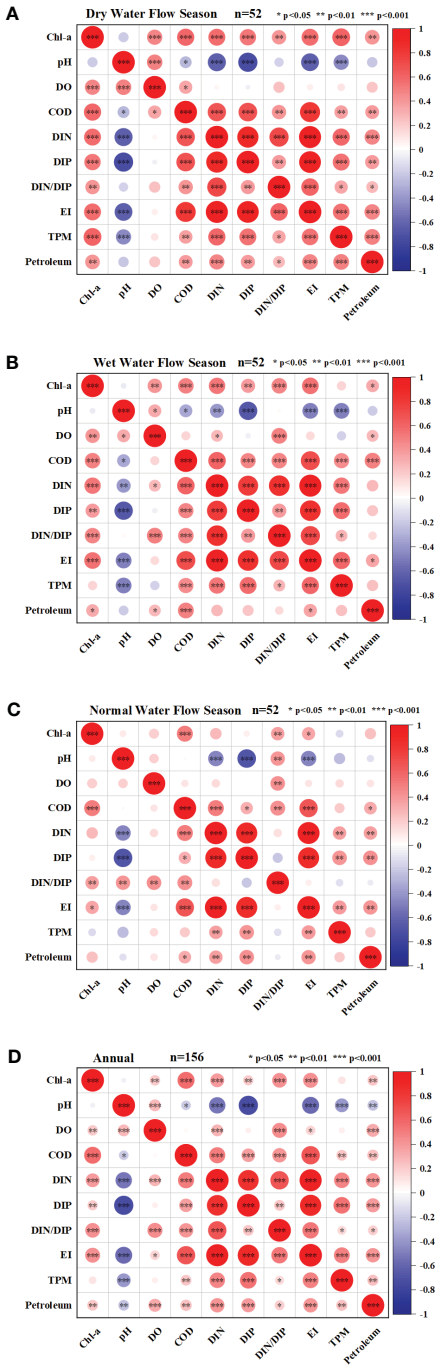

FIGURE 7
Correlation relationships among DIN, DIP, EI and environmental factors during the dry season **(A)**, wet season **(B)**, normal season **(C)** and annual **(D)** in Guangdong coastal waters. (n = 52).

dry and normal water periods (P<0.05). In addition, DIN/DIP was significantly and positively correlated with Chl-*a* in all three water periods (P<0.01) (Figure 7D).

4 Discussion

4.1 Comparison with global estuaries and coastal water

The data of nutrient content, DIN/DIP and EI are listed in this paper. However, in order to further elucidate the pollution levels of nutrients in the nearshore waters of Guangdong Province, it is necessary to compare the results of this study with those of other studies (Table 1). The DIN concentrations in the nearshore waters of Guangdong Province were higher than those previously reported in Hainan Island, Kaohsiung Harbor, Laizhou Bay, Qinzhou Gang, Weizhou Island, and Lianyungang (Chen et al., 2016; Ning et al., 2020; Zhang P, et al., 2020; Lu et al., 2022; Wang et al., 2022; Zhang M, et al., 2022), but lower than those in the Changjiang River, Mississippi River (Turner et al., 2007; Cui and Xian, 2018). However, the DIP concentrations were higher than those in Laizhou Bay, Weizhou Island and Lianyungang (Ning et al., 2020; Wang et al., 2022; Zhang M, et al., 2022), but lower than those in Kaohsiung Harbor, Qinzhou Gang, the Changjiang River and Mississippi River (Turner et al., 2007; Chen et al., 2016; Cui and Xian, 2018; Lu et al., 2022). The DIN/DIP was higher than the previously investigated Qinzhou Gang, Weizhou Island, Lianyungang, and Mississippi River (Turner et al., 2007; Ning et al., 2020; Lu et al., 2022; Wang et al., 2022), but lower than Laizhou Bay and the Changjiang River (Cui and Xian, 2018; Zhang M, et al., 2022). EI is higher than previously reported for Hainan Island, Kaohsiung Harbor Laizhou Bay, Lianyungang (Chen et al., 2016; Zhang P, et al., 2020; Wang et al., 2022; Zhang M, et al., 2022) and lower than the Changjiang River (Cui and Xian, 2018). In addition, the results showed that the DIN pollution level in offshore waters of Guangdong Province in 2020 was higher compared with other river estuaries, and the pollution level of DIP concentration is not low. And in general, the pollution level of DIN is higher than that of DIP. Therefore, DIN/DIP is much higher than 16 and higher than the DIN/DIP values of most other rivers. Besides, the mean value of EI is much lower than the Changjiang River and higher than other estuaries.

4.2 Seasonal DIN and DIP change pattern and eutrophication degree

According to the survey results, compared with the seawater quality standard, the percentage of the number of monitoring stations with DIN concentration exceeding the Grade IV seawater quality standard (DIN ≤ 35.71μmol/L) to the total number of monitoring stations was 28.85%, 19.23% and 23.08% in the dry season, wet season and normal season respectively (Figure 8A). In general, the level of DIN pollution in offshore waters of Guangdong Province is small. Mainly, the DIN concentration of most monitoring stations in the coastal waters of the Pearl River Estuary cannot reach the seawater quality standard of Grade IV or above (Shen et al., 2022), indicating that the coastal area of the Pearl River Estuary is seriously polluted. With the rapid socio-economic development, human activities such as land-based pollutant discharges, marine aquaculture and port shipping along the Pearl River Estuary are increasingly expanding, making the rivers along the Pearl River Estuary carry more nutrients. As a result, DIN concentrations at several monitoring stations in the area exceeded seawater quality standards (Li et al., 2020; Qian et al., 2022). In addition, DIN concentrations were highest during the dry season. Compared to the dry season, the average DIN concentrations in both the wet and normal season were significantly

TABLE 1 Comparison of the nutrient concentrations, EI and DIN/DIP in the coastal waters of Guangdong with global estuaries and coastal water.

Region	Time	DIN (μmol/L)	DIP (μmol/L)	DIN/DIP	EI	References
Hainan Island	2016	8.14 (0.57-27.5)	–	–	0.21 (0.00-3.94)	Zhang P, et al., 2020
Kaohsiung Harbor	2012	11.43 ± 7.86 (2.86-34.29)	5.81 ± 2.26 (1.94-15.16)	–	2.24-139.39	Chen et al., 2016
Laizhou Bay	2021	9.22-54.69	0.05 ± 0.04-0.32 ± 0.79	130.65	0.24-3.21	Zhang M, et al., 2022
Qinzhou Gang	2011-2017	20.1 ± 17.2	1.0 ± 0.9	43 ± 46	–	Lu et al., 2022
Weizhou Island	2018	3.84	0.24	16.0	–	Ning et al., 2020
Lianyungang	2016	10.71	0.42	15.1 (1.6-55)	0.6 (0.1-7.2)	Wang et al., 2022
the Changjiang River	2014	118.4	1.3	91.1	11.0	Cui and Xian, 2018
Mississippi River	1997-2006	99.6	2.6	38.31	–	Turner et al., 2007
Guangdong coastal water	2020	25.84 ± 35.72 (0.92-231.21)	0.59 ± 0.71 (0.01-3.65)	43.77 ± 41.01 (2.05-259.47)	4.16 ± 10.9 (0.00-82.51)	This study

"—" indicated not detected.

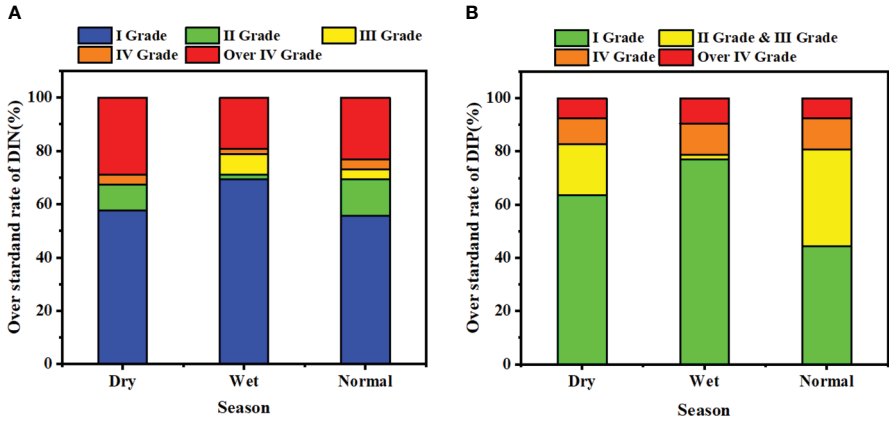

FIGURE 8
Over-standard rate of DIN **(A)** and DIP **(B)** in coastal water quality monitoring stations of Guangdong Province.

lower, because July and August are the rainy season, a high typhoon season, and constantly affected by the intrusion of rainwater, and the resuspended nutrients are quickly diluted.In addition, the temperature in the coastal water gradually increases and there is sufficient light, which is the peak period for algal growth during summer. As the temperature meets the conditions for rapid algal growth, the algae can absorb a large amount of nutrients from the water body while growing, resulting in a relatively low average DIN concentration during the wet period (Ke et al., 2022).

Compared with the national seawater quality standard, the percentage of the number of monitoring stations with DIP concentration exceeding the Grade IV seawater quality standard (DIP ≤ 1.45μmol/L) to the total number of monitoring stations was 7.69%, 9.62% and 7.69% in the dry season, wet season and normal season respectively (Figure 8B). In general, the level of DIP pollution in the offshore waters of Guangdong Province is small, and the DIP concentrations at most monitoring stations meet the seawater quality standard of Grade IV or higher, but there are still individual stations that do not meet the Grade IV standard. The average concentration of DIP is lowest during the wet season, which may be related to the frequent rainy season in July and August, when rainwater replenishes the sea and dilutes the concentration of DIP, or it may be caused by phytoplankton absorbing large amounts of nutrients from the seawater after heavy typhoon rains (Herbeck et al., 2011). The peak of DIP concentration occurs during the normal water period, which is due to the input of fresh water, domestic sewage and industrial wastewater from rivers with greater influence.

4.3 Key environmental factors affecting nutrient concentrations and composition in coastal waters of Guangdong Province

DIN and DIP were significantly negatively correlated with pH in all seasons (P<0.01). With the rapid development of industry in coastal areas, it has led to a great increase in the amount of CO_2 emitted into the atmosphere. The seawater absorbed a large amount of CO_2 from the air, which led to a decrease in the pH of seawater and the phenomenon of ocean acidification (Queré et al., 2014; Stocker, 2014; Rees et al., 2017). However, DIN and DIP were significantly and positively correlated with suspended matter in all seasons (P<0.01), which may be due to the fact that suspended matter in organic pollutants from land-based runoff carries a large amount of DIN and DIP. DIN and DIP were significantly and positively correlated with Chl-*a* in the dry and wet seasons (P<0.01), which may be due to the input of pollutants from land-based sources, promoting the rapid growth of phytoplankton (Han et al., 2023). DIN, DIP and COD are important indicators for evaluating coastal water quality (Ministry of Environmental Protection of the People's Republic of China, 1997) (Tu et al., 2022). In addition, DIN and DIP were significantly and positively correlated with COD in each season (P<0.01) because surface runoff in each season carried a large amount of pollutants of terrestrial origin, which provided a large amount of inorganic and nutrients for a large number of phytoplankton in the water column. DIN and DIP were significantly and positively correlated (P<0.01) with petroleum species during the dry and normal season, probably because DIP in surface seawater has the same source and fate as petroleum hydrocarbons.

Nutrients are important for the growth of phytoplankton. Phytoplankton in the ocean take up nutrients from seawater in a certain ratio, and this constant ratio becomes the Redfield (Turner et al., 2003). Under normal conditions, N:P is about 16. During the survey period, DIN/DIP values ranged from 2.05 to 259.47, with a mean value of 43.77 ± 41.01, which is much higher than the Redfield ratio. And DIN/DIP was significantly and positively correlated with Chl-*a* (p<0.01). High Chl-*a* concentrations can reflect the changes of nutrient content in marine ecosystems, and the extremely strong correlation between DIN/DIP and Chl-*a* indicates that the imbalance of nutrient ratios in coastal waters of Guangdong Province has led to the occurrence of harmful algal blooms, thus exacerbating the eutrophication phenomenon (Schlüter et al., 2000; Qiao et al., 2017). The DIN/DIP ratios in the dry and normal seasons were higher than those in the wet season, which was caused by the higher DIN concentration and relatively lower DIP concentration in the dry and normal season. As can be seen from Figure 5, the DIN/DIP values at the location of the Pearl River

Estuary were significantly higher, up to 259.47, indicating a serious imbalance in the nutrient composition of the offshore waters of the Pearl River Estuary, and the phenomenon of nutrient imbalance indicated that the discharge of industrial wastewater, domestic sewage and agricultural fertilizers near the Pearl River Estuary had a dynamic effect on the DIN/DIP values of the coastal waters. The eutrophication of nearshore water bodies in Guangdong Province is likely to continue due to the continued disturbance of nutrient ratios in these bodies (Wang et al., 2021).

4.4 Suggestions for effective mitigation of eutrophication in coastal waters of Guangdong Province

With rapid socio-economic development and rapid population growth, industrialization and urbanization have accelerated, human pursuit of material culture has been elevated and the scope of activities has been expanded, leading to a gradual increase in the discharge of nutrients imported from outside into water bodies. Under the implementation of the 14th Five-Year Plan for Marine Ecological Protection of Guangdong Province (Department of Ecological Environment in Guangdong Province, 2022), land-based pollutant inputs are reduced to improve water quality according to the characteristics of the near-shore waters of Guangdong Province.Combining the concentrations of Chl-*a*, DIN, DIP, and the DIN/DIP stoichiometry results, we found that the eutrophication of coastal waters in Guangdong Province is low, but the eutrophication problem is still prominent in local waters, especially in the Pearl River Estuary and the waters near Zhanjiang City (Ke et al., 2023). To reduce the eutrophication in coastal waters of Guangdong Province, firstly, numerical nutrient criteria for estuaries and adjacent coastal waters should be developed (Wu et al., 2010; Huo et al., 2018; Yang et al., 2019; Xie et al., 2021; Zhang P, et al., 2022). The application of nutrient standards is not only an effective measure to prevent eutrophication of water bodies, but also a scientific basis for comprehensive monitoring, evaluation and management of nutrients in estuaries. The government should strengthen the comprehensive control of eutrophic waters and the management related to the discharge of river pollutants into the sea. In the time scale, we need further monitor nutrients and Chl-*a* response in the ocean for a long time. Besides, considering the spatial and temporal differences of EI, it is necessary to investigate and analyze Chl-*a* and nutrients according to their distribution characteristics at different locations and times, and to implement suitable management measures.In addition, the publicity of river pollution prevention and control should be strengthened to raise citizens' awareness of coastal environmental protection participation. Integrated land and sea management of coastal water quality should be introduced in the future to control river and coastal water quality efficiently (Zeng-Lin et al., 2012; Gao et al., 2022).

5 Conclusion

Exploring the biogeochemical processes of nitrogen and phosphorus in the coastal waters of Guangdong Province is key to developing countermeasures to mitigate eutrophication. This study focuses on the spatial and temporal patterns of nutrients, their composition and their effects on mitigating eutrophication in the offshore waters of Guangdong Province. The results showed that the nutrients in 2020 showed seasonal variations, with DIN being highest in the dry season and DIP being highest in the normal season. In all seasons of the survey, DIN and DIP pollution levels were more severe in the vicinity of the Pearl River Estuary and Zhanjiang Bay than the other coastal water. Overall, based on the Redfield values, it can be seen that DIN concentrations are higher than DIP concentrations, indicating the presence of P limitation in the nearshore waters of Guangdong Province. The eutrophication index of seawater surface layer was significantly different among the three water seasons. The mean value of eutrophication index in the dry season was higher than that in the wet and normal seasons. In addition, nutrients and EI showed significantly positive correlations with COD($P<0.05$), as well as DIN/DIP was significantly and positively correlated with Chl-*a* ($p<0.01$), which indicated a direct relationship between eutrophication in the water column and the high input of nutrients. Therefore, controlling the input of total nitrogen and total phosphorus from land-based sources can effectively alleviate the eutrophication in the local coastal areas of Guangdong Province. In addition, harmful algal blooms may persist near the coastal waters of Guangdong Province due to the severely imbalanced nutrient ratios in the coastal water. Therefore, further research is needed on how to bring the heavily polluted coastal waters up to the relevant nutrient standards and ratios so as to effectively mitigate eutrophication and suppress harmful algal blooms.

Data availability statement

The original contributions presented in the study are included in the article/supplementary materials. Further inquiries can be directed to the corresponding author.

Author contributions

Conceptualization, PZ. Methodology, PZ and YH. Software, YH and FX. Validation, YH and FX. Formal analysis, YH and FX. Writing-original draft preparation, YH and PZ. Writing-review and editing, YH and PZ. Visualization, PZ, LZ and JZ. Supervision, PZ, LZ and JZ. Project management, PZ, LZ and JZ. Funding acquisition, PZ, LZ and JZ. All listed authors made substantial, direct, and intellectual contributions to the work and are approved for publication.

Funding

This research was financially supported by Research and Development Projects in Key Areas of Guangdong Province (2020B1111020004); the Guangdong Basic and Applied Basic Research Foundation (2023A1515012769); Guangdong Basic and Applied Basic Research Foundation (2020A1515110483); Key Laboratory of Marine Environmental Survey Technology and Application Ministry of Natural Resource, P.R. China (MESTA-2020-B014); Guangdong Ocean University Fund Project (R18021).

Acknowledgments

The authors are grateful for the reviewers' careful review and valuable suggestions to improve the manuscript.

Conflict of interest

The authors declare that the research was conducted in the absence of any commercial or financial relationships that could be construed as a potential conflict of interest.

Publisher's note

All claims expressed in this article are solely those of the authors and do not necessarily represent those of their affiliated organizations, or those of the publisher, the editors and the reviewers. Any product that may be evaluated in this article, or claim that may be made by its manufacturer, is not guaranteed or endorsed by the publisher.

References

Abell, J. M., Özkundakci, D., and Hamilton, D. P. (2010). Nitrogen and phosphorus limitation of phytoplankton growth in New Zealand lakes:implications for eutrophication control. *Ecosystems* 13, 966–977. doi: 10.1007/s10021-010-9367-9

Aranguren-Gassis, M., Kremer, C. T., Klausmeier, C. A., and Litchman, E. (2019). Nitrogen limitation inhibits marine diatom adaptation to high temperatures. *Ecol. Lett.* 22 (11), 1860–1869. doi: 10.1111/ele.13378

Beusekom, J., Carstensen, J., Dolch, T., Grage, A., and Ruiter, H. (2019). Wadden sea eutrophication: long-term trends and regional differences. *Front. Mar. Sci.* 6. doi: 10.3389/fmars.2019.00370

Butusov, M., Jernelöv, A., Butusov, M., and Jernelöv, A. (2013). Phosphorus in the organic life: cells, tissues, organisms. *Phosphorus: Element that could have been called Lucifer* 9, 13–17. doi: 10.1007/978-1-4614-6803-5_2

Chen, S., Chen, M., Wang, Z., Qiu, W., Wang, J., Shen, Y., et al. (2016). Toxicological effects of chlorpyrifos on growth, enzyme activity and chlorophyll a synthesis of freshwater microalgae. *Environ. Toxicol. Pharmacol.* 45, 179–186. doi: 10.1016/j.etap.2016.05.032

Chen, C. W., Ju, Y. R., Chen, C. F., and Dong, C. D. (2016). Evaluation of organic pollution and eutrophication status of kaohsiung harbor, Taiwan. *Int. Biodeterioration Biodegradation* 113, 318–324. doi: 10.1016/j.ibiod.2016.03.024

Chen, Y. L., Zhao, L. S., Zhou, A., and Shen, S. L. (2023). Evaluation of environmental impact of red tide around Pearl River Estuary,Guangdong, China. *Mar. Environ. Res.* 185, 105892. doi: 10.1016/j.marenvres.2023.105892

China National Standardization Management Committee (2007). *The Specification of Oceanographic Survey—Part 4: Survey of Chemical Parameters in Sea Water*.

Conley, D. J., Paerl, H. W., Howarth, R. W., Boesch, D. F., Seitzinger, S. P., Havens, K. E., et al. (2009). Controlling eutrophication: nitrogen and phosphorus. *Am. Assoc. Adv. Sci.* 323 (5917), 1014–10. doi: 10.1126/science.1167755

Cui, L., and Xian, W. (2018). Changjiang nutrient distribution and transportation and their impacts on the estuary. *Continental Shelf Res.* 165, 137–145. doi: 10.1016/j.csr.2018.05.001

Department of Ecological Environment in Guangdong Province. (2022). *In "14th fifive year plan" for marine ecological environment protection in guangdong province*. (Guangdong Province: Department of ecological environment), 1–40.

Falkowski, P., Fenchel, T., and Delong, E. F. (2008). The microbial engines that drive earth's biogeochemical cycles. *Am. Assoc. Adv. Sci.* 320 (5879), 1034–9. doi: 10.1126/science.1153213

Field, C. B., Behrenfeld, M. J., Randerson, J. T., and Falkowski, P. (1998). Primary production of the biosphere: integrating terrestrial and oceanic components. *Science* 281 (5374), 237–240. doi: 10.1126/science.281.5374.237

Gao, J., An, T., Shen, J., Zhang, K., Yin, Y., Zhao, R., et al. (2022). Development of a land-sea coordination degree index for coastal regions of China. *Ocean Coast. Manage.* 230, 106370. doi: 10.1016/j.ocecoaman.2022.106370

Guo, Q., Wang, X. L., Han, X. R., and Wang, J. T. (2005). Spatial distribution of cod and its contribution to the eutrophi-cation in bohai sea. *Mar. Sci.* 09, 73–77. doi: 10.1111/j.1745-7254.2005.00209.x

Han, H., Xiao, R., Gao, G., Yin, B., and Liang, S. (2023). Influence of a heavy rainfall event on nutrients and phytoplankton dynamics in a well-mixed semi-enclosed bay. *J. Hydrology* 617, 128932. doi: 10.1016/j.jhydrol.2022.128932

Herbeck, L. S., Unger, D., Krumme, U., Liu, S. M., and Jennerjahn, T. C. (2011). Typhoon-induced precipitation impact on nutrient and suspended matter dynamics of a tropical estuary affected by human activities in hainan, china. *Estuar. Coast. Shelf Sci.* 93 (4), 375–388. doi: 10.1016/j.ecss.2011.05.004

Howarth, R. W. (2009). Coastal nitrogen pollution: a review of sources and trends globally and regionally. *Harmful Algae* 8 (1), 14–20. doi: 10.1016/j.hal.2008.08.015

Hoyer, M. V., Frazer, T. K., Notestein, S. K., and Canfield, D. E. (2002). Nutrient, chlorophyll, and water clarity relationships in Florida's nearshore coastal waters with comparisons to freshwater lakes. *Can. J. Fisheries Aquat. Sci.* 59 (6), 1024–1031. doi: 10.1139/f02-077

Huang, X. P., Huang, L. M., and Yue, W. Z. (2003). The characteristics of nutrients and eutrophication in the pearl river estuary, south china. *Mar. pollut. Bull.* 47 (1–6), 30–36. doi: 10.1016/S0025-326X(02)00474-5

Huang, J., Zhang, Y., Gao, Qi, et al. (2018). When and where to reduce nutrient for controlling harmful algal blooms in large eutrophic lake chaohu, china? cological Indic. *Integrating Monit. Assess. Manage. Ecological Indicators.* 89, 808–817. doi: 10.1016/j.ecolind.2018.01.056

Huo, S., Ma, C., Xi, B., Zhang, Y., Wu, F., and Liu, H. (2018). Development of methods for establishing nutrient criteria in lakes and reservoirs: a review. *J. Environ. Sci.* 67 (05), 57–69. doi: 10.1016/j.jes.2017.07.013

Ibáñez, C., and Peñuelas, J. (2019). Changing nutrients, changing rivers. *Science* 365 (6454), 637–638. doi: 10.1126/science.aay2723

Justi, D., Rabalais, N. N., and Turner, R. E. (1995). Stoichiometric nutrient balance and origin of coastal eutrophication. *Mar. pollut. Bull.* 30 (1), 41–46. doi: 10.1016/0025-326X(94)00105-I

Ke, S., Zhang, P., Ou, S., Zhang, J., Chen, J., and Zhang, J. (2022). Spatiotemporal nutrient patterns, composition, and implications for eutrophication mitigation in the pearl river estuary, china. *Estuarine Coast. Shelf Sci.* 266, 107749– doi: 10.1016/j.ecss.2022.107749

Ke, S., Cai, Z., Zhang, P, Zhang, J., and Zhang, J. (2023). Effects of river input flux on spatiotemporal patterns of total nitrogen and phosphorus in the Pearl River Estuary, China. *Front. Mar. Sci.* 10, 1129712. doi: 10.3389/fmars.2023.1129712

Li, D., Gan, J., Hui, R., Liu, Z., Yu, L., Lu, Z., et al. (2020). Vortex and biogeochemical dynamics for the hypoxia formation within the coastal transition zone off the pearl river estuary. *J. Geophysical Research: Oceans* 125 (8). doi: 10.1029/2020JC016178

Li, Y. W., Hu, Y. Y., and Chen, S. M. (2013). Distribution and influence factors of nutrients in the north yellow sea in summer and autumn. *Zhongguo Huanjing Kexue/China Environ. Sci.* 33 (6), 1060–1067.

Li, H., Li, X., Xu, Z., Liang, S., Ding, Y., Song, D., et al. (2022). Nutrient budgets for the Bohai Sea: Implication for ratio imbalance of nitrogen to phosphorus input under intense human activities. *Mar. pollut. Bull.* 179, 113665. doi: 10.1016/j.marpolbul.2022.113665

Li, X. Y., Yu, R. C., Richardson, A. J., Sun, C., Eriksen, R., Kong, F. Z., et al. (2023). Marked shifts of harmful algal blooms in the Bohai Sea linked with combined impacts of environmental changes. *Harmful Algae* 121, 102370. doi: 10.1016/j.hal.2022.102370

Li, J. L., Zheng, B. H., Zhang, L. S., Jin, X., Hu, X., Liu, F., et al. (2016). Eutrophication characteristics and variation analysis of estuaries in China. *China Environ. Sci.* 36 (2), 506–516.

Lie, A. A. Y., Wong, C. K., Lam, J. Y. C., Liu, J. H., and Yung, Y. K. (2011). Changes in the nutrient ratios and phytoplankton community after declines in nutrient

concentrations in a semi-enclosed bay in hong kong. *Mar. Environ. Res.* 71 (3), 178–188. doi: 10.1016/j.marenvres.2011.01.001

Liu, J., Feng, Y., Zhang, Y., Liang, N., Wu, H., and Liu, F. (2022). Allometric releases of nitrogen and phosphorus from sediments mediated by bacteria determines water eutrophication in coastal river basins of Bohai Bay. *Ecotoxicol. Environ. Saf.* 235, 113426. doi: 10.1016/j.ecoenv.2022.113426

Liu, Y., Kuang, W., Xu, J., Chen, J., Sun, X., Lin, C., et al. (2022). Distribution, source and risk assessment of heavy metals in the seawater, sediments, and organisms of the daya bay, China. *Mar. pollut. Bull.* 174, 113297–Jan. doi: 10.1016/j.marpolbul.2021.113297

Liu, X., Liu, D., Wang, Y., Shi, Y., Wang, Y., and Sun, X. (2019). Temporal and spatial variations and impact factors of nutrients in bohai bay, China. *Mar. pollut. Bull.* 140 (MAR.), 549–562. doi: 10.1016/j.marpolbul.2019.02.011

Lu, X. Q., Yu, W. W., Chen, B., Ma, Z. Y., Chen, G. C., Ge, F. Y., et al. (2023). Imbalanced phytoplankton C, N, P and its relationship with seawater nutrients in Xiamen Bay, China. *Mar. pollut. Bull.* 187, 114566. doi: 10.1016/j.marpolbul.2022.114566. ISSN 0025.

Lu, D., Zhang, D., Zhu, W., Dan, S. F., Yang, B., Kang, Z., et al. (2022). Sources and long-term variation characteristics of dissolved nutrients in Maowei Sea, Beibu Gulf, China. *J. Hydrology* 615, 128576. doi: 10.1016/j.jhydrol.2022.128576

Mariko, H., Measures, C. I., and Jaromir, R. (2018). Determination of traces of phosphate in sea water automated by programmable flow injection: surfactant enhancement of the phosphomolybdenum blue response. *Talanta* 191, 333–341. doi: 10.1016/j.talanta.2018.08.045

Ming, X., Wang, B., Xia, S., and Xie, L. (2010). The distribution characteristics and seasonal variation of nutrients in guangxi coastal area. *Mar. Sci.* 34 (09), 5–9. doi: 10.3788/HPLPB20102209.2186

Ministry of Environmental Protection of the PRC. (2002). Technical Specifications Requirements for Monitoring of Surface Water and Waste Water. *Ministry of Environment Protection, People's Republic of China*. Standards Press of China, Beijing, China.

Ministry of Environmental Protection of the PRC. (2009). *Specification for Offshore Environmental Monitoring: HJ 442—2008*. China: China Environment Science Press, p. 19.

Ministry of Environmental Protection of the People's Republic of China (PRC). (1997). *Sea Water Quality Standard (GB3097-1997)*, p. 3.

Mourão, F. V., de Sousa, A. C. S. R., da Luz Mendes, R. M., Castro, K. M., da Silva, A. C., El-Robrini, M., et al. (2020). Water quality and eutrophication in the Curuçá estuary in northern Brazil. *Regional Stud. Mar. Sci.* 39, 101450. doi: 10.1016/j.rsma.2020.101450

Murphy, J., and Riley, J. P. (1962). A modified single solution method for the determination of phosphate in natural waters. Anal. Chim. *Acta* 27 (C), 678–681. doi: 10.1016/S0003-2670(00)88444-5

Ning, Z., Fang, C., Yu, K., Yang, B., and Wang, Y. (2020). Influences of phosphorus concentration and porewater advection on phosphorus dynamics in carbonate sands around the weizhou island, northern south china sea. *Mar. pollut. Bull.* 160, 111668. doi: 10.1016/j.marpolbul.2020.111668

Niu, L., Luo, X., Hu, S., Liu, F., and Yang, Q. (2020). Impact of anthropogenic forcing on the environmental controls of phytoplankton dynamics between 1974 and 2017 in the pearl river estuary, China. *Ecol. Indic.* 116, 106484.1–106484.14. doi: 10.1016/j.ecolind.2020.106484

Paerl, H. W., Scott, J. T., Mccarthy, M. J., Newell, S. E., Gardner, W. S., Havens, K. E., et al. (2016). It takes two to tango: when and where dual nutrient (n & p) reductions are needed to protect lakes and downstream ecosystems. *Environ. Sci. Technol.* 50 (20), 10805–10813. doi: 10.1021/acs.est.6b02575

Paerl, H. W., Xu, H., Mccarthy, M. J., Zhu, G., Qin, B., Li, Y., et al. (2011). Controlling harmful cyanobacterial blooms in a hyper-eutrophic lake (lake taihu, china): the need for a dual nutrient (n & p) management strategy. *Water Res.* 45 (5), 1973–1983. doi: 10.1016/j.watres.2010.09.018

Pan, J., Hu, C., Chen, J., Liu, X., Zhou, H.Weidong Ji Key Laboratory of Submarine Geosciences of State Oceanic Administration, et al. (2003). The chemical distribution characteristics of variant form phosphorus in the seawater of the south china sea. *Acta Oceanologica Sin.* 2003 (03), 385–394. doi: 10.1029/2002JC001507

Pei, S., Laws, E. A., Zhu, Y., Zhang, H., and Ding, X. (2019). Nutrient dynamics and their interaction with phytoplankton growth during autumn in liaodong bay, China. *Continental Shelf Res.* 186, 34–47. doi: 10.1016/j.csr.2019.07.012

Philippart, C. J., Beukema, J. J., Cadée, G. C., Dekker, R., Goedhart, P. W., van Iperen, J. M., et al. (2007). Impacts of nutrient reduction on coastal communities. *Ecosystems* 10, 96–119. doi: 10.1007/s10021-006-9006-7

Qian, Ge, Liu, J. ,. P., Xue, Z., et al. (2014). Dispersal of the zhujiang river (pearl river) derived sediment in the holocene. *J. Oceanography: English. Acta Oceanol. Sin.* 33, 1–9. doi: 10.1007/s13131-014-0407-8

Qian, W., Zhang, S., Tong, C., Sardans, J., Peñuelas, J., and Li, X. (2022). Long-term patterns of dissolved oxygen dynamics in the pearl river estuary. *J. Geophysical Research: Biogeosciences* 127 (7), e2022JG006967. doi: 10.1029/2022JG006967

Qiao, Y., Feng, J., Cui, S., and Zhu, L. (2017). Long-term changes in nutrients, chlorophyll a and their relationships in a semi-enclosed eutrophic ecosystem, bohai bay, china. *Mar. pollut. Bull.* 117 (1-2), 222. doi: 10.1016/j.marpolbul.2017.02.002

Qin, B., Gao, G., Zhu, G., Zhang, Y., Song, Y., Tang, X., et al. (2013). Lake eutrophication and its ecosystem response. *Chin. Sci. Bull.* 58, 961–970. doi: 10.1007/s11434-012-5560-x

Quan, W. M., Shen, X. Q., and Han, J. D. (2005). Analysis and assessment on eutrophication status and developing trend in changjiang estuary and adjacent sea. *Mar. Environ. Sci.* 24 (3), 13–16. doi: 10.1007/s10971-005-6694-y

Queré, C. L., Peters, G. P., Andres, R. J., Boden, T. A., and Yue, C. (2014). Global carbon budget 2013. *Earth System Sci. Data Discussions* 6, 235–263. doi: 10.5194/essd-6-235-2014

Rees, A. P., Turk-Kubo, K. A., Al-Moosawi, L., Alliouane, S., Gazeau, F., Hogan, M. E., et al. (2017). Ocean acidification impacts on nitrogen fixation in the coastal western Mediterranean Sea. *Estuarine Coast. Shelf Sci.* 186, 45–57. doi: 10.1016/j.ecss.2016.01.020

Schindler, D. W., Carpenter, S. R., Chapra, S. C., Hecky, R. E., and Orihel, D. M. (2016). Reducing phosphorus to curb lake eutrophication is a success. *Environ. Sci. Technol.* 50 (17), 8923. doi: 10.1021/acs.est.6b02204

Schlüter, L., Mhlenberg, F., Havskum, H., and Larsen, S. (2000). The use of phytoplankton pigments for identifying and quantifying phytoplankton groups in coastal areas: testing the influence of light and nutrients on pigment/chlorophyll a ratios. *Mar. Ecol. Prog. Ser.* 192, 49–63. doi: 10.3354/meps192049

Shen, Y., Zhang, H., and Tang, J. (2022). Hydrodynamics and water quality impacts of large-scale reclamation projects in the Pearl River Estuary. *Ocean Eng.* 257, 111432. doi: 10.1016/j.oceaneng.2022.111432

Shi, Z., Xu, J., Huang, X., Zhang, X., Jiang, Z., and Ye, F. (2017). Relationship between nutrients and plankton biomass in the turbidity maximum zone of the pearl river estuary. *J. Environ. Sci. (China).* 57, 72–84. doi: 10.1016/j.jes.2016.11.013

Smith, V., Wood, S., Mcbride, C., Atalah, J., and Hamilton, D. (2017). Phosphorus and nitrogen loading restraints are essential for successful eutrophication control of lake rotorua, new zealand. *Inland Waters* 6 (2), 273–283. doi: 10.5268/IW-6.2.998

Song, C., Yang, J., Wu, F., Xiao, X., Xia, J., and Li, X. (2022). Response characteristics and influencing factors of carbon emissions and land surface temperature in Guangdong Province, China. *Urban Climate* 46, 101330. doi: 10.1016/j.uclim.2022.101330

Stocker, T. (2014). *Climate change 2013: the physical science basis: Working Group I contribution to the Fifth assessment report of the Intergovernmental Panel on Climate Change* (Cambridge university press). Available at: https://www.researchgate.net/publication/320182295_Climate_change_2013_the_physical_science_basis_Working_Group_I_contribution_to_the_Fifth_assessment_report_of_the_Intergovernmental_Panel_on_Climate_Change.

Sun, X., Dong, Z., Zhang, W., Sun, X., Hou, C., Liu, Y., et al. (2021). Seasonal and spatial variations in nutrients under the influence of natural and anthropogenic factors in coastal waters of the northern yellow sea, China. *Mar. Pollut. Bull.* 175, 113171. doi: 10.1016/j.marpolbul.2021.113171

Tu, J., Wan, M., Chen, Y., Tan, L., and Wang, J. (2022). Biodiversity assessment in the near-shore waters of Tianjin city, China based on the Pressure-State-Response (PSR) method. *Mar. pollut. Bull.* 184, 114123. doi: 10.1016/j.marpolbul.2022.114123

Turner, R. E., Rabalais, N. N., Alexander, R. B., McIsaac, G., and Howarth, R. W. (2007). Characterization of nutrient, organic carbon, and sediment loads and concentrations from the Mississippi River into the northern Gulf of Mexico. *Estuaries Coasts* 30, 773–790. doi: 10.1007/BF02841333

Turner, R. E., Rabalais, N. N., Justic', D., and Dortch, Q. (2003). Future aquatic nutrient limitations. *Mar. pollut. Bull.* 46 (8), 1032–1034. doi: 10.1016/S0025-326X(03)00049-3

Vaquer-Sunyer, R., and Duarte, C. M. (2008). Thresholds of hypoxia for marine biodiversity. *Proc. Natl. Acad. Sci. U.S.A.* 105 (40), 15452–15457. doi: 10.1073/pnas.0803833105

Wang, H., Bouwman, A. F., Van Gils, J., Vilmin, L., Beusen, A. H., Wang, J., et al. (2023). Hindcasting harmful algal bloom risk due to land-based nutrient pollution in the Eastern Chinese coastal seas. *Water Res.* 231, 119669. doi: 10.1016/j.watres.2023.119669

Wang, Y., Liu, D., Lee, K., Dong, Z., Di, B., Wang, Y., et al. (2017). Impact of Water-Sediment Regulation Scheme on seasonal and spatial variations of biogeochemical factors in the Yellow River estuary. *Estuarine Coast. Shelf Sci.* 198, 92–105. doi: 10.1016/j.ecss.2017.09.005

Wang, Q., Wang, X., Xiao, K., Zhang, Y., and Li, H. (2021). Submarine groundwater discharge and associated nutrient fluxes in the greater bay area, china revealed by radium and stable isotopes. *Geosci. Front.* 12 (3–4), 101223. doi: 10.1016/j.gsf.2021.101223

Wang, J. N., Yan, W. J., Chen, N. W., Li, X. Y., and Liu, L. S. (2015). Modeled long-term changes of din:dip ratio in the changjiang river in relation to chl-α and do concentrations in adjacent estuary. *Estuarine Coast. Shelf Sci.* 166 (166), 153–160. doi: 10.1016/j.ecss.2014.11.028

Wang, Y., Zhang, J., Wu, W., Liu, J., Ran, X., Zhang, A., et al. (2022). Variations in the marine seawater environment and the dominant factors in the Lianyungang coastal area. *Regional Stud. Mar. Sci.* 52, 102276. doi: 10.1016/j.rsma.2022.102276

Wang, M., Zhang, Q., Zhou, D. S., Song, X. M., and Chen, K. H. (2011). Preliminary survey and evaluation of water quality in lianyungang inshore. *J. Huaihai Institute Technol. (Natural Sci. Edition).* 20 (04), 50–53. doi: 10.3969/j.issn.1672-6685.2011.01.014

Wei, B., Mollenhauer, G., Hefter, J., Grotheer, H., and Jia, G. (2020). Dispersal and aging of terrigenous organic matter in the pearl river estuary and the northern south china sea shelf. *Geochimica Cosmochimica Acta: J. Geochemical Soc. Meteoritical Soc.* 282 (1), 324–339. doi: 10.1016/j.gca.2020.04.032

Wu, H. Y., Dong, C. F., Zheng, G. C., Zhang, Z. H., Zhang, Y. Y., Tan, Z. J., et al. (2022). Formation mechanism and environmental drivers of Alexandrium catenella bloom events in the coastal waters of Qinhuangdao, China. *Environ. pollut.* 313, 120241. doi: 10.1016/j.envpol.2022.120241

Wu, F., Meng, W., Zhao, X., Li, H., Zhang, R., Cao, Y., et al. (2010). China embarking on development of its own national water quality criteria system. *Environ. Sci. Technol.* 44 (21), 7992–7993. doi: 10.1021/es1029365

Xie, L., Xu, H., Xin, M., Wang, B., and Sun, X. (2021). Regime shifts in trophic status and regional nutrient criteria for the bohai bay, china. *Mar. pollut. Bull.* 170 (1–9), 112674. doi: 10.1016/j.marpolbul.2021.112674

Yang, B., Gao, X., Zhao, J., Lu, Y., and Gao, T. (2020). Biogeochemistry of dissolved inorganic nutrients in an oligotrophic coastal mariculture region of the northern Shandong Peninsula, north Yellow Sea. *Mar Pollut Bull.* 150, 110693. doi: 10.1016/j.marpolbul.2019.110693

Yang, F., Mi, T., Chen, H., and Yao, Q. (2019). Developing numeric nutrient criteria for the yangtze river estuary and adjacent waters in china. *J. Hydrology* 579, 124188. doi: 10.1016/j.jhydrol.2019.124188

Yu, R. C., Lü, S. H., and Liang, Y. B. (2018). "Harmful Algal Blooms in the Coastal Waters of China," in *Global Ecology and Oceanography of Harmful Algal Blooms*, vol. 232 . Eds. P. Glibert, E. Berdalet, M. Burford, G. Pitcher and M. Zhou (Cham: Springer).

Yuan, H., Xing, J., Li, J., Li, X., Duan, N., Qu, L., et al. (2018). Spatial and seasonal variations, partitioning and fluxes of dissolved and particulate nutrients in jiaozhou bay. *Continental Shelf Research: A Companion J. to Deep-Sea Res. Prog. Oceanography* 171, 140–149. doi: 10.1016/j.csr.2018.11.004

Zeng-Lin, H., Qian-Bin, D. I., and Le-Ping, Z. (2012). Discussion on the connotation and target of sea-land coordination. *Marine Economy*. doi: CNKI:SUN:SEJJ.0.2012-01-004

Zhang, P., Chen, Y., Peng, C., Dai, P., and Zhang, J. (2020). Spatiotemporal variation, composition of din and its contribution to eutrophication in coastal waters adjacent to hainan island, china. *Regional Stud. Mar. Sci.* 37 (25), 101332. doi: 10.1016/j.rsma.2020.101332

Zhang, P., Ou, S., Zhang, J., Zhao, L., and Zhang, J. (2022). Categorizing numeric nutrients criteria and implications for water quality assessment in the Pearl River Estuary, China. *Front. Mar. Sci.* 9, 1004235. doi: 10.3389/fmars.2022.1004235

Zhang, C., Lim, P., Li, X., Gu, H., Li, X., and Anderson, D. (2020). Wind-driven development and transport ofgymnodinium catenatumblooms along the coast of fujian, china. *Regional Stud. Mar. Sci.* 39, 101397. doi: 10.1016/j.rsma.2020.101397

Zhang, M., Lu, Q., Wang, D., Ding, D., Cui, Z., and Shi, H. (2022). Spatiotemporal evolution of nutrients and the influencing factors in Laizhou Bay over the past 40 years. *Mar. pollut. Bull.* 184, 114186. doi: 10.1016/j.marpolbul.2022.114186

Zhang, L., Yan, W., Xie, Z., Cai, G., Mi, W., and Xu, W. (2020). Bioaccumulation and changes of trace metals over the last two decades in marine organisms from Guangdong coastal regions, South China. *J. Environ. Sci.* 98, 103–108. doi: 10.1016/j.jes.2020.05.007

Zhen, W. A., Yong, L., Zl, A., Sw, A., and Hg, A. (2017). Internal cycling, not external loading, decides the nutrient limitation in eutrophic lake: a dynamic model with temporal bayesian hierarchical inference - sciencedirect. *Water Res.* 116, 231–240. doi: 10.1016/j.watres.2017.03.039

Zhou, A. G., and Cai, H. S. (1998). The theory and application of geological environment quality evaluation. *Press Chin. Geology Univ.* pp, 70–83.

Zhou, Z. X., Yu, R. C., and Zhou, M. J. (2022). Evolution of harmful algal blooms in the East China Sea under eutrophication and warming scenarios. *Water Res.* 221, 118807. doi: 10.1016/j.watres.2022.118807

Zou, J. Z., Dong, L. P., and Qin, B. P. (1983). The primary research on the eutrophication and red tide in Bohai Bay. *Mar. Environ. Sci.* 2 (2), 41–55.

Zou, W., Zhu, G., Xu, H., Zhu, M., Zhang, Y., and Qin, B. (2022). Temporal dependence of chlorophyll a–nutrient relationships in lake taihu: drivers and management implications. *J. Environ. Manage.* 306, 114476–. doi: 10.1016/j.jenvman.2022.114476

frontiers | Frontiers in Marine Science

TYPE Brief Research Report
PUBLISHED 16 August 2023
DOI 10.3389/fmars.2023.1215627

OPEN ACCESS

EDITED BY
Ram Kumar,
Central University of Bihar, India

REVIEWED BY
Jawed Equbal,
National Centre for Coastal Research, India
Diwakar Prakash,
Central University of South Bihar, India
Malayaj Rai,
Silliman University, Philippines

*CORRESPONDENCE
P. Sathish Kumar
marinesathis@gmail.com

RECEIVED 02 May 2023
ACCEPTED 10 July 2023
PUBLISHED 16 August 2023

CITATION
Sathish Kumar P, Dharani G, Santhanakumar J, Jha DK, Pandey V, Venkatnarayanan S, Jebakumar JPP, Muthukumar C and James RA (2023) Assessment of phytoplankton diversity, distribution, and environmental variables along the southeast coast of India. *Front. Mar. Sci.* 10:1215627. doi: 10.3389/fmars.2023.1215627

Assessment of phytoplankton diversity, distribution, and environmental variables along the southeast coast of India

P. Sathish Kumar[1,2*], G. Dharani[1], J. Santhanakumar[1], Dilip Kumar Jha[1], Vikas Pandey[1,3], S. Venkatnarayanan[1], J. Prince Prakash Jebakumar[4], C. Muthukumar[2,5] and R. Arthur James[2]

[1]Ocean Science and Technology for Islands, National Institute of Ocean Technology (NIOT), Ministry of Earth Sciences, Government of India, Chennai, Tamil Nadu, India, [2]Department of Marine Science, Bharathidasan University, Tiruchirappalli, Tamil Nadu, India, [3]Biological Oceanography Division, CSIR - National Institute of Oceanography, Dona Paula, Goa, India, [4] Coastal and Environmental Engineering, National Institute of Ocean Technology, Ministry of Earth Sciences, Government of India, Chennai, Tamil Nadu, India, [5]National Centre for Coastal Research, Ministry of Earth Sciences, Government of India, Chennai, Tamil Nadu, India

Coastal waters are dynamic because of anthropogenic activities that contribute nutrients and contaminants. These changes have the potential to alter patterns of primary production and thus pelagic food webs. Here, we investigated the spatial variation of the phytoplankton community and its response to changing environmental variables at 84 stations along the five coastal districts of Tamil Nadu (TN). During the present study, 85 phytoplankton species were recorded, such as diatoms (64), dinoflagellates (18), silicoflagellates (1), and Cyanophyceae (2). The maximum phytoplankton abundance was recorded on the Thanjavur coast and gradually decreased towards the south coast of Tamil Nadu. Among the phytoplankton community, 50% was dominated by pennate diatoms, attributed to higher NO_3^- concentrations in the coastal waters due to agricultural discharge. Cluster analysis revealed that Ramanathapuram and Tirunelveli formed a closed cluster, whereas Thanjavur and Pudukottai formed a separate closed cluster associated with higher nutrient and metal concentrations, highlighting the difference in physicochemical parameters between the northern and southern districts of the TN coast. Relatively high nutrient concentrations in the coastal waters of northern districts are of greater concern, which could impact the coastal ecosystem. Coastal eutrophication is becoming a widespread phenomenon, causing disruption in the food chain and ecosystem balances and hence requiring regular monitoring and management.

KEYWORDS

phytoplankton, nutrient, heavy metal, multivariate, Gulf of Mannar, Tamil Nadu

Introduction

Phytoplankton is key component in coastal ecosystems and serve as primary producers in the marine food chain (Ananthan et al., 2004; Tas and Gonulol, 2007). In addition to being the foundation of the marine food web, they are responsible for adding oxygen to the ocean and play a key role in carbon sequestration. The growth and abundance of phytoplankton are predominantly controlled by interactions between biotic and abiotic factors (Dayala et al., 2014). Ambient temperature can significantly influence the growth and distribution of phytoplankton in coastal waters by affecting the photosynthetic activity of these primary producers (Trombetta et al., 2019). Similarly, salinity also plays a major role in controlling the structure and composition of phytoplankton communities because each species responds to salinity differently (Larson and Belovsky, 2013). Changes in salinity can affect the mixing and transport of nutrients throughout the water column, which can affect nutrient availability (Marcarelli et al., 2006). Nitrogen and phosphorus are critical nutrients for phytoplankton growth and metabolism, and variations in nutrient availability can have a significant impact on phytoplankton diversity (Smith et al., 1999). Therefore, understanding the interaction between these variables is critical for estimating phytoplankton communities in coastal ecosystems (Sin et al., 1999).

Several studies have been conducted along the east coast of India to examine the seasonal and spatial pattern of coastal waters and their impact on phytoplankton productivity (Naqvi et al., 1978; Satpathy et al., 2011; Sahu et al., 2012; Prakash et al., 2023). The nearshore and estuaries, which are impacted by both natural and anthropogenic disturbances (Jarvie et al., 1998), vary significantly depending on the local environmental setup, such as rainfall, amount of freshwater inflow, tidal incursion, and biological activities (Satpathy et al., 2011). The primary source of organic and inorganic variables (including nutrients) in the coastal ecosystem is wastewater discharges (Specchiulli et al., 2010). Previous studies have shown that such discharges can alter the dynamics of food webs in coastal environments (Nixon, 1995; Halpern et al., 2008). One of the key environmental parameters that reflect the turbidity of an eroding coastline or the introduction of suspended materials into coastal waters via land runoff is total suspended solids (TSS), which also affect the composition and abundance of the plankton community (Wu et al., 2011; Kumar et al., 2022).

Tamil Nadu (TN) has the third-longest coastline in India, comprising the Palk Bay (PB) and the Gulf of Mannar (GoM), which account for approximately 15% of the country's total coastline (Pandey et al., 2022). Thousands of traditional fisherfolk in both GoM and PB rely on seagrass beds for their fishing and livelihood (Balasubramanian et al., 2011). Rainfall occurs in the TN region from late August (southwest monsoon) to early November (northeast monsoon). The average annual rainfall in TN is approximately 950 mm (IMD). The coastal waters of the PB resemble the Bay of Bengal in terms of low salinity and higher turbidity, whereas the coastal waters of the GoM exhibit a mixed character of both the Bay of Bengal and the Arabian Sea (Rao et al., 2008). The objectives of the present study were: 1) to investigate the spatial patterns of environmental variables; and 2) to investigate the spatial variations of the phytoplankton community and its response to changing environmental factors.

Materials and methods

Sampling was conducted at 84 stations in five coastal districts, namely Thanjavur (THA1 to THA10), Pudukottai (PUD1 to PUD10), Ramanathapuram (RAM1 to RAM9), Thoothukudi (THO1 to THO7), and Tirunelveli (TIR1 to TIR6), covering 537 km along the coastal waters of TN, on the southeast coast of India. A total of 84 samples were collected from 42 locations offshore (within 15 km from the shore) and nearshore (within 1 km from the shore) (Figure 1). Sample collection and analysis of physio-chemical and biological parameters were conducted from January to March 2020. Seawater samples were collected from the surface (~0.5 m) using a 5 L Niskin sampler for the analysis of dissolved oxygen (DO), biochemical oxygen demand (BOD), total suspended solids (TSS), nutrients, trace metals, chlorophyll-*a* (Chl-*a*), and phytoplankton. Air temperature (AT) was measured with a mercury thermometer (accuracy ±0.1°C). A calibrated portable multi-parameter water quality instrument (model HI 9829, Hanna) was used to measure sea surface temperature (SST), salinity, and pH. The DO and BOD were measured using the modified Winkler's method of Carrit and Carpenter (1966). TSS was determined by filtering a known volume of seawater through pre-dried and pre-weighed filter paper (0.45 µm, Millipore GF/C) (APHA, 2012). Analysis of nutrients like ammonia (NH_4^+), nitrite (NO_2^-), nitrate (NO_3^-), phosphate (PO_4^{3-}), and silicate ($SiO^2_4^-$) was performed using standard spectrophotometric techniques described by Grasshoff et al. (1999). The heavy metal analysis was carried out according to the US Environmental Protection Agency's (USEPA, 2001) technique. A detailed methodology for heavy metal analysis was adopted by Jha et al. (2019). The standard method for spectrofluorometric analysis of Chl-a was followed (Parsons et al., 1984). For phytoplankton assessment, 1L of the surface seawater sample was collected and preserved with Lugol's iodine solution. Qualitative and quantitative analysis of phytoplankton was carried out using Utermöhl's (1958) method. The conventional taxonomic keys were used for the identification (Subrahmanyan, 1946, 1959; Tomas, 1997). The Shannon-Wiener diversity index (H'), Margalef species richness (d), and Pielou evenness (J') of univariate measures were calculated using PRIMER-6 (PRIMER–E Ltd., Plymouth, UK). The linear relationship between phytoplankton abundance and environmental variables was assessed using Pearson correlation and multivariate regression analysis. A one-way ANOVA was performed using XLSTAT software to determine the significant variation in physicochemical parameters. The spatial pattern of environmental variables was examined using hierarchical agglomerative clustering with group average linkage using Euclidean distance in PRIMER-6. Factor analysis (FA) of environmental variables was performed using SPSS software (version 18.0), and the results were categorized as strong (> 0.75), moderate (0.75-0.50), and weak (0.50-0.30) factor loadings. The Kaiser-Meyer-Olkin (KMO) criterion was adopted for sample

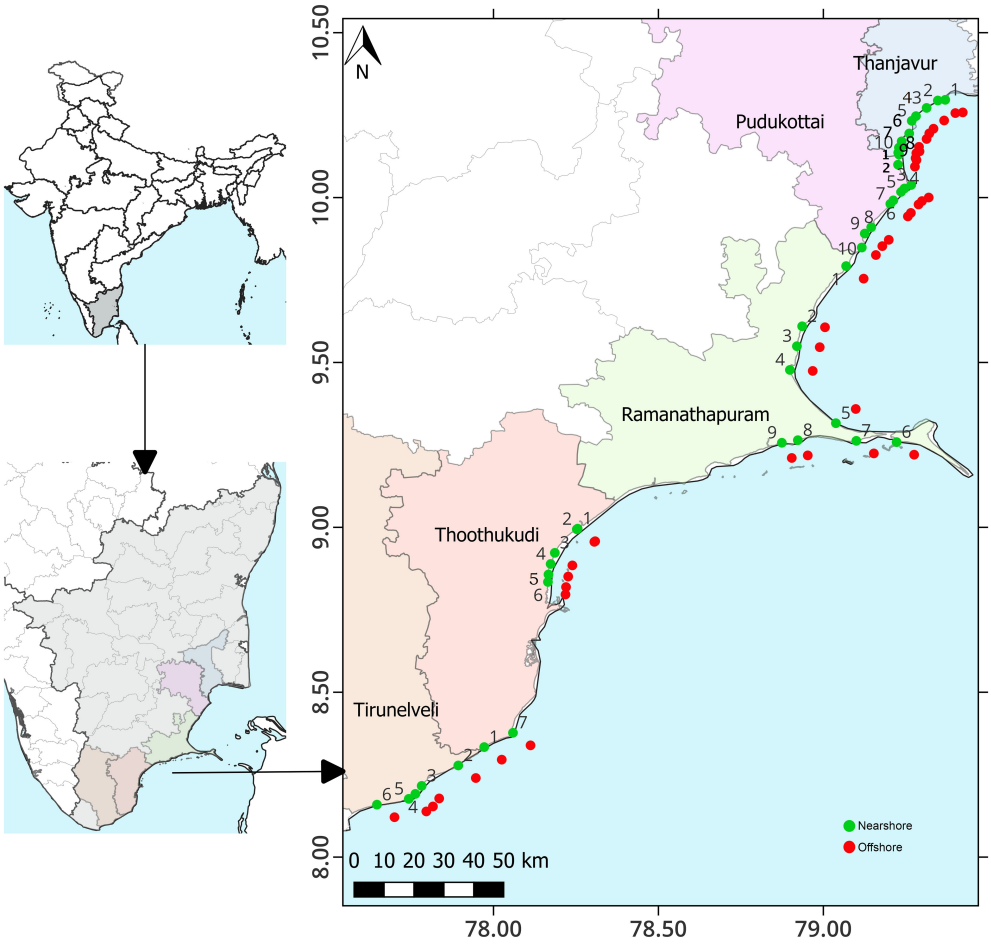

FIGURE 1
Map showing study locations along the coastal waters of Tamil Nadu on the southeast coast of India.

adequacy, and the parameters were standardized using a Z-scale transformation (mean = 0; variance = 1) before analysis to make the data dimensionless.

Results and discussion

Environmental parameters

The spatial variation of physicochemical parameters observed during the present study is shown in Figure 2. The SST ranged from 26.54 to 30.01°C, with the highest and lowest SST recorded at RAM (offshore) and THA (offshore) stations, respectively. The pH decreased from north to south, with a maximum (8.47) at PUD and a minimum (8.05) at the TIR region. Salinity ranged from 28.35 to 34.38 PSU, with higher and lower salinities observed offshore of RAM (RAM7) and PUD (PUD3), respectively. The mean salinity was higher (31.96 ± 1.42 PSU) at RAM. Compared to the nearshore, the offshore recorded optimal DO and TSS, which might be attributed to less disturbance in the water column leading to good transparency and productivity. The THA stations recorded lower DO and higher BOD, which could be attributed to organic influx from sewage discharge into the marine environment causing oxidative degradation by bacteria, resulting in high BOD and reduced DO (Sahu et al., 2013; Pandey and Ganesh, 2019). TSS showed a significant spatial variation ($F=11.785$, $p < 0.01$), which ranged from 15.8 to 67.8 mg/L, with a maximum recorded at the nearshore stations. Freshwater input from many perennial (Krishna, Godavari, and Mahanadi) and seasonal (Palar, Vellar, and Coleroon) rivers in the nearshore region could be attributed to the higher TSS (Shanthi et al., 2013). In addition, three minor rivers, Tamiraparani, Vembar, and Vaipar, drain into the GoM (Rao et al., 2008). Variations in dissolved nutrient levels between the nearshore and offshore of each district are shown in Figure 2. Most of the nutrients were recorded as comparatively high at the northern stations and low at the southern stations, which could be attributed to anthropogenic activities in the surrounding vicinity. Nutrients such as NO_3^-, PO_4^{3-}, and SiO_4^{2-} were low in the southern stations and increased toward the north, which could be due to anthropogenic activities such as untreated domestic sewage, industrial wastewater, and agricultural runoff (Xu et al., 2010; Kumar et al., 2018). SiO_4^{2-} (18.95 ± 11.1 µM) and NH_4^+ (4.85 ± 1.9 µM) were found to be high at PUD and RAM nearshore stations, respectively, while NO_3^- (3.49 ± 0.4 µM) was found to be high at THA stations.

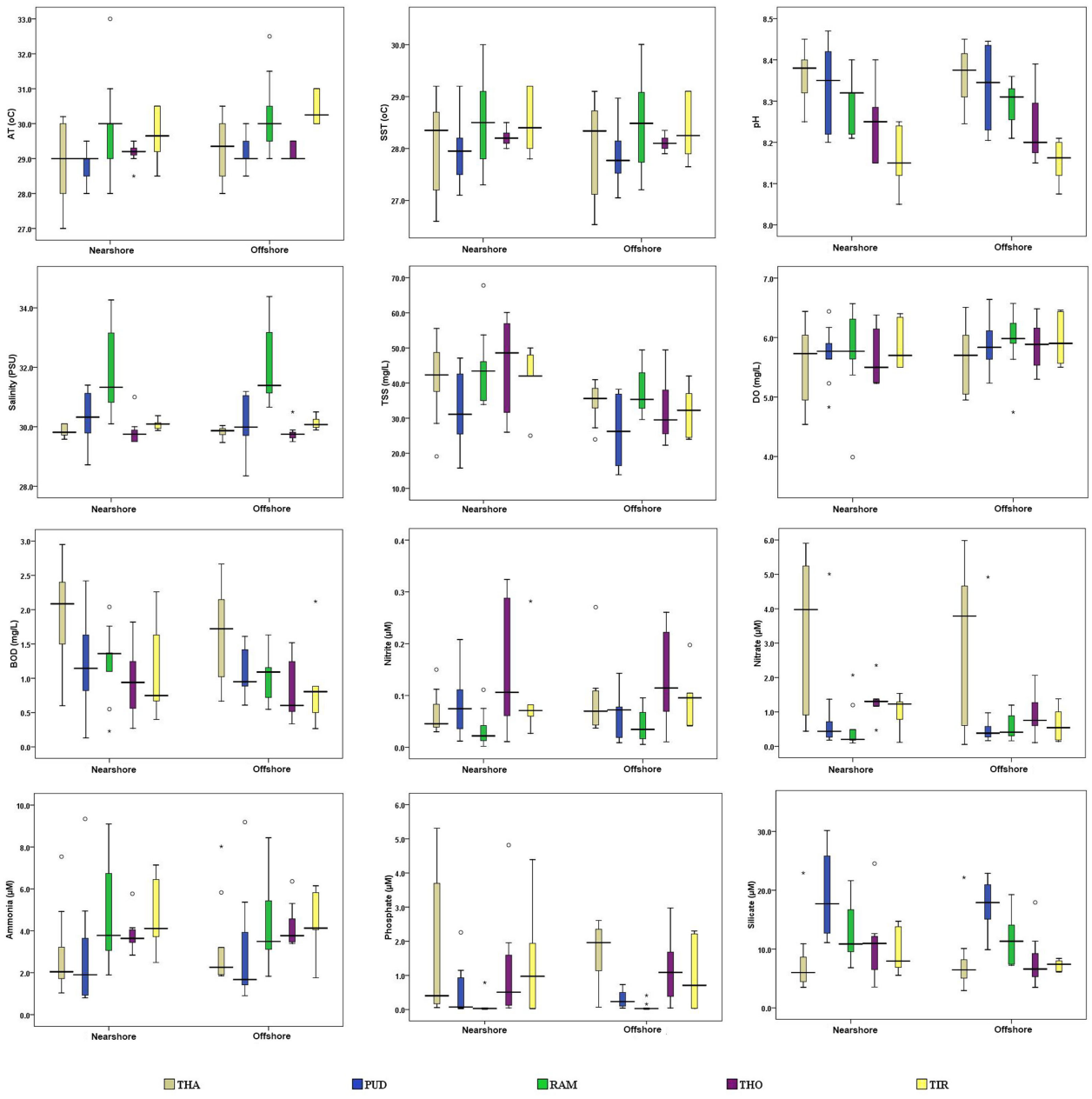

FIGURE 2
Spatial variations of physicochemical parameters along the coastal waters of Tamil Nadu on the southeast coast of India (* indicates extreme outliers, and ° indicates mild outliers). THA, Thanjavur district; PUD, Pudukottai district; RAM, Ramanathapuram district; THO, Tuthukudi district; TIR, Tirunelveli district.

In addition to the hydrographic parameters, 11 important heavy metals were also examined in the present study and are summarized in Table 1, with Cd and Hg being below the detection limit (BDL). The mean concentration of heavy metals were in the order of Al >Fe >Zn >Cu >Mn >Cr >Pb >Ni >Co. Al ranged from 14.4 to 420.3 ppb, with a maximum recorded at the THA station, which was above the permissible level (Conama, 2003). The concentrations of Fe (225.6 ppb) and Zn (67.2 ppb) were high at RAM. The concentrations of Cu (26.01 ppb) and Mn (12.5 ppb), which were found to be high in the PUD region, could be due to the usage of biocides attributed to anthropogenic activities (Anbuselvan et al., 2018). Ni (0.51 ppb) was high at THA stations, while Cr (1.52 ppb) was high at THO and PUD stations. Higher Ni concentrations at THA stations could increase phytoplankton production as Ni is essential for algal growth (Price and Morel, 1991). However, the recorded Fe and Ni concentrations were comparatively lower than in nearby coastal regions (Jha et al., 2019). During the present study, most of the metal concentrations were comparatively higher at northern stations. However, the lower concentration of metals like Fe at southern stations could be one of the reason for the lower phytoplankton abundance. Continuous monitoring could help regulate coastal water quality and thus support the fishing

TABLE 1 Spatial variation of trace metal concentrations in the coastal waters of Tamil Nadu on the southwest Bay of Bengal.

Parameters	THA	PUD	RAM	THO	TIR
Al (ppb)	14.4-420.3	25.2-220.5	25.2-75.4	45.1-115.2	25.6-225.3
	(108.9 ± 119.28)	(106.4 ± 59.82)	(53.0 ± 15.49)	(75.83 ± 32.02)	(80.2 ± 80.44)
Fe (ppb)	BDL-201.2	BDL-125.1	3.0–225.6	15.3–115.3	9.2-125.2
	(33.08 ± 65.28)	(46.30 ± 46.83)	(58.80 ± 74.47)	(43.67 ± 40.15)	(51.67 ± 55.08)
Cr (ppb)	BDL-0.38	BDL-1.52	BDL	0.35-1.52	BDL-0.99
	(0.07 ± 0.13)	(0.50 ± 0.51)		(0.63 ± 0.45)	(0.21 ± 0.40)
Cu (ppb)	BDL-17.0	BDL-26.01	BDL-2.51	BDL-0.92	0.21-7.88
	(2.16 ± 5.26)	(4.02 ± 7.90)	(1.08 ± 0.87)	(0.53 ± 0.38)	(2.31 ± 2.86)
Mn (ppb)	BDL-2.76	BDL-12.50	BDL-2.11	BDL-3.27	BDL-1.90
	(0.81 ± 0.92)	(1.72 ± 3.92)	(0.68 ± 0.82)	(1.54 ± 1.41)	(0.83 ± 0.81)
Ni (ppb)	BDL-0.51	BDL-0.42	BDL	BDL	BDL-0.42
	(0.13 ± 0.22)	(0.05 ± 0.13)			(0.07 ± 0.17)
Zn (ppb)	BDL-26.3	BDL-36.2	BDL-67.2	BDL	BDL
	(4.8 ± 9.45)	(9.83 ± 12.15)	(13.4 ± 24.99)		
Co (ppb)	BDL-0.07	BDL	BDL	BDL	BDL
	(0.01 ± 0.02)				
Pb (ppb)	BDL-4.44	BDL	BDL	BDL	BDL
	(2.38 ± 1.80)				

Values in open and parentheses represent the minimum – maximum, and mean values with ± standard error, respectively. (BDL, below detectable limit). THA, Thanjavur district; PUD, Pudukottai district; RAM, Ramanathapuram district; THO, Tuthukudi district; TIR, Tirunelveli district.

industry. Additionally, metal analysis can help identify the sources of contamination and prevent further pollution of the marine ecosystem.

Cluster analysis was used to assess the relationship of physicochemical parameters among the five coastal districts, and the study revealed two statistically significant clusters (Figure 3A). In the present study, lower activities such as industrial and pesticides use might have contributed fewer contaminants and nutrients in PUD, RAM, and TIR districts, thus forming cluster 1. Wherein RAM and TIR districts formed clusters with less distance could be attributed to similar sea water quality with lower nutrient and anthropogenic activity, which resulted these two districts as undisturbed (Pandey et al., 2022). Higher concentrations of $NO_3^-$and PO_4^{3-} could be the reason for the formation of cluster 2 between THO and THA. This could be attributed to higher domestic sewage, solid waste disposal, industries, agriculture, and aquaculture activities around the coastal districts. The results are similar to earlier observations that indicated a higher concentration of $NO_3^-$and PO_4^{3-} in THO due to domestic and industrial waste through anthropogenic runoff (Muthukumar et al., 2022).

KMO values were used to assess the sampling efficiency, which revealed variance significance. For the nearshore (Figure 3B) data, the KMO was 0.52, indicating that FA can significantly reduce the dimensionality of the original dataset (Wu et al., 2010). Four factors (eigenvalue >1) identified by factor analysis explained 62.5% of the overall variation in the dataset, but the first two factors were selected for detailed discussion (Table S1; Supplementary Material). Factor 1 showed strong positive loadings of BOD (0.85) and pH (0.84) with a 21.2% variance. In factor 2, moderate positive loadings of PO_4^{3-} (0.64), NO_2^- (0.59), and moderate negative loadings of salinity (-0.71) and NH_4^+ (-0.53) were observed, accounting for 16.2% of the total variation. This could be attributed to higher nutrient loading in the nearshore area due to river inflow (Zhou et al., 2007; Sahu et al., 2013). The offshore area (Figure 3C) indicated a significant reduction of the original dataset with 0.565 KMO, and FA explained 65.2% of the total variance with four factors (>1 eigenvalue). Factors 1 and 2 explained 20.9% and 18.2% of the total variance, respectively. Factor 1 showed strong positive loadings of NO_3^-(0.78), PO_4^{3-}(0.75), and moderate negative loading of $SiO^2{}_4^-$ (-0.73). On the other hand, factor 2 showed strong and moderate positive loadings of pH (0.81) and BOD (0.68), respectively. Nevertheless, a similar hydrographic condition was observed in the nearshore and offshore areas. However, TSS and nutrients were comparatively high at the nearshore, which could be due to the anthropogenic input from land runoff (Iscen et al., 2008). The FA analysis revealed a significant correlation matrix between different environmental parameters and their influence on phytoplankton density and diversity.

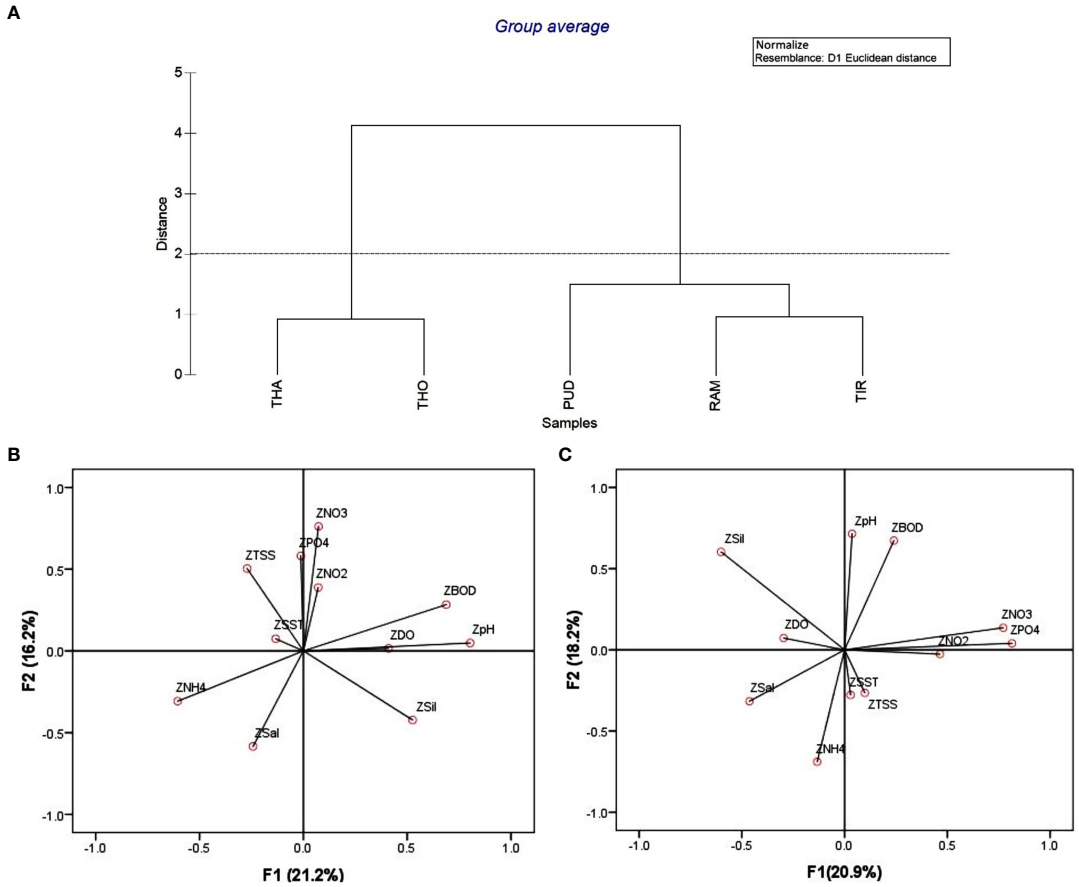

FIGURE 3
(A) Cluster analysis of physicochemical parameters, **(B)** Factor analysis of water quality parameters at nearshore, and **(C)** offshore locations. THA, Thanjavur district; PUD, Pudukottai district; RAM, Ramanathapuram district; THO, Tuthukudi district; TIR, Tirunelveli district.

Spatial variation of phytoplankton diversity, distribution, and biomass

Phytoplankton biomass (Chl-*a*) ranged from 0.03 to 0.5 mgm^{-3} (Table S2; Supplementary Material). The mean Chl-*a* concentration was higher in TIR (0.30 ± 0.03 mgm^{-3}) and lower in RAM (0.15 ± 0.02 mgm^{-3}). A similar trend was observed for pheophytin concentrations, which ranged from 0.05 to 0.60 mgm^{-3}. However, nearshore stations showed comparatively higher biomass than offshore stations, which could be attributed to higher nutrient loading from land runoff. During the present study, 85 phytoplankton species were recorded, such as diatoms (64), dinoflagellates (18), silicoflagellates (1), and cyanophyceae (2). A detailed list of phytoplankton recorded in the present study is shown in Table S3 (Supplementary Material). As with Chl-*a*, phytoplankton abundance was comparatively higher in the nearshore than the offshore stations due to the nutrient input from the land. Phytoplankton densities ranged from 0.7 to 210×10^{3}cells L^{-1}, with lower and higher densities observed in the THA at offshore (Stn-8) and nearshore (Stn-2) stations, respectively. The mean phytoplankton density was observed as being maximum at THA (59.8 ± 16.2×10^{3}cells L^{-1}) and decreasing abruptly toward the southern stations, with the lowest density at THO (6.3 ± 1.4×10^{3}cells L^{-1}). Although THO receives more nutrients from the land runoff, the phytoplankton biomass and abundance were low. This could be due to changes in the hydrographic features, such as a decrease in salinity, pH and an increase in turbidity due to the inflow of freshwater (Bharathi et al., 2018). THA alone contributed 60% of the total phytoplankton abundance, which was ~6 times higher than the other coastal stations in TN. This could be attributed to higher nutrient concentrations at THA, resulting in higher phytoplankton abundance. The phytoplankton community was dominated by diatoms (75.2%), followed by cyanophyceae (17.4%), and dinoflagellates (7.3%). Among the diatoms, pennate diatoms contributed 66% and centric diatoms contributed 34%. The dominance of pennate diatoms could lead to higher fouling rates (Mitbavkar and Anil, 2008). During the present study, seven species dominated the phytoplankton community, i.e., *Pseudo-nitzschia* sp., *Cylindrotheca closterium, Chaetoceros diversus, Cyanobacteria* sp. 1 in nearshore stations and *Rhizosolenia styliformis, Pleurosigma* sp. 1, *Rhizosolenia* sp. 2 in offshore stations. Most of the species belonged to the pennate diatoms at many stations.

The Shannon-Wiener diversity index (H') ranged from 0.16 to 2.50 (Table S2). The mean high diversity was observed in TIR (1.99 ± 0.13), followed by RAM (1.80 ± 0.08), and lower in THA (1.43 ± 0.17). Phytoplankton taxa ranged from 4 to 18 at nearshore stations and from 2 to 26 at offshore stations. Optimal hydrographic conditions may have supported the higher phytoplankton taxa at RAM and TIR, while anthropogenic disturbance may have reduced the taxa at THO stations. Maximum phytoplankton abundance and minimum species diversity & evenness were observed at THA, which could be attributed to the dominance of one phytoplankton species (*Pseudo-nitzschia* sp.) as reported previously (Sahu et al., 2012; Kumar et al., 2018). Species richness and evenness ranged from 0.11 to 2.49 and 0.07 to 1.0, respectively, in the present study. Higher diversity, richness, and evenness were recorded at the TIR stations, where the maximum number of phytoplankton taxa (26) was also recorded. In contrast, lower phytoplankton species richness and diversity were recorded in the THO region, both nearshore and offshore, due to intense anthropogenic activities such as power plants, ports, and various other industrial activities (Bharathi et al., 2018; Jha et al., 2022a).

Influence of hydrographic parameters on phytoplankton communities

Pearson correlation was used to identify the significant relationships between phytoplankton and hydrographic factors. In offshore stations, phytoplankton density was positively correlated with NO_3^- ($r = 0.67$, $P< 0.05$), followed by PO_4^{3-}($r = 0.51$, $P< 0.05$), pH ($r = 0.32$, $P< 0.05$) and negatively correlated with SiO_4^{2-}($r = -0.27$, $P< 0.05$). A similar result was also observed through multivariate regression analysis, which revealed a positive correlation of NO_3^- with phytoplankton ($r^2 = 0.18$, $P< 0.05$) and pennate diatoms ($r^2 = 0.33$, $P< 0.05$). The Chl-*a* biomass was positively and negatively correlated with NO_2^-($r = 0.22$, $P < 0.05$), and salinity ($r = -0.31$, $P< 0.05$), respectively. In the nearshore, phytoplankton showed the positive and negative correlation with NO_3^-($r = 0.36$, $P< 0.05$) and SiO_4^{2-}($r = -0.24$, $P< 0.05$). Compared to the offshore, $NO_3^-$and SiO_4^{2-} were comparatively high in the nearshore, which might be due to the nutrient input from land runoff (Zhou et al., 2008). However, the low nutrient concentration leads to low phytoplankton abundance under natural oceanic conditions, which was evident in the present study except for THA stations. At the same time, increased TSS concentrations in the southern stations may also be one of the reasons for the lower phytoplankton productivity. Previous studies also indicated that increasing TSS as a primary limiting factor by reducing light penetration resulted in lower phytoplankton abundance (Yuvaraj et al., 2018; Kumar et al., 2022). It is understood that NO_3– was the main factor that influenced the phytoplankton especially the pennate diatoms in the present study. The ability of diatoms to quickly absorb and store NO_3^- resulted in rapid growth (Cermeno et al., 2011), which could support fisheries by implementing artificial reefs. One earlier study also revealed the importance of fisheries production by maintaining good water quality, productivity and through the deployment of artificial reefs (Jha et al., 2022b).

Conclusion

The present study revealed that Ramanathapuram is an undisturbed coastal area due to fewer anthropogenic activities in the surrounding area. On the other hand, increased anthropogenic activities resulted in lower phytoplankton productivity in the Thoothukudi district. Increased TSS levels limited phytoplankton productivity in the southern stations. The present investigation revealed that the northern stations were found to be dominated by pennate diatoms due to higher NO_3^- concentrations. Comparatively higher metal concentrations in the northern stations could be attributed to anthropogenic discharges, which could pose a threat to fish and other seafood products if left unregulated. As these areas are highly dependent on the fishing industry, continuous monitoring will help identify the source of contamination and may promote the adoption of mitigation measures.

Data availability statement

The original contributions presented in the study are included in the article/Supplementary Material. Further inquiries can be directed to the corresponding author.

Author contributions

PSK: Conceptualization, sample collection, laboratory analysis, data processing, and writing-original manuscript. GD: Reviewing the manuscript, suggestion, and project administration, JS: Data validation, and manuscript review. DKJ: Data validation, and manuscript review. VP: Field investigation. SV: Field investigation. JPPJ: Reviewing the manuscript, suggestion. CM: Analysis of nutrient samples and data processing. RAJ: Data validation, suggestion, and manuscript review. All authors contributed to the article and approved the submitted version.

Acknowledgments

The authors are grateful to the Ministry of Earth Sciences, Government of India, for funding the present study. We are grateful to Dr. G. A. Ramadass, Director, NIOT, Chennai, for his continuous encouragement, support, and guidance. We would also like to thank the scientific and support staff of NIOT and NCCR for their field and laboratory assistance throughout the course of this study. Finally, we are thankful to our colleagues, Mr. S. Ragumaran, Mr. B. Ranjan Babu, and Mr. G. Nanadhagopal, for their kind support during the fieldwork.

Conflict of interest

The authors declare that the research was conducted in the absence of any commercial or financial relationships that could be construed as a potential conflict of interest.

The reviewer JE declared a shared affiliation with the author MC to the handling editor at the time of review.

Publisher's note

All claims expressed in this article are solely those of the authors and do not necessarily represent those of their affiliated organizations, or those of the publisher, the editors and the reviewers. Any product that may be evaluated in this article, or claim that may be made by its manufacturer, is not guaranteed or endorsed by the publisher.

Supplementary material

The Supplementary Material for this article can be found online at: https://www.frontiersin.org/articles/10.3389/fmars.2023.1215627/full#supplementary-material

References

Ananthan, G., Sampathkumar, P., Soundarapandian, P., and Kannan, L. (2004). Observations on environmental characteristics of Ariyankuppam estuary and Verampattinam coast of Pondicherry. *J. Aqua. Biol.* 19, 67–72.

Anbuselvan, N., Senthil Nathan, D., and Sridharan, M. (2018). Heavy metal assessment in surface sediments off Coromandel Coast of India: implication on marine pollution. *Mar. pollut. Bull.* 131, 712–726. doi: 10.1016/j.marpolbul.2018.04.074

APHA (2012). "Standard methods for the examination of water and wastewater," in *Total Suspended Solids Dried at 103–105, 22nd edition* (Washington, DC: APHA), 2–56.

Balasubramanian, T., Anantharaman, P., and Thangaradjou, T. (2011). "Seagrass productivity and mapping in the Gulf of Mannar Biosphere Reserve," in *Compendium of Research Findings on Biodiversity Conservation and Sustainable Use in the Gulf of Mannar Bioshere Reserve, Gulf of Mannar Biosphere Reserve Trust* (Ramnathapuram, India:Science Outreach Series), 1, 18–40.

Bharathi, M. D., Patra, S., Sundaramoorthy, S., Madeswaran, P., Chandrasekar, D., and Sundaramanickam, A. (2018). Seasonal variability in plankton food web composition in Tuticorin coastal waters, South east coast of India. *Mar. pollut. Bull.* 137, 408–417. doi: 10.1016/j.marpolbul.2018.10.042

Carrit, D. E., and Carpenter, J. H. (1966). Recommendation procedure for Winkler analyses of sea water for dissolved oxygen. *J. Plankton Res.* 24, 313–318.

Cermeno, P., Lee, J. B., Wyman, K., Schofield, O., and Falkowski, P. G. (2011). Competitive dynamics in two species of marine phytoplankton under non-equilibrium conditions. *Mar. Ecol. Prog. Ser.* 429, 19–28. doi: 10.3354/meps09088

Conama, (2003). *Proyecto def initivo de normas de calidad primaria para la protección de las aguas marinas* (Comisión Nacional de Medioambiente, Santiago, Chile), 20.

Dayala, V. T., Salas, P. M., and Sujatha, C. H. (2014). Spatial and seasonal variations of phytoplankton species and their relationship to physicochemical variables in the Cochin estuarine waters, Southwest Coast of India. *Ind. J. Mar. Sci.* 43, 937–947.

Grasshoff, K., Kremling, K., and Ehrhardt, M. (1999). Methods of seawater analysis -chapter 10- nutrients. *Methods Seawater Anal.*, 159–228. doi: 10.1002/9783527613984

Halpern, B. S., Walbridge, S., Selkoe, K. A., Kappel, C. V., Micheli, F., d'Agrosa, C., et al. (2008). A global map of human impact on marine ecosystems. *science* 319 (5865), 948–952.

Iscen, C. F., Emiroglu, O., Ilhan, S., Arslan, N., Yilmaz, V., and Ahiska, S. (2008). Application of multivariate statistical techniques in the assessment of surface water quality in Uluabat Lake, Turkey. *Environ. Monit. Assess.* 144, 269–276. doi: 10.1007/s10661-007-9989-3

Jarvie, H. P., Whitton, B. A., and Neal, C. (1998). Nitrogen and phosphorus in east coast Britishrivers: speciation, sources and biological significance. *Sci. Total Environ.* 210–211, 79–109. doi: 10.1016/S0048-9697(98)00109-0

Jha, D. K., Pandey, V., Muthukumar, C., Sathish Kumar, P., Venkatnarayanan, S., Jebakumar, J. P. P., et al. (2022a). Investigation of coastal water characteristics along the Southeast Coast of India: A multivariate approach. *Front. Mar. Sci.* 9, 269. doi: 10.3389/fmars.2022.945495

Jha, D. K., Pandey, V., Santhanakumar, J., Sathish Kumar, P., Venkatnarayanan, S., Jebakumar, J., et al. (2022b). Evaluation of site suitability for artificial reefs deployment in southeast coast of India using geographical information system as a management tool. *Front. Mar. Sci.* 8, 2028. doi: 10.3389/fmars.2021.817975

Jha, D. K., Ratnam, K., Rajaguru, S., Dharani, G., Devi, M. P., and Kirubagaran, R. (2019). Evaluation of trace metals in seawater, sediments, and bivalves of Nellore, Southeast coast of India, by using multivariate and ecological tool. *Mar. pollut. Bull.* 146, 1–10. doi: 10.1016/j.marpolbul.2019.05.044

Kumar, P. S., Kumaraswami, M., Rao, G. D., Ezhilarasan, P., Sivasankar, R., Rao, V. R., et al. (2018). Influence of nutrient fluxes on phytoplankton community and harmful algal blooms along the coastal waters of Southeastern Arabian Sea. *Cont. Shelf Res.* 161, 20–28. doi: 10.1016/j.csr.2018.04.012

Kumar, P. S., Venkatnarayanan, S., Pandey, V., Ratnam, K., Jha, D. K., Rajaguru, S., et al. (2022). Multivariate approach to evaluate the factors controlling the phytoplankton abundance and diversity along the coastal waters of Diu, Northeastern Arabian Sea. *Oceanologia* 64 (2), 267–275. doi: 10.1016/j.oceano.2021.11.005

Larson, C. A., and Belovsky, G. E. (2013). Salinity and nutrients influence species richness and evenness of phytoplankton communities in microcosm experiments from Great Salt Lake, Utah, USA. *J. Plankton Res.* 35 (5), 1154–1166. doi: 10.1093/plankt/fbt053

Marcarelli, A. M., Wurtsbaugh, W. A., and Griset, O. (2006). Salinity controls phytoplankton response to nutrient enrichment in the Great Salt Lake, Utah, USA. *Can. J. Fish. Aquat* 63 (10), 2236–2248. doi: 10.1139/f06-113

Mitbavkar, S., and Anil, A. C. (2008). Seasonal variations in the fouling diatom community structure from a monsoon influenced tropical estuary. *Biofouling* 24 (6), 415–426. doi: 10.1080/08927010802340317

Muthukumar, C., Balasubramaniyan, S., Garlapati, D., Bharathi, M. D., Kumar, B. C., James, R. A., et al. (2022). Impact of untreated sewage and thermal effluent discharges on the air-sea CO_2 fluxes in a highly urbanized tropical coastal region. *Mar. pollut. Bull.* 175, 113166. doi: 10.1016/j.marpolbul.2021.113166

Naqvi, S. W. A., De Souza, S. N., and Reddy, C. V. G. (1978). Relationship between nutrients and dissolved oxygen with special references to water masses in western Bay of Bengal. *Ind. J. Mar. Sci.* 7, 15–17.

Nixon, S. W. (1995). Coastal marine eutrophication: A definition, social causes, and future concerns. *Ophelia* 41, 199–219. doi: 10.1080/00785236.1995.10422044

Pandey, V., and Ganesh, T. (2019). Spatial and temporal variability of sandy intertidal macrobenthic communities and their relationship with environmental factors in a tropical island. *Estuar. Coast. Shelf Sci.* 224, 73–83. doi: 10.1016/j.ecss.2019.04.045

Pandey, V., Jha, D. K., Kumar, P. S., Santhanakumar, J., Venkatnarayanan, S., Jebakumar, J. P. P., et al. (2022). Effect of multiple stressors on the functional traits of sub-tidal macrobenthic fauna: A case study of the southeast coast of India. *Mar. pollut. Bull.* 175, 113355. doi: 10.1016/j.marpolbul.2022.113355

Parsons, T. R., Maita, Y., and Lalli, C. M. (1984). *A manual of chemical and biological methods for seawater analysis*. Pergamon Press, Oxford 173 pp.

Prakash, D., Tiwary, C. B., and Kumar, R. (2023). Ecosystem variability along the estuarine salinity gradient: A case study of hooghly river estuary, West Bengal, India. *J. Mar. Sci.* 11 (1), 88. doi: 10.3390/jmse11010088

Price, N. M., and Morel, F. M. M. (1991). Co-limitation of phytoplankton growth by nickel and ni- trogen. *Limnol. Oceanogr.* 36, 1071–1077. doi: 10.4319/lo.1991.36.6.1071

Rao, S. D. V., Rao, S. K., Iyer, C. S. P., and Chittibabu, P. (2008). Possible ecological consequences from the Sethu Samudram Canal Project, India. *Mar. pollut. Bull.* 56, 170–186. doi: 10.1016/j.marpolbul.2007.10.018

Sahu, B. K., Begum, M., Khadanga, M. K., Jha, D. K., Vinithkumar, N. V., and Kirubagaran, R. (2013). Evaluation of significant sources influencing the variation of physico chemical parameters in Port Blair Bay, South Andaman, India by using multivariate statistics. *Mar. pollut. Bull.* 66, 246–251. doi: 10.1016/j.marpolbul.2012.09.021

Sahu, G., Satpathy, K. K., Mohanty, A. K., and Sarkar, S. K. (2012). Variations in community structure of phytoplankton in relation to physicochemical properties of coastal waters, Southeast Coast of India. *Indian J. Mar. Sci.* 41, 223–241.

Satpathy, K. K., Mohanty, A. K., Sahu, G., Sarguru, S., Sarkar, S. K., and Natesan, U. (2011). Spatio-temporal variation in physico-chemical properties of coastal waters off Kalpakkam, Southeast Coast of India, during summer, pre-monsoon and post-monsoon period. *Environ. Monit. Assess.* 180, 41–62. doi: 10.1007/s10661-010-1771-2

Shanthi, R., Poornima, D., Raja, S., Sethubathi, G. V., Thangaradjou, T., Balasubramanian, T., et al. (2013). Validation of OCM-2 sensor performance in retrieving chlorophyll and TSM along the Southwest Bay of Bengal coast. *J. Earth Syst. Sci.* 122, 479–489. doi: 10.1007/s12040-013-0286-y

Sin, Y., Wetzel, R. L., and Anderson, I. C. (1999). Spatial and temporal characteristics of nutrient and phytoplankton dynamics in the York River estuary, Virginia: analyses of long-term data. *Estuaries* 22, 260–275. doi: 10.2307/1352982

Smith, V. H., Tilman, G. D., and Nekola, J. C. (1999). Eutrophication: impacts of excess nutrient inputs on freshwater, marine, and terrestrial ecosystems. *Environ. pollut.* 100 (1-3), 179–196. doi: 10.1016/S0269-7491(99)00091-3

Specchiulli, A., Scirocco, T., Cilenti, L., Florios, M., Renzi, M., and Breber, P. (2010). Spatial and temporal variations of nutrients and chlorophyll a in a Mediterranean coastal lagoon: Varano Lagoon, Italy. *Transit. Water Bull.* 2, 49–62.

Subrahmanyan, R. (1946). A systematic account of the marine plankton diatoms of the Madras coast. *Proc. Indian Acad. Sci.* 24, 85-197.

Subrahmanyan, R. (1959). Studies on the phytoplankton of the west coast of India. parts I and II. *Proc. Indian Acad. Sci.* 50B, 113-187.

Tas, B., and Gonulol, A. (2007). An ecologic and taxonomic study on phytoplankton of a shallow lake, Turkey. *J. Environ. Biol.* 28, 439.

Tomas, C. R. (1997). San Diego. Academic Press, California: Identifying Marine Phytoplankton.

Trombetta, T., Vidussi, F., Mas, S., Parin, D., Simier, M., and Mostajir, B. (2019). Water temperature drives phytoplankton blooms in coastal waters. *PLoS One* 14 (4), e0214933. doi: 10.1371/journal.pone.0214933

USEPA (2001). *Methods for Collection, Storage and Manipulation of Sediments for Chemical and Toxicological Analyses: Technical Manual. EPA-823-B-01-002* (Washington, DC: Office of Water).

Utermöhl, H. (1958). Zur vervollkommnung der quantitativen phytoplankton Methodik. *Mitt. int. Ver. ther. angew. Limnol.* 9, 1–38.

Wu, N., Schmalz, B., and Fohrer, N. (2011). Distribution of phytoplankton in a German lowland river in relation to environmental factors. *J. Plankton Res.* 33 (5), 807–820. doi: 10.1093/plankt/fbq139

Wu, M. L., Wang, Y. S., Sun, C. C., Wang, H., Dong, J. D., Yin, J. P., et al. (2010). Identification of coastal water quality by statistical analysis methods in Daya Bay, South China Sea. *Mar. pollut. Bull.* 60, 852–860. doi: 10.1016/j.marpolbul.2010.01.007

Xu, H., Paerl, H. W., Qin, B., Zhu, G., and Gao, G. (2010). Nitrogen and phosphorus inputs control phytoplankton growth in Eutrophic Lake. *Limno. Oceanogr.* 55, 420e432. doi: 10.4319/lo.2010.55.1.0420

Yuvaraj, P., Satheeswaran, T., Damotharan, P., Karthikeyan, V., Jha, D. K., Dharani, G., et al. (2018). Evaluation of the environmental quality of Parangipettai, Southeast Coast of India, by using multivariate and geospatial tool. *Mar. pollut. Bull.* 131, 239–247. doi: 10.1016/j.marpolbul.2018.04.022

Zhou, F., Guo, H. C., Liu, Y., and Jiang, Y. M. (2007). Chemometrics data analysis of marine water quality and source identification in Southern Hong Kong. *Mar. pollut. Bull.* 54, 745–756. doi: 10.1016/j.marpolbul.2007.01.006

Zhou, M. J., Shen, Z. L., and Yu, R. C. (2008). Responses of a coastal phytoplankton community to increased nutrient input from the Changjiang (Yangtze) River. *Cont. Shelf Res.* 28 (12), 1483–1489. doi: 10.1016/j.csr.2007.02.009

frontiers | Frontiers in Marine Science

TYPE Original Research
PUBLISHED 23 August 2023
DOI 10.3389/fmars.2023.1206332

OPEN ACCESS

EDITED BY
Dilip Kumar Jha,
National Institute of Ocean Technology, India

REVIEWED BY
Gopalakrishnan Thilagam,
Pachaiyappa's College for Men, India
Gajendra Joshi,
National Institute of Ocean Technology, India
Naseera Kottangodan,
National Institute of Ocean Technology, India

*CORRESPONDENCE
Wenhua Liu
whliu@stu.edu.cn

RECEIVED 15 April 2023
ACCEPTED 07 August 2023
PUBLISHED 23 August 2023

CITATION
Wang L, Zhao H, Sanganyado E, Liang B, Chen X, Ma Q, Lin J and Liu W (2023) B vitamins supplementation induced shifts in phytoplankton dynamics and copepod populations in a subtropical coastal area. *Front. Mar. Sci.* 10:1206332. doi: 10.3389/fmars.2023.1206332

B vitamins supplementation induced shifts in phytoplankton dynamics and copepod populations in a subtropical coastal area

Lin Wang[1,2], Hancheng Zhao[1], Edmond Sanganyado[3], Bo Liang[1], Xiaohan Chen[1], Qun Ma[1], Jianqing Lin[1] and Wenhua Liu[1]*

[1]Guangdong Provincial Laboratory of Marine Biotechnology, Institute of Marine Sciences, Shantou University, Shantou, China, [2]College of Chemical and Environmental Engineering, Hanshan Normal University, Chaozhou, China, [3]Department of Applied Chemistry, Northumbria University, Newcastle upon Tyne, United Kingdom

Introduction: B vitamins play a crucial role in shaping phytoplankton and zooplankton communities in marine ecosystems, yet their impact on community dynamics remains poorly understood.

Methods: We carried out *in situ* incubation experiments of B vitamins supplementation to explore the response pattern of phytoplankton and zooplankton community compositions.

Results: The results showed that vitamins B_1, B_2, B_6 and B_{12} promoted the growth of phytoplankton, and the total Chl α in 87.5% of the supplemented B vitamin treatments showed a significant positive response ($p < 0.05$). Supplementation with these B vitamins significantly altered the community composition of phytoplankton, and 75% of the B vitamin-supplemented treatments showed an increase in the relative abundance of *Minutocellus*, Thalassiosirales, *Odontella*, Prymnesiales and *Ditylum*, considered mainly to be the result of B vitamin auxotrophy. In contrast, a significant decrease in Copepoda, including Calanoida and Cyclopoida, was observed in 87.5% of treatments. The observed shifts in community composition were attributed to the auxotrophy of certain diatoms and Prymnesiales for B vitamins. These shifts subsequently led to negative correlations (Spearman Rho < -0.8) between the abundance of these phytoplankton species and Copepoda populations.

Discussion: These findings advance our understanding of the complex interactions between micronutrient availability and plankton community dynamics.

KEYWORDS

B vitamins, phytoplankton communities, copepods, auxotrophy, plankton dynamics

1 Introduction

B vitamins are water-soluble micronutrients and act as key coenzyme factors in catalyzing many important biochemical reactions in biological central metabolism. These reactions include C-C bond rearrangement reduction and methyl transfer reactions, deoxyribose/fatty acid/carbohydrate/branched amino acid synthesis, electron transfer in redox reactions and the fixation of CO_2 (Matthews et al., 2003; Frank et al., 2007; Dowling et al., 2012; Waldrop et al., 2012). For the past few decades, scientists have been studying the production, transfer, and circulation of nutrients in the ocean. However, previous studies have focused on the roles of C, N, P and Si in the regulation of marine ecological processes (Sañudo-Wilhelmy et al., 2014). The importance of vitamin B in aquatic products was first considered in the early 20th century (Helliwell, 2017). B vitamins in the ocean are mainly derived from bacteria and/or phytoplankton. Croft et al. (2006) showed that 76% of the 400 marine bacteria surveyed synthesized vitamin B_1, and 50% of sequenced phytoplankton had B_1 synthesis pathways. Vitamin B_2 and B_6 can be synthesized by plants and bacteria (Monteverde et al., 2017). 78% of marine bacteria and some of phytoplankton in Sañudo-Wilhelmy et al. (2014) had a pathway to synthesize vitamin B_7 *de novo*. However, it was generally believed that eukaryotic couldn't synthesize vitamin B_{12}(Bertrand et al., 2011; Helliwell, 2017). It could only be synthesized by some bacteria and archaea (Rodionov et al., 2002). At the same time, B vitamins auxotrophy were also widespread in the ocean (Croft et al., 2006; Sañudo-Wilhelmy et al., 2014). Without an exogenous source of B vitamins, some effects can occur: impaired central metabolism of organisms deficient in B vitamins, blocked cell growth, and significant impacts on many biological processes in the ocean. These processes include primary productivity, phytoplankton community structure, and biocarbon pumps (Giovannoni, 2012; Sañudo-Wilhelmy et al., 2012; Monteverde et al., 2017).

Marine microbial loop supplements to the main food chain. As the main energy flow path in the sea, it converts dissolved organic matter difficult to transfer into granular organic matter, and then return it to the main food chain (Nichols, 2003; Pomeroy et al., 2007). Phytoplankton, which are primary producers in the ocean, play a key role in the microbial loop; however, their growth and reproduction are affected by certain B vitamins. Previous studies have shown that although vitamin B_{12} cannot be synthesized by phytoplankton *de novo*, more than half of phytoplankton species require it (Croft et al., 2005; Croft et al., 2006; Watanabe and Bito, 2018). While most phytoplankton species are deficient of vitamin B_1, it is produced by most diatoms (Tang et al., 2010; Heal et al., 2017). Previous field and laboratory nutrient amendment studies showed that the availability of vitamins B_1 and B_{12} strongly affected the abundance and community composition of phytoplankton and bacteria (Sañudo-Wilhelmy et al., 2006; Bertrand et al., 2011; King et al., 2011; Koch et al., 2011; Koch et al., 2012; Joglar et al., 2020; Joglar et al., 2021). Some phytoplankton rely on B_7 during their growth process (Helliwell, 2017).

Zooplankton feed on phytoplankton, bacteria and debris, and also food for fish and other aquatic animal, thus act as an important link in the vertical circulation of marine nutrients (Chiba et al., 2018; Abo-Taleb, 2019). In addition, due to their small size and short life cycle, zooplankton are very sensitive to environmental stress, with their biomass and community structure altering significantly following a disturbance. These changes alter nutrient linkages in marine microbial food webs, affecting fish and other marine animal stocks (Chiba et al., 2018; Srichandan et al., 2021). Several fish species, such as bighead carp, herring, mackerel, various juvenile fishes and baleen whales rely on zooplankton, particularly Copepoda, as a food source. In fact, the yield of herring in Europe was shown to be closely related to the abundance and distribution of Copepoda (Bils et al., 2022; Randall et al., 2022).

However, most studies of phytoplankton and bacterial responses to B vitamins are only limited to vitamins B_1 and B_{12}. There is little coverage of the effect of other B vitamins. Moreover, most studies have focused on the factors influencing transfer dynamics of B vitamins from phytoplankton and bacteria to zooplankton (e.g., seasonal variations (Fridolfsson et al., 2019), species variations (Fridolfsson et al., 2020), and local environmental conditions (Majaneva et al., 2020). Knowledge on the effects of B vitamins on zooplankton abundance and community compositions, especially for Copepoda, remains scarce. In this context, we conducted a series of *in situ* experiments to evaluate the response of prokaryote, phytoplankton and Copepoda biomasses/relative abundance to the addition of B_1, B_2, B_6 and B_{12}. The aims of our study were to explore the effects of different B vitamins on phytoplankton biomass and community composition and, more importantly, to further analyze the roles of B vitamins on the growth limitation of Copepoda.

2 Materials and methods

2.1 Study site

Fieldwork and sampling were conducted at the coastal experimental station of Shantou University, located on Nan'ao Island (23.48°N, 117.11°E, Figure 1), Guangdong, China: Shantou. Nan'ao Island features multiple bays with typical tropical and subtropical characteristics. Its surrounding waters exhibit complex hydrological conditions (Cai et al., 2011; Shu et al., 2018) due to the influence of surface runoff from the Hanjiang and Huanggang Rivers and upwelling from the Taiwan Shoal, which usually occurs in summer (June to September) (Jiang & Wang, 2018; Huang et al., 2021). These unique current conditions promote rich marine life. Enrichment experiments were conducted in autumn (November 2020) and spring (April 2021) to capture diverse initial ecological conditions.

2.2 Experimental design

Surface water samples (1 m depth) for enrichment experiments were collected using Niskin metal-free bottles. Chlorophyll α (Chl α), B vitamins, and microbial plankton community samples were obtained at the beginning (day 0). Portable hand-held water quality meters (HACH, USA) measured physicochemical indices such as

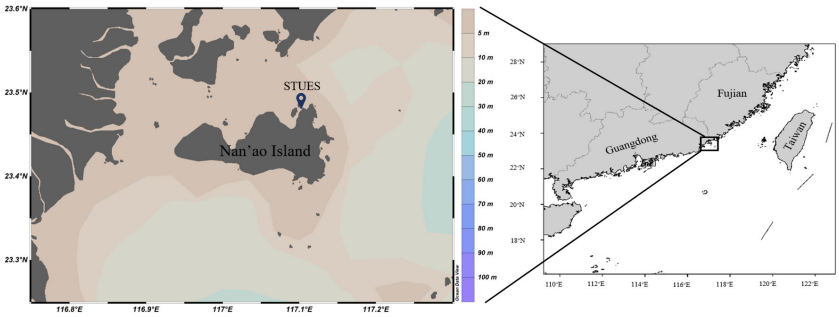

FIGURE 1
The location of the experimental site (STUES, Shantou University Experimental Station).

pH, DO, temperature, and salinity. Subsequently, 300 mL of seawater was filtered through a 200 µm mesh to remove larger zooplankton and debris and added to photosynthetically active radiation (PAR) and ultraviolet radiation (UVR) transparent, sterile, and nontoxic (Whirl-Pak) bags along with nutrients or B vitamins, as shown in Table 1. The bags and nutrient concentrations were consistent with those used in previous enrichment experiments (Martínez-García et al., 2010; Joglar et al., 2020). The added amounts of B_1, B_2, B_6, and B_{12} were approximated to the maximum concentrations observed in earlier studies (Sañudo-Wilhelmy et al., 2006; Sañudo-Wilhelmy et al., 2012; Heal et al., 2014). Each treatment had five replicates. Experimental bags were incubated *in situ* in coastal floating cages at a depth of 1 m for 5 days. Untreated groups served as control treatments (C) alongside B vitamin addition treatments, while inorganic nutrient addition was set as another control treatment (I) with inorganic nutrients and B vitamin addition treatments.

2.3 Size-fractionated chlorophyll α (Chl α)

The Chl α concentration was measured initially and after a 5-day incubation. Seawater samples (300 mL) were sequentially filtered through 3 and 0.2 µm Millipore polycarbonate (PC) filters, which were then frozen at -20 °C until analysis. Chl α extraction involved 90% acetone and 5 minutes of vortexing, followed by overnight storage in darkness at 4 °C. Finally, samples were analyzed using a spectrophotometer (General Administration of Quality Supervision et al., 2007, China).

2.4 B vitamins

2.4.1 Dissolved B vitamin preconcentration

Dissolved B vitamin samples were collected on day 0 and day 5 of the enrichment experiments, filtered through 0.2 µm Millipore polycarbonate (PC) filters, and stored at -20 °C until further analysis. Dissolved B vitamins were determined following the methods described by Sañudo-Wilhelmy et al. (Sañudo-Wilhelmy et al., 2012) and Heal et al. (Heal et al., 2014), with minor modifications. Samples (300 mL) were adjusted to pH 5.5-6.5 using 1 M HCl and preconcentrated with HLB solid-phase extraction columns (500 mg, 6 mL, Shimadzu) at a rate of 1 mL min^{-1} using a peristaltic pump with tygon tubing. Columns were rinsed with 20 mL of Milli-Q water to remove salts and eluted with 20 mL HPLC grade methanol. Eluents were dried under clean N_2 gas without heat and reconstituted in 500 µL of Milli-Q water. Samples were stored at −20°C until UHPLC/MS/MS analysis within 24 h. Preconcentration was conducted in the dark to minimize photodegradation.

TABLE 1 List of amendment treatments: (1) control treatment (C), no nutrients added; (2) vitamin B_1 treatment (B_1), 500 pM; (3) vitamin B_2 treatment (B_2), 500 pM; (4) vitamin B_6 treatment (B_6), 500 pM; (5) vitamin B_{12} treatment (B_{12}), 100 pM; (6) inorganic nutrients treatment (I), 5 µM nitrate, 5 µM ammonium, 1 µM phosphate, 5 µM silicate; (7) inorganic nutrients and vitamin B_1 treatment (IB_1); (8) inorganic nutrients and vitamin B_2 treatment (IB_2); (9) inorganic nutrients and vitamin B_6 treatment (IB_6); (10) inorganic nutrients and vitamin B_{12} treatment (IB_{12}).

Treatment	Nutrient	Concentration
(1) Control (C)	None	–
(2) Vitamin B_1 (B_1)	B_1	500pM
(3) Vitamin B_2 (B_2)	B_2	500pM
(4) Vitamin B_6 (B_6)	B_6	500pM
(5) Vitamin B_{12} (B_{12})	B_{12}	100pM
(6) Inorganic nutrients (I)	NO_3^-	5µM
	NH_4^+	5µM
	HPO_4^{2-}	1µM
	SiO_4^{2-}	5µM
(7) I+B_1 (IB_1)	I	Same as treatment (6)
	B_1	500pM
(8) I+B_2(IB_2)	I	Same as treatment (6)
	B_2	500pM
(9) I+B_6(IB_6)	I	Same as treatment (6)
	B_6	500pM
(10) I+B_{12}(IB_{12})	I	Same as treatment (6)
	B_{12}	100pM

2.4.2 Particulate B vitamin extraction

Particulate B vitamin extraction followed the method described by Suffridge et al. (Suffridge et al., 2017). Frozen filters were placed in 15 mL thick-walled polypropylene centrifuge tubes containing 5 mL of lysis solution (5% methanol solution, pH adjusted to 3.5) and 2 mL of 0.5 mm zirconia beads. Samples were vortexed for 5 min and placed in an ice bath for 1 min to maintain a temperature below 30°C, and this process was repeated six times. After cell lysis, samples were incubated in a dark water bath at 30 °C for 30 min to fully extract target analytes. Liquid phase extraction (LPE) removed hydrophobic components from cell lysates using chloroform (5 mL), vigorous shaking for 3 min, and centrifugation at 5000 rpm for 10 min. The aqueous phase was transferred to a new centrifuge tube, and the extraction process was repeated. Sample pH was adjusted to 6.5 after liquid extraction, filtered into a brown bottle with a 0.22 μm filter, and stored at -20 °C until UHPLC–MS/MS analysis.

2.4.3 HPLC–MS/MS analysis

B_1, B_2, B_6, and B_{12} were quantitatively detected using a UHPLC–MS/MS system. Standards for B_1 (thiamine hydrochloride), B_2 (riboflavin), B_6 (pyridoxine), and B_{12} (cyanocobalamin) were purchased from Sigma Aldrich. A Thermo Scientific Ultimate 3000 UHPLC system with an Agilent Zorbax Eclipse Plus C18 column (2.1×100 mm, 3.5-micron) at 30 °C separated B vitamins. A 17-min gradient flow was employed with mobile phases of acetonitrile (solvent A) and 0.1% formic acid solution (solvent B). The flow rate was set at 0.3 mL min^{-1}, and the sample injection volume was 100 μL. A Thermo Scientific TSQ Endura triple quadrupole mass spectrometer operating in selective response monitoring (SRM) mode with positive polarity was used for mass spectrometry. The H-ESI spray voltage was set at 3000 V, with sheath gas and aux gas velocities at 35 Arb and 10 Arb, respectively. The ion transfer tube and vaporizer temperatures were maintained at 325 °C and 300°C, respectively. SRM specifications are detailed in Table 2. Average B vitamin recovery percentages after preconcentration and extraction of B-vitamin-spiked samples, as well as their limits of detection (LOD) and limits of quantitation (LOQ), are presented in Table 3.

2.5 Phytoplankton and zooplankton communities

Samples were filtered through 0.22 μm polycarbonate filters, immediately frozen in liquid nitrogen, and stored at -80 °C until analysis. Phytoplankton and zooplankton communities were assessed by sequencing the entire 18S rRNA gene (18S rDNA). DNA extraction was performed using the PowerSoil DNA Isolation Kit (MoBio Laboratories Inc., CA, USA) following the kit's instructions. Eukaryotes were amplified using the primers "Euk-A: AACCTGGTT GATCCTGCCAGT and Euk-B: GATCCTTCTGCAGGTTCAC CTAC"(Countway et al., 2005). The KOD One PCR Master Mix (TOYOBOLife Science) was used to perform 25 cycles of PCR amplification, with initial denaturation at 95°C for 5 min, followed by 25 cycles of denaturation at 95°C for 30 s, annealing at 50°C for 30 s, and extension at 72°C for 1 min, and a final step at 72°C for 7 min. Amplified regions were sequenced with the PacBio platform at Biomarker Technologies (Beijing, China). CCS sequences were derived from the original data, and chimeras were removed to obtain effective CCS. Effective CCS sequences were clustered/denoised, OTUs/ASVs (features) were classified, and species classification was obtained according to feature sequences. The coverages of the samples ranged from 0.9936 to 0.9998. Finally, the SILVA reference database was used for taxonomic assignment of 18S ASVs through the Naive Bayes classifier combination comparison method.

2.6 Statistical analysis

Response ratios (RRs) were calculated to intuitively illustrate the responses of phytoplankton and bacteria to B vitamin supplementation (Barber-Lluch et al., 2019; Joglar et al., 2020). Phytoplankton and bacterial biomass of B vitamin amendment treatments were divided by control treatment values, and when combined with inorganic nutrients and B vitamins, treatments were divided by inorganic nutrient (I) treatment values. RR values >1 indicate a positive response, RR values = 1 imply no response, and RR values <1 signify a negative response; the further RR values deviate from 1, the more pronounced the response. One-way ANOVA and *t*-tests were employed to test significant differences between treatments. Principal coordinates analysis (PCoA) and non-metric multidimensional scaling (NMDS) were used to display community composition differences across seasons at the OTU level. Pearson/Spearman correlation analysis and redundancy analysis (RDA) were employed to assess correlations between specific copepods and phytoplankton. Detrended correspondence analysis (DCA) for biological data was applied to determine whether to use linear or unimodal ordination methods. Correlation networks were constructed using OmicStudio tools at https://www.omicstudio.cn/tool. All statistical analyses were considered significant at the 0.05 significance level.

TABLE 2 MS conditions and retention times for each analyte.

Compound	SRM Precursor-product (m/z)	Collision Energy (V)	RF Lens (V)	Retention Time (min)
B_1	265- 122, 144, 81	10, 10, 26	77	1.24
B_2	377- 243, 198, 172	19, 32, 32	150	1.69
B_6	170- 152, 134, 77	10, 16, 30	82	1.37
B_{12}	678- 912, 998, 636	32, 19, 18	198	1.40

TABLE 3 Recoveries, limits of detection and limits of quantification of each analyte.

Compound	Dissolved VB Recovery (%)	Particle VB Recovery (%)	LOD(pM)	LOQ(pM)
B_1	98.30 ± 14.64	98.83 ± 13.11	2.40	8.01
B_2	98.17 ± 16.14	94.57 ± 5.01	1.81	6.04
B_6	87.69 ± 7.47	96.87 ± 1.38	1.83	6.09
B_{12}	96.08 ± 8.88	86.94 ± 8.17	7.38	24.59

3 Results

3.1 Initial conditions at the experimental site

The initial environmental conditions in November and April were compared to assess changes in hydrographic and biochemical conditions during the *in situ* amendment experiments (Table 4). Differences in pH, temperature, dissolved oxygen, and salinity were observed between the two months, with November having slightly lower temperature salinity. Phytoplankton biomass was 1.16 times higher in April, particularly for smaller phytoplankton, which were 2.44 times higher in April. The B vitamin content in the experimental field exhibited seasonal variation, with B_1 and B_2 concentrations 37.08% and 80.14% lower in November than in April, while B_6 and B_{12} concentrations were 3.03 times and 5.92 times higher in November, respectively.

3.2 Changes in phytoplankton biomass and community composition

The total chlorophyll α (Chl α) was measured to assess phytoplankton biomass (Figure 2A). After the end of the experiments, the phytoplankton biomass of all treatments increased significantly in November compared with the initial biomass (T0), and the total Chl α ranged from 12.10-29.52 μg L^{-1}, while that in April was only 0.64-4.58 μg L^{-1}. In 87.5% of the eight treatments supplemented with B vitamins, total Chl α showed significant positive responses compared to the control treatment (ANOVA, $p < 0.05$). In terms of response rate (RR) (Figure 2B), the range of positive RR of treatments in November was 1.22-2.08, while in April, the highest was as high as 7.12, and the average positive RR was 3.75. The positive response ratios in April were 1.54-8.96 times higher than those in November (Figure 2B). Only 50% of treatments comprising a mixture of B vitamins and inorganic nutrients had a slight secondary response, and there were IB_1 and IB_6 treatments with RRs slightly greater than 1. The response rates of IB_2 and IB_{12} were less than 1, indicating that there was no secondary response of phytoplankton to vitamin B in these two treatments.

Analysis of different particle sizes of phytoplankton revealed that smaller phytoplankton (0.22-3 μm) exhibited strong positive responses to B vitamins in November treatments and mixed inorganic nutrients and B vitamins treatments in April, regardless of inorganic nutrient levels. The average Chl α (0.22-3 μm) RR of the treatments supplemented with B vitamins reached 4.27 in November, and that of the mixed inorganic nutrients and B vitamins treatments in April was 3.83 (Figure 2C). Conversely, larger phytoplankton (> 3 μm) showed stronger positive responses in the April than in the November experiments, with a maximum Chl α (> 3 μm) RR of 12.18 in April (Figure 2D). These findings suggest that B_1, B_2, B_6, and B_{12} vitamins may ultimately limit phytoplankton growth in the marine environment.

Community composition analysis revealed the impact of vitamin B supplementation on phytoplankton communities. The initial community compositions differed between November and April, with diatoms dominating in November and *Picochlorum* dominating in April. In both seasons, B vitamin supplemented treatments showed increases in the relative abundance of several phytoplankton compared to the control treatments, such as Thalassiosirales, *Odontella* in B_6 and B_{12} treatments, Prymnesiales, Thalassiosirales and Ditylum in B_1 treatment, *Minutocellus* in B_2 treatment in November (Figure 3A), and then *Picochlorum* in both of the B vitamin supplemented treatments in April (Figure 3B). Principal coordinate analysis (PCoA) and nonmetric multidimensional scaling (NMDS) based on Bray –Curtis distance at the endpoint of each experiment confirmed that the community composition of phytoplankton in each treatment was obviously different from that in the control treatment after B vitamin supplementation (Figures 4A-1, 2). The points of each B vitamin treatment in PCoA and NMDS were far from the points represented by the control treatment. These results demonstrate that B vitamins have a substantial impact on phytoplankton community composition.

TABLE 4 Water quality data and vitamin B content for experimental initial states in two months.

	pH	Temperature°C	DO mg L^{-1}	Salinity	Chl a μg L^{-1}			B_1 pM	B_2 pM	B_6 pM	B_{12} pM
					0.2-3 μm	>3 μm	Total				
November	8.12	22.1	8.77	33.99	0.3179	0.9216	1.2395	3.222	9.4277	6.7762	1.3900
April	8.05	24.1	8.39	34.52	1.0924	1.5818	2.6742	5.1207	47.4730	1.6826	0.2008

10.3389/fmars.2023.1206332

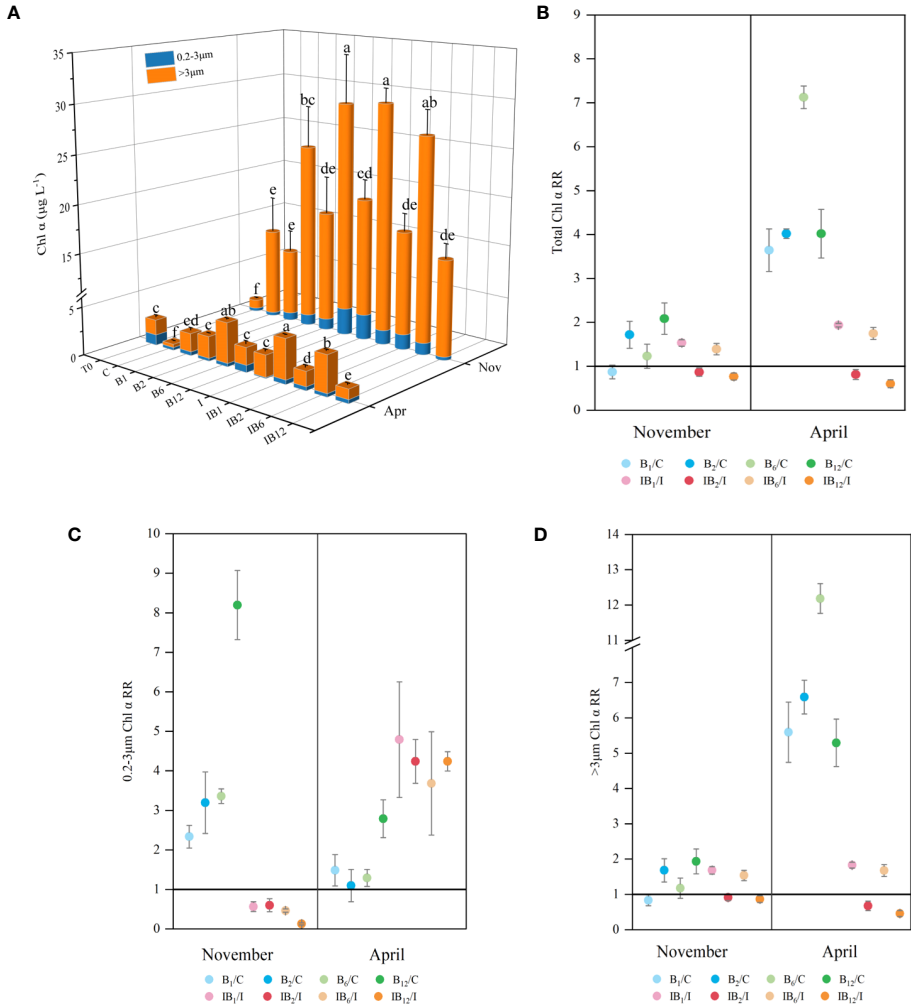

FIGURE 2
Chlorophyll α concentration (μg L^{-1}) and response ratio (RR) of Chl α for each treatment. **(A)** Chlorophyll α concentration; **(B)** Response ratios of total Chl α; **(C, D)**: Response ratios of size-fractionated Chl α. The value of RR >1 means a positive response, and the value of RR = 1 implies no response, while RR <1 shows a negative response, and the farther the RR is from 1, the more obvious the response is. Among them, the treatments of adding B vitamins alone were compared with the control group, and the treatments of adding inorganic nutrients and B vitamins were compared with the treatment of inorganic nutrients. Different alphabets above columns in **(A)** denote significant differences ($p < 0.05$) between treatments. The bars in the **(B–D)** indicates standard error of mean.

3.3 Changes in zooplankton community composition

The initial community compositions of the identified zooplankton were similar in the two experimental seasons, with Calanoida (Copepoda) predominating, which was not the case with phytoplankton. In addition, their relative abundances were at low levels, at 0.2 in November and less than 0.02 in April. However, compared with the C treatment, the relative abundance of identified zooplankton in 87.5% of the treatments supplemented with B vitamins had negative responses (Figure 3). Calanoida showed a decrease in the B_1 and B_6 treatments, which decreased to almost undetectable levels in November. The decline also occurred in April, when the relative abundance of Cyclopoida and *Paracalanus* sharply decreased in all B vitamin treatments, and the maximum reduction was in the B_1 treatment, decreasing to less than 0.02, while that of the C treatment was greater than 0.8.

We also used PCoA and NMDS analysis to show the differences in identified zooplankton communities between experiments (Figures 4B-1, 2). The first principal coordinate explained 53.08% and 58.47% of the total variation in November and April, respectively, and the second principal coordinate explained 25.53% and 26.28% of the total variation in November and April, respectively. Both stress values of the NMDS analysis were less than 0.01. Accordingly, significant differences between B vitamin treatments and C treatments were observed. Besides, we used RDA analysis to show the relationship between specific phytoplankton and zooplankton as the first axis lengths of gradient in the DCA analysis is less than 3.0. The RDA results showed that different patterns of response in phytoplankton and zooplankton to B-vitamin amendments appeared to be mostly explained by the certain phytoplankton and zooplankton (Figure 5). In details, Calanoida dominated the plankton community changes in the vitamin B_2 treatments, while

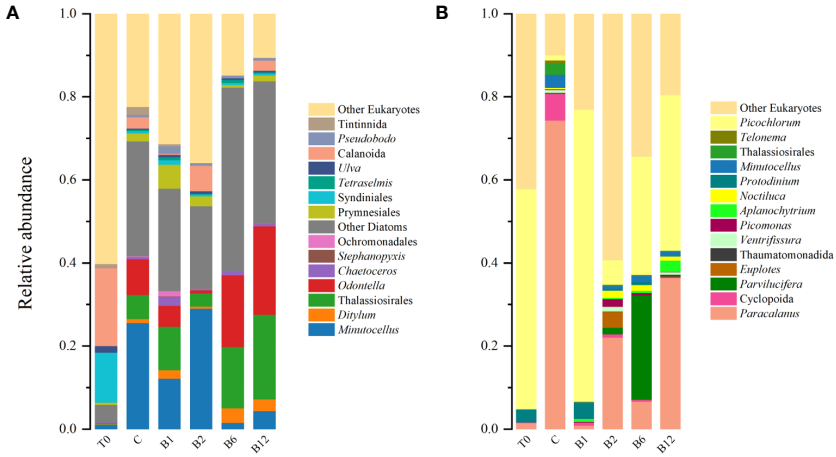

FIGURE 3
Relative abundance of sequence reads assigned to the major taxonomic groups of eukaryotes at the initial (T0) and endpoint of control treatment (C) and each B vitamins supplementation experiment conducted **(A)** in November and **(B)** in April.

Thalassiosirales, *Ditylum*, *Odontella*, *Chaetoceros* dominated the plankton community changes in the vitamin B_1, B_6, and B_{12} treatments in November. The changes of plankton community composition in the B vitamins treatments in April were mostly dominated by *Paracalanus*, *Protodinium* and *Picochlorum*. At the same time different correlations were observed between different species of zooplankton and phytoplankton, most phytoplankton species showed negative correlation with zooplankton, such as Calanoida with Thalassiosirales, *Ditylum*, *Odontella*, Prymnesiales and *Chaetoceros* in November (Figure 5A), *Paracalanus* with *Protodinium* and *Picochlorum* in April (Figure 5B).

4 Discussion

4.1 B vitamin auxotrophy may dominate the changes in phytoplankton communities

Our study highlights the importance of B vitamins, including B_2 and B_6, in addition to B_1 and B_{12}, in stimulating phytoplankton growth. These findings challenge the conventional belief that only B_1 and B_{12} are significant to phytoplankton (Barber-Lluch et al., 2019; Joglar et al., 2020). Additionally, our results demonstrate distinct response patterns among phytoplankton of different sizes in relation to B vitamins. For example, since the inorganic nutrient content was higher in spring and lowest in autumn in the experimental area, the probability of nitrogen restriction in autumn is higher than that in spring (Ke et al., 2019; Chen et al., 2020). Therefore, smaller phytoplankton (0.22-3 μm) exhibited strong positive responses to B vitamins in the autumn when inorganic nutrition was relatively limited, suggesting that they may have an advantage in the absorption and assimilation of B_1, B_2, B_6, and B_{12} under nutrient-limited conditions (Koch et al., 2012; Fridolfsson et al., 2019). In contrast, larger phytoplankton (> 3 μm) were mainly limited by inorganic nutrients under nutrient-limited conditions, exhibiting less pronounced responses to B vitamin supplementation. However, when inorganic nutrients were abundant, larger phytoplankton outcompeted smaller species, and vitamin B limitation emerged as the primary constraint (Gobler, 2007). The observed limitation of single B vitamins in spring implies that organic micronutrient reserves may be insufficient during more productive seasons (Barber-Lluch et al., 2019).

Previous studies have found that vitamin B_1 (Barber-Lluch et al., 2019; Joglar et al., 2020) and B_{12} (Sañudo-Wilhelmy et al., 2006; Koch et al., 2011; Barber-Lluch et al., 2019) supplementation increased phytoplankton biomass. There is widespread auxotrophy for B vitamins among phytoplankton (Giovannoni, 2012; Sañudo-Wilhelmy et al., 2014). In fact, most phytoplankton (80%) are auxotrophic for B_1 (Croft et al., 2006; Paerl et al., 2015), and 50% of sequenced phytoplankton, including most diatoms, possess a pathway for B_1 synthesis (Sañudo-Wilhelmy et al., 2014). Our study observed an increased relative abundance of diatom species (Thalassiosirales, *Chaetoceros*, and *Ditylum*) and Prymnesiales following B_1 supplementation. However, eukaryotic phytoplankton are widely believed to be incapable of *de novo* B_{12} synthesis (Bertrand and Allen, 2012; Helliwell, 2017), and more than half of marine phytoplankton require B_{12}, indicating widespread B_{12} auxotrophy in the ocean (Tang et al., 2010). *Chaetoceros*, *Ditylum*, and Thalassiosirales have also been reported as B_{12} auxotrophs (Croft et al., 2006), which accounts for the increase in the relative abundance of these species following B_{12} supplementation observed in this study and another (Koch et al., 2011).

Limited information exists about B_2 and B_6 auxotrophy, but our study demonstrated changes in phytoplankton community composition following their supplementation. We hypothesize that *Chaetoceros, Ditylum*, and Thalassiosirales may also be B_6 auxotrophs, given the similarity of their relative abundance trends in the B_1 and B_{12} treatments. In contrast, the relative abundance of *Minutocellus* decreased in most treatments compared to the control, which suggests that they might not have significant B vitamin dependence. The increase in *Picochlorum* abundance in April

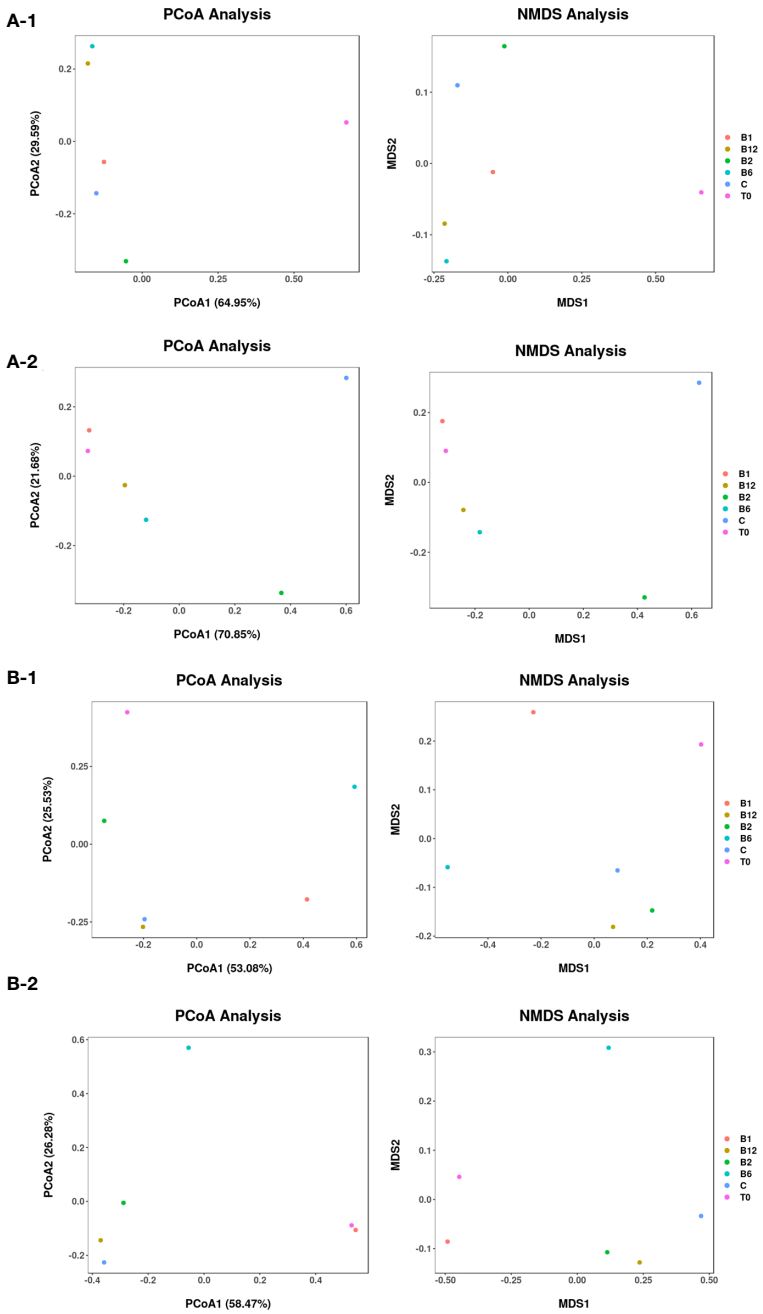

FIGURE 4
Principal coordinate analysis (PCoA) and nonmetric multidimensional scaling (NMDS) based on Bray–Curtis distance at the operational taxonomic unit (OTU) level of phytoplankton **(A)** and zooplankton **(B)** at the initial (T0) and endpoint of experiments, which were conducted in November **(A-1, B-1)** and April **(A-2, B-2)**.

suggests an obvious stimulation by B vitamins, particularly B_1, B_6, and B_{12}. *Picochlorum*, a member of the Chlorophyta phylum, is a group of small, fast-growing nanoplanktonic algae known for high oil-producing potential and applications in wastewater remediation, biomass production, and aquaculture feedstock (Henley et al., 2004; De la Vega et al., 2011; Chen et al., 2012b; Zhu and Dunford, 2013; Wang et al., 2016; Watanabe and Fujii, 2016; Kumar et al., 2017). However, the B vitamin auxotrophy of *Picochlorum* remains unclear. Our findings highlight the need for further research on the relationship of *Picochlorum* with B vitamins to better understand their ecological role and potential applications.

4.2 Phytoplankton effects on Copepoda and potential underlying mechanisms

Our study identified a decrease in the relative abundance of Copepoda, including Calanoida, *Paracalanus*, and Cyclopoida,

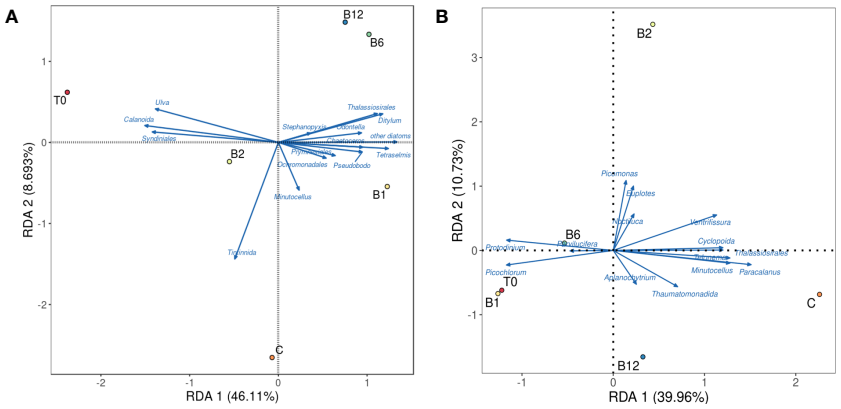

FIGURE 5
Redundancy analysis (RDA) of B vitamin responses by specific species phytoplankton and zooplankton. Filled symbols represent B vitamins supplementation samples in **(A)** November and **(B)** April.

following B vitamin amendments. A network diagram based on Spearman's rank correlation analysis (Figure 6) and redundancy analysis (RDA) (Figure 5) revealed negative correlations between Copepoda and several phytoplankton species, such as Thalassiosirales, *Chaetoceros*, *Ditylum*, *Picochlorum*, and *Protodinium*.

The addition of B vitamins stimulated the abundance of specific diatoms (*Odontella*, Thalassiosirales, *Ditylum*, and *Chaetoceros*), which may be auxotrophic for B vitamins. These diatoms displayed significant negative correlations with Copepoda, with Spearman Rho values greater than 0.8 ($p < 0.05$ or 0.01) (Figure 7). Copepoda were known to feed on phytoplankton. Fridolfsson et al. (2018) found in their study on marine vitamin B_1 that the presence of filamentous cyanobacteria could negatively affect copepods reproduction through phytoplankton and copepods vitamin B_1 content. Previous research has demonstrated that high concentrations of certain diatoms can inhibit Copepoda reproduction (Carotenuto et al., 2002; Miralto et al., 2003; Pierson et al., 2005), with two prevailing hypotheses: the "nutritional deficiency hypothesis", suggesting that diatom nutrient composition is insufficient for Copepoda growth and reproduction (Irigoien et al., 2002), and the "toxicity hypothesis", proposing that diatoms produce toxic secondary metabolites that directly affect Copepoda (Ianora et al., 2003). Thalassiosirales have been shown to produce mitogenic aldehydes at peak levels, which then affect copepods hatching and survival (Halsband-Lenk et al., 2005; Ask et al., 2006). At the same time, laboratory studies have reported negative effects of specific diatoms on Copepoda spawning and/or hatching (Ceballos and Ianora, 2003; Poulet et al., 2007; Dutz et al., 2008). Based on the above discussion, we believed that vitamin B induced changes in phytoplankton community composition may negatively affect Copepoda through food inhibition.

In addition to some certain diatoms, *Protodinium* and *Picochlorum* also showed significant negative correlations with Copepoda, with Spearman Rho values greater than 0.8 ($p < 0.05$) (Figure 7). Previous studies have reported that Copepoda biomass did not increase with phytoplankton biomass in some coastal waters (Vadstein et al., 2004; Hong et al., 2013). Copepoda were known to exhibit adaptive food selection to meet their growth and reproduction requirements (Chen et al., 2012a), and their ingestion rate was linearly related to food concentration (Frost,

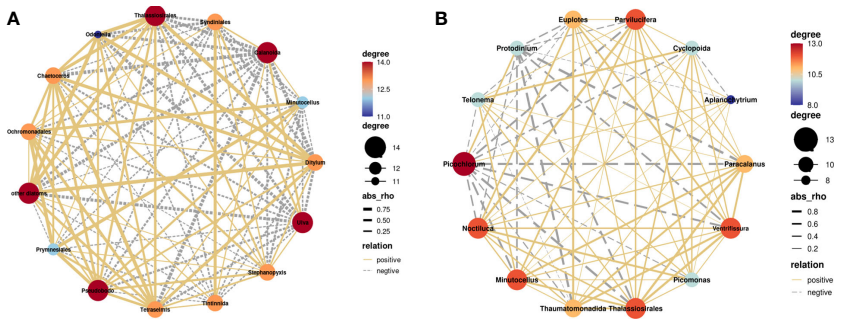

FIGURE 6
Correlation networks between the top 15 taxonomic groups of phytoplankton or zooplankton with relative abundance at the endpoint of each B vitamin addition experiment conducted **(A)** in November and **(B)** in April. The solid yellow lines indicate positive relationships, and the dashed gray lines indicate negative relationships. The thicker the line is, the larger the value of Rho.

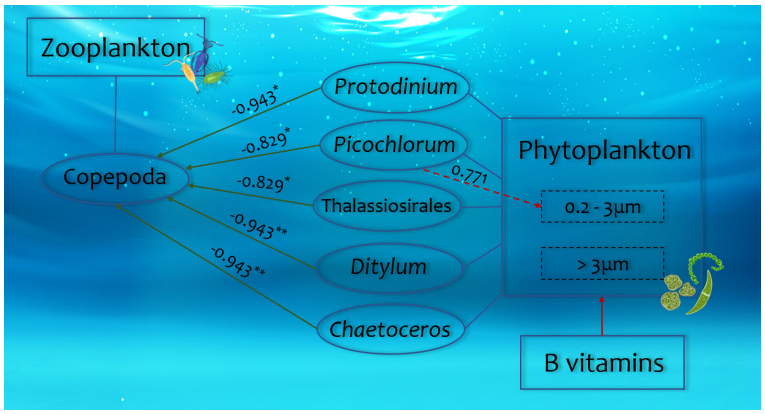

FIGURE 7
The correlation of certain species of phytoplankton and zooplankton after B vitamin amendments. Red arrows represent positive correlations, and green arrows represent negative correlations. The numbers represent the values of the correlation coefficients (Rho), "*" symbols represent $p < 0.05$ and "**" symbols represent $p < 0.01$.

1972). Copepods increase their ingestion rate when food concentration is low, but when it exceeds a certain threshold, their feeding rate decreases. Copepoda typically preferred phytoplankton that were nutritious and within a suitable size range (Liu et al., 2010; Lee et al., 2012; Fridolfsson et al., 2019). *Picochlorum* has been reported to be too small for Copepoda to graze effectively, making top-down control of their bloom less likely (Ma et al., 2021). Thus, our study suggests that B vitamin-induced changes in phytoplankton community composition may also negatively affect Copepoda through feeding inhibition.

5 Conclusion

This study used *in situ* amendments to demonstrate the effects of vitamins B_1, B_2, B_6 and B_{12} on the growth of phytoplankton. We found that B vitamin supplementation, particularly B_1, B_{12}, and to a lesser extent B_2 and B_6, led to significant shifts in phytoplankton community composition. Certain phytoplankton species, including diatoms and Prymnesiales, were found to be potentially auxotrophic for B vitamins and exhibited increased relative abundance in response to B vitamin supplementation. And the resulting changes in phytoplankton communities had a negative impact on Copepoda populations, leading to a decrease in their relative abundance. In conclusion, our findings augmented our knowledge on the effect of B vitamins other than B_1 and B_{12} on phytoplankton and had important implications for our understanding of the dynamics of zooplankton community composition under the influence of different B vitamins.

Data availability statement

The datasets presented in this study can be found in online repositories. The names of the repository/repositories and accession number(s) can be found below: BioProject, PRJNA956500.

Author contributions

LW: Methodology, Formal analysis, Investigation, Writing – original draft. HZ: Investigation, Formal analysis, Writing – review & editing. ES: Formal analysis, Writing – review & editing. BL: Methodology, Formal analysis, Resources. XC: Methodology, Formal analysis, Resources. QM: Investigation, Writing – review & editing. JL: Methodology, Writing – review & editing. WL: Conceptualization, Funding acquisition, Project administration, Writing – review & editing. All authors contributed to the article and approved the submitted version.

Funding

This study was supported by the National Natural Science Foundation of China (42230413) and the Key Special Project for Introduced Talents Team of Southern Marine Science and Engineering Guangdong Laboratory (Grant No. GML2019ZD0606).

Conflict of interest

The authors declare that the research was conducted in the absence of any commercial or financial relationships that could be construed as a potential conflict of interest.

Publisher's note

References

Abo-Taleb, H. A. (2019). Key to the Red Sea *Labidocera* (Crustacea; Calanoida: Pontellidae) copepods, the distribution of the species in various habitats, with special reference to two new records, and a historical correction. *Egyptian J. Aquat. Res.* 45, 367–374. doi: 10.1016/j.ejar.2019.11.004

Ask, J., Reinikainen, M., and Bamstedt, U. (2006). Variation in hatching success and egg production of Eurytemora affinis (Calanoida, Copepoda) from the Gulf of Bothnia, Baltic Sea, in relation to abundance and clonal differences of diatoms. *J. Plankton Res.* 28 (7), 683–694. doi: 10.1093/plankt/fbl005

General Administration of Quality Supervision, Inspection and Quarantine of the People's Republic of China & Standardization Administration of the People's Republic of China. (2007). *Sepcifications for oceanographic survey – Part 6: Marine biological survey* (Beijing, China: Standards Press of China). GB/T12763.6-2007.

Barber-Lluch, E., Hernandez-Ruiz, M., Prieto, A., Fernandez, E., and Teira, E. (2019). Role of vitamin B_{12} in the microbial plankton response to nutrient enrichment. *Mar. Ecol. Prog. Ser.* 626, 29–42. doi: 10.3354/meps13077

Bertrand, E. M., and Allen, A. E. (2012). Influence of vitamin B auxotrophy on nitrogen metabolism in eukaryotic phytoplankton. *Front. Microbiol.* 3, 375. doi: 10.3389/fmicb.2012.00375

Bertrand, E. M., Saito, M. A., Lee, P. A., Dunbar, R. B., Sedwick, P. N., and Ditullio, G. R. (2011). Iron limitation of a springtime bacterial and phytoplankton community in the ross sea: implications for vitamin B_{12} nutrition. *Front. Microbiol.* 2, 160. doi: 10.3389/fmicb.2011.00160

Bils, F., Aberle, N., van Damme, C. J. G., Peck, M. A., and Moyano, M. (2022). Role of protozooplankton in the diet of North Sea autumn spawning herring (*Clupea harengus*) larvae. *Mar. Biol.* 169, 90. doi: 10.1007/s00227-022-04076-1

Cai, S. Z., Wu, R. S., and Xu, J. D. (2011). Characteristics of upwelling in eastern Guangdong and southern Fujian coastal waters during 2006 summer. *Jouranl Oceanography Taiwan Strait* 30, 4. doi: 10.3969/J.ISNN.1000-8160.2011.04.006

Carotenuto, Y., Ianora, A., Buttino, I., ROmano, G., and Miralto, A. (2002). Is postembryonic development in the copepod *Temora stylifera* negatively affected by diatom diets? *J. Exp. Mar. Biol. Ecol.* 276, 49–66. doi: 10.1016/S0022-0981(02)00237-X

Ceballos, S., and Ianora, A. (2003). Different diatoms induce contrasting effects on the reproductive success of the copepod *Temora stylifera*. *J. Exp. Mar. Biol. Ecol.* 294, 189–202. doi: 10.1016/S0022-0981(03)00263-6

Chen, D., Ke, Z., Tan, Y., and Liu, J. (2020). Seasonal distribution of nutrients concentrations and the potential limitation for phytoplankton growth in the coastal region of Nan'ao-Dongshan. *Ecol. Sci.* 39 (4), 41–50. doi: 10.14108/j.cnki.1008-8873.2020.04.006

Chen, T. Y., Lin, H. Y., Lin, C. C., Lu, C. K., and Chen, Y. M. (2012b). Picochlorum as an alternative to *Nannochloropsis* for grouper larval rearing. *Aquaculture* 338, 82–88. doi: 10.1016/j.aquaculture.2012.01.011

Chen, M. R., Liu, H. B., and Chen, B. Z. (2012a). Effects of dietary essential fatty acids on reproduction rates of a subtropical calanoid copepod, *Acartia erythraea*. *Mar. Ecol. Prog. Ser.* 455, 95–110. doi: 10.3354/meps09685

Chiba, S., Batten, S., Martin, C. S., Ivory, S., Miloslavich, P., and Weatherdon, L. V. (2018). Zooplankton monitoring to contribute toward addressing global biodiversity conservation challenges. *Jouranl Plankton Res.* 40, 509–518. doi: 10.1093/plankt/fby030

Countway, P. D., Gast, R. J., Savai, P., and Caron, D. A. (2005). Protistan diversity estimates based on 18S rDNA from seawater inCubations in the Western North Atlantic. *J. Eukaryotic Microbiol.* 52 (2), 95–106. doi: 10.1111/j.1550-7408.2005.05202006.x

Croft, M. T., Lawrence, A. D., Raux-Deery, E., Warren, M. J., and Smith, A. G. (2005). Algae acquire vitamin B_{12} through a symbiotic relationship with bacteria. *Nature* 438, 90–93. doi: 10.1038/nature04056

Croft, M. T., Warren, M. J., and Smith, A. G. (2006). Algae need their vitamins. *Eukaryotic Cell* 5, 1175–1183. doi: 10.1128/EC.00097-06

De la Vega, M., Diaz, E., Vila, M., and Leon, R. (2011). Isolation of a new strain of *Picochlorum* sp and characterization of its potential biotechnological applications. *Biotechnol. Prog.* 27, 1535–1543. doi: 10.1002/btpr.686

Dowling, D. P., Croft, A. K., and Drennan, C. L. (2012). Radical use of Rossmann and TIM barrel architectures for controlling coenzyme B_{12} chemistry. *Annu. Rev. Biophysics* 41, 403–427. doi: 10.1146/annurev-biophys-050511-102225

Dutz, J., Koski, M., and Jonasdottir, S. H. (2008). Copepod reproduction is unaffected by diatom aldehydes or lipid composition. *Limnology Oceanography* 53, 225–235. doi: 10.4319/lo.2008.53.1.0225

Frank, R. A. W., Leeper, F. J., and Luisi, B. F. (2007). Structure, mechanism and catalytic duality of thiamine-dependent enzymes. *Cell. Mol. Life Sci.* 64, 892–905. doi: 10.1007/s00018-007-6423-5

Fridolfsson, E., Lindehoff, E., Legrand, C., and Hylander, S. (2020). Species-specific content of thiamin (vitamin B_1) in phytoplankton and the transfer to copepods. *J. Plankton Res.* 42, 274–285.

Fridolfsson, E., Bunse, C., Legrand, C., Lindehoff, E., Majaneva, S., and Hylander, S. (2019). Seasonal variation and species-specific concentrations of the essential vitamin B_1 (thiamin) in zooplankton and seston. *Mar. Biol.* 166, 70. doi: 10.1007/s00227-019-3520-6

Fridolfsson, E., Lindehoff, E., Legrand, C., and Hylander, S. (2018). Thiamin (vitamin B_1) content in phytoplankton and zooplankton in the presence of filamentous cyanobacteria. *Limnology Oceanography* 63, 2423–2435. doi: 10.1002/lno.10949

Frost, B. W. (1972). Effects of size and concentration of food particles on the feeding behavior of the marine plankton copepod *Calanus pacificus*. *Limnology Oceanography* 17, 805–815. doi: 10.4319/lo.1972.17.6.0805

Giovannoni, S. J. (2012). Vitamins in the sea. *Proceedings of the National Academy of Sciences.* 109, 13888–13889.

Gobler, C. J. (2007). Effect of B-vitamins (B_1, B_{12}) and inorganic nutrients on algal bloom dynamics in a coastal ecosystem. *Aquat. Microbial Ecol.* 49, 181–194. doi: 10.3354/ame01132

Halsband-Lenk, C., Pierson, J. J., and Leising, A. W. (2005). Reproduction of Pseudocalanus newmani (Copepoda : Calanoida) is deleteriously affected by diatom blooms - A field study. *Prog. Oceanography* 67 (3-4), 332–348. doi: 10.1016/j.pocean.2005.09.003

Heal, K. R., Carlson, L. T., Devol, A. H., Armbrust, E. V., Moffett, J. W., Stahl, D. A., et al. (2014). Determination of four forms of vitamin B_{12} and other B vitamins in seawater by liquid chromatography/tandem mass spectrometry. *Rapid Communcation Mass Spectrometry* 28, 2398–2404. doi: 10.1002/rcm.7040

Heal, K. R., Qin, W., Ribalet, F., Bertagnolli, A. D., Coyote-Maestas, W., Hmelo, L. R., et al. (2017). Two distinct pools of B12 analogs reveal community interdependencies in the ocean. *Proceedings of the National Academy of Sciences* 114, 364–369.

Helliwell, K. E. (2017). The roles of B vitamins in phytoplankton nutrition: New perspectives and prospects. *New Phytol.* 216, 62–68. doi: 10.1111/nph.14669

Henley, W. J., Hironaka, J. L., Guillou, L., Buchheim, M. A., Buchheim, J. A., Fawley, M. W., et al. (2004). Phylogenetic analysis of the '*Nannochloris*-like' algae and diagnoses of *Picochlorum oklahomensis* gen. et sp nov (Trebouxiophyceae, Chlorophyta). *Phycologia* 43, 641–652. doi: 10.2216/i0031-8884-43-6-641.1

Hong, Y., Burford, M. A., Ralph, P. J., Udy, J. W., and Doblin, M. A. (2013). The cyanobacterium *Cylindrospermopsis raciborskii* is facilitated by copepod selective grazing. *Harmful Algae* 29, 14–21. doi: 10.1016/j.hal.2013.07.003

Huang, Z., Hu, J., and Shi, W. (2021). Mapping the coastal upwelling East of Taiwan using geostationary satellite data. *Remote Sens* 13, 170. doi: 10.3390/rs13020170

Ianora, A., Poulet, S. A., and Miralto, A. (2003). The effects of diatoms on copepod reproduction: a review. *Phycologia* 42, 351–363. doi: 10.2216/i0031-8884-42-4-351.1

Irigoien, X., Harris, R. P., Verheye, H. M., Joly, P., Runge, J., Starr, M., et al. (2002). Copepod hatching success in marine ecosystems with high diatom concentrations. *Nature* 419, 384–389. doi: 10.1038/nature01055

Jiang, R., and Wang, Y. S. (2018). Modeling the ecosystem response to summer coastal upwelling in the northern South China Sea. *Oceanologia* 60, 32–51. doi: 10.1016/j.oceano.2017.05.004

Joglar, V., Pontiller, B., Martinez, S., Fuentes-Lema, A., Perez-Lorenzo, M., Lundin, D., et al. (2021). Microbial plankton community structure and function responses to vitamin B_{12} and B_1 amendments in an upwelling system. *Appl. Environ. Microbiol.* 87, e01525–e01521. doi: 10.1128/AEM.01525-21

Joglar, V., Prieto, A., Barber-Lluch, E., Hernández-Ruiz, M., Fernández, E., and Teira, E. (2020). Spatial and temporal variability in the response of phytoplankton and prokaryotes to B-vitamin amendments in an upwelling system. *Biogeosciences* 17, 2807–2823. doi: 10.5194/bg-17-2807-2020

Ke, Z., Chen, D., Tan, Y., Liu, H., and Liu, J. (2019). Temporal and spatial variations in primary production in the coastal region of Dongshan-Nan'ao. *J. Fishery Sci. China* 26 (1), 44–52. doi: 10.3724/SP.J.1118.2019.18208

King, A. L., Sañudo-Wilhelmy, S. A., Leblanc, K., Hutchins, D. A., and Fu, F. (2011). CO_2 and vitamin B_{12} interactions determine bioactive trace metal requirements of a subarctic Pacific diatom. *ISME J.* 5, 1388–1396. doi: 10.1038/ismej.2010.211

Koch, F., Hattenrath-Lehmann, T. K., Goleski, J. A., Sañudo-Wilhelmy, S. A., Fisher, N. S., and Gobler, C. J. (2012). Vitamin B_1 and B_{12} uptake and cycling by plankton communities in coastal ecosystems. *Front. Microbiol.* 3, 363. doi: 10.3389/fmicb.2012.00363

Koch, F., Marcoval, M. A., Panzeca, C., Bruland, K. W., Sañudo-Wilhelmy, S. A., and Gobler, C. J. (2011). The effect of vitamin B_{12} on phytoplankton growth and community structure in the Gulf of Alaska. *Limnology Oceanography* 56, 1023–1034. doi: 10.4319/lo.2011.56.3.1023

Kumar, S. D., Santhanam, P., Ananth, S., Kaviyarasan, M., Nithya, P., Dhanalakshmi, B., et al. (2017). Evaluation of suitability of wastewater-grown microalgae (*Picochlorum maculatum*) and copepod (*Oithona rigida*) as live feed for white leg shrimp *Litopenaeus vannamei* postlarvae. *Aquaculture Int.* 25, 393–411. doi: 10.1007/s10499-016-0037-6

Lee, D. B., Song, H. Y., Park, C., and Choi, K. H. (2012). Copepod feeding in a coastal area of active tidal mixing: diel and monthly variations of grazing impacts on phytoplankton biomass. *Mar. Ecol.* 33, 88–105. doi: 10.1111/j.1439-0485.2011.00453.x

Liu, H. B., Chen, M. R., Suzuki, K., Wong, C. K., and Chen, B. Z. (2010). Mesozooplankton selective feeding in subtropical coastal waters as revealed by HPLC pigment analysis. *Mar. Ecol. Prog. Ser.* 407, 111–123. doi: 10.3354/meps08550

Ma, X., Jacoby, C. A., and Johnson, K. B. (2021). Grazing by the copepod *Parvocalanus crassirostris* on Picochlorum sp. at harmful bloom densities and the role of particle size. *Front. Mar. Sci.* 8, 1–8. doi: 10.3389/fmars.2021.664154

Majaneva, S., Fridolfsson, E., Casini, M., Legrand, C., Lindehoff, E., Margonski, P., et al (2020). Deficiency syndromes in top predators associated with large-scale changes in the Baltic Sea ecosystem. *PLoS One* 15, e0227714..

Martínez-García, S., Fernandez, E., Calvo-Diaz, A., Maranon, E., Moran, X. A. G., and Teira, E. (2010). Response of heterotrophic and autotrophic microbial plankton to inorganic and organic inputs along a latitudinal transect in the Atlantic Ocean. *Biogeosciences* 7, 1701–1713. doi: 10.5194/bg-7-1701-2010

Matthews, R. G., Smith, A. E., Zhou, Z. H. S., Taurog, R. E., Bandarian, V., Evans, J. C., et al. (2003). Cobalamin-dependent and cobalamin-independent methionine synthases: Are there two solutions to the same chemical problem? *Helv. Chimica Acta* 86, 3939–3954. doi: 10.1002/hlca.200390329

Miralto, A., Guglielmo, L., Zagami, G., Buttino, I., Granata, A., and Ianora, A. (2003). Inhibition of population growth in the copepods *Acartia clausi* and *Calanus helgolandicus* during diatom blooms. *Mar. Ecol. Prog. Ser.* 254, 253–268. doi: 10.3354/meps254253

Monteverde, D. R., Gomez-Consarnau, L., Suffridge, C., and Sañudo-Wilhelmy, S. A. (2017). Life's utilization of B vitamins on early Earth. *Geobiology* 15, 3–18. doi: 10.1111/gbi.12202

Nichols, D. S. (2003). Prokaryotes and the input of polyunsaturated fatty acids to the marine food web. *FEMS Microbiol. Lett.* 219, 1–7. doi: 10.1016/S0378-1097(02)01200-4

Paerl, R. W., Bertrand, E. M., Allen, A. E., Palenik, B., and Azam, F. (2015). Vitamin B_1 ecophysiology of marine picoeukaryotic algae: Strain-specific differences and a new role for bacteria in vitamin cycling. *Limnology Oceanography* 60, 215–228. doi: 10.1002/lno.10009

Pierson, J. J., Halsband-Lenk, C., and Leising, A. W. (2005). Reproductive success of *Calanus pacificus* during diatom blooms in Dabob Bay, Washington. *Prog. Oceanography* 67, 314–331. doi: 10.1016/j.pocean.2005.09.002

Pomeroy, L. R., Williams, P. J. I., Azam, F., and Hobbie, J. E. (2007). The microbial loop. *Oceanography* 20, 28–33. doi: 10.5670/oceanog.2007.45

Poulet, S. A., Escribano, R., Hidalgo, P., Cueff, A., Wichard, T., Aguilera, V., et al. (2007). Collapse of *Calanus Chilensis* reproduction in a marine environment with high diatom concentration. *J. Exp. Mar. Biol. Ecol.* 352, 187–199. doi: 10.1016/j.jembe.2007.07.019

Randall, J. R., Murphy, H. M., Robert, D., and Geoffroy, M. (2022). Forage fish as a predator: summer and autumn diet of Atlantic herring in Trinity Bay, Newfoundland. *Fisheries Res.* 252, 106331. doi: 10.1016/j.fishres.2022.106331

Rodionov, D. A., Vitreschak, A. G., Mironov, A. A., and Gelfand, M. S. (2002). Comparative genomics of thiamin biosynthesis in procaryotes: new genes and regulatory mechanisms. *J. Biol. Chem.* 277 (50), 48949–48959. doi: 10.1074/jbc.M208965200

Sañudo-Wilhelmy, S. A., Cutter, L. S., Durazo, R., Smail, E. A., Gomez-Consarnau, L., Webb, E. A., et al. (2012). Multiple B-vitamin depletion in large areas of the coastal ocean. *Proceedings of the National Academy of Sciences* 109, 14041–14045.

Sañudo-Wilhelmy, S. A., G´omez-Consarnau, L., Suffridge, C., and Webb, E. A. (2014). The role of B vitamins in marine biogeochemistry. *Annu. Reviwe Mar. Sci.* 6, 339–367. doi: 10.1146/annurev-marine-120710-100912

Sañudo-Wilhelmy, S. A., Gobler, C. J., Okbamichael, M., and Taylor, G. T. (2006). Regulation of phytoplankton dynamics by vitamin B-12. *Geophysical Res. Lett.* 33, L04604. doi: 10.1029/2005GL025046

Shu, Y. Q., Wang, Q., and Zu, T. T. (2018). Progress on shelf and slope circulation in the northern South China Sea. *Sci. China Earth Sci.* 48, 276–287. doi: 10.1007/s11430-017-9152-y

Srichandan, S., Baliarsingh, S. K., Lotliker, A. A., Sahu, B. K., Roy, R., and Nair, T. M. B. (2021). Unraveling tidal effect on zooplankton community structure in a tropical estuary. *Environ. Monit. Assess.* 193, 362. doi: 10.1007/s10661-021-09112-z

Suffridge, C., Cutter, L., and Sañudo-Wilhelmy, S. A. (2017). A new analytical method for direct measurement of particulate and dissolved B-vitamins and their congeners in seawater. *Front. Mar. Sci.* 4, 1–11. doi: 10.3389/fmars.2017.00011

Tang, Y. Z., Koch, F., and Gobler, C. J. (2010). Most harmful algal bloom species are vitamin B_1 and B_{12} auxotrophs. *Proceedings of the National Academy of Sciences* 107, 20756–20761.

Vadstein, O., Stibor, H., Lippert, B., Loseth, K., Roederer, W., Sundt-Hansen, L., et al. (2004). Moderate increase in the biomass of omnivorous copepods may ease grazing control of planktonic algae. *Mar. Ecol. Prog. Ser.* 270, 199–207. doi: 10.3354/meps270199

Waldrop, G. L., Holden, H. M., and St Maurice, M. (2012). The enzymes of biotin dependent CO_2 metabolism: What structures reveal about their reaction mechanisms. *Protein Sci.* 21, 1597–1619. doi: 10.1002/pro.2156

Wang, S. Y., Shi, X. G., and Palenik, B. (2016). Characterization of *Picochlorum* sp use of wastewater generated from hydrothermal liquefaction as a nitrogen source. *Algal Research-Biomass Biofuels Bioproducts* 13, 311–317. doi: 10.1016/j.algal.2015.11.015

Watanabe, F., and Bito, T. (2018). Vitamin B_{12} sources and microbial interaction. *Exp. Biol. Med.* 243, 148–158. doi: 10.1177/1535370217746612

Watanabe, K., and Fujii, K. (2016). Isolation of high level CO_2 preferring *Picochlorum* sp strains and their biotechnological potential. *Algal Research-Biomass Biofuels Bioproducts* 18, 135–143. doi: 10.1016/j.algal.2016.06.013

Zhu, Y., and Dunford, N. T. (2013). Growth and biomass characteristics of *Picochlorum oklahomensis* and *Nannochloropsis oculata*. *J. Am. Oil Chem. Soc.* 90, 841–849. doi: 10.1007/s11746-013-2225-0

frontiers | Frontiers in Marine Science

TYPE Original Research
PUBLISHED 25 October 2023
DOI 10.3389/fmars.2023.1280753

OPEN ACCESS

EDITED BY
Dilip Kumar Jha,
National Institute of Ocean Technology, India

REVIEWED BY
Shrikant D. Khandare,
National Institute of Ocean Technology, India
Nithyanandam Marimuthu,
Zoological Survey of India, India
Vikas Pandey,
Council of Scientific and Industrial Research (CSIR), India

*CORRESPONDENCE
Hui Zhao
huizhao1978@163.com
Hui Gao
huigao109@163.com

†These authors share first authorship

RECEIVED 21 August 2023
ACCEPTED 09 October 2023
PUBLISHED 25 October 2023

CITATION
Chen Y, Sun Y, Shi H, Zhao H, Gao H, Pan G and Tian K (2023) Environmental capacity and fluxes of land-sourced pollutants around the Leizhou Peninsula in the summer.
Front. Mar. Sci. 10:1280753.
doi: 10.3389/fmars.2023.1280753

Environmental capacity and fluxes of land-sourced pollutants around the Leizhou Peninsula in the summer

Ying Chen[1,2,3†], Yan Sun[1,4†], Haiyi Shi[1,2,3], Hui Zhao[1,2,3,5*], Hui Gao[1,2,3,5*], Gang Pan[1,2,6,7] and Kai Tian[1,2,3]

[1]College of Chemistry and Environmental Science, Guangdong Ocean University, Zhanjiang, China, [2]Cooperative Research Center for Nearshore Marine Environmental Change, Guangdong Ocean University, Zhanjiang, China, [3]Research Center for Coastal Environmental Protection and Ecological Resilience, Guangdong Ocean University, Zhanjiang, China, [4]College of Electronic and Information Engineering, Guangdong Ocean University, Zhanjiang, China, [5]Southern Marine Science and Engineering Guangdong Laboratory, Zhuhai, China, [6]School of Humanities, York St John University, York, United Kingdom, [7]Jiangsu Jiuguan Institute of Environment and Resources, Yixing, China

Although the water environment has certain self-purification capability, the natural balance is disrupted, leading to water quality deterioration when the discharge load of wastewater exceeds a certain threshold. This problem implies the urgency of evaluating marine environmental capacity as a necessary parameter for marine sustainable development of marine ecosystems. Through principal component analysis (PCA), clustering, and other methods, we analyzed the average concentration and fluxes of land-sourced pollutants and determined the pollution level around the Leizhou Peninsula. Combined with the Delft3D hydrodynamic numerical model, tidal hydrodynamic forces and pollutants migration and diffusion were calculated. Based on *in-situ* measured data, the model was validated. The sharing rate method was used to calculate the marine environmental capacity in Zhanjiang Bay and analyzed their impact on seawater eutrophication. The results showed that: (1) The average concentrations of chemical oxygen demand (COD), ammonia nitrogen (NH_4^+), total nitrogen (TN), and total phosphorus (TP) around Leizhou Peninsula were 22.56 mg/L, 0.69 mg/L, 6.69 mg/L, and 0.69 mg/L, respectively. (2) Six areas (Area A-F) can be divided into, based on the discharge of land-sourced pollutants into the sea area. According to the results of PCA, clustering, and other methods, the average concentration and fluxes of land-sourced pollutants in Area B (i.e. Zhanjiang Bay) were very high. (3) The environmental capacity of Zhanjiang Bay was calculated through Delft3D numerical simulation, and it was found that the COD and TN environmental capacity of 6 sewage outlets exceeded the standard, while the TP environmental capacity of 3 sewage outlets exceeded the standard. (4) According to the statistical research result, most of the Zhanjiang Bay waters has been restricted by nitrogen for over a decade. Therefore, we speculate that although TN environmental capacity exceeds the standard, its impact on eutrophication in Zhanjiang Bay is still limited to a certain extent.

KEYWORDS

Leizhou Peninsula, Zhanjiang Bay, land-sourced pollutants, Delft 3D, environmental capacity

1 Introduction

The nearshore is a hub for terrestrial and marine ecosystems as well as an ecosystem that is jointly influenced by biological, chemical, and physical processes. Marine biodiversity is significantly impacted by the nearshore environment. In recent years, the increase in pollutant load caused by industrialization and urbanization has become a major constraint on the development of many regions of the world, resulting in water pollution (Wang et al., 2014; Chen et al., 2019). Chemical oxygen demand (COD), nitrogen, and phosphorus are generally the key components in the monitored rivers with water quality parameters exceeding the standard in the "2018 China Marine Ecological Environment Status Bulletin". There are many environmental pressures on estuaries and bays. The natural world has always existed as a system and is capable of self-regulation to a certain extent (Bui and Pham, 2023). However, when human-caused pollution loads rise, there will be a significant increase in the transfer of land-sourced pollutants to coastal waters, leading to water pollution, eutrophication, and so on. Its biodiversity, community makeup, and seawater quality are all significantly impacted (Huang et al., 2003; Kalnejais et al., 2010; Kang and Xu, 2012; Parette and Pearson, 2014; Dou et al., 2015; Zhou et al., 2017; Jia et al., 2018). This may have a negative impact on ecosystems, habitat quality, and human health (Zhou et al., 2017). Excessive nutrient input, such as nitrogen and phosphorus, may promote the growth of harmful algae, forming red tides, etc. This not only damages the marine ecological structure, but also leads to the death of phytoplankton and zooplankton, seriously damaging the coastal ecological environment (Wang et al., 2021). Recent researches have shown a new wave of environmental problems, including the resurgence of eutrophication (Kemp et al., 2009; Andersen et al., 2017; Le Moal et al., 2019; Wu et al., 2019). Therefore, it is vital to address this issue with suitable pollution management measures for sustainable development.

Limiting the concentration of pollutant discharges is the principal strategy used in traditional management of marine water environments. In recent years, the concentration of pollutant emissions has been managed, and the majority of coastal areas have accomplished both standard emissions and pollutant concentration management. However, there has been no improvement in the quality of the nearshore waters, and pollution discharge has generally increased (Yang et al., 2018; Yu et al., 2019). On the one hand, controlling the concentration of pollutant discharges alone is not enough. The total number of pollutant emissions is heavily influenced by the amount of sewage discharged from sewage outlets and river runoff into the sea. As the total amount of emissions rises, so will the impact on the marine ecosystem. On the other hand, the management method of controlling the concentration of pollutant discharges only considers a single emission, ignoring the superposition of pollutant discharges from multiple sewage outlets in the region (Sun, 2020).

The ocean has a strong self-cleaning ability and can accommodate a large number of pollutants. It can transfer, dilute, degrade, and purify pollutants through physical, chemical, and biological processes. But the amount of pollutants that the ocean can hold is not infinite. Environmental capacity, also known as environmental bearing capacity, environmental tolerance, is the maximum quantity of pollutants that the ocean is capable of tolerating while still maintaining a healthy marine ecosystem. Important coastal countries have conducted research on marine environmental capacity, including the Black Sea of Russia (Mironov et al., 1975), Kastela Bay of Yugoslavia (Margeta et al., 1989), Haifa Bay of Israel (Krom et al., 1990), Buk Bay of South Korea (Woo-Jeung et al., 1991), and the Seto Inland Sea of Japan (Song, 1999). Chinese scholars have also conducted research on marine environmental capacity in Laizhou Bay (Jiang et al., 1991), Bohai Sea (Guo, 2005), Dapeng Bay (Li et al., 2005), and other areas. Additionally, scientists are dedicated to creating and enhancing marine environmental capacity assessment models and techniques. Researchers were committed to developing and improving marine environmental capacity assessment models and methods to evaluate the environmental capacity of diverse coastal regions based on multiple dimensions such as ecosystem services, physical environmental factors, and biodiversity indicators (Van der Wulp et al., 2016; Xu and Chua, 2017; Yamamoto and Nadaoka, 2018). These models take into account all of the ecological processes, energy flow, and material cycle of marine ecosystems, providing a scientific foundation for management and decision-making of marine environments. If the total amount of pollutants entering the ocean does not exceed its pollutant carrying capacity, the self-purification function of the ocean can maintain a healthy state of the marine environment. However, both the marine environment and its functions will be harmed and may even be impossible to recover when the total amount of pollutants emitted reaches the upper limit of the ocean's environmental capacity (Yang, 2001). Controlling the total amount of pollutants entering the sea can more effectively improve and protect the marine environment. Therefore, it has become a hot topic in current marine environmental research to determine the capacity value of the marine environment in a scientifically sound and reasonable manner.

Diverse coastal marine ecosystems, including coral reefs, mangroves, seagrass beds, etc., surround the sea area surrounding the Leizhou Peninsula and have abundant marine biological resources. However, its ecological system is more delicate and perilous (Zhang et al., 2008). In recent years, with the increase of human activities and the impact of climate change, oceans are facing serious environmental problems, such as marine pollution, overfishing, ocean acidification, etc., which pose a huge challenge to the sustainable development of marine ecosystems and human beings. Studying the marine environmental capacity is crucial because it can provide scientific basis and decision-making support for marine protection and sustainable utilization. The purpose of this research is to sample 81 significant sewage outlets into the sea along the Leizhou Peninsula and discuss the distribution of land-sourced pollutants and their affecting elements (Figure 1). Combining the Delft3D model, the sharing rate method is used to calculate the environmental capacity and explore the impact of land-sourced pollutants on the study areas.

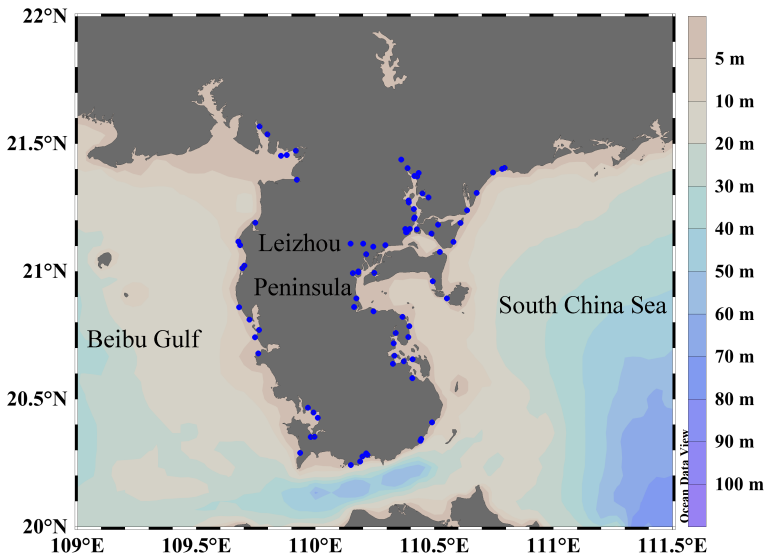

FIGURE 1
Study area and spatial distribution of sampling stations.

2 Material and methods

2.1 Study area and sampling

Leizhou Peninsula is located between 20–22°N and 109–111.5°E near the southernmost of the Chinese Mainland (Figure 1). It is bordered to the west by the northeastern Beibu Gulf, to the east by the northwest South China Sea, and to the south by Hainan Island. Its coastline is winding, with numerous harbors and islands, unique ecosystems such as mangroves and seagrass beds, as well as abundant marine biological resources (Gong et al., 2012). Due to the impact of human activities and external interference, the water quality in the coastal waters of Leizhou Peninsula has significantly decreased, and the environmental pressure has gradually increased over the past few years (Lei et al., 2016). In addition, due to the uneven distribution and development of industry and agriculture, as well as the impact of the sea areas, coastal runoff, the water quality, ecological environment, marine biological resources and ecological environment factors around the Leizhou Peninsula are complex and changeable (Zhang et al., 2021).

In the summer of 2020, we conducted an investigation around the Leizhou Peninsula and arranged 81 sampling stations, including river sewage outlets, industrial sewage outlets, domestic sewage outlets, and aquaculture sewage outlets (Figure 1). The sampling depth of each station is about 0.5 m. In addition, we also measured various indicators of these outfalls, including temperature, salinity, pH, dissolved oxygen (DO), COD, ammonia nitrogen (NH_4^+), total nitrogen (TN), and total phosphorus (TP). The temperature, salinity, pH, and DO are measured using a portable multi-parameter water quality analyzer. COD and NH_4^+ use dichromate titration (river water)/basic potassium permanganate method (seawater), and hypobromate oxidation method. TN and TP use potassium persulfate oxidation method (The specification for marine monitoring – Part 4: Seawater analysis) (National Marine Environmental Monitoring Center, 2007). The *in-situ* measured data used to validate the model is also from the sampling data of Zhanjiang Bay in the summer of 2020 (Figure 2H). Importantly, the nutrient data in Table 1 for Zhanjiang Bay over the past 10 years have been accumulated from our team's voyages sampling.

2.2 Calculation of the fluxes of land-sourced pollutants

$$F_{(i)} = C_{(i)} \times Q_{(i)} \times 10^{-3} \quad \text{(Zhang et al., 2021)} \quad (1)$$

Where $F_{(i)}$ is the fluxes of land-sourced pollutants (COD, NH_4^+, TN, and TP) (kg/day); $C_{(i)}$ is the concentration of land-sourced pollutants (COD, NH_4^+, TN, and TP) (mg/L); $Q_{(i)}$ is the flow rate at the sewage outlets (m^3/day).

2.3 Water quality evaluation index

Nemerow Pollution Index (NPI) is a popular approach for assessing the quality of both surface water and groundwater (Nemerow, 1974). This approach can overcome the drawbacks of the single factor index method and effectively address the effects of outlier or a portion of high values on the overall assessment of water quality.

The traditional *NPI*:

$$NPI = \sqrt{\frac{F_{max}^2 + F_{ave}^2}{2}} \quad (2)$$

$$F_{ave} = \frac{1}{n}\sum_{i=1}^{n} F_i \quad (3)$$

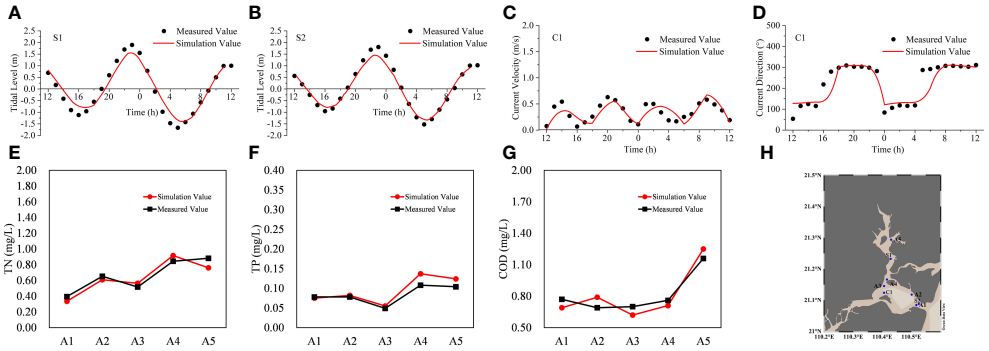

FIGURE 2
The results of simulation value and measured value in **(A)**&**(B)** Tidal level, **(C)** Current velocity, **(D)** Current direction, **(E)** COD, **(F)** TN, **(G)** TP, **(H)** The sampling stations of validation.

$$F_i = \frac{C_i}{S_{ij}} \tag{4}$$

Where *NPI* is the Nemerow Pollution Index; F_{max} is the maximum pollution index; F_{ave} is the average pollution index; F_i is the pollution index; C_i is the measured value of evaluation index i at the sampling stations; S_{ij} is the standard value of evaluation index i in Class j water; n is the number of assessment indicators. The Class III water quality standard from "surface water quality standard (GB 3838-2002)" is chosen as the evaluation standard in this study (State environmental protection administration, 2002).

TABLE 1 Percentage of the stations of nitrogen and phosphorus limitation in Zhanjiang Bay from 2010 to 2021.

Time	N Limitation	P Limitation	Stations Number
2021.03	76%	24%	41
2020.10	58%	42%	24
2019.01	100%	0	22
2018.11	78%	22	27
2017.11	96%	4%	25
2016.03	95%	5%	20
2015(Yuan et al., 2016)	91%	9%	11
2014(Yuan et al., 2016)	55%	45%	11
2013(Yuan et al., 2016)	27%	73%	11
2012.01	100%	0	11
2011.11	100%	0	11
2011.06	100%	0	11
2011.03	78%	22%	11
2010.10	70%	30%	27
2010.07	74%	26%	27
2010.04	44%	56%	25

However, the traditional NPI is based on a single factor evaluation method that could overstate the importance of the largest pollution factor and undervalue the importance of each indicator. In recent years, domestic and foreign researchers have continuously improved and optimized this method (Swati, 2015; Ji et al., 2016). The improved NPI (CNPI) (Table 2) is as follows:

$$CNPI = \sqrt{\frac{F_{max}^{'2} + F_{ave}^2}{2}} \tag{5}$$

$$F_{max}^{'} = \frac{F_{max} + F_w}{2} \tag{6}$$

Where $F_{max}^{'}$ is a correction to traditional NPI (F_{max}); F_w is the pollution factor F_i value with the highest weight value.

The calculation of weight value W_i:

In general, the lower the concentration of pollution indicators in the "surface water quality standard (GB 3838-2002)", the greater the harm to water quality, and the link between the two is inversely proportional (Yang et al., 2012). Arrange the water standards j for various evaluation factors W_{ij} in descending order. Compare their maximum value S_{max} with S_i, and set R_i as the correlation ratio of the evaluation factor i to obtain:

$$R_i = \frac{S_{max}}{S_i} \tag{7}$$

$$W_i = \frac{R_i}{\sum_{i=1}^{n} R_i} \tag{8}$$

TABLE 2 The classifications of water quality based on the CNPI (Chen et al., 2020).

CNPI	Classification
CNPI ≤ 0.63	Safe
0.63<CNPI ≤ 0.74	Warming
0.74<CNPI ≤ 1	Slight pollution
1<CNPI ≤ 7.28	Moderate pollution
CNPI>7.28	Heavy pollution

Where W_i is the weight value of the pollution factor i; S_{max} is the maximum standard value S_i; R_i is the correlation ratio of the evaluation indicator i.

2.4 Principal component analysis

Principal component analysis (PCA) is a statistical method for dimensionality reduction of data (Liu et al., 2003; Gimenez and Giussani, 2018). It can increase the interpretability of data while retaining the maximum amount of information in the data and can achieve visualization of multidimensional data. The steps are as follows:

(1) On the basis of the raw data, create a sample matrix X and carry out standardization processing.

$$X = (X_{ij})_{n \times p},\ i = 1, 2, \cdots,\ n; j = 1, 2, \cdots,\ p \tag{9}$$

$$Z_{ij} = \frac{x_{ij} - \bar{x}_j}{\sigma_j},\ i = 1, 2, \cdots,\ n; j = 1, 2, \cdots,\ p \tag{10}$$

Where n is the number of sampling stations with p indicators. $\bar{x}_j$ is the mean of the indicator j, $\bar{x}_j = \frac{\sum_{i=1}^{n} x_{ij}}{n}$; σ_j is the standard deviation of the indicator j, $\sigma_j = \sqrt{\sum_{i=1}^{n} \frac{(x_{ij} - \bar{x}_j)^2}{n-1}}$; Z_{ij} is the standardized value of indicator j for station i; x_{ij} is the measured value of indicator j for station i.

(2) Checkout of Kaiser-Meyer-Olkin-Measure of Sampling Adequacy (KMO) and Bartlett Test of Sphericity. KMO is an indicator that compares partial and simple correlation coefficients between variables, with values ranging from 0 to 1. The KMO indicates the strength of the correlation between variables, and the original variables are better suited for factor analysis when it is closer to 1.The Bartlett Test of Sphericity is a method to determine whether the variables in the data matrix are independent of one another and whether the data matrix is an identity matrix. If p< 0.05, the data correlation matrix is not an identity matrix, allowing for the possibility of factor analysis; if p > 0.05, the data correlation matrix is an identity matrix, making factor analysis inappropriate. Finally, PCA can be used to determine the relationship between the variables in the data when the KMO > 0.5 and the p< 0.001.

(3) Create a correlation coefficient matrix $R = (r_{ij})_{p \times p}$ based on normalized data matrix for the variables. Calculate the eigenvalues $\lambda_i (i=1,2,\ldots,p)$ of R, which is the variance of PCA, using the characteristic equation $|R - \lambda I| = 0$. The eigenvalues are ordered in descending order $\lambda_1 \geq \lambda_2 \geq \ldots \lambda_p$. The variance contribution rate and cumulative variance contribution rate are $e_g = \lambda_g / \sum_{g=1}^{p} \lambda_g$ and $\sum_{g=1}^{k} \lambda_g / \sum_{g=1}^{p} \lambda_g$, respectively. Standardized data is converted into primary components using the eigenvector corresponding to various eigenvalues $I_g = (I_{g1}, I_{g2,\ldots,} I_{gp})^T$ $(g = 1,2, \ldots, p)$.

(4) Based on the tenet that the characteristic value of the cumulative contribution rate of primary component variance is larger than 1, determine the total number of PCA.

2.5 Cluster analysis

In order to reveal the underlying characteristics and connections among samples, cluster analysis (including hierarchical clustering, K-Means, etc.) is used to divide samples of unknown categories into several class families, cluster similar samples into the same class cluster, and divide dissimilar samples into different class clusters (Wu et al., 2009). Each sample is treated as a cluster in this study's bottom-up method for hierarchical clustering, which involves finding the two clusters with the shortest distance between them and merging them until all samples are in the same cluster. The steps are as follows:

(1) Use n data objects as initial clustering centers (i.e. cluster centroids).

(2) Calculate the distance between the centroids of each cluster (Euclidean distance).

$$D_{min}(C_i, C_j) = minx - z_2\ (x \in C_i, z \in C_j) \tag{11}$$

(3) Find two clusters C_i and C_j with the smallest distance and merge them into a new cluster.

(4) Repeat step 2 until just one cluster is left or the predetermined criteria are met.

(5) Output the results of cluster analysis.

2.6 Numerical model

The Delft3D model, developed by the Dutch Delft Hydraulic Institute, is one of the most reliable numerical models in the world. It is widely used in coastal, estuarine, and riverine applications and also has good applicability in inter-tidal and beach topography. In this study, the Delft3D-Flow module is used to build a numerical model of the local two-dimensional tidal hydrodynamics and the transport and dispersion of pollutants to support the subsequent calculation of the environmental capacity of pollutants.

The computational domain of the model is Zhanjiang Bay and part of the outer bay, with an area of about 5.6×10^3 km^2 (Figure 3). In order to make the model computationally stable, the outer sea open boundary is set as a circular arc shape. The overall change in grid resolution is adapted to the hydrodynamic environment of Zhanjiang Bay, and the resolution of the grid is gradually reduced from inside the bay to outside the bay and locally encrypted in the key area, with a finest grid resolution of 30 m. The entire computational domain has 174 × 110 grid points.

The underwater topographic data in the computational domain is taken from ETOPO1 and calibrated with high-precision electronic charts in the bay. Tidal harmonic constants for the eight major subtidal tides (M_2, S_2, N_2, K_2, K_1, O_1, P_1, and Q_1) provided by Oregon State University's global tidal database were used to drive the boundary tidal levels at the open boundary in the outer sea (Egbert and Erofeeva, 2002). For the model parameter settings, we used the previously validated numerical model parameters of Zhanjiang Bay with necessary rate improvements (Wei et al., 2023). Among them, the roughness coefficient is expressed by the Manning coefficient. The bottom drag coefficient is set to 0.015–0.022 according to different underwater topographies, and the eddy viscosity coefficient is set to 10 m^2/s. In addition, for the pollutant calculations in this study, the initial field of the pollutant with fluxes on the boundary is defined by interpolating the measured summer data. The sources of pollutants

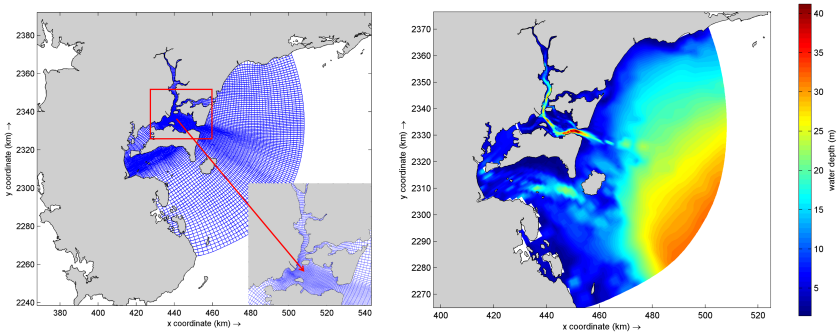

FIGURE 3
Modeling grid (left) and model water depth (right).

were determined from the outfall and river measured value. COD, TN, and TP are considered as conservative substances, and only hydrodynamic transport processes such as advection and diffusion are considered without considering biochemical processes.

2.7 Calculation of environmental capacity

The sharing rate method is also a commonly used method for calculating environmental capacity (Han et al., 2011). By creating a water quality model, the percentage of a single source of pollution in the total pollution may be computed, indicating how much that source contributed to the overall regional pollution. The sharing rate approach is easy to use and practical for administration and operation. This approach has been used successfully in numerous coastal regions (Zhang and Sun, 2007; Wang et al., 2012).

The response coefficient reflects the response relationship between pollutant input and sea water, which is the key to controlling sea water quality and total pollutant input. It is the concentration formed under the source intensity of the unit intensity of pollution source emissions ($a_{ij}(x,y)$), where i represents the pollution source and j represents the water quality control point, that is, the response coefficient of the water quality control point j under the input of the pollution source i.

The calculation of the sharing rate is as follows:

$$\gamma_{ij}(x,y) = \frac{C_{ij}(x,y)}{C_i(x,y)} \tag{12}$$

Where $C_{ij}(x,y)$ is the concentration formed by the pollution source i at the water quality control point j; $C_i(x,y)$ is the concentration input for each pollution source.

Using the response coefficient and sharing rate, obtain the contribution concentration value $C_{0i}(x,y)$ of the pollution source i. Then calculate the allowable emission Q_{0i} of the pollution source i based on $C_{0i}(x,y)$, which is:

$$C_{0i}(x,y) = \gamma_i(x,y) \cdot C_0(x,y) \tag{13}$$

$$Q_{0i} = \frac{C_{0i}(x,y)}{a_i(x,y)} \tag{14}$$

3 Results and discussion

3.1 Spatial distribution of COD, NH_4^+, TN, and TP around Leizhou Peninsula

COD is a crucial metric for assessing the quality of water and serves as an indirect indicator of the amount of organic matter in water bodies. TP is an indicator that shows the overall quantity of phosphorus compounds in the water, whereas NH_4^+ and TN reflect the various kinds of nitrogen content in the water. The elements nitrate and phosphorus play a significant role in eutrophication and the degradation of water quality. The COD around the Leizhou Peninsula exhibits a general spatial tendency in the summer that is high in the east, low in the west, high in the north, and low in the south (Figure 4). The range of the COD concentration is 0.96 to 199 mg/L, with a mean value of 21.08 mg/L. Some stations with high COD values are primarily found in the east and south, flowing into Bomao Port, Leizhou Bay, and Qiongzhou Strait. The concentration of NH_4^+ is an important component of terrestrial TN and an important indicator for the country's total pollutant control. The NH_4^+ concentration in the whole area around Leizhou Peninsula has individual high values, and the low-value area is mainly located in the eastern area (Figure 4). The average NH_4^+ concentration is 0.71 mg/L, with a range of 0.003 to 4.94 mg/L. The TN concentration shows an overall spatial trend of high in the east, low in the west, and high in the north and low in the south (Figure 4). The TN concentration value ranges from 0.089 to 348 mg/L, with a total average of 6.87 mg/L. Some high-value stations are mainly located in the eastern region and flow into Zhanjiang Bay. The TP concentration shows an overall spatial trend of high in the east and west, high in the north, and low in the south (Figure 4). The TP concentration value ranges from 0.058 to 4.62 mg/L, with a total average of 0.70 mg/L. Some high-value

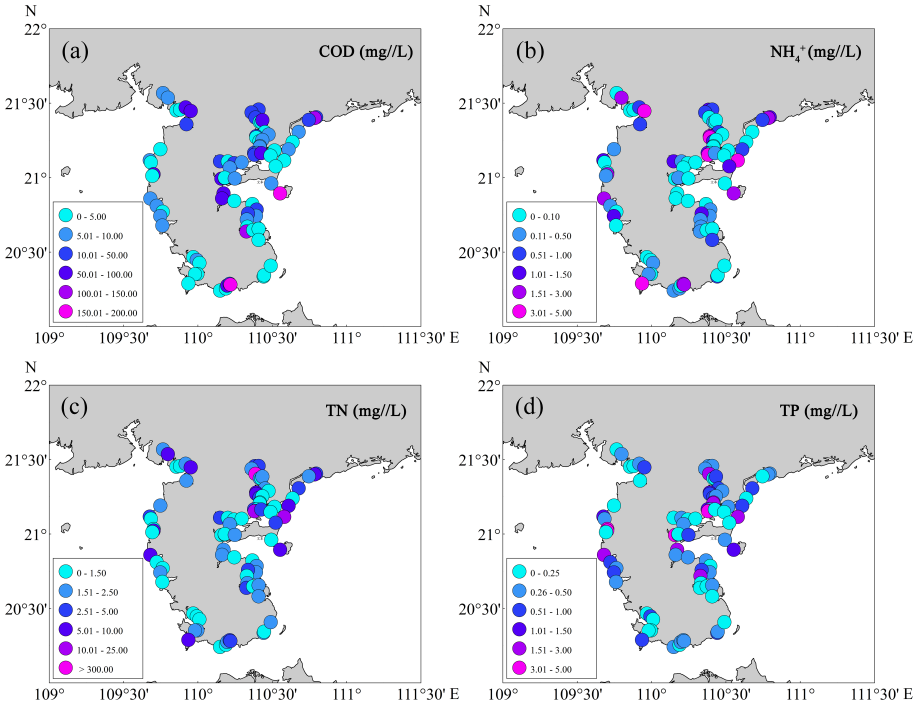

FIGURE 4
Concentration range of **(A)** COD (mg/L), **(B)** NH_4^+ (mg/L), **(C)** TN (mg/L), and **(D)** TP (mg/L) around Leizhou Peninsula in the summer of 2020.

stations are mainly located in the eastern region and flow into Zhanjiang Bay, Leizhou Bay, and Anpu Bay.

3.2 The fluxes of COD, NH_4^+, TN, and TP and other environmental factors

We have designed a total of 81 sampling stations, including river sewage outlets, industrial sewage outlets, domestic sewage outlets, and aquaculture sewage outlets. Each sewage outlet ultimately flows into a different sea area. In order to better evaluate the pollution discharge and water pollution of the whole area around the Leizhou Peninsula, we choose to classify the 81 sewage outlets according to their final inflow into the sea areas, and the results are divided into 6 sea areas (Figure 5).

Early studies have shown that nearshore waters are affected by land-sourced pollutants, leading to increased nutrient concentrations and eutrophication in seawater (Huang et al., 2003; Kalnejais et al., 2010; Parette and Pearson, 2014). In order to evaluate the impact of land-sourced pollutants on the regional water quality around Leizhou Peninsula, this study calculated the fluxes and average concentration of COD, NH_4^+, TN, and TP pollutants in 6 sea areas (Figure 6).

It is obvious that the fluxes of COD, NH_4^+, TN, and TP [$F_{(COD)}$, $F_{(NH4+)}$, $F_{(TN)}$, and $F_{(TP)}$] in Area B (Zhanjiang Bay) are the highest. $F_{(COD)}$ is at least 200 times larger than other regions; $F_{(NH4+)}$ is at least 1500 times larger than other regions; $F_{(TN)}$ is at least 500 times larger than other regions; $F_{(TP)}$ is at least 100 times larger than other regions. However, the average concentration of COD and NH_4^+ is not the highest in Area B, indicating that the discharge outlet in Area B has a very large flux. Since the 1980s, with the economic and social development of Zhanjiang City, a large amount of industrial and domestic wastewater has been discharged into the bay through rivers, leading to increased pollution of seawater quality and the frequent occurrence of red tide disasters. According to the "Guangdong Provincial Marine Environmental Quality Bulletin", the coastal areas of Zhanjiang City have become one of the most severe areas for red tide outbreaks, except for the Pearl River Delta region. The significant input of land-sourced pollutants is one of the important reasons for the deterioration of water quality near the Zhanjiang Bay.

Among the 6 sea areas, except for Area D, the temperature and salinity of other sea areas maintained a good trend, that is, areas with higher temperatures also have higher salinities (Figure 6). The temperature in Area D is low (33.29°C) compared to other areas, but the salinity is high (20.01), which is related to its location. It is located in Qiongzhou Strait, and the current velocity is very fast. Area A has the lowest temperature (32.58°C) and the lowest salinity (12.14), which is speculated to be related to the high input of rivers at this location. The temperature (35.37°C) and salinity (25.83) in the Area E are both the highest, which is speculated to be related to the low input of runoff at this location. The distribution of pH and DO shows a good trend, that is, areas with higher pH also have higher DO. It is obvious that the economically developed Area B and Area F have the lowest DO (4.11 mg/L and 4.09 mg/L) and PH (7.70 and 7.56), which may be related to anthropogenic pollutant emissions.

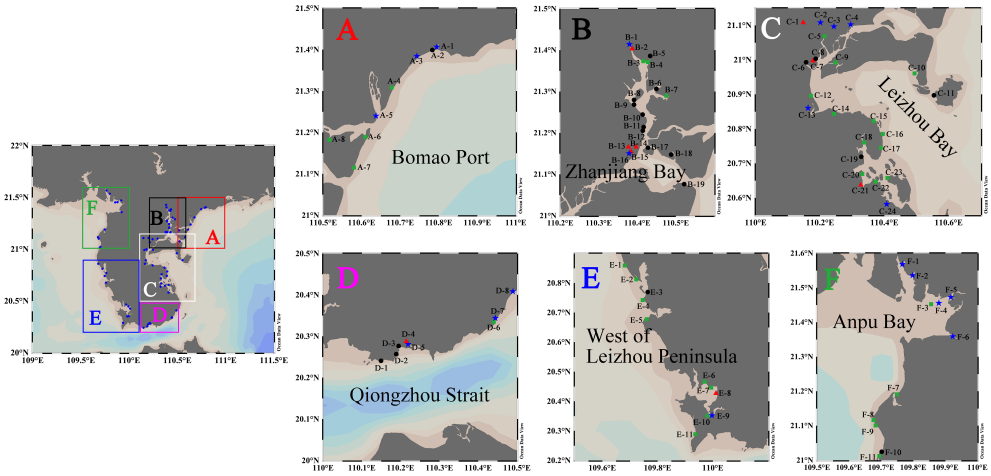

FIGURE 5
According to their final inflow into the sea areas, the study region is classified into 6 sea areas (**A:** Bomao Port **B:** Zhanjiang Bay **C:** Leizhou Bay **D:** Qiongzhou Strait **E:** West of Leizhou Peninsula **F:** Anpu Bay). Blue pentagram: river sewage outlets. Black dots: domestic sewage outlets. Green box: aquaculture sewage outlets. Red triangle: industrial sewage outlets.

3.3 CNPI index

According to the Class III water quality standard in the "Surface Water Quality Standard (GB 3838-2002) (State environmental protection administration, 2002)", CNPI is used to express the pollution index of land-sourced pollutants in the sea area around Leizhou Peninsula. The CNPI considers the weight of the impact of various water quality indicators on water quality, which can reasonably reflect the water quality pollution status. The correction of the maximum index value takes into account the harmfulness of the important pollution factor, and the evaluation results are relatively close to reality.

According to the weight values (Table 3), it can be concluded that TP accounts for the largest proportion among various pollution indicators, followed by TN and NH_4^+, meaning that nitrogen and phosphorus indicators are the greatest impact on water quality.

Overall, the water quality in Area B is generally worse than other areas, with CNPI: B>A>F>C>D>E (Table 4). In summer, the CNPI range in Area A is 0.35–6.50, including three water quality levels: 1 "Safe" sewage outlet, 1 "Warming" sewage outlet, and 6 "Moderate Pollution" sewage outlets, and the average value of CNPI is 2.03 (Table 4, Figure 7). The CNPI range in Area B is 0.41–123.13, including five water quality levels: 4 "Safe" sewage outlets, 1 "Warming" sewage outlet, 1 "Slight Pollution" sewage outlets, 12 "Moderate Pollution" sewage outlets, and 1 "Heavy Pollution" sewage outlet. The average value of CNPI is 7.13 in Area B, and the high TN value of B-2 in Area B is 348 mg/L, resulting in a larger CNPI (Table 4, Figure 7). The CNPI range in Area C is 0.31–3.93, including four water quality levels: 4 "Safe" sewage outlets, 3 "Warming" sewage outlets, 9 "Slight Pollution" sewage outlets, and 8 "Moderate Pollution" sewage outlets, and the average value of CNPI is 1.22 (Table 5, Figure 7). The CNPI range in Area D is 0.53–2.53, including three water quality levels: 2 "Safe" sewage outlets, 2 "Slight Pollution" sewage outlets, and 4 "Moderate Pollution" sewage outlets, and the average value of CNPI is 1.15 (Table 4, Figure 7). The CNPI range in Area E is 0.55–2.57,

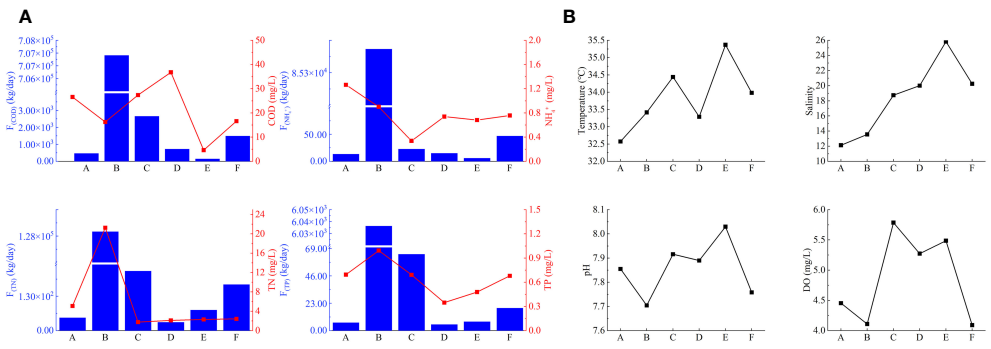

FIGURE 6
(A) Average concentration and fluxes of COD, NH_4^+, TN and TP in the sewage outlets in Area A, Area B, Area C, Area D, Area E, and Area F around Leizhou Peninsula in summer. **(B)** Average temperature, salinity, PH and DO in the sewage outlets in Area A, Area B, Area C, Area D, Area E, and Area F around Leizhou Peninsula in summer.

TABLE 3 Weight values of COD, NH_4^+, TN, and TP.

Index	Class III water standard	Wi
COD	≤20	0.007
NH_4^+	≤1.0	0.142
TN	≤1.0	0.142
TP	≤0.2	0.709

including three water quality levels: 4 "Safe" sewage outlets, 4 "Slight Pollution" sewage outlets, and 3 "Moderate Pollution" sewage outlets, and the average value of CNPI is 1.10 (Table 5, Figure 7). The range of CNPI in Area F is 0.52–4.85, including four water quality levels: 2 "Safe" sewage outlets, 3 "Warming" sewage outlets, 2 "Slight Pollution" sewage outlets, and 4 "Moderate Pollution" sewage outlets, and the average value of CNPI is 1.31 (Table 4, Figure 7).

3.4 PCA and cluster analysis

The PCA was used to analyze the land-sourced pollutants and environmental factors from six sea areas around the Leizhou Peninsula. There was a correlation between the variables, as shown by the Kaiser Meyer Olkin (KMO) test value of 0.643 and the Bartlett test result of $p<0.001$. Through PCA, we explored the relationship between land-sourced pollutants (COD, NH_4^+, TN, and TP) and environmental factors (temperature, salinity, DO, and pH) at 81 sewage outlets around Leizhou Peninsula (Figure 8). PC1 and PC2 explained 56.1% of the total variance (Figure 8). The main contribution of PC1 (34.1%) comes from the fluxes of land-sourced pollutants, including $F_{(COD)}$ (0.48), $F_{(NH4+)}$ (0.48), $F_{(TN)}$ (0.48), and $F_{(TP)}$ (0.48). The contribution of PC2 (22.2%) comes from environmental factors such as temperature (0.39), DO (0.39), salinity (0.35), and pH (0.42). In PCA, B-1 and B16 showed anomalies, which may be due to the large flux in these two stations.

Cluster analysis was conducted on the land-sourced pollutants and environmental factors in 81 sewage outlets, and the clustering results were presented in the form of heat maps (Figure 9). It can be seen that the station cluster tree can be divided into six categories, with B-2 having a particularly small correlation with other stations. Even when it is classified into six categories, B-2 is still separated separately, which is related to the high TN concentration (348 mg/L) in B-2. The first type is mainly composed of river sewage outlets with high $F_{(COD)}$. The second type mainly consists of aquaculture sewage outlets with high temperatures, high salinities, high $F_{(TN)}$, and $F_{(COD)}$. The third type includes all types of sewage outlets with high temperatures and salinities. The fourth type is industrial sewage outlets with high temperatures and COD concentrations. The fifth type is mainly domestic sewage outlets with high temperatures and COD concentrations. The sixth type only has B-2 with a high TN concentration.

TABLE 4 The range of CNPI and the average CNPI in Area A–F.

Study areas	range	mean
Area A	0.35-6.50	2.03
Area B	0.41-123.13	8.06
Area C	0.31-3.93	1.22
Area D	0.53-2.53	1.15
Area E	0.55-2.57	1.10
Area F	0.52-4.85	1.31

3.5 Model validation and results

In the previous analysis, we found that the $F_{(COD)}$, $F_{(TN)}$ and $F_{(TP)}$ in Area B of the six receiving sea areas around the Leizhou Peninsula are much larger than those in other areas (Figure 6). The CNPI index and cluster analysis also show that there is a serious pollution station (B-2) in Area B (Figures 7, 9). Moreover, the PCA also indicates that B-1 and B-16 have a significant impact on Area B (Figure 8). Based on the above analysis, Area A, Area C, Area D, Area E, and Area F belong to open sea areas with fast flow velocity and fast metabolism, while Area B belongs to a semi-enclosed bay with fast economic development and severe pollution. Therefore, it is necessary to analyze the environmental capacity in Area B through a model.

It can be seen that the measured values and simulated values have a good fit in tidal level verification (S1: RMSE=0.26, r=0.98; S2: RMSE=0.19, r=0.99; C1: RMSE=0.07, r=0.68; TN: RMSE=0.07, r=0.93; TP: RMSE=0.016, r=0.97;COD: RMSE=0.08, r=0.95) (Figure 2). Overall, the errors in phase and amplitude are basically within a reasonable range, and the changes in simulated values and measured values tend to be consistent (Figures 2A, B). The measured and simulated values have a good fit in the verification of flow velocity and direction, and the changes between the simulated and measured values tend to be consistent (Figures 2C, D). It can be considered that they can reasonably reflect the characteristics of the tidal current field in Zhanjiang Bay. In this study, the concentration accuracy of the model in Zhanjiang Bay was verified by combining the COD, TN, and TP from the sampled data (Figures 2E-G). The variability of simulated values of COD, TN, and TP concentrations is generally consistent with the measured values.

3.6 Environmental capacity and remaining environmental capacity

Through calculation, a total of 6 sewage outlets have exceeded the environmental capacity of COD and TN, and 3 sewage outlets have exceeded the environmental capacity of TP. In the study, the response coefficients of B-1 and B-16 reach over 90%, so we only provide the figures of response coefficients and sharing rates in B-1 and B-16 (Figure 10).

The response coefficient can reflect the quantitative relationship between the pollution source and the receiving water. The different dynamic environments in different sea areas cause the response coefficient to change with location, thus forming a response coefficient field. The response coefficient field is defined based on

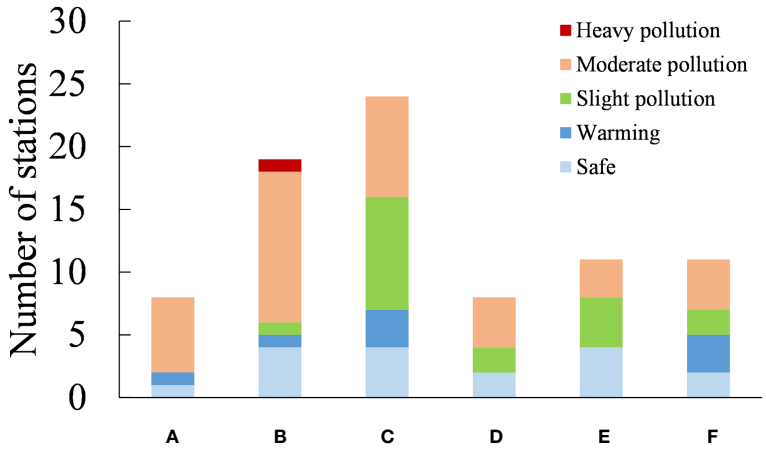

FIGURE 7
The number of stations of CNPI in Area A–Area F.

the equilibrium concentration field of land-sourced pollutants by each sewage outlets when discharged separately in a unit volume. The response coefficient field undergoes periodic changes under the influence of tides. In this study, COD, TN, and TP are regarded as conservative substances; that is, only the physical processes of hydrodynamic transport such as advection diffusion are considered, and biological chemical processes are not considered. Therefore, when the three pollutants are discharged with unit source intensity, the pollutant response coefficient fields formed are the same. From the sharing rate field of each sewage outlet, it can be seen that each sewage outlet has the greatest impact on the nearby sea area, and the impact gradually weakens as the distance from the pollution source increases. This also proves that the response coefficient field is related to the geographical location of sewage outlets because different geographical locations have different hydrodynamic environments. In areas with strong water mixing, the response coefficient of land-sourced pollutants has a wider impact, while the distribution area of high-value areas is smaller. On the contrary, in areas with weak water mixing, the range of land-sourced pollutants transport and diffusion is relatively small, which will generate a certain amount of land-sourced pollutants accumulation in the sea area near the sewage outlets.

The sharing rate refers to the percentage of the impact of each pollution source on the overall pollution of the sea area, which represents the contribution of each pollution source to the pollution of each spatial point in the sea area when it is actually discharged. Based on the statistics of 19 major sewage outfalls in Zhanjiang Bay, This study calculates the ratio of the concentration distribution field emitted by each pollution source alone to the concentration distribution field emitted by all pollution sources simultaneously. Overall, the sharing rate of the three pollutants generally decreases from the discharge point to the distance, with the highest sharing rate occurring in the waters near the sewage outfalls. In addition, due to the fact that the sharing rate is calculated using measured values, the pollutant fluxes in B-1 and B-16 are much greater than those at other sewage outfalls, making B-1 and B-16 with high and most widely distributed sharing rates in the Zhanjiang Bay. Near the sewage outlets with smaller pollutant discharge flux, the sharing rates of B-1 and B-16 can also be higher than 90%, indicating that the COD, TN, and TP of these two sewage outlets have an important impact on the entire sea area.

TABLE 5 The theoretical environmental capacity, remaining environmental capacity, and theoretical environmental capacity of sewage outlets with excessive environmental capacity.

Station	COD (t/a)			TN (t/a)			TP (t/a)		
	Theoretical environmental capacity	Used environmental capacity	Remaining environmental capacity	Theoretical environmental capacity	Used environmental capacity	Remaining environmental capacity	Theoretical environmental capacity	Used environmental capacity	Remaining environmental capacity
B-1	2.1×10^{3}	2.6×10^{5}	0	32.167	4.5×10^{4}	0	5.887	1.7×10^{3}	0
B-2	0.005	0.063	0	0.251	1.829	0	0.006	0.010	0
B-3	1.397	10.762	0	0.985	4.769	0	/	/	/
B-4	2.417	17.199	0	0.802	4.559	0	/	/	/
B-5	2.726	10.220	0	0.093	0.280	0	/	/	/
B-16	542.445	2.3×10^{3}	0	124.700	1.2×10^{3}	0	27.759	482.940	0

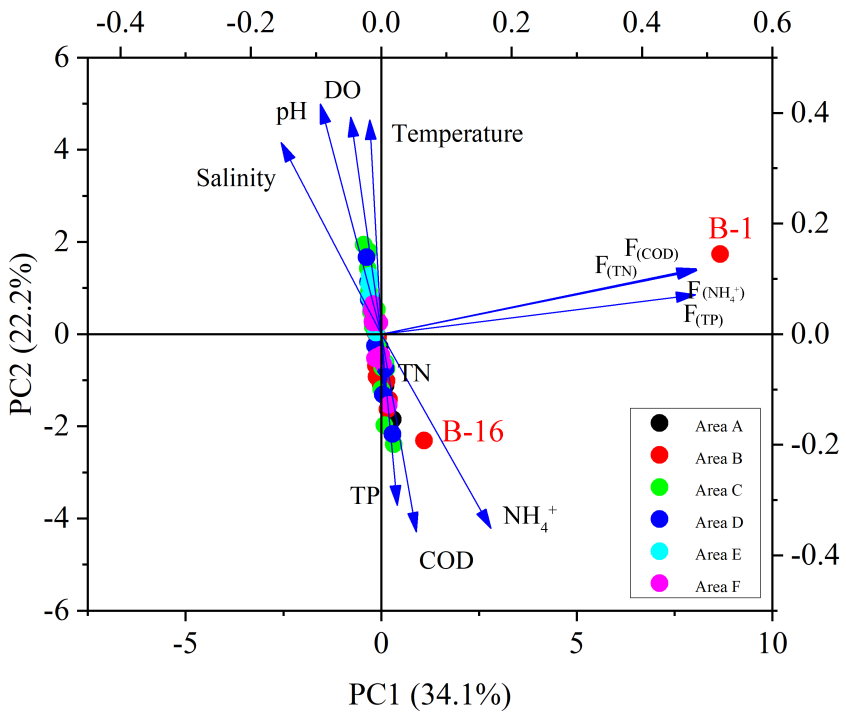

FIGURE 8
The PCA shows the relationship between the land-sourced pollutants and environmental factors around the Leizhou Peninsula. (The vector shows the direction and intensity of environmental variables relative to the overall distribution; the color dots correspond at 81 stations).

The environmental capacity of the sea area near a total of 6 sewage outlets has exceeded the standard, with B-1 and B-16 estuaries being the most severely exceeded (Table 5). The COD exceeded 2.5×10^5 t/a at B-1 and 1.7×10^3 t/a at B-16, respectively. The TN exceeded 4.5×10^4 t/a at B-1 and 1.0×10^3 t/a at B-16, respectively. The TP exceeded 1.7×10^3 t/a at B-1 and 455 t/a at B-16, respectively. It was found that the areas with excessive environmental capacity in Zhanjiang Bay are mainly located at the top of the bay. The large flow rate and high concentration of pollutants at the B-1 and B-16 sewage outlets contribute to the majority of TN and TP in the Zhanjiang Bay, thereby also affecting the environmental capacity of other sewage outlets in the sea area. Therefore, it is necessary to focus on renovating these two sewage outlets in order to protect the seawater quality and environmentally sensitive areas in Zhanjiang Bay.

3.7 The impact of land-sourced pollutants flux into the sea and environmental capacity of Zhanjiang Bay on seawater eutrophication

Eutrophication usually occurs in the transitional zone between terrestrial and aquatic ecosystems, such as coastal zones, bays, lakes, especially in areas that are strongly affected by human activities and have poor water exchange capacity, such as river estuaries. In nearshore waters, human activities can cause a sharp increase in eutrophic substances in seawater through various channels, such as the discharge of industrial wastewater, domestic sewage, and the inflow of agricultural fertilizers. Under certain conditions, nearshore eutrophication will also trigger marine disasters such as

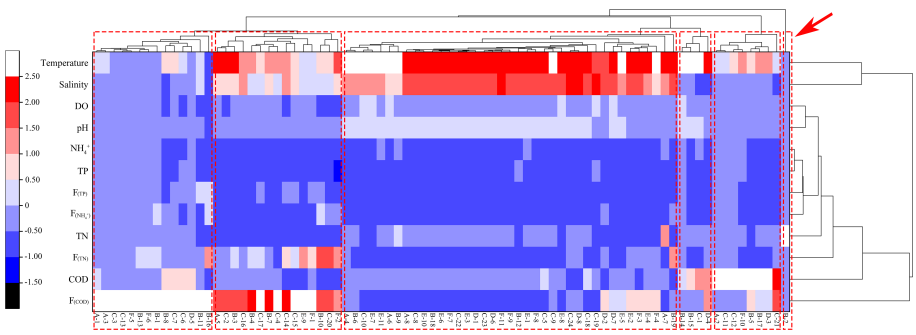

FIGURE 9
The Mondrian plot (inverse heat map) shows the land-sourced pollutants and environmental factors in 81 stations around Leizhou Peninsula.

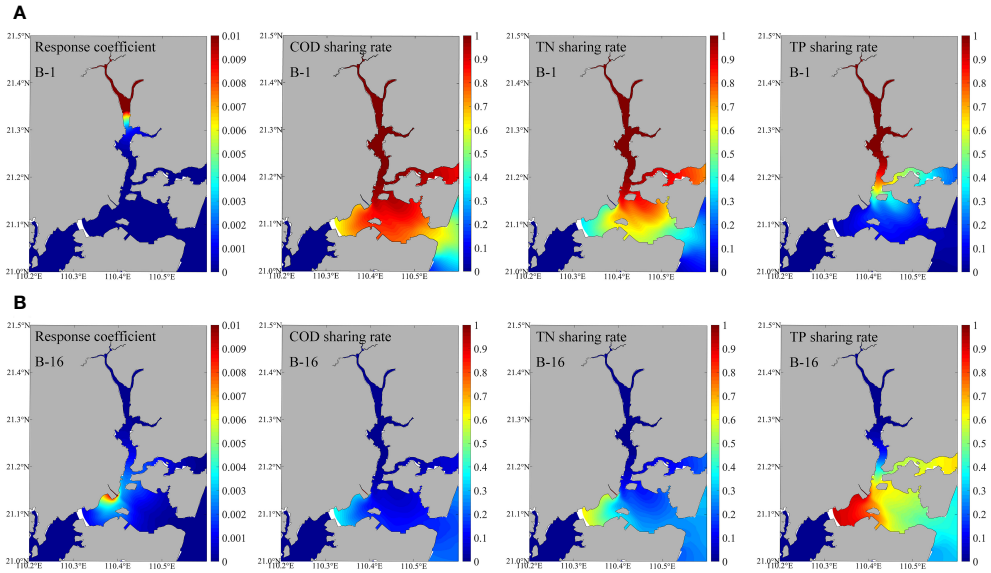

FIGURE 10
Response coefficient and land-sourced pollutants sharing rate in B-1 and B-16.

red tides, thereby endangering the marine ecological environment and coastal production and human health. In recent decades throughout the world, the increasing occurrence of phytoplankton blooms suggests an unsettling trend that has become a serious ecological issue (Liu et al., 2013; Mohamed, 2018). Eutrophication as a result of human-induced nutrient enrichment has become a concern in the Zhanjiang Bay.

The optimal ratio for phytoplankton to absorb nutrients is N: P=16:1 (Redfield et al., 1963). If the ratio of a certain nutrient in the water deviates from this ratio, it will potentially limit its growth. This ratio can reflect the nutritional status of the water environment, thereby better identifying the eutrophication status of the water environment and better controlling and managing the water environment. After analyzing our existing data, it was found that Zhanjiang Bay has generally been restricted by nitrogen in the past decade (Table 1). Although our calculations show that the pollutants in the upstream discharge outlets of the bay exceed the standard, including TN, TP, and COD, the actual impact of nitrogen emissions on eutrophication in Zhanjiang Bay may be negligible. At present, for eutrophication in Zhanjiang Bay, although the nitrogen and phosphorus environmental capacity exceeds the standard, it is still within the controllable range due to nitrogen limitations. Therefore, we found that simply controlling the nitrogen concentration in the area can effectively change the eutrophication situation in Zhanjiang Bay.

The self purification ability of water bodies varies in different water environments. Some sewage outlets with high discharge flux have limited impact on the environment due to their strong exchange capacity in the water or their distance from environmentally sensitive areas. In other cases, some sewage outlets with low discharge flux may have a significant impact on the local sea area due to their location in areas with weak water exchange capacity or high water quality requirements. Therefore, the discharge flux and location of sewage outlets play an important role. In future sewage outlets planning, it is necessary to comprehensively consider the local natural water environment, distribution of ecological functional areas, and policy planning requirements.

4 Conclusion

In this study, based on the water quality factors in the coastal waters of the Leizhou Peninsula, the spatial distribution and fluxes of land-sourced pollutants were analyzed and the pollution level of these sea areas was determined. In addition, using a modelling approach combined with measured values, environmental capacity was calculated in the Zhanjiang Bay. The following results were obtained:

(1) Although the average concentration of COD and NH_4^+ is not the highest in Area B, the $F_{(COD)}$, $F_{(NH4+)}$, $F_{(TN)}$, and $F_{(TP)}$ in Area B are the highest. $F_{(COD)}$ is at least 200 times larger than other areas; $F_{(NH4+)}$ is at least 1500 times larger than other areas; $F_{(TN)}$ is at least 500 times larger than other areas; $F_{(TP)}$ is at least 100 times larger than other areas.

(2) The CNPI index and cluster analysis showed that there was a serious pollution at B-2 in Area B. Moreover, the PCA also indicates that the station of B-1 and B-16 have a significant impact on Area B.

(3) There are 6 sewage outlets exceeding the environmental capacity of COD and TN and 3 sewage outlets exceeding the environmental capacity of TP. The stations of the environmental capacity exceeding the standard in Zhanjiang Bay are mainly located at the top of the bay.

(4) Although the pollutants in the upstream discharge outlets of the bay exceed the standard, including TN, TP, and COD, the actual

impact of nitrogen emissions on eutrophication in Zhanjiang Bay may be negligible because Zhanjiang Bay has generally been restricted by nitrogen in the past decade.

Data availability statement

The original contributions presented in the study are included in the article/supplementary material. Further inquiries can be directed to the corresponding authors.

Author contributions

YC: Conceptualization, Formal Analysis, Methodology, Visualization, Writing – original draft, Writing – review & editing. YS: Conceptualization, Formal Analysis, Methodology, Visualization, Writing – original draft, Writing – review & editing. HS: Data curation, Methodology, Writing – review & editing. HG: Conceptualization, Funding acquisition, Supervision, Writing – review & editing. HZ: Conceptualization, Funding acquisition, Supervision, Writing – review & editing. KT: Supervision, Writing – review & editing. GP: Supervision, Writing – review & editing.

Funding

The author(s) declare financial support was received for the research, authorship, and/or publication of this article. The present research is supported by the National Natural Science Foundation of China (No. 42076162) and the project was supported by the Innovation Group Project of Southern Marine Science and Engineering Guangdong Laboratory (Zhuhai) (No. 311020004).

Conflict of interest

The authors declare that the research was conducted in the absence of any commercial or financial relationships that could be construed as a potential conflict of interest.

Publisher's note

References

Andersen, J. H., Carstensen, J., Conley, D. J., Dromph, K., Lehtinen, V. F., Gustafsson, B. G., et al. (2017). Long-term temporal and spatial trends in eutrophication status of the Baltic Sea. *Biol. Rev.* 92, 135–149. doi: 10.1111/brv.12221

Bui, L. T., and Pham, H. T. H. (2023). Linking hydrological, hydraulic and water quality models for river water environmental capacity assessment. *Sci. Total Environment* 857, 159490. doi: 10.1016/j.scitotenv.2022.159490

Chen, X., Wang, Y., Cai, Z., Zhang, M., and Ye, C. (2020). Response of the nitrogen load and its driving forces in estuarine water to dam construction in Taihu Lake, China. *Environ. Sci. pollut. Res.* 27, 31458–31467. doi: 10.1007/s11356-020-09454-0

Chen, Y., Cheng, W., Zhang, H., Qiao, J., Liu, J., Shi, Z., et al. (2019). Evaluation of the total maximum allocated load of dissolved inorganic nitrogen using a watershed–coastal ocean coupled model. *Sci. Total Environment* 673, 734–749. doi: 10.1016/j.scitotenv.2019.04.036

Dou, M., Ma, J. X., Li, G. Q., and Zuo, Q. (2015). Measurement and assessment of water resources carrying capacity in Henan Province, China. *Water Sci. Eng.* 8 (2), 12. doi: 10.1016/j.wse.2015.04.007

Egbert, G. D., and Erofeeva, S. Y. (2002). Efficient inverse modeling of barotropic ocean tides. *J. Atmospheric Oceanic Technol.* 19, 183–204. doi: 10.1175/1520-0426(2002)019<0183:EIMOBO>2.0.CO;2

Gimenez, Y., and Giussani, G. (2018). Searching for the core variables in principal components analysis. *Braz. J. Probability Statistics* 32 (4), 730–754. doi: 10.48550/arXiv.1308.6626

Gong, Y., Zhang, C., Sun, X., Zhang, Y., Shi, Y., Xie, Q., et al. (2012). Community characteristics of phytoplankton in the coastal area of Leizhou Peninsula and their relationships with primary environmental factors in the summer of 2010. *Acta Ecol. Sinica* 32, 5972–5985. doi: 10.0.22.214/stxb201109011280

Guo, L. (2005). *A Study on the Bohai Sea in Environmental Capacity of Petroleum Hydrocarbon* (China: Ocean University of China).

Han, H., Li, K., Wang, X., Shi, X., Qiao, X., and Liu, J. (2011). Environmental capacity of nitrogen and phosphorus pollutions in Jiaozhou Bay, China: Modeling and assessing. *Mar. pollut. Bull.* 63, 262–266. doi: 10.1016/j.marpolbul.2010.12.017

Huang, X. P., Huang, L. M., and Yue, W. Z. (2003). The characteristics of nutrients and eutrophication in the Pearl River estuary, South China. *Mar. pollut. Bull.* 47, 30–36. doi: 10.1016/S0025-326X(02)00474-5

Ji, X., Dahlgren, R. A., and Zhang, M. (2016). Comparison of seven water quality assessment methods for the characterization and management of highly impaired river systems. *Environ. Monit. Assessment* 188, 15. doi: 10.1007/s10661-015-5016-2

Jia, Z., Cai, Y., Chen, Y., and Zeng, W. (2018). Regionalization of water environmental carrying capacity for supporting the sustainable water resources management and development in China. *Resources Conserv. Recycling* 134, 282–293. doi: 10.1016/j.resconrec.2018.03.030

Jiang, T., Song, W., and Fang, X. (1991). Physical self-cleaning capacity in the southwest of Laizhou Bay. *Mar. Sci. Bull.*, 53–79.

Kalnejais, L. H., Martin, W. R., and Bothner, M. H. (2010). The release of dissolved nutrients and metals from coastal sediments due to resuspension. *Mar. Chem.* 121, 224–235. doi: 10.1016/j.marchem.2010.05.002

Kang, P., and Xu, L. (2012). Water environmental carrying capacity assessment of an industrial park. *Proc. Environ. Sci.* 13, 879–890. doi: 10.1016/j.proenv.2012.01.082

Kemp, W. M., Testa, J. M., Conley, D. J., Gilbert, J. D., and Hagy, J. D. (2009). Temporal responses of coastal hypoxia to nutrient loading and physical controls. *Biogeosciences;* 6, 2985–3008. doi: 10.5194/bg-6-2985-2009

Krom, M., Hornung, H., and Cohen, Y. (1990). Determination of the environmental capacity of Haifa Bay with respect to the input of mercury. *Mar. pollut. Bull.* 21, 349–354. doi: 10.1016/0025-326X(90)90798-D

Lei, G., Zhang, Y., Pan, D., and Fu, D. Y. (2016). Parameter selection and model research on remote sensing evaluation for nearshore water quality. *Acta Oceanol. Sin.* 35, 114–117. doi: 10.1007/s13131-016-0802-4

Le Moal, M., Gascuel-Odoux, C., Ménesguen, A., Souchon, Y., Etrillard, C., Levain, A., et al. (2019). Eutrophication: A new wine in an old bottle? *Sci. Total Environment* 651, 1–11. doi: 10.1016/j.scitotenv.2018.09.139

Li, S., Li, H., and Xia, J. (2005). Dapeng bay water environment capacity analysis on the base of delft 3D model. *Res. Environ. Sci.* 18 (5) 91–95. doi: 10.13198/j.res.2005.05.93.lisw.023

Liu, R. X., Kuang, J., Gong, Q., and Hou, X. L. (2003). Principal component regression analysis with SPSS. *Comput. Methods Programs Biomed.* 71, 141–147. doi: 10.1016/S0169-2607(02)00058-5

Liu, L., Zhou, J., Zheng, B., Cai, W., Lin, K., and Tang, J. (2013). Temporal and spatial distribution of red tide outbreaks in the Yangtze River Estuary and adjacent waters, China. *Mar. pollut. Bull.* 72, 213–221. doi: 10.1016/j.marpolbul.2013.04.002

Margeta, J., Baric, A., and Gacic, M. (1989). *Environmental capacity of the Kastela Bay.*

Mironov, O., Kiryukhina, L., and Kucherenko, M. (1975). Self-purification in the coastal area of the Black Sea. *Naukova Dumka Kiev (USSR)* 143, 1975.

Mohamed, Z. A. (2018). Potentially harmful microalgae and algal blooms in the Red Sea: Current knowledge and research needs. *Mar. Environ. Res.* 140, 234–242. doi: 10.1016/j.marenvres.2018.06.019

National Marine Environmental Monitoring Center (2007). *The specification for marine monitoring - Part 4: Seawater analysis (GB17378.4–2007)* (China: Standards Press of China).

Nemerow, N. L. C. (1974). Scientific stream pollution analysis. *Environmental Science*.

Parette, R., and Pearson, W. N. (2014). doi: 10.1016/j.chemosphere.2014.03.076

Redfield, A. C., Ketchum, B. H., and Richards, F. A. (1963). The influence of organisms on the composition of sea-water. *Sea*.

Song, D. (1999). Pollution control in the seto inland sea of Japan from the 1970s to the 1980s. *J. Japan Stud. Forum*, 23–29.

State environmental protection administration (2002). *Surface water quality standard: GB 3838-2002* (Beijing: China Environmental Science Press).

Sun, L. (2020). Research on the changes and mechanisms of marine environmental capacity in haizhou bay from 2006 to 2016. *Nanjing Normal University*. doi: 10.27245/d.cnki.gnjsu.2020.000001

Swati, S. S. (2015). Nemerow's pollution index: for ground water quality assessment.

Van der Wulp, S. A., Damar, A., Ladwig, N., and Hesse, K. J. (2016). Numerical simulations of river discharges, nutrient flux and nutrient dispersal in Jakarta Bay, Indonesia. *Mar. pollut. Bull.* 110, 675–685. doi: 10.1016/j.marpolbul.2016.05.015

Wang, Y., Liu, D., Xiao, W., Zhou, P., Tian, C., Zhang, C., et al. (2021). Coastal eutrophication in China: Trend, sources, and ecological effects. *Harmful Algae* 107, 102058. doi: 10.1016/j.hal.2021.102058

Wang, S., Xu, L., Yang, F., and Wang, H. (2014). Assessment of water ecological carrying capacity under the two policies in Tieling City on the basis of the integrated system dynamics model. *Sci. Total Environment* 472, 1070–1081. doi: 10.1016/j.scitotenv.2013.11.115

Wang, X., Zhao, Q., and Zhao, S. (2012). Research progress on marine environmental capacity and total amount control of marine pollutant. *Mar. Environ. Sci.* 31, 765–769. doi: 10.1007/s11783-011-0280-z

Wei, S., Fu, D., Wang, D., Yu, G., Luo, Y., and Xu, H. (2023). Tracer study of CDOM for nitrogen and phosphorus pollution in the offshore Leizhou Peninsula, China. *Ecol. Indicators* 148, 110019. doi: 10.1016/j.ecolind.2023.110019

Woo-Jeung, C., Na, G. H., Young-Yell, C., and Chung-Kill, P. (1991). Self-purification capacity of eutrophic buk bay by DO mass balance. *Korea J. Herbol.* 24 (1).

Wu, G., Cao, W., Wang, F., Su, X., Yan, Y., and Guan, Q. (2019). Riverine nutrient fluxes and environmental effects on China's estuaries. *Sci. Total Environment* 661, 130–137. doi: 10.1016/j.scitotenv.2019.01.120

Wu, J., Hui, X., and Jian, C. (2009). Towards understanding hierarchical clustering: A data distribution perspective. *Neurocomputing* 72, 2319–2330. doi: 10.1016/j.neucom.2008.12.011

Xu, M., and Chua, V. P. (2017). A numerical study on land-based pollutant transport in Singapore coastal waters with a coupled hydrologic-hydrodynamic model. *J. Hydro-environment Res.* 14, 119–142. doi: 10.1016/J.JHER.2016.09.002

Yamamoto, T., and Nadaoka, K. (2018). Analyzing coastal turbidity under complex terrestrial loads characterized by a 'stress connectivity matrix' with an atmosphere-watershed-coastal ocean coupled model. *Estuarine Coast. Shelf Sci.* 203, 44–58. doi: 10.1016/j.ecss.2018.01.025

Yang, J. (2001). The theory and practice of implementing total pollutant emission control in coastal waters. *Mar. Inf.*, 24–26.

Yang, L., Lu, W., Huang, H., and Chu, H. (2012). Application of improved nemerow pollution exponential method and fuzzy comprehensive evaluation method used in water quality assessment. *Water Resour. Power* 30, 41–44.

Yang, F., Wei, Q., Chen, H., and Yao, Q. (2018). Long-term variations and influence factors of nutrients in the western North Yellow Sea, China. *Mar. pollut. Bull.* 135, 1026–1034. doi: 10.1016/j.marpolbul.2018.08.034

Yu, C., Huang, X., Chen, H., Godfray, H. C. J., Wright, J. S., Hall, J. W., et al. (2019). Managing nitrogen to restore water quality in China. *Nature;* 567, 516–520. doi: 10.1038/s41586-019-1001-1

Yuan, Q., Xu, Z. Y., Peng, H. Q., Lu, J. M., Huang, L. C., Liang, X. J., et al. (2016). Research on nitrogen and phosphorus variation trend in Zhanjiang harbor and its near waters in recent five years. *J. Green Sci. Technol.* 24, 41–45. doi: 10.16663/j.cnki.lskj.2016.24.016

Zhang, P., Dai, P. D., Zhang, J. B., Li, J. X., Zhao, H., and Song, Z. G. (2021). Spatiotemporal variation, speciation, and transport flux of TDP in Leizhou Peninsula coastal waters, South China Sea. *Mar. pollut. Bull.* 167, 112284. doi: 10.1016/j.marpolbul.2021.112284

Zhang, X., and Sun, Y. (2007). Study on the environmental capacity in Jiaozhou Bay. *Mar. Environ. Sci.* 26 (4), 347–350+359. doi: 10.1002/cem.1038

Zhang, Z., Sun, W., and Zhou, Y. (2008). Quantitatively assessment of eco-environmental vulnerability in tropic coastal arid area: A case study of Leizhou Peninsula. *J. Desert Res.* 28 (01), 125–130.

Zhou, X. Y., Lei, K., Meng, W., and Khu, S. (2017). Industrial structural upgrading and spatial optimization based on water environment carrying capacity. *J. Cleaner Prod.* 165, 1462–1472. doi: 10.1016/j.jclepro.2017.07.246

frontiers | Frontiers in Marine Science

TYPE Brief Research Report
PUBLISHED 27 October 2023
DOI 10.3389/fmars.2023.1255466

OPEN ACCESS

EDITED BY
Dilip Kumar Jha,
National Institute of Ocean Technology, India

REVIEWED BY
Vikas Pandey,
Council of Scientific and Industrial Research (CSIR), India
Gopalakrishnan Thilagam,
Pachaiyappa's College for Men, India

*CORRESPONDENCE
Subrat Naik
naiksubrat@gmail.com

RECEIVED 08 July 2023
ACCEPTED 02 October 2023
PUBLISHED 27 October 2023

CITATION
Naik S, Pradhan U, Karthikeyan P, Bandyopadhyay D, Sahoo RK, Panda US, Mishra P and Murthy MVR (2023) Ecological risk assessment of heavy metals in the coastal sediment in the South-western Bay of Bengal. *Front. Mar. Sci.* 10:1255466. doi: 10.3389/fmars.2023.1255466

Ecological risk assessment of heavy metals in the coastal sediment in the South-western Bay of Bengal

Subrat Naik*, Umakanta Pradhan, P. Karthikeyan, Debasmita Bandyopadhyay, Rabindra Kumar Sahoo, Uma Sankar Panda, Pravakar Mishra and M. V. Ramana Murthy

National Centre for Coastal Research (NCCR), Ministry of Earth Sciences, Chennai, India

Dynamic coastal waters are often polluted by chemical pollutants, affecting coastal ecosystems. A total of four scientific coastal cruises up to 10 km offshore from the coastline along the Chennai-Puducherry coast during 2019-20 were conducted. This study examined the spatiotemporal distribution of heavy metals (Cr, Cu, Pb, Cd, Ni, Zn, As, Co, Mn) in the coastal sediments using various geochemical indices, including the Geo-accumulation Index (Igeo), Enrichment Factor (EF), Contamination Factor (CF), and Ecological Risk Index (ERI), to understand the impacts, environmental risks, and pollution status in coastal and marine systems. The heavy metal concentrations of Cr, Cu, Pb, Cd, Ni, Zn, As, Co, and Mn in sediments are 16.48-74.70 µg/g, 2.01-3.78 µg/g, 1.37-17.54 µg/g, 0.20-21.76 µg/g, and 5.73-40.53 µg/g, 4.73-53.54 µg/g, 2.09-28.18 µg/g, 1.80-9.02 µg/g, 70.27-346.22 µg/g, respectively. The I*geo* results revealed that none of the metals reached up to the contamination level except for Cd and As which showed a slightly contaminated level of the sediment. ERI indicated that coastal sediments are at moderate to high ecological risk from heavy metals. This study will help policymakers make informed decisions for combating or remediating metal pollution to safeguard the coastal environment.

KEYWORDS

heavy metals, geochemical indices, ecological risk index, sediment quality, Bay of Bengal

Introduction

The accumulation of heavy metals in marine and coastal ecosystems is a serious global issue that has recently received significant attention due to its environmental persistence, biogeochemical cycling, and ecological concerns. There are several reports of industrial activities that directly discharge wastewater and solid waste, as well as processes that recycle electrical and electronic trash (Youssef and El-Said, 2011; Pan and Wang, 2012; Wang et al., 2013; Ra et al., 2014). Globally, an estimated 160 thousand industries discharge 41-57

thousand tons of toxic chemicals and 68 thousand tons of toxic metals into coastal waters (UNEP and UN-HABITAT, 2005). The heavy metal (As, Cd, and Pb) concentrations higher than the background levels are considered hazardous to marine life and human health (Persaud et al., 1993). The most toxic heavy metals, Cd, As, and Hg pose serious ecological threats to marine flora and fauna. They are carried in the water column, build up in sediments, and bio-accumulate in the food chain (Neff, 1997; Mason et al., 2000; Cotin et al., 2011; Nance et al., 2012). Several studies have also reported metal contamination from desalination plant effluents in coastal sediments in the Gulf States (de Mora et al., 2004; Naser, 2012; Naser, 2013).

Heavy metals are widely present in industrial effluents, anti-fouling paint on fishing boats, ships, and municipal wastewater, and large accumulations of industrial wastes and effluents have the potential to pollute the coastal environment (Jha et al., 2021; Xie et al., 2023). Several studies have found that heavy metal accumulation in sediments along the southeast coast of India may be caused by point sources such as direct discharge of significant amounts of industrial and domestic wastes into rivers and coastal waters (Muthu and Jayaprakash, 2008; Satpathy et al., 2012; Barath Kumar et al., 2017; Gopal et al., 2017; Tholkappian et al., 2018; Jha et al., 2019; Jha et al., 2021; Kannan et al., 2023). When heavy metals enter the aquatic environment, only a fraction of the metal ions dissolve in the water; the remainder is deposited in sediments through adsorption, hydrolysis, and co-precipitation, posing a risk to the environment, the biota, and human health (Li et al., 2013; Ke et al., 2017). However, sediments may move from the sink to the source of the water column when environmental conditions change as a result of a reversal in wind patterns (Prica et al., 2008; Zhuang and Gao, 2015). As a result, heavy metal concentrations in sediments are frequently investigated to provide information for assessing environmental risk (Long et al., 1995; SEPA (State Environmental Protection Administration of China), 2002). As far as the Indian coast is concerned, lots of heavy metals are being handled in the major ports available along the east and west coasts of India, and many industries have been established along the Indian coast, which releases lots of pollutants into the Bay of Bengal and Arabian seas (Sundararajan et al., 2016; Jha et al., 2019; Satheeswaran et al., 2019). Therefore, many possibilities and opportunities exist to monitor the heavy metal concentration in the coastal environment to avoid the major environmental potential loss due to heavy metal accumulation in water and marine sediments. Further, the species available in benthic sediments are very susceptible to the ingress of toxic heavy metals, which form the building block in the marine food chain (Nance et al., 2012).

The present investigation aimed to (i) evaluate the contamination status of metals (Cr, Cu, Pb, Cd, Co, Mn, Ni, Zn, and As) in the sediment and their spatio-temporal distribution, (ii) quantify and identify the sources and pollution status in the coastal sediments/marine system, and (iii) estimate the ecological risk of heavy metal contamination using various geochemical indices, including geo-accumulation index (I*geo*), enrichment factor (EF), contamination factor (CF), and ecological risk index (ERI). Data on heavy metals in coastal sediments were collected during pre- and post-Covid-19 scenarios, where most of the industries and port operations were under lockdown. The metal concentrations reported in this study would be useful as reference values for the future evaluation of marine sediment quality and help government strategies for addressing environmental pollution, particularly heavy metal pollution, which not only has human hazard implications but also the power to paralyze the aquatic environment and associated species for a longer time scale.

Materials and methods

Study area

The study area extends within the geographical limits of (13° 03' 59.99" N, 80° 17' 25.63" E and 12° 31' 18.59" N, 80° 9' 56.60" E) and a coastal stretch of about 170 km extending from north Chennai to the south of Puducherry along the southeast coast of India (Figure 1). Sediment samples were collected at 11 transects (1 km, 5 km, and 10 km from the coast) such as Chennai Port (CP-1, CP-5, CP-10), Marina (MA-1, MA-5, MA-10), Adyar (AD-1, AD-5, AD-10), Kovalam (KO-1, KO-5, KO-10), Mahabalipuram (MH-1, MH-5, MH-10), Kalpakkam (KP-1, KP-5, KP-10), Edaikazhinadu (ED-1, ED-5, ED-10), Pondicherry University (PU-1, PU-5, PU-10), Gandhi statue (GS-1, GS-5, GS-10), Fishing harbor (FH-1, FH-5, FH-10), and Paradise beach (PB-1, PB-5, PB-10). The coast of Tamil Nadu has 3 major ports, 7 state ports, 16 minor ports, fishing ports, and various coastal industries such as nuclear power plants, thermal power plants, oil refineries, and fertilizer production. The megacity Chennai, the capital of Tamilnadu, has also experienced rapid industrial and population growth as well as seeing untreated domestic and industrial wastes discharged into the coastal waters (Rosado et al., 2023). Such coastal cities have an estimated population of around 20 million people (Ramesh et al., 2008). More than 10 million people live along the coast in the mega city of Chennai alone, resulting in more than 75 million gallons of waste being discharged into the sea every day (Ramesh et al., 2008). The Buckingham Canal, which is located within the study area, runs parallel to the coast and transports largely untreated sewage from the city and industrial effluents to the backwaters of the Cooum, Adyar, Muthukadu, Edaiyur, and Sadras. Additionally, the Madras Atomic Power Station (MAPS) on the Kalpakkam coast draws seawater through an intake structure that is submerged in water about 500 meters from the coastline. The hot seawater is discharged into the sea through an outfall canal after being heated by the condenser during the cooling process. The coast is characterized by a semi-diurnal tide of a maximum ~1.2 m tidal range. Coastal currents vary seasonally; with an average of 15 cm/s, northeasterly during the southwest (SW) monsoon and 17 cm/s in a southerly direction during the northeast (NE) monsoon. Five important tourist beaches *viz*., Marina (MA), Elliot (EL), Thiruvanmiyur (TH), and Kovalam (KO) in Chennai, and Paradise Beach (PB) in Puducherry, are located along the southeast coast of India.

A total of four scientific coastal cruises up to 10 km from the coast along the Chennai-Puducherry region were conducted during 2019-20. The research vessels of the Ministry of Earth Sciences, Govt. of India were engaged for these on-board samplings. Details of the cruises are: first cruise- Mar 2019 by CRV Sagar Purvi, second

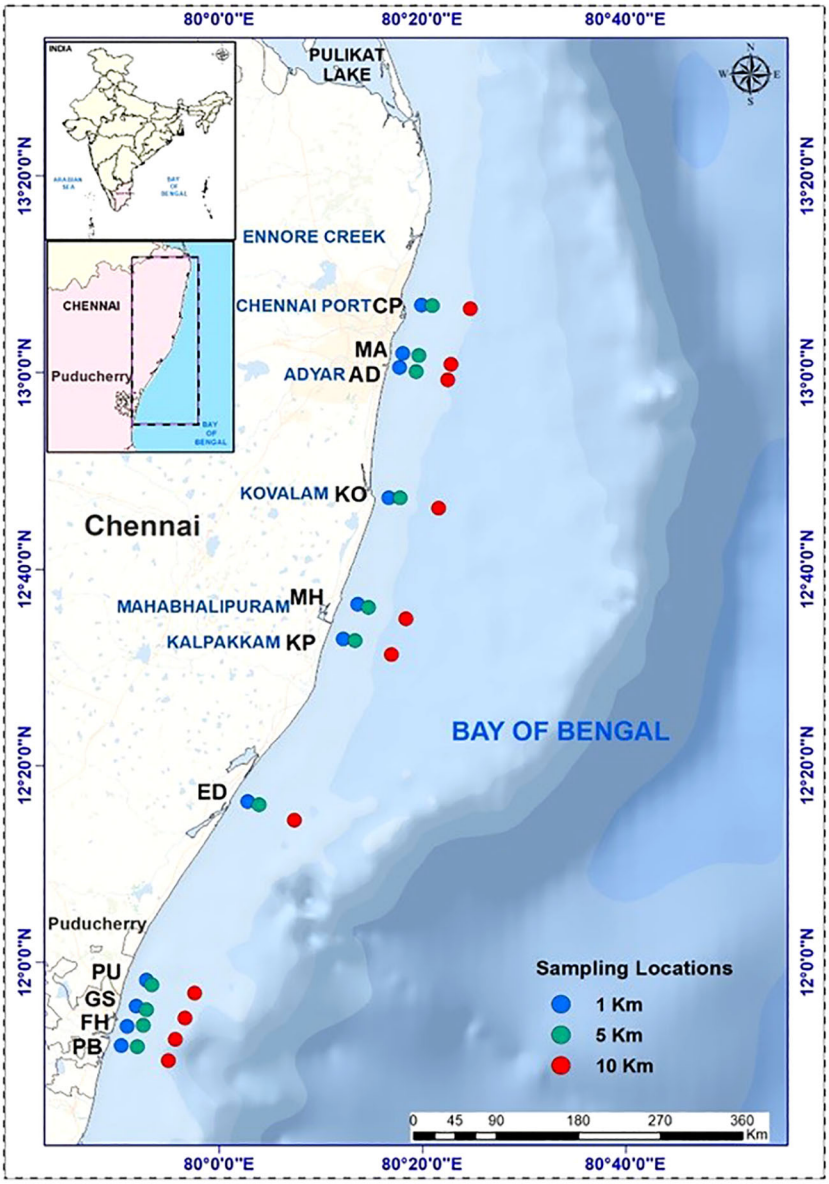

FIGURE 1
Sampling locations.

cruise-January 2020 by ORV Sagar Manjusha, third cruise-July 2020 by CRV Sagar Anveshika, and fourth cruise-September 2020 by CRV Sagar Anveshika. The four cruise data sets were separated into two seasons. Depending on the amount of precipitation (IMD, 2020), the seasons are classified into dry periods (January and March) and wet periods (July and September). A total of 132 coastal sediment samples were collected from the Chennai-Puducherry coast. After collection, the sediment samples were air-dried for one week, then ground using a porcelain mortar and pestle, sieved through a 63 μ size, and stored in polyethylene bags at ambient room temperature. All analyses were carried out in duplicate and the results were expressed as mean. Briefly, 0.2 g of the sediment samples were digested with 1 ml H_2O_2, 4 ml HNO_3, and 1 ml HCL in a 1:4:1 ratio. Samples were digested at 195°C in a microwave digestor for 90 min. The digested samples were then filtered through the Whatman No.1 filter and made up to 10 ml with Milli Q water (USEPA, 2007). Metal concentrations in extracted samples were measured by Inductively Coupled Plasma Optical Emission Spectrometry (ICP-OES, Make: Agilent; Model: 5110 VDV). The instrument was calibrated using a trace metals mix (Agilent Technologies) standard. The certified reference materials (CRMs) for marine sediment (PACS-3, Lot G 4169010, NRC, Canada) were used to validate the analysis of heavy metals (Persaud et al., 1993; MacDonald et al., 2000; ECMDEQ, 2007; Simpson et al., 2013) (Supplementary Table 1). The same acid digestion process used for the sediment samples was also used for CRMs. Sediment organic carbon (SOC) was determined using the Walkley-Black wet oxidation method (Walkley, 1935).

The pollution level and environmental quality status in marine sediments were assessed by using pollution indices such as enrichment factor (EF), contamination factor (CF), geo-accumulation index (Igeo), and ecological risk index (ERI). The background metal concentration is considered the standard value for reliable interpretation of the geochemical data. The average metal concentrations in sediments were measured following Turekian and Wedepohl (1961).

A popular normalization technique used to distinguish metals with natural variability from those with anthropogenic variability is the enrichment factor (EF) (Sinex and Helz, 1981; Selvaraj et al., 2004). To assess the anthropogenic impact on heavy metals in sediments, the EF for each element was determined as follows.

$$EF = \frac{(\frac{C_x}{C_{Al}})_{Sample}}{(\frac{C_x}{C_{Al}})_{Background}}$$

Where EF is the ratio of the relevant samples to background shale average values, and C_X and C_{Al} stand for the concentrations of metals X and Al, respectively.

According to Bam et al. (2011), EF is categorized as background concentration<1; depletion to minimum enrichment 1-2; moderate enrichment 2-5; significant enrichment 5-20, very high enrichment 20-40, and extremely high enrichment >40.

To measure the contamination in sediments from specific metals, the contamination factor (CF) was calculated using the following equation:

$$CF = \frac{C_{heavy\ metal}}{C_{background}}$$

"$C_{background}$" in the equation above refers to the metal content in the sediments before any anthropogenic input. According to Hakanson (1980), CF<1 represents low contamination, 1< CF< 3 suggests moderate contamination, 3< CF< 6 denotes considerable contamination, and CF> 6 refers to high contamination.

The geoaccumulation index (I*geo*) is the estimate of probable metal enrichment of metals in the sediments (Muller, 1979). The equation for the derivation of I*geo* is provided here under,

$$I_{geo} = \log_2\left(\frac{C_n}{1.5 \times B_n}\right)$$

Where B_n is the background concentration value for metal n and C_n is the concentration of metal n in the sediments (Turekian and Wedepohl, 1961), factor 1.5 is used to account for any variations in the background data due to lithological variances. Using the world average shale values, I*geo* was effectively computed. Muller (1979) defined five levels of sediment pollution: non-polluted (I*geo*< 1), very slightly polluted (1<I*geo*< 2), slightly polluted (2<Igeo< 3), moderately polluted (3<Igeo< 4), highly polluted (4<I*geo*< 5), and very highly polluted (I*geo*> 5).

Overall, the ecological impact of metal contamination in the sediment is evaluated using the ecological risk index (ERI) (Hakanson, 1980). The ERI is calculated by the formula,

$$ERI = \sum Ef^i$$

$$Ef^i = Tr^i x\, Cf^i$$

Where Tr^i stands for the toxic response factor for a certain metal, Cf^i for contamination of a chosen metal, and Ef^i for the enrichment of a particular metal. The degree of ecological risk is quantified using the following categories of ERI:

ERI< 40, which indicates low ecological risk due to metal pollution; 40 ≤ ERI< 80, which indicates moderate ecological risk; 80 ≤ ERI< 160, which indicates Considerable ecological risk; 160 ≤ ERI< 320 - high ecological risk; ≥ 320 - very high ecological risk.

Results and discussion

Coastal sediments are the ultimate storeroom for pollutants, hence monitoring and regulation are highly essential to conserve the ecosystem. Sediment quality guidelines (SQG) and environmental quality indices are widely recognized for the assessment of hazards from the toxic metals in the sediment (Oves et al., 2012; Kwok et al., 2014). The findings of the measurements made of the heavy metals and organic carbon in the coastal sediments at 33 different sites are shown in Table 1. A total of 132 numbers of coastal sediment samples were collected from the Chennai-Puducherry coast. Heavy metals (Cr, Cu, Pb, Cd, Co, Mn, Ni, Zn, As), as well as sediment organic carbon, were analyzed during the dry and wet periods. Overall higher metal concentrations were observed during the dry season attributing to accumulation and precipitation due to the lesser flow rate and dilution (Duncan et al., 2018; Santhosh et al., 2023). The concentration of chromium (Cr) ranged from 16.48 to 74.70 µg/g and maximum concentration was observed at ED-1 during the dry period. Copper (Cu) concentrations ranged between 2.01 µg/g and 53.78 µg/g and the concentration of Cu was higher at FH-5 in the dry period. Lead (Pb) concentration was observed from 1.37 to 17.54 µg/g and the ED-1 site was recorded with high levels during the dry period. Cadmium (Cd) was found in the range between 0.20 and 21.76 µg/g. The higher Cd concentration was recorded at MA-5 during the dry period. Higher Cobalt (Co) concentration was found during the wet period at KO-10 with an overall range of 1.80 - 9.02 µg/g. Manganese (Mn) varied from 70.27 to 346.22 µg/g and the highest concentration was found at ED-1 during the dry period. Nickel (Ni) varied from 5.73 to 40.53 µg/g and the highest concentration was found at PU-5 in the wet period. The Ni concentration observed in this study is lesser than the reported concentration of Ni from 15.6 to 23.6 µg/g in 2018 in Chennai coastal sediments (Tholkappian et al., 2018). Zinc (Zn) concentration ranged from 4.73 to 53.54 µg/g and the highest concentration was found at FH-5 during the wet period. Similarly, Tholkappian et al. (2018) reported the concentrations of Cr, Ni, Zn, Co, and Mn in the sediments of Chennai coastal waters. The mean concentrations of Cr, Ni, Zn, Co, and Mn were reported as 31.14, 18.79, 29.12, 2.85, and 160.8 mg/kg respectively. These concentrations are comparable with the metal levels observed in this study. The difference in the metal concentrations with the reported data may be due to various reasons such as reduced

TABLE 1 Distribution of heavy metals (Cr, Cu, Pb, Cd, Co, Mn, Ni, Zn, As) and SOC in the coastal sediment.

STATION CODE	DRY PERIOD										WET PERIOD									
	Cr (µg/g)	Cu (µg/g)	Pb (µg/g)	Cd (µg/g)	Co (µg/g)	Mn (µg/g)	Ni (µg/g)	Zn (µg/g)	As (µg/g)	SOC (%)	Cr (µg/g)	Cu (µg/g)	Pb (µg/g)	Cd (µg/g)	Co (µg/g)	Mn (µg/g)	Ni (µg/g)	Zn (µg/g)	As (µg/g)	SOC (%)
CP-1	37.22	6.34	5.11	0.58	4.46	187.0	14.13	16.28	7.14	0.95	35.50	6.12	6.16	1.34	4.05	180.6	14.21	22.35	9.99	0.80
CP-5	29.65	2.81	4.52	0.39	4.25	74.6	9.20	12.39	8.34	0.62	52.53	5.26	7.51	2.43	4.49	254.5	23.06	11.63	28.18	0.78
CP-10	24.64	3.55	3.20	0.34	2.45	138.5	9.37	7.51	13.31	0.78	45.63	10.03	6.32	11.23	5.14	157.3	19.60	19.34	9.07	1.08
MA-1	26.75	9.14	9.84	0.41	3.16	106.3	7.43	13.26	5.61	0.67	16.48	2.01	2.25	0.30	1.83	76.8	5.73	7.73	4.70	0.63
MA-5	45.41	3.13	2.62	21.76	2.85	101.3	19.45	7.28	10.13	0.68	28.68	3.53	3.32	0.78	2.50	105.6	11.11	10.23	12.83	0.36
MA-10	26.07	2.32	3.89	0.25	2.48	251.6	8.76	4.37	18.64	1.03	39.59	8.32	4.50	0.52	4.16	175.2	17.54	16.58	8.16	1.06
AD-1	29.07	3.63	2.75	0.26	2.64	90.8	10.84	9.07	6.50	1.08	56.60	9.48	5.32	1.29	4.70	141.1	24.65	23.91	7.35	0.59
AD-5	32.16	2.33	2.42	9.86	1.92	132.0	14.24	6.27	9.97	0.48	32.80	3.31	3.21	4.24	2.54	83.9	13.59	10.34	7.18	0.46
AD-10	26.56	10.35	5.38	0.44	4.82	170.8	12.46	16.49	3.88	1.05	33.97	10.55	5.07	0.48	4.86	154.8	14.54	19.14	7.35	0.78
KO-1	40.27	11.35	5.62	0.53	5.49	209.9	15.89	21.34	7.27	1.00	38.57	7.06	6.66	0.53	4.08	212.7	13.35	18.13	11.24	1.23
KO-5	41.23	4.35	2.96	15.47	3.32	88.5	16.89	11.01	8.99	0.65	64.73	7.47	9.43	5.08	4.49	121.0	31.34	16.83	7.39	0.67
KO-10	39.84	15.91	5.66	0.58	6.69	175.3	20.07	23.14	3.31	1.13	58.17	21.32	8.02	1.01	9.02	232.4	27.21	32.48	4.79	1.00
MH-1	39.94	11.09	5.96	0.53	5.84	188.0	15.57	21.75	4.38	0.68	43.38	9.93	4.42	0.67	4.42	214.6	15.43	22.23	10.72	1.00
MH-5	40.22	2.15	2.62	0.85	3.38	131.5	17.87	6.41	11.04	0.63	44.00	5.49	3.48	1.37	3.85	147.5	16.95	12.71	12.28	0.27
MH-10	41.81	11.19	8.72	0.68	5.52	256.9	13.00	23.05	5.90	1.14	54.33	13.46	4.77	0.87	7.06	223.4	19.09	27.12	5.98	1.48
KP-1	22.33	2.12	2.96	0.20	2.73	84.6	7.60	7.20	3.78	0.68	38.88	8.29	3.51	0.74	2.81	156.7	16.80	18.16	7.96	0.82
KP-5	41.88	3.50	3.76	3.59	3.54	102.4	17.70	8.98	5.82	0.45	46.01	9.08	3.67	0.70	3.86	177.6	19.21	18.77	9.41	0.73
KP-10	34.22	9.95	5.77	0.47	4.90	152.0	12.98	16.96	3.42	1.03	37.22	9.47	4.20	1.27	4.39	156.2	15.08	18.42	5.94	0.89
ED-1	74.70	9.26	17.54	0.85	5.62	346.2	10.47	18.70	14.04	0.86	28.70	6.46	2.89	0.72	3.51	152.1	14.06	32.50	6.12	0.67
ED-5	35.11	4.28	3.64	1.74	3.45	101.1	13.54	9.66	5.74	0.93	70.79	3.59	3.90	0.84	2.65	93.2	34.22	13.17	7.17	1.11
ED-10	22.34	4.81	4.28	0.46	4.30	132.3	7.52	11.88	4.87	0.78	48.25	9.36	4.86	0.51	3.83	150.9	19.26	20.91	4.24	0.64
PU-1	55.07	6.51	13.42	0.46	5.11	148.6	10.74	15.65	7.09	0.78	37.83	4.79	3.69	0.67	3.29	108.3	24.46	12.03	16.84	0.69
PU-5	51.06	12.98	6.98	0.74	6.36	204.3	19.75	26.21	4.54	1.19	39.89	5.37	4.77	1.16	2.83	172.6	40.53	11.84	11.08	1.19

(Continued)

10.3389/fmars.2023.1255466

TABLE 1 Continued

STATION CODE	DRY PERIOD										WET PERIOD									
	Cr (µg/g)	Cu (µg/g)	Pb (µg/g)	Cd (µg/g)	Co (µg/g)	Mn (µg/g)	Ni (µg/g)	Zn (µg/g)	As (µg/g)	SOC (%)	Cr (µg/g)	Cu (µg/g)	Pb (µg/g)	Cd (µg/g)	Co (µg/g)	Mn (µg/g)	Ni (µg/g)	Zn (µg/g)	As (µg/g)	SOC (%)
PU-10	64.33	4.28	4.23	6.31	5.60	195.5	28.52	12.42	18.25	0.81	26.87	3.73	1.37	3.72	1.80	70.3	17.93	11.71	4.28	0.75
GS-1	22.64	2.59	3.22	0.24	2.80	82.9	6.34	9.02	3.21	0.90	30.80	7.24	3.51	0.47	3.71	108.9	16.90	25.15	5.59	0.95
GS-5	45.25	3.99	5.44	5.79	4.47	110.3	14.49	16.75	7.17	0.76	30.85	13.24	1.80	2.74	3.64	97.3	21.73	17.92	7.44	1.23
GS-10	32.48	3.46	3.63	0.48	4.18	123.1	10.08	11.72	5.08	0.98	24.15	11.42	2.53	0.70	2.88	105.8	18.92	18.04	6.07	0.96
FH-1	48.28	6.35	9.39	1.03	4.86	182.8	10.92	15.22	8.73	0.91	33.66	7.20	3.82	0.82	3.48	151.0	11.33	34.95	5.82	1.00
FH-5	73.71	4.23	3.41	9.04	3.31	187.4	32.87	9.19	18.63	1.23	27.52	53.78	1.64	2.55	2.32	116.7	10.65	53.54	10.94	1.07
FH-10	28.59	7.55	3.67	0.41	3.73	109.3	11.20	19.38	2.61	1.20	22.56	6.83	2.87	0.80	2.59	94.4	12.30	14.21	7.23	1.03
PB-1	23.86	2.70	1.69	0.41	3.02	85.6	9.87	14.14	2.09	0.85	32.47	5.91	2.96	2.23	2.80	114.1	10.62	16.65	5.18	0.73
PB-5	42.88	4.08	2.86	11.57	4.17	113.7	18.54	13.95	4.52	0.93	25.46	10.04	1.53	4.16	2.76	93.4	11.34	30.39	5.73	1.32
PB-10	37.67	9.16	4.18	0.67	4.59	128.5	15.00	19.75	2.80	1.11	27.04	10.65	4.50	0.60	3.71	138.6	10.07	18.45	5.39	0.92

10.3389/fmars.2023.1255466

discharges due to Covid-19 restrictions. Arsenic (As) varied from 2.09 to 28.18 µg/g and the highest concentration was found at CP-5 during the wet period (Table 1). Miao et al. (2022) have recorded higher concentrations of metal in the sediment in the wet season. This is attributed to the large amounts of metals brought from various sources through monsoonal river run-off. The concentration of Cd and As exceeded the permissible limit according to Dutch standards and Persaud et al., 1993. Higher concentrations of Cd and As were detected at MA and CP stations, which were attributed to the Cooum River's passage of industrial and municipal wastes as well as proximity to the major Chennai Port. Similarly, a high concentration of Cd was found in the sediment of the Gulf of Mannar and Palk Bay (Palanichamy and Rajendran, 2000). The sediment organic carbon (SOC) content in the sediments was found between 0.27% and 1.48% during the study period. A high SOC was noticed at MH-10 in the wet period (Table 1). Generally, the concentrations of SOC were higher in the silt and clay in both near-shore and offshore sediments, indicating that SOC is derived from marine and terrestrial inputs (Goslin et al., 2017).

Geo accumulation index

Geo accumulation index (I*geo*) is a measure of metal deposit in the sediment in comparison with the contextual concentration of the specific metal. The I*geo* values of the heavy metals are depicted in Figure 2A. The I*geo* value of the surface sediments in the study area showed that Cr ranged from -2.6 to -1.3 (mean -1.9), Cu -4.4 to -2.9 (mean -3.6), Cd -0.1 to 2.2 (mean 1.1), Pb -4.8 to -2.0 (mean -3.2), Ni -3.8 to -2.2 (mean -2.9), Zn -4.2 to -2.8 (mean -3.3), and As from 0.4 to 2.4 (mean 1.6). The I*geo* index categorized Cd and As under the slightly polluted category. The I*geo* values of other metals such as Cr, Cu, Pb, Ni, and Zn were less than 1, so these metals are shown to be non-polluted (Figure 2A). The I*geo* values obtained in this study are in agreement with the previously reported values in Chennai coastal sediments (Tholkappian et al., 2018). However, the I*geo* value of Cd was >2 for sediments during the dry period (CP, KO, ED, FH), but the I*geo* value of As was >2 during both dry and wet periods (CP, MA, MH, PU) locations, which indicates that these locations are slightly polluted. The heavy metals (Cd and As) pollution tends to be higher in the study area during both dry and wet periods, possibly due to anthropogenic inputs such as untreated sewage discharge, fertilizers, pharmaceuticals, paints, distilleries, cement clinker, refineries, and ship breaking. Similar observations are reported along the southeast coast of India (Ranjan et al., 2008; Sundaramanickam et al., 2016). The I*geo* value of metals is in the following order: As >Cd >Cr >Ni >Pb>Cu (Figure 2A).

Enrichment factor

The EF values for heavy metal pollution in the sediment are shown in Figure 2B. The EF value of the sediment for Cr ranged from 0.3 to 0.6 (mean 0.4), Cu 0.1 to 0.5 (mean 0.2), Cd 1.4 to 24.3 (mean 8.1), Pb 0.1 to 0.4 (mean 0.2), Ni 0.1 to 0.4 (mean 0.2), Zn 0.1 to 0.3 (mean 0.2), and As from 2 to 10 (mean 5.1), Cd showed the highest EF value followed by As among the other metals (Figure 2B). As was classified as moderate to significant enrichment whereas Cd was moderate to very high, while Cr, Cu, Pb, Ni, and Zn were classified as minimal enrichment which corroborates Figure 2B. Cd showed very high enrichment during the dry period whereas, As showed significant enrichment during the wet period. Except for MH and KP locations, the EF value of Cd was >5, while As was >5 at CP, MA, ED, PU, and FH. The average EF for Cr, Cu, Pb, Ni, and Cd was less than 1, while As was between

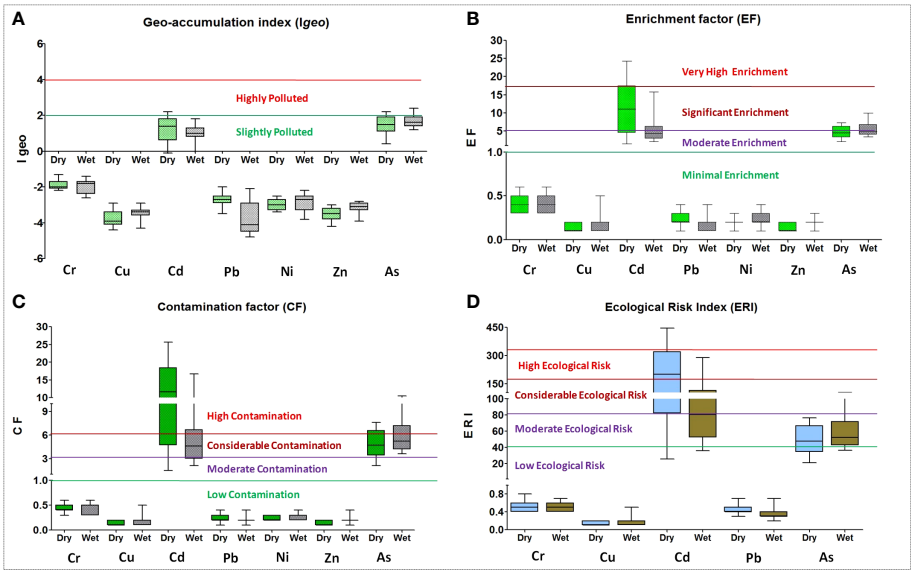

FIGURE 2
(A-D) Geoaccumulation index (Igeo), **(B)** Enrichment factor (EF), **(C)** Contamination factor (CF), **(D)** Ecological risk index (ERI) of the coastal sendiments.

2 and 20, indicating that these metals were depleted to minimum to moderate enrichment in the sediments. The EF results revealed that the higher values for Cd and As are primarily attributable to contamination from metal-based industries such as electroplating and metallurgy, as well as automobile exhaust (Karthikeyan et al., 2020) The average order of EF values of metals was Cd > As > Cr >Ni >Pb>Cu (Figure 2B). Similarly, Rubalingeswari et al. (2021) found higher enrichment of Cr and Cu based on EF values of more than 30 in the sediment samples of the Adyar estuary on the Chennai coast. This indicates the metal load to the coastal sediments from the highly contaminated estuaries in the Chennai coastal region.

Contamination factor

CF values describe the level of metal contamination in the coastal environment. The CF values for heavy metal contamination in the sediment are shown in Figure 2C. The CF value of Cr ranged from 0.3 to 0.6 (mean 0.4), Cu 0.1 to 0.5 (mean 0.2), Cd 1.5 to 25.6 (mean 8.5), Pb 0.1 to 0.4 (mean 0.2), Ni 0.2to 0.4 (mean 0.2), Zn 0.1 to 0.4 (mean 0.2), and As from 2.1 to 10.5 (mean 5.4), Cd shows the highest CF value followed by As (Figure 2C). Cd and As were classified as considerable to high contamination, while Cr, Cu, Pb, Ni, and Zn were classified as low contamination in the study area. The coastal sediments are highly contaminated by Cd during the dry, whereas As was during the wet period. The CF of metals is in the following order: Cd > As >Cr >Ni >Pb>Cu (Figure 2C).

Ecological risk index

The ERI values for heavy metals in the sediment are shown in Figure 2D. The ERI value of Cr varied from 0.4 to 0.8 (mean 0.5), Cu 0.1 to 0.5 (mean 0.2), Cd 25.2 to 444.1 (mean 147.7), Pb 0.2 to 0.7 (mean 0.4), and As from 20.9 to 105 (mean 53.9), Cd shows the highest ERI value followed by As (Figure 2D). ERI classified the sediments as moderate to very high ecological risk from Cd during the dry period, while the coastal sediments are under moderate to considerable ecological risk by As during the wet period in the study area. This coastal region has low ecological risk from metals such as Cr, Cu, and Pb. The ERI of metals in the sediment samples are in the following order: Cd > As > Cr > Pb > Cu (Figure 2D). In a similar observation, an ERI value of less than 150 was reported in the southern tropical estuarine sediments of the Indian coast (Nishitha et al., 2022). These values indicate that the aquatic organisms are not at risk from these metals.

Correlation coefficient matrix

The correlation coefficient for Cr, Cu, Pb, Cd, Co, Mn, Ni, Zn, As, SOC, Sand, Silt, and Clay components are depicted in Table 2. The sand showed strong positive correlation with Cd (r^2 = 0.986), Mn (r^2 = 0.983), Co (r^2 = 0.828), and Zn (r^2 = 0.702), while Silt and clay showed strong positive correlation with SOC (r^2 = 0.936), Ni (r^2 = 0.933), Cr (r^2 = 0.811), Pb (r^2 = 0.756), and Cu (r^2 = 0.753). This implies that these metals bond better to finer sand particles than to larger sand particles (Sundaramanickam et al., 2016) The SOC was strongly correlated with As (r^2 = 0.981), and Zn (r^2 = 0.703). This suggests that the sediment organic matter and its properties act as metal binders, with SOC playing an important role in its distribution pattern (Samuel and Phillips, 1988; Sundaramanickam et al., 2016). Additionally, As was strongly positively correlated with Cr (r^2 = 0.982), Co (r^2 = 0.853), and Pb (r^2 = 0.619). Mn substantially correlated with Cd (r^2 =0.900) and Pb (r^2 =0.707), whereas Co positively correlated with Pb (r^2 =0.877), Cu (r^2 =0.865), Cr (r^2 =0.811), and Cd (r^2 =0.634), which shown in Table 2.

TABLE 2 Pearson's correlation coefficient of heavy metals, SOC, Sand, Silt, and Clay in the coastal sediment.

	Cr	Cu	Pb	Cd	Co	Mn	Ni	Zn	As	SOC	Sand	Silt	Clay
Cr	1.000	0.206	0.502	0.167	0.811**	0.564	0.692*	0.059	0.982**	0.123	0.485	0.811**	0.810**
Cu		1.000	0.000	0.310	0.865**	0.186	0.130	0.019	0.419	0.131	0.367	0.753*	0.753*
Pb			1.000	0.292	0.877**	0.707*	-0.179	0.134	0.619*	0.059	0.304	0.756*	0.756*
Cd				1.000	0.634*	0.900**	0.613*	0.155	0.276	0.435	0.986**	0.056	0.056
Co					1.000	0.545	0.774*	0.027	0.853**	0.285	0.828**	0.443	0.443
Mn						1.000	0.307	0.549	0.444	0.378	0.983**	0.344	0.343
Ni							1.000	0.151	0.333	0.171	0.383	0.933**	0.933**
Zn								1.000	0.031	0.703*	0.702*	0.092	0.091
As									1.000	0.981**	0.492	0.181	0.180
SOC										1.000	0.428	0.936**	0.936**
Sand											1.000	0.761*	0.758*
Silt												1.000	0.989**
Clay													1.000

** Correlation is significant at the 0.01 level.
* Correlation is significant at the 0.05 level.

Conclusion

In the present study, the coastal sediment shows elevated Cd and As concentrations. The results of I*geo* suggested that the coastal sediments are slightly polluted by Cd and As, whereas, the sediment is uncontaminated by other metals. The CF shows high sediment contamination by Cd whereas, with considerable contamination by As. The ERI indicated that the coastal sediments are under threat with moderate to high ecological risk from As and Cd. The higher Cd and As concentrations than the background value were recorded, which are considered prime contributors to ecological risk. Geogenic and anthropogenic may be the major sources of the contamination. The level of pollutants, particularly metals (Cr, Cu, Pb, Cd, Co, Mn, Ni, Zn, As), would increase over time as a result of emerging industries such as ceramic, painting, glass, pesticides, herbicides, and battery manufacturing along the entire estuarine and coastal regions of Tamilnadu and therefore, further long-term monitoring is required. The finding of this study suggested that the increased heavy metals (Cd and As) concentration in the study area increases the toxicity in the coastal environment and affects the ecological balance. The study will enhance the awareness of policymakers/environmental agencies on heavy metal pollution and facilitate appropriate pollution control measures in the coastal waters.

Data availability statement

The original contributions presented in the study are included in the article/Supplementary Material. Further inquiries can be directed to the corresponding author.

Ethics statement

This study is based on coastal sediment sample, animal tests are not performed in the study.

Author contributions

SN: Conceptualization, Data curation, Investigation, Methodology, Validation, Writing – original draft. UP: Formal Analysis, Investigation, Methodology, Writing – review & editing. PK: Data curation, Formal Analysis, Writing – review & editing. DB: Investigation, Methodology, Writing – review & editing. RKS Writing – review & editing. USP: Investigation, Writing – review & editing. PM: Supervision, Writing – review & editing. MR: Project administration, Writing – review & editing.

Funding

The author(s) declare that no financial support was received for the research, authorship, and/or publication of this article.

Acknowledgments

The authors are grateful to the Secretary, Ministry of Earth Sciences (MoES), Government of India for his continuous support and encouragement. This manuscript has an NCCR contribution no. NCCR/MS/398.

Conflict of interest

The authors declare that the research was conducted in the absence of any commercial or financial relationships that could be construed as a potential conflict of interest.

Publisher's note

Supplementary material

The Supplementary Material for this article can be found online at: https://www.frontiersin.org/articles/10.3389/fmars.2023.1255466/full#supplementary-material

References

Bam, E. K. P., Akiti, T. T., Osea, S. D., Ganyaglo, S. Y., and Gibrilla, A. (2011). Multivariate cluster analysis of some major and trace elements distribution in an unsaturated zone profile, Densu river Basin, Ghana. *Afr. J. Environ. Sci. Technol.* 5 (3), 155–167.

Barath Kumar, S., Padhi, R. K., Mohanty, A. K., and Satpathy, K. K. (2017). Elemental distribution and trace metal contamination in the surface sediment of the southeast coast of India. *Mar. pollut. Bull.* 114 (2), 1164–1170. doi: 10.1016/j.marpolbul.2016.10.038

Cotin, J., García-Tarrasón, M., Sanpera, C., Jover, L., and Ruiz, X. (2011). Sea, freshwater or saltpans? Foraging ecology of terns to assess mercury inputs in a wetland landscape: the Ebro Delta. *Estuar. Coast. Shelf Sci.* 92 (1), 118–194. doi: 10.1016/j.ecss.2010.12.024

de Mora, S., Fowler, S., Wyse, E., and Azemard, S. (2004). Distribution of heavy metals in marine bivalves,fish and coastal sediments in the Gulf and Gulf of Oman. *Mar. pollut. Bull.* 49, 410–424. doi: 10.1016/j.marpolbul.2004.02.029

Duncan, A. E., de Vries, N., and Nyarko, K. B. (2018). Assessment of heavy metal pollution in the sediments of the River Pra and its tributaries. *Water Air Soil pollut.* 229, 1–10. doi: 10.1007/s11270-018-3899-6

ECMDEQ (Environment Canada and Ministère du Développement durable, de l'Environnement et des Parcs du Québec) (2007). *Criteria for the assessment of sediment*

quality in Quebec and application frameworks: prevention, dredging and remediation (Quebec, Canada: Environment Canada and Ministère du Développement durable, de l'Environnement et des Parcs du Québec), 27. Available at: http://www.planstlaurent.qc.ca/fileadmin/publications/diverses/Registre_de_dragage/Criteria_sediment_2007E.pdf.

Gopal, V., Krishnakumar, S., Simon Peter, T., Nethaji, S., Suresh Kumar, K., Jayaprakash, M., et al. (2017). Assessment of trace element accumulation in surface sediments off the Chennai coast after a major flood event. *Mar. Pollut. Bull.* 114 (2), 1063–1071. doi: 10.1016/j.marpolbul.2016.10.019

Goslin, J., Sansjofre, P., Van Vliet-Lanoe, B. V., and Denmark, C. (2017). Carbon Stable Isotope and Elemental (TOC, TN) geochemistry in Salymarsh Surface sediments (Western Brittany, France): a Useful Tool for reconstructing Holocene Relative Sea-Level. *J. Quat. Sci.* 32 (7), 987–1007. doi: 10.1002/jqs.2971

Hakanson, L. (1980). Ecological risk index for aquatic pollution control, a sedimentological approach. *Water Res.* 14 (8), 975–1001. doi: 10.1016/0043-1354(80)90143-8

IMD. (2020). Rainfall statistics of India-2020, India meteorological department, ministry of earth sciences, *government of India, New Delhi, Report No.ESSO/IMD/HS/Rainfall Report*. 133.

Jha, D. K., Dharani, G., Verma, P., Ratnam, K., Kumar, R. S., and Rajaguru, S. (2021). Evaluation of factors influencing the trace metals in Puducherry and Diu coasts of India through multivariate techniques. *Mar. Pollut. Bull.* 167, 112342. doi: 10.1016/j.marpolbul.2021.112342

Jha, D. K., Ratnam, K., Rajaguru, S., Dharani, G., Devi, M. P., and Kirubagaran, R. (2019). Evaluation of trace metals in seawater, sediments, and bivalves of Nellore, southeast coast of India, by using multivariate and ecological tool. *Mar. pollut. Bull.* 146, 1–10. doi: 10.1016/j.marpolbul.2019.05.044

Kannan, G., Mghili, B., Di Martino, E., Sanchez-Vidal, A., and Figuerola, B. (2023). Increasing risk of invasions by organisms on marine debris in the Southeast coast of India. *Mar. Pollut. Bull.* 195, 115469. doi: 10.1016/j.marpolbul.2023.115469

Karthikeyan, P., Marigoudar, S. R., Mohan, D., Nagarjuna, A., and Sharma, K. V. (2020). Ecological risk from heavy metals in Ennore estuary, South East coast of India. Environ. *Chem Ecotoxicol.* 2, 182–193. doi: 10.1016/j.enceco.2020.09.004

Ke, X., Gui, S., Huang, H., Zhang, H., Wang, C., and Guo, W. (2017). Ecological risk assessment and source identification for heavy metals in surface sediment from the Liaohe River protected area, China. *Chemosphere* 175, 473–481. doi: 10.1016/j.chemosphere.2017.02.029

Kwok, K. W., Batley, G. E., Wenning, R. J., Zhu, L., Vangheluwe, M., and Lee, S. (2014). Sediment quality guidelines: challenges and opportunities for improving sediment management. *Environ. Sci. pollut. Res.* 21, 17–27. doi: 10.1007/s11356-013-1778-7

Li, F., Huang, J., Zeng, G., Yuan, X., Li, X., Liang, J., et al. (2013). Spatial risk assessment and sources identification of heavy metals in surface sediments from the Dongting Lake, Middle China. *J. Geochem. Explor.* 132, 75–83. doi: 10.1016/j.gexplo.2013.05.007

Long, E. R., Macdonald, D. D., Smith, S. L., and Calder, F. D. (1995). Incidence of adverse biological effects within ranges of chemical concentrations in marine and estuarine sediments. *Environ. Manage.* 19, 81–97. doi: 10.1007/BF02472006

MacDonald, D., Ingersoll, C., and Berger, T. (2000). Development and evaluation of consensus-based sediment quality guidelines for freshwater ecosystems. *Arch. Environ. Contam. Toxicol.* 39, 20–31. doi: 10.1007/s002440010075

Mason, R. P., Laporte, J. M., and Andres, S. (2000). Factors controlling the bioaccumulation of mercury, methyl mercury, arsenic, selenium and cadmium by freshwater invertebrates and fish. *Arch. Environ. Contam. Toxicol.* 38, 283–297. doi: 10.1007/s002449910038

Miao, X., Liang, J., Hao, Y., Zhang, W., Xie, Y., and Zhang, H. (2022). The influence of the reduction in clay sediments in the level of metals bioavailability—An investigation in Liujiang river basin after wet season. *Int. J. Environ. Res. Public Health* 19 (22), 14988. doi: 10.3390/ijerph192214988

Muller, G. (1979). Schwermetalle in den sedimenten des Rheins-VeraÈnderungenseit. *Umschau* 79, 778–783.

Muthu, S. R., and Jayaprakash, M. (2008). Distribution and enrichment of trace metals in marine sediments of Bay of Bengal, off Ennore, south-east coast of India. *Environ. Geol.* 56, 207–217. doi: 10.1007/s00254-007-1156-1

Nance, P., Patterson, J., Willis, A., Foronda, N., and Dourson, M. (2012). Human health risks from mercury exposure from broken compact fluorescent lamps (CFLs). *Regul. Toxicol. Pharmacol.* 62 (3), 542–552. doi: 10.1016/j.yrtph.2011.11.008

Naser, H. A. (2012). "Metal concentrations in marine sediments influenced by anthropogenic activitiesin Bahrain, Arabian Gulf," in *Metal contaminations: sources, detection andenvironmental impacts*. Ed. H. B. Shao (New York: NOVA Science Publishers, Inc.), 157–175.

Naser, H. A. (2013). Assessment and management of heavy metal pollution in the marine environment of the Arabian Gulf: a review. *Mar. pollut. Bull.* 72 (1), 6–13. doi: 10.1016/j.marpolbul.2013.04.030

Neff, J. M. (1997). Ecotoxicology of arsenic in the marine environment. *Environ. Toxicol. Chem.* 16 (5), 917–927. doi: 10.1002/etc.5620160511

Nishitha, D. S., Amrish, V. N., Arun, K., Warrier, A. K., Udayashankar, H. N., and Balakrishna, K. (2022). Study of trace metal contamination and ecological risk assessment in the sediments of a tropical river estuary, Southwestern India. *Environ. Monit. Assess.* 194 (2), 94. doi: 10.1007/s10661-021-09728-1

Oves, M., Khan, M. S., Zaidi, A., and Ahmad, E. (2012). "Soil contamination, nutritive value, and human health risk assessment of heavy metals: an overview," in *Toxicity of heavy metals to legumes and bioremediation*. Eds. A. Zaidi, P. A. Wani and M. S. Khan (Vienna: Springer), 1–27. doi: 10.1007/978-3-7091-0730-0_1

Palanichamy, S., and Rajendran, A. (2000). Heavy metal concentration in seawater and sediment of Gulf of Mannar and Palk Bay, southeast coast of India. *Indian J. Mar. Sci.* 29, 116–119.

Pan, K., and Wang, W.-X. (2012). Trace metal contamination in estuarine and coastal environments in China. *Sci. Total Environ.* 421-422, 3–16. doi: 10.1016/j.scitotenv.2011.03.013

Persaud, D., Jaaguagi, R., and Hayton, A. (1993). *Guidelines for the protection and management of aquatic sediment quality in Ontario* (Toronto: Ontario Ministry of the Environment), 27. Available at: http://hdl.handle.net/10214/15797.

Prica, M., Dalmacija, B., Roncˇevic´, S., Krcˇmar, D., and Becˇelic´, M. (2008). A comparison of sediment quality results with acid volatile sulfide (AVS) and simultaneously extracted metals (SEM) ratio in Vojvodina (Serbia) sediments. *Sci. Total Environ.* 389 (2-3), 235–244. doi: 10.1016/j.scitotenv.2007.09.006

Ra, K., Kim, J. K., Hong, S. H., Yim, U. H., Shim, W. J., Lee, S. Y., et al. (2014). Assessment of pollution and ecological risk of heavy metals in the surface sediments of Ulsan Bay, Korea. *Ocean Sci. J.* 49, 279–289. doi: 10.1007/s12601-014-0028-3

Ramesh, R., Nammalwar, P., and Gowri, V. S. (2008). *Database on coastal information of Tamilnadu* (Chennai: Environmental Information System (ENVIS) Centre, Department of Environment, Government of Tamilnadu), 133. Available at: https://tnenvis.nic.in/tnenvis_old/coastal%20data.pdf.

Ranjan, R. K., Ramanathan, A. L., Singh, G., and Chidambaram, S. (2008). Assessment of metal enrichments in tsunamigenic sediments of Pichavaram mangroves, southeast coast of India. *Environ. Monit. Assess.* 147, 389–411. doi: 10.1007/s10661-007-0128-y

Rosado, D., Castillo, F., Nambi, I., Sadhasivam, R., Valleru, H., and Fohrer, N. (2023). Evaluating heavy metal levels and their toxicity risks in an urban lake in Chennai, India. *Int. J. Environ. Sci. Technol.* doi: 10.1007/s13762-023-05086-2

Rubalingeswari, N., Thulasimala, D., Giridharan, L., Gopal, V., Magesh, N. S., and Jayaprakash, M. (2021). Bioaccumulation of heavy metals in water, sediment, and tissues of major fisheries from Adyar estuary, southeast coast of India: An ecotoxicological impact of a metropolitan city. *Mar. Pollut. Bull.* 163, 111964. doi: 10.1016/j.marpolbul.2020.111964

Samuel, N. L., and Phillips, D. J. H. (1988). Distribution, variability and impacts of trace elements in San Francisco Bay. *Mar. Pollut. Bull.* 19 (9), 413–425. doi: 10.1016/0025-326X(88)90396-7

Santhosh, A. P., Pyary, A., Biju, A., Partheeban, E. C., Vethanayaham, J., Rajendran, R., et al. (2023). Heavy metal contamination along different tidal zones of a tropical Bay of Bengal coastal environment influenced by various anthropogenic activities. *Environ. Sci. Pollut Res.* 30 (10), 27980–27995. doi: 10.1007/s11356-022-24112-3

Satheeswaran, T., Yuvaraj, P., Damotharan, P., Karthikeyan, V., Jha, D. K., Dharani, G., et al. (2019). Assessment of trace metal contamination in the marine sediment, seawater, and bivalves of Parangipettai, southeast coast of India. *Mar. Pollut. Bull.* 149, 110499. doi: 10.1016/j

Satpathy, K. K., Mohanty, A. K., Prasad, M. V. R., Natesan, U., and Sarkar, S. K. (2012). Studies on the variations of heavy metals in the marine sediments off Kalpakkam, East Coast of India. *Environ. Earth Sci.* 65, 89–101. doi: 10.1007/s12665-011-1067-z

Selvaraj, K., Mohan, V. R., and Szefer, P. (2004). Evaluation of metal contamination in coastal sediments of the Bay of Bengal, India: geochemical and statistical approaches. *Mar. pollut. Bull.* 49, 174–185. doi: 10.1016/j.marpolbul.2004.02.006

SEPA (State Environmental Protection Administration of China) (2002). *Marine sediment quality (GB 18668-2002)*. (Beijing: Standards Press of China).

Simpson, S. L., Batley, G. B., and Chariton, A. A. (2013). *Revision of the ANZECC/ARMCANZ sediment quality guidelines. CSIRO land and water science report*. Available at: http://hdl.handle.net/102.100.100/126155?index=1.

Sinex, S. A., and Helz, G. R. (1981). Regional geochemistry of trace elements in Chesapeake Bay sediments. *Environ. Geol.* 3, 315–323. doi: 10.1007/bf02473521

Sundaramanickam, A., Shanmugam, N., Cholan, S., Kumaresan, S., Madeswaran, P., and Balasubramanian, T. (2016). Spatial variability of heavy metals in estuarine, mangrove and coastal ecosystems along Parangipettai, Southeast coast of India. *Environ. pollut.* 218, 186–195. doi: 10.1016/j.envpol.2016.07.048

Sundararajan, S., Khadanga, M. K., Kumar, J., Raghumaran, S., Vijaya, R., and Jena, B. K. (2016). Ecological risk assessment of trace metal accumulation in sediments of Veraval Harbor, Gujarat, Arabian Sea. *Mar. pollut. Bull.* 114 (1), 592–601. doi: 10.1016/j.marpolbul.2016.09.016

Tholkappian, M., Ravisankar, R., Chandrasekaran, A., Jebakumar, J. P. P., Kanagasabapathy, K. V., Prasad, M. V. R., et al. (2018). Assessing heavy metal toxicity in sediments of Chennai Coast of Tamil Nadu using Energy Dispersive X-Ray Fluorescence Spectroscopy (EDXRF) with statistical approach. *Toxicol. Rep.* 5, 173–182. doi: 10.1016/j.toxrep.2017.12.020

Turekian, K. K., and Wedepohl, K. H. (1961). Distribution of the elements in some major units of the Earth's crust. *Geol. Soc Am. Bull.* 72, 175. doi: 10.1130/0016-7606(1961)72[175:DOTEIS]2.0.CO;2

UNEP and UN-HABITAT (2005) *Coastal area pollution – the role of cities*. Available at: http://www.unep.org/urban_environment/PDFs/Coastal_Pollution_Role_of_Cities.pdf (Accessed 01 Jan 2015).

USEPA. (2007). *Method 3051A (SW-846): Microwave assisted acid digestion of sediments, sludges, and oils (Revision 1)* (Washington, DC), 30. Available at: http://www.jonesenv.com/PDF/3051a.pdf.

Walkley, A. (1935). An examination of methods for determining organic carbon and nitrogen in Soils1.(With one text-figure.). *J. Agric. Sci.* 25 (4), 598–609. doi: 10.1017/S0021859600019687

Wang, S. L., Xu, X. R., Sun, Y. X., Liu, J. L., and Li, H. B. (2013). Heavy metal pollution in coastal areas of South China: a review. *Mar. pollut. Bull.* 76 (1-2), 7–15. doi: 10.1016/j.marpolbul.2013.08.025

Xie, S., Jiang, W., Sun, Y., Yu, K., Feng, C., Han, Y., et al. (2023). Interannual variation and sources identification of heavy metals in seawater near shipping lanes: Evidence from a coral record from the northern South China Sea. *Sci. Total Environ.* 854, 158755. doi: 10.1016/j.scitotenv.2022.158755

Youssef, D. H., and El-Said, G. F. (2011). Assessment of some heavy metals in surface sediments of the Aqaba Gulf, Egypt. *Environ. Monit. Assess.* 180, 229–242. doi: 10.1007/s10661-010-1784-x

Zhuang, W., and Gao, X. L. (2015). Distributions, sources and ecological risk assessment of arsenic and mercury in the surface sediments of the southwestern coastal Laizhou Bay, Bohai Sea. *Mar. Pollut. Bull.* 99, 320–327. doi: 10.1016/j.marpolbul.2015.07.037

frontiers | Frontiers in Marine Science

TYPE Original Research
PUBLISHED 04 December 2023
DOI 10.3389/fmars.2023.1303497

OPEN ACCESS

EDITED BY
Meilin Wu,
Chinese Academy of Sciences (CAS), China

REVIEWED BY
Kaizhi Li,
Chinese Academy of Sciences (CAS), China
Peng Zhang,
Guangdong Ocean University, China

*CORRESPONDENCE
Xuebao He
hexuebao@tio.org.cn
Hui Lin
linhui@tio.org.cn

†These authors share first authorship

RECEIVED 28 September 2023
ACCEPTED 15 November 2023
PUBLISHED 04 December 2023

CITATION
Wang Y, Wang W, Huang Y, Chang L, Tang X, He X and Lin H (2023) Scenarios of temporal environmental alterations and phytoplankton diversity in a changing bay in the East China Sea.
Front. Mar. Sci. 10:1303497.
doi: 10.3389/fmars.2023.1303497

Scenarios of temporal environmental alterations and phytoplankton diversity in a changing bay in the East China Sea

Yu Wang†, Weibo Wang†, Yaqin Huang, Lin Chang, Xiaoming Tang, Xuebao He* and Hui Lin*

Third Institute of Oceanography, Ministry of Natural Resources, Xiamen, China

In the context of global change, the stressors of warming and eutrophication have significant ecological implications in coastal waters. In order to examine the diversity of phytoplankton and its relationship with water quality, we conducted a survey of phytoplankton community compositions and their correlation with environmental changes over four seasons in a eutrophic bay located in the East China Sea. Through a systematic analysis, we identified diatoms and dinoflagellates as the primary dominant groups, with the species *Skeletonema costatum*, *Skeletonema marinoi*, *Biddulphia sinensis*, *Thalassiosira eccentrica*, *Leptocylindrus danicus*, *Coscinodiscus oculus-iridis*, *Coscinodiscus jonesianus*, and *Chaetoceros knipowitschi* as the most abundant species in all seasons. Significant seasonal alterations were observed in both environmental settings and phytoplankton species richness, dominance, and abundance. The phytoplankton community varied in its response to diverse aquatic environments and was principally affected by temperature, silicic acid concentrations, and suspended solids. Elevated temperatures were found to promote an increase in phytoplankton abundance. However, no clear evidence of diatom and dinoflagellate succession in relation to N:P ratio was observed across seasons. Water quality analysis illustrated that the majority of the study area exhibited a mid-eutrophic with severe organic pollution. The abundance of phytoplankton was significantly influenced by eutrophication and organic pollution. The accelerated warming process related to coastal nuclear power plants and nutrient regime alterations significantly affect the temporal shift of the phytoplankton community. These findings contribute valuable insights into the effects of eutrophic environments on the structure of phytoplankton communities in coastal aquatic systems.

KEYWORDS

phytoplankton shift, seasonal variation, Sanmen Bay, water quality assessment, elevated temperature, nutrient regime alterations

1 Introduction

Coastal aquatic ecosystems possess significant global socioeconomic importance (Martínez et al., 2007), and are subject to substantial impacts from human activities and land–ocean interactions (Tagliani et al., 2003; Zhao et al., 2005). The introduction of terrestrial nutrients into coastal waters and the release of greenhouse gases have been expedited by various anthropogenic factors, including port services and shipping, aquaculture, urban domestic sewage, and industrial and agricultural wastewater, as well as agricultural nonpoint source pollution. Consequently, these human-induced activities have resulted in eutrophication and water warming (Cloern, 2001; Rice et al., 2015; Wang et al., 2018). The subsequent negative impacts, including algal blooms, organic pollution, hypoxia, and stratification, pose significant threats to the marine environment and ecosystem health (Meyer-Reil and Köster, 2000; Marcus, 2004). Within the context of global climatic change, the combined effects of rising temperatures and increased nutrient levels from eutrophication serve as prominent stressors with interconnected ecological implications in coastal waters (Miyamoto et al., 2019; Cheung et al., 2021; Wei et al., 2022), ultimately influencing the physicochemical processes of aquatic systems (Xia et al., 2016; Freeman et al., 2019; Song et al., 2022).

Phytoplankton, as the primary producer in aquatic ecosystems, play a crucial role in the microbial food web due to their ability to utilize nutrients and fix carbon (Cloern and Dufford, 2005; Zhou et al., 2008; Garmendia et al., 2011). The impact of anthropogenic nutrient inputs and global warming on marine phytoplankton has been significant (Novak et al., 2019; Wu et al., 2021). In coastal ecosystems across the globe, such as the East China Sea, the discharge of wastewater from tributaries has resulted in frequent harmful algal blooms (HABs) and subsequent fish mortality. This is primarily attributed to the increased availability of nitrogen and phosphate compared to silicon (Carstensen et al., 2007; Wang et al., 2019; Xin et al., 2019). Frequent HABs are increasingly associated with the eutrophication of coastal waters (Carstensen et al., 2007). The nutrient regime shifts have been found to impact the diversity and complexity of phytoplankton composition and biomass (Song et al., 2016; Xin et al., 2019), resulting in an increase in HAB phytoplankton species (Carstensen et al., 2007; Wells et al., 2015; Song et al., 2016) and a shift in dominant phytoplankton groups from primarily diatoms to a more balanced presence of diatoms and dinoflagellates (Wells et al., 2015; Xin et al., 2019; Song et al., 2022). Long-term studies conducted in coastal East China Sea, using extensive datasets, have revealed a decrease in diatom abundance and an increase in dinoflagellate abundance in response to higher temperatures and eutrophication. This suggests that diatoms and dinoflagellates exhibit distinct responses to warming and eutrophication (Chen et al., 2017; Xiao et al., 2018; Gao et al., 2022).

Located in the heart of China's coastal region, Sanmen Bay serves as the primary access point to eastern Zhejiang. The region's copious marine resources have played a pivotal role in fostering regional economic and social progress. However, the excessive exploitation of these resources, coupled with the haphazard allocation of marine territories and the extensive reclamation of land, have exerted significant strain on the natural environment and delicate ecosystems. Existing scholarly research on Sanmen Bay has primarily examined its structural density and the biodiversity of macrobenthos and fishery resources, along with their temporal and spatial distribution patterns (Yan et al., 2020; Qiu et al., 2022). Additional investigations have focused on environmental quality, interannual variation, and the correlation with macrobenthic communities (Liang et al., 2020; Meng et al., 2022). Furthermore, certain studies have explored the response of Sanmen Bay to alterations in water nutrients, wetland areas, and vegetation resulting from human activities, utilizing remote sensing and geographic information systems (Chen et al., 2015; Liu et al., 2021). In addition, previous research has examined phytoplankton extensively (Zhu et al., 2012; Liu et al., 2015; Xie et al., 2015; Chen et al., 2017). However, these studies have been constrained by the utilization of the net collection method, which proves inadequate in capturing a multitude of noncolonial small-celled (<76 μm) phytoplankton species. Consequently, this method leads to an underestimation of depth-averaged phytoplankton abundance by one to two orders of magnitude when compared to the water collection method (Jiang et al., 2020). Notably, certain investigations employing the water collection method have revealed significant heterogeneity in community composition across three distinct subregions within Sanmen Bay (Gao et al., 2022). Typically, Sanmen Bay is characterized as a partially enclosed harbor with an exposed entrance adjacent to the East China Sea. The bay's ecological dynamics are primarily influenced by the confluence of riverine influxes, the Zhemin Coastal Current, and the Taiwan Warm Current (Zhu et al., 2012), potentially impacting the diversity and intricacy of phytoplankton composition (Xie et al., 2015; Chen et al., 2017; Jiang et al., 2020; Gao et al., 2022). Consequently, the phytoplankton composition in the bay consists of both freshwater or brackish species originating from tributaries, such as *Pediastrum simplex*, *Phormidium tenesmue*, and *Melosira granulata* v. *austissima*. Additionally, the presence of neritic eurytopic and low-salinity species, including *Coscinodiscus jonesianus*, *Ditylum brightwellii*, *Synedra ulna* and *Prorocentrum minimum*, can be attributed to the Zhemin Coastal Current (Jiang et al., 2012; Jiang et al., 2014; Gao et al., 2022). These species are the primary dominant organisms during the spring, autumn, and winter seasons (Jiang et al., 2012; Jiang et al., 2014; Gao et al., 2022). Furthermore, the presence of warm-water and high-salinity species, namely *Cerataulina pelagica*, *Chaetoceros pseudocurvisetus*, and *Chaetoceros lorenzianus*, has experienced a notable surge during the summer season, primarily attributed to the influence of the Taiwan Warm Current (Jiang et al., 2012; Chen et al., 2017; Gao et al., 2022). Recently, the degradation of the aquatic environment in Sanmen Bay has exerted significant strain on its natural resources and ecosystems. The ecological alterations resulting from eutrophication and escalating water temperature in the coastal region are believed to be the primary catalysts for the augmentation of phytoplankton abundance and shifts in dominant species composition (Xiao et al., 2018; Xin et al., 2019; Gao et al., 2022; Song et al., 2022).

Coastal waters exhibit the greatest susceptibility to the impacts of human activities. Given the intricate and diverse nature of

anthropogenic pressure (Borja et al., 2015), the manifestations and magnitude of these effects can differ significantly across geographical locations, and even within the same area over time (Wu et al., 2021; Gao et al., 2022; Wei et al, 2022). Hence, this study uses a systematic analysis treating the temporal data as various groups to describe the shift in phytoplankton composition, abundance, and response to environmental changes in four continuous seasons in Sanmen Bay. Our objective was to examine the influence of physiochemical factors, specifically eutrophication and warming, on seasonal biotic assemblages in relation to the various sources of pollution.

2 Materials and methods

2.1 Study area

Sanmen Bay (SMB) is located on the coast of the East China Sea (Figure 1). It is a macro-tidal turbid estuary, with four tributaries and a maximum tidal range of approximately 2 m at the bay mouth and suspended sediment concentration of 1.192 kg/m^3 in the middle of the bay (Shou and Zeng, 2015). Stratification in the bay is negligible due to the strong physical mixing and relatively modest freshwater input. Tidal current velocities in the bay exceed 30 cm/s at spring tide and 20 cm/s at neap tide. These velocities are greater than the critical velocity for sediment motion; therefore, turbidity in the bay is high, with average annual suspended solids (SS) of 367 mg/L (Editorial Committee of the Bay Chorography in China (ECBCC), 1992). With the rapid development of human activities, pollution in the bay is increasing, with ecological consequences (Shi, 2013; Chen et al., 2017).

2.2 Sample collection

Four survey cruises were conducted in the SMB over the spring (April), summer (July), autumn (November), and winter (January) periods from January 2020 to November 2020, at 30 sampling stations (Figure 1). Surface seawater samples from each station were collected with 5 L Niskin bottles at 0.5 m depth. Temperature and salinity were measured *in situ* using a YSI salinity meter (model 30). Water samples for dissolved inorganic nutrient (nitrogen, phosphate, and silicon) analysis were filtered through a 0.45 μm cellulose acetate filter and then measured by colorimetric methods according to The Specification for Marine Monitoring (General Administration of Quality Supervision, Inspection and Quarantine (GAQSIQ, 2007a). SS samples were filtered through preweighed GF/C filters dried to a constant mass at 105°C and weighed. The dry mass of particles retained on each filter was calculated by subtracting the filter mass from the dried mass. The chemical oxygen demand (COD) was measured using alkalic potassium permanganate according to the specification of standard GB 17378.7–2007 (GAQSIQ, 2007b). The pH values of the seawater were manually measured using a pH meter (NBS scale, Mettler-Toledo, S210-k). Dissolved oxygen (DO) levels were determined via the Winkler titration method (Strickland and Parsons, 1968).

2.3 Eutrophication and organic pollution assessment

The eutrophication index (Ei) was calculated based on nutrients, using the following equation (Zhu et al., 2020).

Ei = COD × DIN × DIP × Sc, where Sc (10^6/4500) is the mean product of the standard concentrations of COD, dissolved inorganic nitrogen (DIN), and dissolved inorganic phosphorous (DIP). Ei < 1: no eutrophication; 1 < Ei ≤ 3: low eutrophication; 3 < Ei ≤ 9: mid-eutrophication; Ei > 9: heavy eutrophication.

The degree of organic pollution assessment was assessed using four indicators: COD, DIN, DIP, and DO (Liu et al., 2011).

$Ci = COD_i/COD_s + DIN_i/DIN_s + DIP_i/DIP_s - DO_i/DO_s$, where Ci is the organic pollution index; COD_i, DIN_i, DIP_i, and DO_i are the measured values; and COD_s, DIN_s, DIP_s, and DO_s are the standard

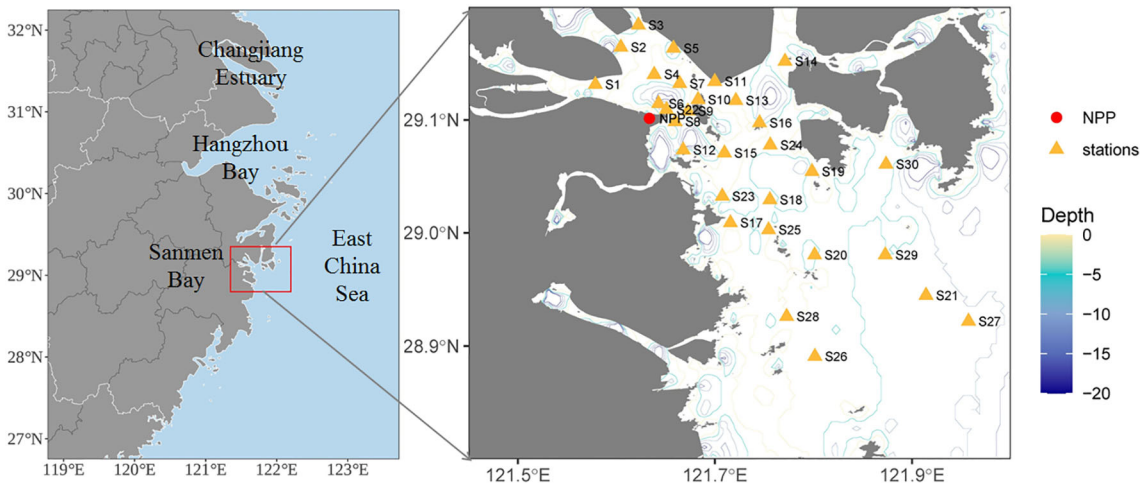

FIGURE 1
Location of the study area and sampling sites over four seasons in the coastal waters of Sanmen Bay, East China Sea. Red dot represents the nuclear power plant (NPP). Green rectangle represents a total of 30 stations for water sampling.

type I seawater quality values of 2, 0.2, 0.015, and 6 (mg/L), respectively. For Ci, if 1 ≤ Ci ≤ 3, organic pollution is low; if Ci > 3, organic pollution is severe.

2.4 Phytoplankton identification and abundance

To determine phytoplankton composition and abundance, 500 mL of seawater was collected and preserved in formalin solution at a final concentration of 2%. In the laboratory, a 100 mL subsample was used for phytoplankton cell identification and enumeration using an inverted microscope (Zeiss Imager Z1) at 400× or 200× magnification, following previously described methods (Utermöhl, 1958). Microscopic observations were conducted according to a previous study (Fukuyo et al., 1990; Tomas, 1997; Sun and Liu, 2002). A quantitative list of dominant species was established based on the dominance index according to Tsirtsis and Karydis, 1998.

2.5 Statistical analysis

Data are given as mean values ± standard deviation (SD). One-way analysis of variance (ANOVA) and significance testing were used to compare differences among phytoplankton groups using SPSS 20.0 software (SPSS Inc., Chicago, USA). Prior to conducting the ANOVA, a normal distribution test was executed. In the event that the dataset satisfied the criteria for normal distribution ($p>0.05$), a T-test was employed. Conversely, if the dataset did not meet the normal distribution requirements ($p<0.05$), a non-parametric Wilcoxon-test was utilized for significance testing. Linear regression models and *t*-tests were used to explore the dynamic trends in various biological and environmental parameters. Spearman correlation analysis and least squares regression (regression variance, R^2) were applied to establish relationships between groups of data, such as temperature, pH versus Ei and Ci. Canonical correspondence analysis (CCA) and aggregated boosted tree (ABT) analyses were performed to assess the relationships between environmental settings and phytoplankton communities, and to quantify the effect of key environmental settings on biological parameters. Structural equation modeling (SEM) analysis was employed to assess the relative direct and indirect impact of key explanatory variables on different phytoplankton groups. The ABT was constructed in R using the gbmplus package with 500 trees for boosting and the mgcv package with GCV smoothness estimation (Rv4.0.2). SEM results were visualized using the semPlot package (Rv4.0.2). Statistical significance was set at $p < 0.05$.

3 Results

3.1 Environmental settings in the SMB

Environmental settings differed significantly ($p < 0.05$) between seasons in most cases. The temperature in the study region had high temporal variability from 12.12 to 31.59°C in the winter and summer, respectively (Figure 2A). The variation in salinity (14.86–28.96) was classically driven by land-based influxes, with the highest in winter and a decrease from spring to autumn (Figure 2B). The average SS content reached its maximum during winter (313.74 ± 212.43) and minimum in the summer (37.09 ± 22.20), with no significant difference between spring and autumn (Figure 2C). The average DO content varied from 5.87 to 8.91 mg/L, with the highest concentration in winter (Figure 2D). The average pH varied within the range of 7.91–8.16, and the values in autumn and winter were generally higher than those in spring and summer. Nevertheless, there was no significant difference in pH between spring and summer (Figure 2E). In contrast, COD (0.31–2.94 mg/L) showed a temporally increasing trend but no significant seasonal difference from summer to winter (Figure 2F). Analogously, nutrient concentrations (i.e., DIN, DIP, and SiO_3) showed explicit seasonal patterns (Figures 2G–I); especially DIN and DIP (0.20–0.85 and 0.018–0.038 mg/L, respectively), increased in the autumn.

3.2 Eutrophication and organic pollution in the SMB

The average Ei index ranged between 0.90 and 21.9, with higher values during autumn and winter (Figure 3A). According to the Ei, sea areas (>20% coverage) were defined as heavily eutrophic areas year round (Ei > 9), while mid-eutrophic areas (3 < Ei ≤ 9) covered >30%, indicating a eutrophic in the entire surveyed area. In most cases, the average Ci index ranged from 2.20 to 7.43, indicating severe organic pollution. Overall, the organic pollution status in autumn was worse than in other seasons (Figure 3B). Furthermore, the temporal trends for the Ei and Ci indices were broadly similar. pH was positively correlated with both Ei and Ci indices ($p < 0.001$) (Figure 3C), suggesting that variation in pH has a large impact on the level of eutrophication and organic pollution. It is possible that water acidification owing to reduced pH gradually would alleviate this eutrophication and organic pollution. Both Ei and Ci indices were correlated with water temperature, but with different interactions (Figure 3D): the Ei index was positively correlated with temperature, implying that elevated temperatures (i.e., ocean warming) would intensify coastal eutrophication, in comparison, the Ci index was negatively correlated with temperature, suggesting that ocean warming would mitigate organic pollution.

3.3 Phytoplankton community structure

A total of 118 taxa were identified over all seasons (including species, varieties, and forms), comprising 84 diatoms, 28 dinoflagellates, 1 euglenophyte, 3 cyanobacteria, and 2 chrysophytes. Diatoms were the dominant group, accounting for approximately 71.2% of the taxa and 82.6% of phytoplankton abundance on average, while dinoflagellates accounted for 23.7% of the taxa and 10.8% of phytoplankton abundance on average. There were remarkable seasonal variations in phytoplankton compositions (Figure 4), with species richness increasing from spring to summer and decreasing in

10.3389/fmars.2023.1303497

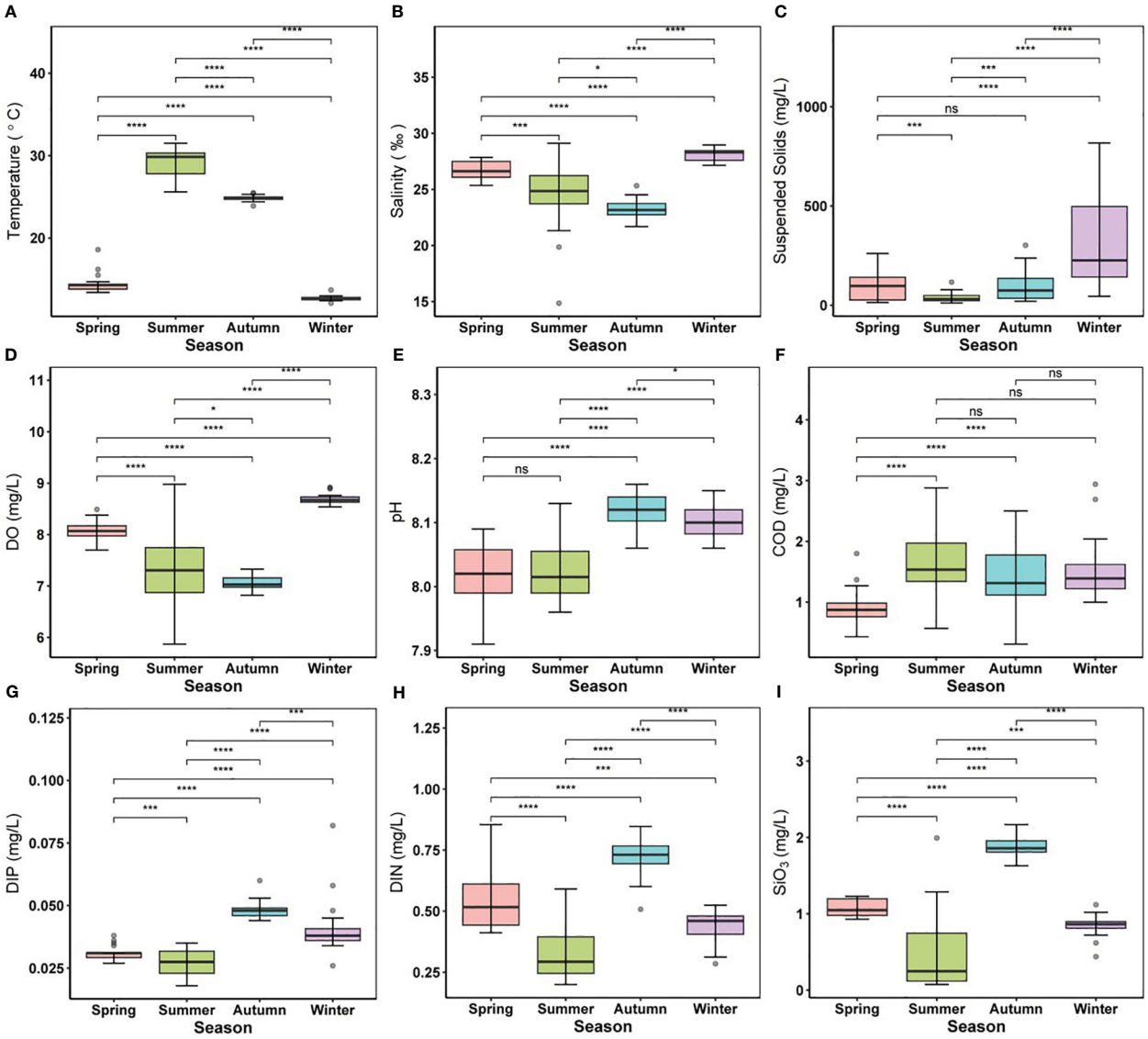

FIGURE 2
Alternations of environmental parameters in different seasons. **(A)** temperature, **(B)** salinity, **(C)** suspended solids, **(D)** DO, **(E)** pH, **(F)** COD, **(G)** DIN, **(H)** DIP, **(I)** SiO_3. Different colored boxes represent four different seasons. For boxplot figures, the box border: the interquartile range; the horizontal line in the box: average value; the upper and lower vibrissae: range beyond the upper and lower quartiles, respectively; grey dots: outliers. Significance indicated by the asterisks (*p*-value: * <0.05, *** <0.001, **** <0.0001). ns indicates nonsignificance.

cold seasons (Figure 4A). Phytoplankton abundance was also markedly higher in summer (80.04 ± 53.14 × 10^3 cells/L on average with a maximum of 213.8 × 10^3 cells/L) than in other seasons, with a nonsignificant difference between spring and autumn (Figure 4B). The abundance of the diatoms (from 4.2 to 205.8 × 10^3 cells/L) followed the same seasonal trend, with a nonsignificant difference between spring and autumn (Figure 4C), and the abundance of dinoflagellates in summer (3.83 ± 2.55 × 10^3 cells/L) was slightly greater than in other seasons, with a significant temporal difference across the four seasons (Figure 4D).

The dominant species were mainly colonial diatoms of either single-celled or multicellular cells (Figure 5). The chain-forming diatoms *Skeletonema* spp. and *Paralia sulcata* dominated in all seasons (Y > 0.20). The chain-forming *Skeletonema*. spp. was the most abundant species in all seasons (Y > 0.15) except in summer, when the dominance of *Skeletonema marinoi* was 0.095. The most abundant chain-forming *P. sulcata* and *Skeletonema costatum* in spring had the greatest dominances, which matched their large proportions in total phytoplankton abundance. The most dominant species in summer was small single-celled *Ditylum brightwellii* with a dominance of 0.218, followed by chain-forming *Leptocylindrus danicus* (0.196) and large single-celled *Biddulphia sinensis* (0.158). Some chain-forming diatoms, such as *Chaetoceros lorenzianus* and *Chaetoceros knipowitschi*, were dominant in the summer. In autumn, the predominant species were largely chain-forming *Thalassionema nitzschioides*, with a dominance index of up to 0.16. Colonial *Thalassiosira subtilis* had its highest dominance (0.083) in autumn. In winter, the maximum dominance value

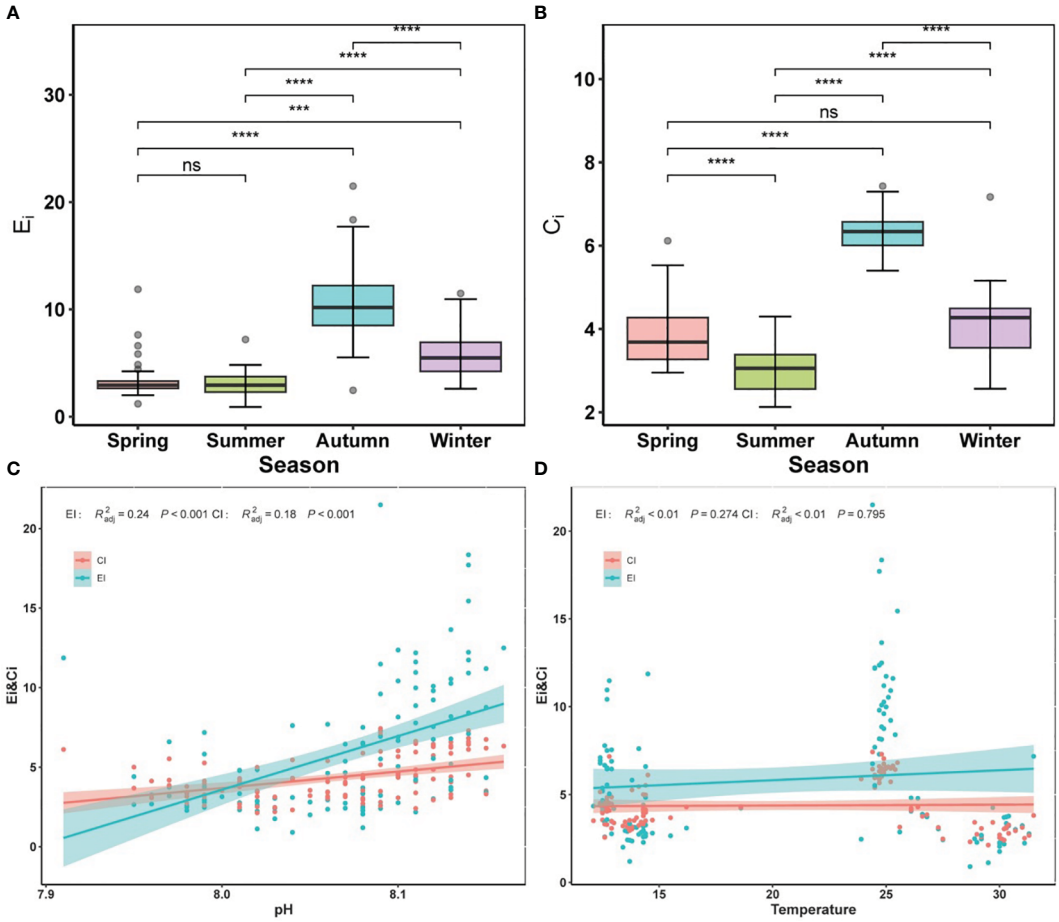

FIGURE 3
Alternations of eutrophication index (Ei), and organic pollution comprehensive index (Ci) in different seasons. **(A)** Ei, **(B)** Ci. **(C)** significant relationships between pH and Ei and Ci, **(D)** significant relationships between temperature and Ei and Ci. Colored lines in panels **(C, D)** represent the least squares regression, which shows statistically significant for both cases (R^2 and *p*-value). Shaded areas are 95% confidence bands. Significance indicated by the asterisks (*p*-value: *** <0.001, **** <0.0001). ns indicates nonsignificance.

(0.114) was attributed to small single-celled *Coscinodiscus radiates*. Some large single-celled diatoms, such as *Coscinodiscus oculus-iridis*, *Coscinodiscus jonesianus*, and *Coscinodiscus subtilis*, were also dominant in winter. Consequently, phytoplankton community was primarily dominated by diatoms. *Skeletonema marinoi*, *S. costatum*, *P. sulcata*, *B. sinensis*, and *C. oculus-iridis* always dominated in this region, even though the top eight dominant species varied widely with season. These results suggest that environmental changes could affect the phytoplankton community, but that some dominant diatoms have a strong adaptability or tolerance to these changes.

3.4 Relationships between phytoplankton and water quality indicators

A CCA (Figure 6) and Spearman matrix (Figure 7A) were performed to examine the relationships between phytoplankton communities and environmental settings. Nutrients, temperature, and SS were the major variables associated with phytoplankton abundance throughout the year. Weak correlations between phytoplankton abundance and the N:P ratio were found in all seasons. The common HAB species, *Skeletonema* spp., was positively correlated with nutrients and the N:P ratio in spring and summer, and positively correlated with salinity and DO in autumn and winter. The chain-forming diatoms (e.g., genus Chaetoceros, *P. sulcata*, *T. nitzschioides*, and genus Thalassiosira) were highly correlated with SS and salinity. Small single-celled diatoms (e.g., *Cyclotella striata*, *Nitzschia clostrium*, and *D. brightwellii*) showed less correlation with environmental settings, but large single-celled diatoms (genus Coscinodiscus and *B. sinensis*) were correlated with high nutrients and high SS concentrations. These findings suggest that the temporal variation in dominant phytoplankton species was largely influenced by SS concentrations and N:P ratio in spring, nutrients and salinity in summer, nutrients and temperature and autumn, and nutrients in winter, respectively.

An ABT analysis was ran to further quantify the effects of environmental settings on major phytoplankton populations (Figure 7B), which revealed that the major predictors were population specific. Specifically, SiO_3 was the major predictor of diatom abundance. In contrast, *Gymnodinium catenatum* and *Akashiwo sanguinea*, which are dinoflagellates, experienced

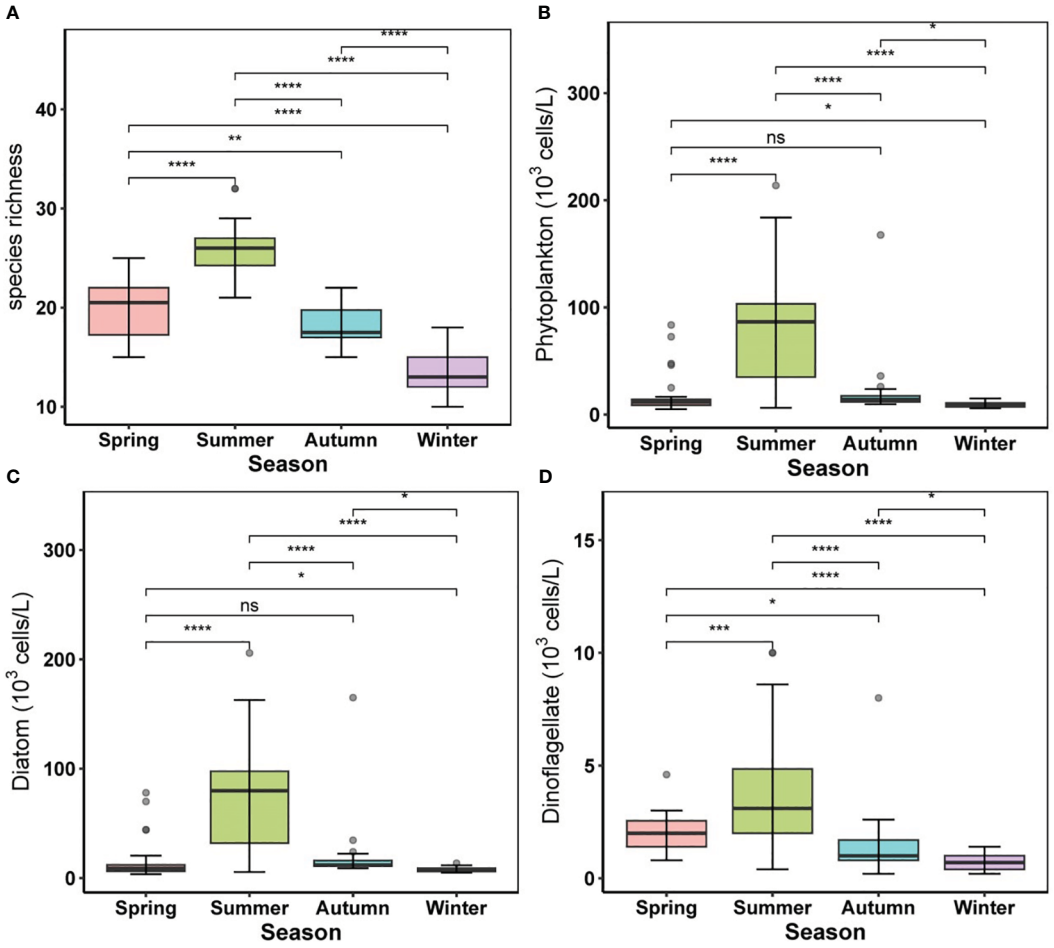

FIGURE 4
Alternations of phytoplankton community in different seasons. **(A)** species richness, **(B)** phytoplankton abundance, **(C)** diatom abundance, **(D)** dinoflagellate abundance. For boxplot figures, the box border: the interquartile range; the horizontal line in the box: average value; the upper and lower vibrissae: range beyond the upper and lower quartiles, respectively; grey dots: outliers. Significance indicated by the asterisks (*p*-value: * <0.05, ** <0.01, *** <0.001, **** <0.0001).

favorable conditions in the form of warm temperatures, low salinity, and low DIP concentrations. Thus, temperature emerged as the primary determinant of dinoflagellate abundance, and temperature, SiO_3, and SS were identified as the primary predictors of overall phytoplankton, diatoms, and dinoflagellates. The relative influence of each factor was not high (<20%), except for temperature (>30%).

Consequently, the causal relationships between phytoplankton abundance and relevant environmental parameters were examined using SEM (Figure 8). We focused on interactions between temperature, salinity, N:P ratio, SiO_3, Ei and Ci index (water quality assessment indices) as the importance of these variables was indicated in the above mentioned analysis (Figures 6 and 7).

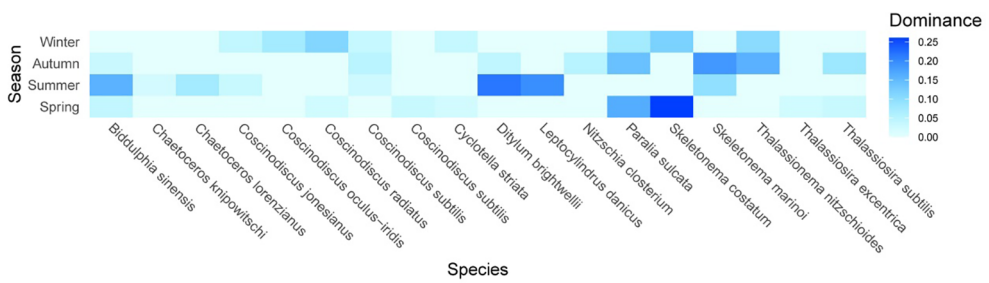

FIGURE 5
Alternations of phytoplankton dominant species in different seasons. The magnitude of dominance index (Y) for phytoplankton species is indicated by color intensity changing from light blue to dark blue.

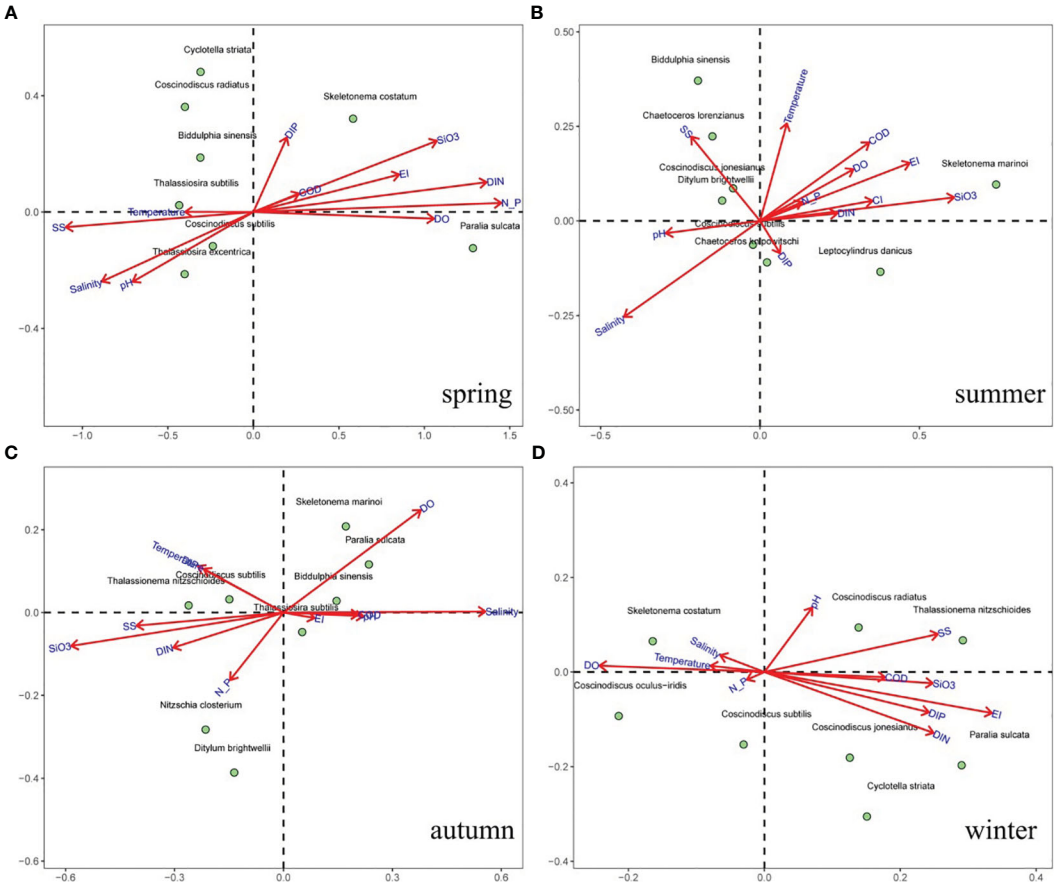

FIGURE 6
The CCA ordination biplots of phytoplankton abundance and environmental settings in different seasons. **(A)** spring, **(B)** summer, **(C)** autumn, and **(D)** winter.

The model results showed that both Ei and Ci indices had a significant direct effect on phytoplankton abundance. Ei had a significant positive effect on phytoplankton abundance but a nonsignificant negative effect on diatom abundance. The Ci index had a nonsignificant negative effect on both diatom and dinoflagellate abundance. The Ei and Ci indices exhibited a positive interaction with each other. Temperature and SiO_3 had positive direct effects on phytoplankton and diatom abundance, while salinity and N:P ratio had negative direct effects on phytoplankton and diatom abundance. Temperature, and N:P ration demonstrated positive direct effects on dinoflagellates, while salinity had a negative direct effect. An indirect effect of SiO_3 on dinoflagellates was also indicated. Overall, temperature had the greatest total positive effect and salinity had the greatest total negative effect (Figure 8).

4 Discussion

4.1 Nutrient regime and water temperature dynamics in the SMB

SMB has demonstrated a longstanding commitment to mariculture and related industries since the 1980s (Chen et al., 2015; Liu et al., 2021). The expansion of these activities has been extensively expanded (Jiang et al., 2012; Ye et al., 2017). The ecological integrity of the area has been persistently jeopardized by thermal discharges originating from a coastal power plant. in this area have also threatened the ecological status for a long time (Liang et al., 2021; Wang et al., 2022). Consequently, these anthropogenic activities have resulted in the excessive introduction of pollutants and nutrients, particularly nitrogen (N) and phosphorus (P), into the nearshore marine environment. This influx has not only disrupted the composition of phytoplankton communities but has also accelerated their growth. In this study, it was observed that environmental factors and water quality in the SMB exhibited noteworthy significant seasonal variation (Figures 2 and 3). Furthermore, the phytoplankton displayed distinct responses to these temporal alternations (Figures 5–8).

Eutrophication and surface warming pose significant threats to marine ecosystems, as evidenced by multiple studies (Laurent et al., 2018; Deininger and Frigstad, 2019; Freeman et al., 2019; Wei et al., 2022). The influence of nutrients on the phytoplankton community is widely acknowledged (Irwin et al., 2006; Song et al., 2016; Cloern, 2018; Lee et al., 2021). The findings from the CCA and ABT analyses provide further confirmation that seasonal variation in the phytoplankton community are primarily driven by nutrient levels (Figures 6 and 7B). Table 1 presents a comprehensive

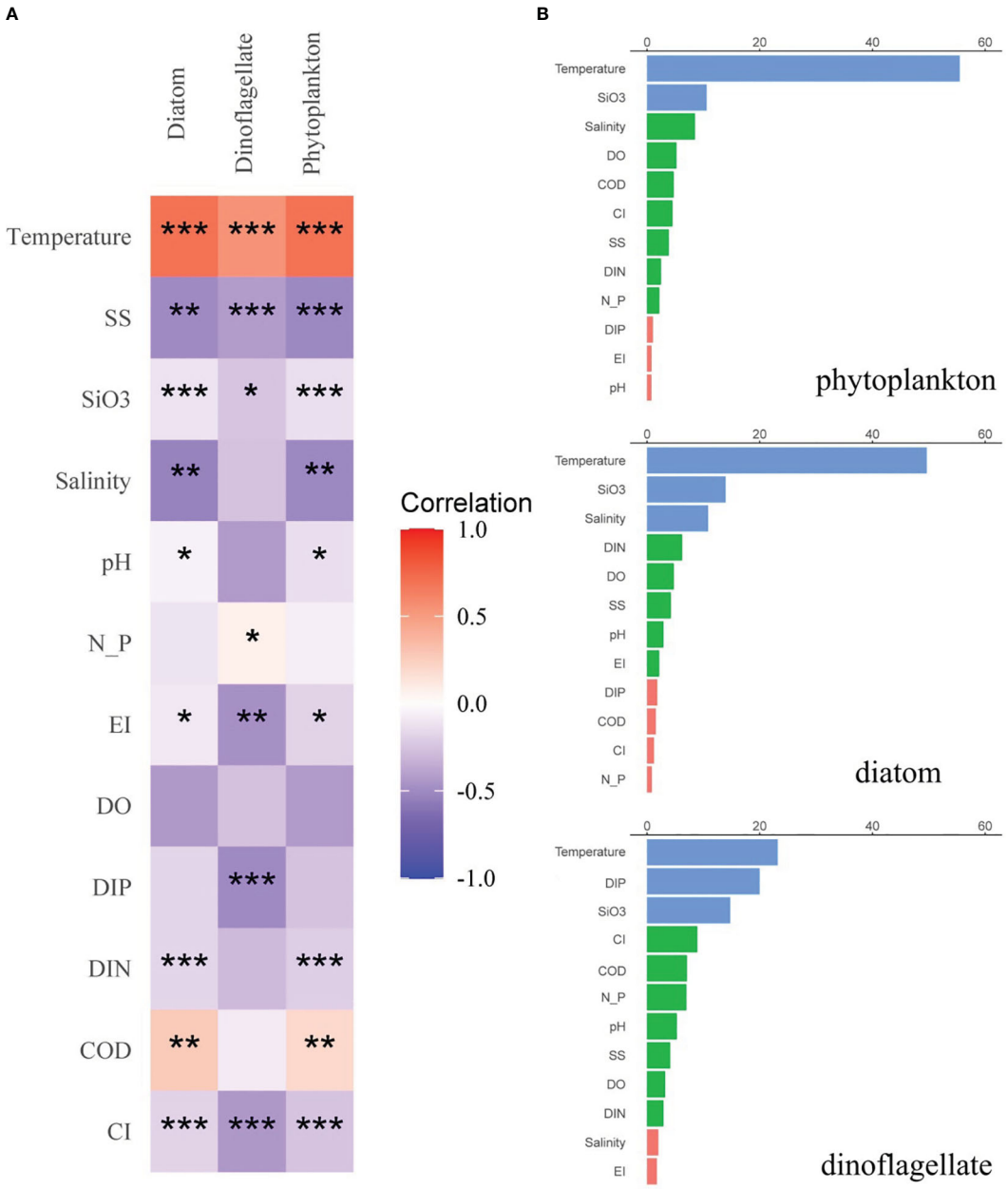

FIGURE 7
(A) Correlation matrix among the various environmental parameters and major phytoplankton groups over all seasons. Spearman correlation coefficients ranged from negative to positive and are indicated by color intensity changing from blue to red, respectively. Significance indicated by the asterisks (*p*-value: * <0.05, ** <0.01, *** <0.001). **(B)** ABT analysis for the relative effects of environmental settings on abundance of major phytoplankton groups over all seasons. The blue, green, and red bars represent the ranges of relative effect in >10%, 2–10%, and <2%, respectively.

depiction of the prolonged fluctuations in averaged DIN, DIP, N/P, Ei (the eutrophication index), and dominant phytoplankton species from the 1980s to 2020. Over the course of the past five decades, there has been a discernible upward trajectory in nutrient content and N/P ratio. In comparison to the 1980s, the annual average DIN content in this investigation has experienced an approximate threefold increase, while the N/P ratio has doubled. Specifically, the N:P ratio has increased from 13.3 to 28.6 in the SMB (Gao et al., 2022), and showed an increasing trend from the 1980s to 2015 (Table 1). It was generally higher than the Redfield ratio of 16 (Redfield, 1958), with an average N:P ratio as high as 22 in spring in this study. The strong negative association between most of the dominant phytoplankton species and N:P ratio, and the positive relationship with SS, supports the inference that phytoplankton distribution in spring was principally controlled by lower SS and a higher N:P ratio (Figure 6). In addition, the SMB has experienced prolonged eutrophication as a result of its limited water exchange capacity and excessive input from tributaries. Consequently, the level of eutrophication (Ei) has significantly escalated (Table 1), leading to an increase in HAB occurrences and alterations in species composition caused by human activities (Jiang et al., 2012; Chen et al., 2017; Gao et al., 2022).

10.3389/fmars.2023.1303497

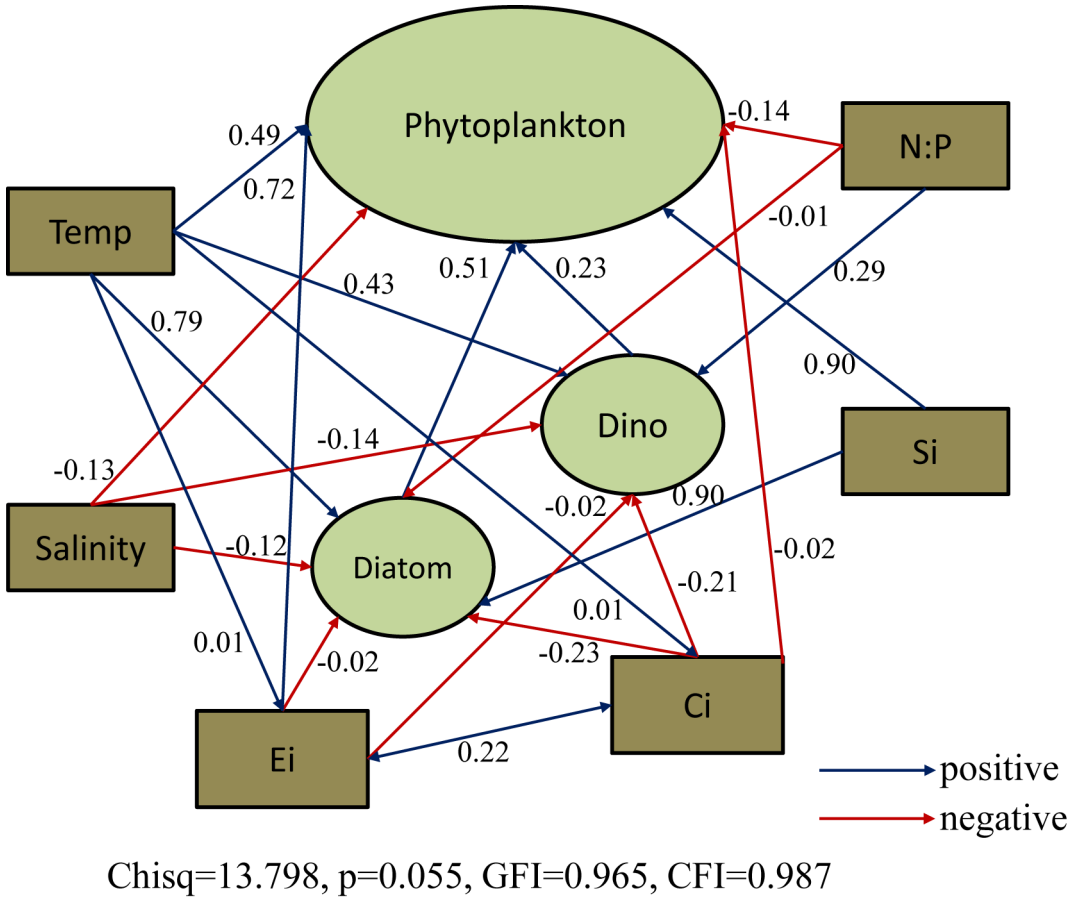

FIGURE 8
Structural equation model (SEM) analysis examining the effects of relevant environmental parameters (temperature, salinity, N:P ratio, SiO_3) and water quality assessment indices (Ei and Ci index) on major phytoplankton groups over all seasons. Solid blue and red lines indicate significant positive and negative effects at $p < 0.05$, respectively, and dashed blue and red lines indicate nonsignificant positive and negative effects, respectively. Values associated with arrows represent standardized path coefficients.

TABLE 1 Long-term variation in SMB in averaged nutrient concentration, N/P ratio, eutrophication index and dominant species of phytoplankton in all seasons.

Time	Nutrient concentration (mg/L)		N/P ratio	Ei index	Phytoplankton dominant species in all seasons	Reference
	DIN	DIP				
The 1980s	0.26	0.032	17.80	4.59	*Coscinodiscus* spp., *D. brightwellii*, and *Nitzschia* spp.	Committee of Chronicles in China Gulf, 1992
Year 2002-2003	0.49	0.026	42.35	2.35	*S. costatum*, *P. punges*, *C. pseudocurvisetus*, *and D. brightwellii*	Ning, 2005
Year 2006-2007	0.62	0.033	41.90	4.18	*Coscinodiscus* spp., *C. lorenzianus*, *C. pseudocurvisetus*, and *C. fusus*	Committee of Zhejiang Coastal Ecology and Environmental Capacity, 2015
Year 2015-2016	0.63	0.036	39.18	6.57	*C. jonesianus*, *C. oculus-iridis*, *C. pseudocurvisetus*, *Skeletonema* spp., and *T. frauenfeldii*	Chen et al., 2017
Year 2020	0.57 ± 0.18	0.038 ± 0.010	21.73 ± 9.30	5.95± 3.95	*S. costatum*, *S. marinoi*, *B. sinensis*, *T. eccentrica*, *L. danicus*, *C. oculus-iridis*, *C. jonesianus*, and *C. knipowitschi*	This study

In the past 50 years, the composition of dominant species in the SMB has been influenced by the presence of chain-forming diatoms, which have partially constrained the dominance of large single-celled diatoms (Table 1). The proliferation of chain-forming diatoms has been observed to occur at a faster rate under conditions of high nutrient content, as supported by studies conducted by Finkel et al. (2010); Wang et al. (2019), and Song et al. (2016). Furthermore, there has been a significant increase in the N/P ratio in the SMB over time. This increase has created a favorable environment for the growth of small-celled chain-forming diatoms, which have a lower demand for DIP compared to large single-celled diatoms and dinoflagellates. (Glibert and Burkholder, 2011; Xiao et al., 2018; Xin et al., 2019). Hence, the increasing prevalence of chain-forming diatoms surpassing large-cell dinoflagellates, such as genera Ceratium and Prorocentrum, may have contributed to the disappearance of dinoflagellates as the dominant species in this study (Figure 5). Throughout the entire duration of the study, the succession of diatoms and dinoflagellates in relation to N:P ratios did not exhibit seasonal variation (Figures 5 and 6). Correlation and ABT analysis (Figure 7) indicated that dinoflagellates possessed a stronger competitive advantage over diatoms in environments with limited biogenic factors. Furthermore, the presence of silicates exerted a substantial impact on diatoms, in addition to their utilization of nitrogen.

Phytoplankton experiencing nutrient limitations are compelled to adapt to the warming of seawater. The increase in temperatures has the potential to expedite the absorption of nutrients by phytoplankton, as evidenced by studies conducted by Berges et al., 2002; Wu et al., 2021 and Wei et al., 2022. The presence of the coastal nuclear power plant (NPP) in SMB plays a significant role in this phenomenon, as NPPs produce substantial quantities of warm water effluent (Hu, 2004), thereby substantially raising the temperature of the surrounding aquatic environment (Langford, 1990; Krishnakumar et al., 1991; Zhang et al., 2023). The thermal discharge from NPPs has the potential to affect phytoplankton survival, growth, and reproduction (Langford, 1990; Lo et al., 2004; Poornima et al., 2006; Zhang et al., 2023), resulting in changes to the upper trophic levels and modification of the ecosystem. The study observed a clear seasonal fluctuation in temperature, which, in conjunction with salinity, had a significant impact on the temporal distribution of phytoplankton (Figure 6) (e.g., Jiang et al., 2014; Song et al., 2016; Wei et al., 2022). Our findings suggest that temperature was significantly positively correlated with phytoplankton abundance, and thus ocean warming would favor high phytoplankton populations (Figures 7 and 8). Further, elevated temperatures would intensify the progress of coastal eutrophication (Figure 3D). Numerous studies have demonstrated that the concurrent effects of warming and eutrophication have the potential to amplify the growth and metabolic rates of phytoplankton, consequently leading to an increase in both the magnitude and occurrence of phytoplankton blooms, including HABs (Winder and Sommer, 2012; Xiao et al., 2018; Lee et al., 2019). Specifically, the occurrence and duration of algal blooms in subtropical eutrophic waters are frequently linked to thermal discharge from power plants (Yu et al., 2007; Jiang et al., 2019a; Jiang et al., 2019b). Nevertheless, this study did not observe any blooms throughout the four seasons (Figures 4 and 5). Previous research has shown that under eutrophic conditions, an increase in temperature resulting from thermal discharge has led to an augmentation in phytoplankton abundance in the SMB (Chen et al., 2017; Gao et al., 2022). The sequence of prevailing species in the local area was significantly influenced by the thermal discharge originating from the NPP in SMB. This discharge facilitated the growth and reproductive activities of *C. jonesianus* (Yang et al., 2013), ultimately resulting in the prevalence of Coscinodiscus during the winter and spring seasons, as depicted in Figures 5 and 6 of this study.

4.2 Phytoplankton community shift in the SMB

Phytoplankton, as a primary producer in aquatic ecosystems, experiences alterations in its community structure due to nutrient load and hydrologic regimes (Hart et al., 2015; Song et al., 2022). The present study reveals noteworthy seasonal fluctuations in the phytoplankton community (Figures 4–6). Additionally, the hydrologic conditions exhibited temporal variability, thereby inducing dynamic fluctuations in the phytoplankton community (Figures 4–6). In particular in spring, the low concentration of suspended solids and high transparency of the water facilitated the growth of phytoplankton, leading to an increase in both abundance and species richness (Cloern and Dufford, 2005; Jiang et al., 2019b) as depicted in Figures 2C and 4. During the summer, the Taiwan Warm Current intensified, causing a significant influx of neritic warm-water species into the bay (Zhu et al., 2012; Jiang et al., 2014). Concurrently, the intrusion of oligotrophic and highly transparent seawater resulted in reduced levels of suspended solids and nutrients (Figure 2). However, the highest abundance and species richness were found in summer accordingly (Figure 4). A previous study in the Atlantic coast of the Brazil, which had lower nutrient loads but greater light availability, also suggested a stimulated phytoplankton abundance (Cavalcanti et al., 2020). In autumn, the Zhemin Coast Current, characterized by low salinity and high nutrient content, exerted control over the system (Zhu et al., 2012; Jiang et al., 2014). This resulted in an increase in suspended solids concentration and a decrease in transparency, which disrupted the water environment (Figure 2C). Consequently, the growth of phytoplankton species was constrained, leading to a significant decline in abundance and species richness compared to the summer season (Figure 4) (Chen et al., 2017; Gao et al., 2022). However, due to the persistence of warmer water temperatures, a certain abundance of warm-water species managed to survive (Shou and Zeng, 2015; Gao et al., 2022). During the winter season, the bay experienced elevated levels of suspended solids primarily attributed to the intensified hydrodynamic forces. Additionally, the suboptimal temperature conditions hindered the growth of phytoplankton, resulting in diminished abundance and species diversity. Furthermore, phytoplankton species richness index exhibited a value of 19 across the four seasons, signifying a notable seasonal change in species composition. This occurrence has been previously recorded, as a study by Tang et al. (2018)

reported a total of 12 shared species annually in the vicinity of Zhoushan Island in the East China Sea. The presence of a relatively diverse local community plays a crucial role in stabilizing the ecosystem by preserving the proportional abundance of certain species (Carr et al., 2002). Generally, coastal eutrophication had profound effects on the diversity and complexity of phytoplankton composition and biomass. Specifically, it enhanced the frequency of HAB events accompanied by severe Si limitation (Lin et al., 2001; Carstensen et al., 2007; Wang et al., 2019; Xin et al., 2019). The ABT revealed that Si was a major predictor of total phytoplankton, diatoms, and dinoflagellates (Figure 7B), indicating that the Si concentration had a significant impact on the relative proportion of dinoflagellates to diatoms. The significant impact of Si on dinoflagellates in SMB may be attributed to the presence of a widely distributed harmful algal bloom specie, *A. sanguinea*, which showed substantial abundance during the summer and autumn in this study. Prior research has indicated that *A. sanguinea* may have a preference for nitrate uptake over silicon, as evidenced by the low nitrate concentration observed (Du et al., 2011). This finding aligns with the observed negative correlation between dinoflagellates and DIN concentration throughout the present study (Figure 7A). The prevalence of *A. sanguinea* was observed to be prominent along the coast of Korea, resulting in blooms in autumn (Kim et al., 2019). Conversely, during the spring and summer seasons, while interspecific interactions, such asallelopathy exhibited by centric diatoms, were found to hinder the formation of these blooms (Figure 5) (e.g. Matsubara et al., 2008). This dominance of *A. sanguinea* aligns with the P–Si limitation observed in recent decades (Wang et al., 2019; Xin et al., 2019; Song et al., 2022).

Diatoms and dinoflagellates are of significant concern in coastal waters due to their pivotal role in aquatic ecosystems (Agustí et al., 2015). These groups exacerbate the impacts of eutrophication and ocean warming. Chen et al. (2017) demonstrated, through net collection of phytoplankton, that warm-water species such as *Chaetoceros pseudocurvisetus* and *Palmeria hardmaniana*, which became dominant in SMB in winter, facilitated the dominance of abundances. This increased dominance of genus Chaetoceros and *P. hardmaniana* indicates that warming influences the phytoplankton composition in SMB. Gao et al. (2022) posited that the community structure of phytoplankton in SMB was undergoing a transition towards cell miniaturization, resulting in a shift in the net collection of phytoplankton dominant species as warm-water species became more prevalent. However, our findings based on phytoplankton collected from water samples indicated that the dominance of genus Chaetoceros only increased in summer in SMB, and this genus was not dominant in other seasons (Figure 5). The dominance of small-celled chain-forming diatoms (particularly genera Skeletonema and Thalassiosira) increased from spring to autumn, while the dominance of large single-celled diatoms (e.g., genus Coscinodiscus and species *D. brightwellii*) increased in winter, suggesting that the shifting of phytoplankton composition toward cell miniaturization was not evident across seasons (Figures 5 and 6). This is in contradiction to reports from Hangzhou Bay in East China Sea (Zhang et al., 2015) and Daya Bay in south China Sea (Wu et al., 2017). Large diatoms such as genus Coscinodiscus and species *D. brightwellii* exhibit a notable ability to absorb and assimilate nutrients, enabling them to sustain a rapid growth rate (Philippart et al., 2000). This heightened nutrient consumption results in diminished nutrient levels. Consistent with the presence of the diatom genus Coscinodiscus, the winter season witnessed the second lowest nutrient concentrations in this study (Figures 2 and 6).

Dinoflagellates have been observed to dominate in conditions of lower DIP and are less sensitive to temperature compared to diatoms (Glibert et al., 2010; Wells et al., 2015). Previous studies have indicated a decrease in the proportion of diatom species in waters as the abundance of dinoflagellate species increases (Chen et al., 2017; Gao et al., 2022). This shift has been attributed to the competitive advantage of dinoflagellates over diatoms in environments characterized by higher N:P ratios and elevated temperatures (Xiao et al., 2018; Zhang et al., 2021; Wei et al., 2022). The proportions of dinoflagellates to phytoplankton abundance in the SMB were constrained by the lower temperature, higher DIP, and lower light availability (high SS) across the four seasons (Figures 7 and 8). Nitrophilous diatoms, particularly the overwhelmingly dominant genera Skeletonema, Thalassiosira and Thalassionema, were present throughout the year due to their greater tolerance to environmental variability, including low salinity and abundant nutrients (Figures 2 and 6). This finding is consistent with previous studies by Philippart et al., 2000; Shou and Zeng, 2015; Chen et al., 2017; Jiang et al., 2019a; Cavalcanti et al., 2020; and Song et al., 2022. The most dominant eurythermal species, *Skeletonema* spp., shows a high level of dominance in the coastal waters of the East China Sea, particularly in areas such as the Changjiang estuary (Jiang et al., 2014) and Hangzhou Bay (Zhang et al., 2015). This dominance is attributed to its ability to exploit community competition within eutrophic, low-salinity, and turbid waters. The restructuring of diatom and dinoflagellate communities in coastal ecosystems is observed to be influenced by eutrophication and warming (Glibert et al., 2010; Wells et al., 2015; Song et al., 2022). This restructuring is attributed to changes in nutrient ratios, leading to a transition from siliceous phytoplankton to nonsiliceous phytoplankton and a reduction in cell size (Liu et al., 2009; Finkel et al., 2010; Gao et al., 2022). However, further investigation is needed to fully understand the impact of warming and nutrient ratio dynamics on the succession of diatoms and dinoflagellates in the SMB, necessitating the collection of long-term datasets.

5 Conclusions

The main reason for the deterioration of the coastal environment is that a large number of pollutants produced on land are discharged into it, including inorganic nitrogen, active phosphate, and heavy metals, etc. This study conducted a systematical analysis of phytoplankton diversity in a eutrophic area of the coastal East China Sea, integrating environmental changes and water quality. This study employed a high temporal resolution. Highly significant seasonal variations in the abundance and community structure of water-collected phytoplankton and

environmental settings were identified in the SMB. The results revealed significant seasonal differences in the phytoplankton community, primarily driven by variations in temperature, Si concentrations, and SS. The succession of diatoms and dinoflagellates related to N:P ratio dynamics was not evident across seasons, requiring more long-term datasets. In addition, eutrophication and organic pollution had significant direct effects on phytoplankton abundance. The significance of NPPs should not be disregarded or undervalued, particularly in relation to their impact on phytoplankton responses to eutrophication under thermal stress. As the construction of NPPs persists along China's coastline, it is imperative to allocate additional resources towards the investigation of these responses. Additionally, unreasonable development and layout of the marine space, as well as high-intensity land reclamation, have put intense pressure on natural resources and ecosystems in SMB. These all need to bring to the attention and worth pondering with the discussion. A preliminary understanding of the current state of phytoplankton community structures and their regulation in SMB will facilitate forthcoming investigations in evaluating changes across broader spatial and extended temporal dimensions.

Data availability statement

The original contributions presented in the study are included in the article/supplementary materials, further inquiries can be directed to the corresponding author/s.

Author contributions

YW: Data curation, Investigation, Methodology, Resources, Visualization, Writing – original draft, Writing – review & editing. WW: Conceptualization, Data curation, Formal analysis, Investigation, Resources, Visualization, Writing – review & editing. YH: Data curation, Formal analysis, Investigation, Resources, Visualization, Writing – review & editing. LC: Conceptualization, Data curation, Investigation, Methodology, Writing – review & editing. XT: Conceptualization, Data curation, Investigation, Methodology, Writing – review & editing. XH: Data curation, Formal analysis, Funding acquisition, Project administration, Supervision, Validation, Writing – review & editing. LH: Data curation, Formal analysis, Funding acquisition, Project administration, Supervision, Validation, Writing – review & editing.

Funding

The author(s) declare financial support was received for the research, authorship, and/or publication of this article. This research was funded by the National Key Research and Development Program of China (contract Nos. 2022YFC2804003 and 2022YFC3102401), the National Natural Science Foundation of China (contract Nos. 42006127, 41506136 and 41306115) and the Project of Ministry of Science and Technology (contract No. GASI-01-02-04).

Acknowledgments

The authors acknowledge Dr. Senming Tang from Hongkong University for fruitful discussion and for helping to organize the manuscript. Thanks to the staff workers from Second Institute of Oceanography for their logistical support. We would also like to thank Dr. Xiuwu Sun from Third Institute of Oceanography for assistance with the determination of environmental parameters. We would like to thank MogoEdit (https://www.mogoedit.com) for its English editing during the preparation of this manuscript. We sincerely appreciate the constructive comments and suggestions of the anonymous reviewers.

Conflict of interest

The authors declare that the research was conducted in the absence of any commercial or financial relationships that could be construed as a potential conflict of interest.

Publisher's note

References

Agustí, S., González-Gordillo, J. I., Vaqúe, D., Estrada, M., Cerezo, M. I., Salazar, G., et al. (2015). Ubiquitous healthy diatoms in the deep sea confirm deep carbon injection by the biological pump. *Nat. Commun.* 6, 1–8. doi: 10.1038/ncomms8608

Berges, J. A., Varela, D. E., and Harrison, P. J. (2002). Effects of temperature on growth rate, cell composition and nitrogen metabolism in the marine diatom Thalassiosira pseudonana (Bacillariophyceae). *Mar. Ecol. Prog. Ser.* 225, 139–146. doi: 10.3354/meps225139

Borja, A., Marin, L., Muxika, I., Pino, L., and Rodriz, J. G. (2015). Is there a possibility of ranking benthic quality assessment indices to select the most responsive to different human pressure? *Mar. pollut. Bull.* 97 (1–2), 85–94. doi: 10.1016/j.marpolbul.2015.06.030

Carr, M. H., Anderson, T. W., and Hixon, M. A. (2002). Biodiversity, population regulation, and the stability of coral-reef fish communities. *Proc. Natl. Acad. Sci. U. S. A.* 99 (17), 11241–11245. doi: 10.1073/pnas.162653499

Carstensen, J., Henriksen, P., and Heiskanen, A. S. (2007). Summer algal blooms in shallow estuaries: definition, mechanisms, and link to eutrophication. *Limnol. Oceanogr.* 52, 370–384. doi: 10.4319/lo.2007.52.1.0370

Cavalcanti, L. F., Cutrim, M. V. J., Lourenço, C. B., Karoline, A., Sá, D. D., Oliveira, A. L. L., et al. (2020). Patterns of phytoplankton structure in response to environmental gradients in a macrotidal estuary of the Equatorial Margin (Atlantic coast, Brazil). *Estuarine Coast. Shelf Sci.* 245, 106969. doi: 10.1016/j.ecss.2020.106969

Chen, X., Zhang, J., Ma, Y., and Cui, T. (2015). Monitoring and analysis of coastline changes of the Sanmen Bay with remote sensing during the past 40 years. *Mar. Sci.* 39 (2), 43–49. doi: 10.11759/hykx20141011004

Chen, Y., Liu, J. J., Gao, Y. X., Shou, L., Liao, Y. B., Huang, W., et al. (2017). Seasonal variation and the factors on net-phytoplankton in Sanmen bay. *Oceanologia Limnologia Sin.* 48 (1), 101–112. doi: 10.11693/ hyhz20160700153

Cheung, Y. Y., Cheung, S., Mak, J., Liu, K., Xia, X., Zhang, X., et al. (2021). Distinct interaction effects of warming and anthropogenic input on diatoms and dinoflagellates in an urbanized estuarine ecosystem. *Glob. Change Biol.* 27, 3463–3473. doi: 10.1111/gcb.15667

Cloern, J. E. (2001). Our evolving conceptual model of the coastal eutrophication problem. *Mar. Ecol. Prog. Ser.* 210, 223–253. doi: 10.3354/meps210223

Cloern, J. E. (2018). Why large cells dominate estuarine phytoplankton? *Limnology Oceanography* 63 (S1), S392–S409. doi: 10.1002/lno.10749

Cloern, J. E., and Dufford, R. (2005). Phytoplankton community ecology: Principles applied in san Francisco bay. *Mar. Ecol. Prog. Ser.* 285, 11–28. doi: 10.3354/meps285011

Committee of Chronicles in China Gulf (1992). "Sanmen Bay," in *Committee of chronicles in China Gulf Ed. Volume 5 of China gulf chronicles (Shanghai and Northern Gulf of Zhejiang Province)* (Beijing: Ocean Press), 234–308.

Committee of Zhejiang Coastal Ecology and Environmental Capacity (2015). "Comprehensive evaluation of the trend of changes in marine environmental quality in Sanmen Bay," in *Zhejiang coastal ecology and environmental capacity*. Eds. L. Sou and J. N. Zeng (Beijing: Ocean Press), 136–228.

Deininger, A., and Frigstad, H. (2019). Reevaluating the role of organic matter sources for coastal eutrophication, oligotrophication, and ecosystem health. *Front. Mar. Sci.* 6, 210. doi: 10.3389/fmars.2019.00210

Du, X., Peterson, W., Mcculloch, A., and Liu, G. (2011). An unusual bloom of the dinoflagellate akashiwo sanGuinea off the Central Oregon, USA, coast in autumn 2009. *Harmful Algae* 10, 784–793. doi: 10.1016/j.hal.2011.06.011

Editorial Committee of the Bay Chorography in China (ECBCC) (1992). *The bay chorography in China: part 5* (Beijing: China Ocean Press), 166–233.

Finkel, Z. V., Beardall, J., Flynn, K. J., Quiqq, A., Rees, T. A., and Raven, J. A. (2010). Phytoplankton in a changing world: Cells size and elemental stoichiometry. *J. Plankton Res.* 32 (1), 119–137. doi: 10.1093/plankt/fbp098

Freeman, L. A., Corbett, D. R., Fitzgerald, A. M., Lemley, D. A., Quigg, A., and Steppe, C. N. (2019). Impacts of urbanization and development on estuarine ecosystems and water quality. *Estuar. Coasts* 42 (7), 1821–1838. doi: 10.1007/s12237-019-00597-z

Fukuyo, Y., Hideaki, T., Chihara, M., and Matsuoka, K. (1990). *Red Tide Organisms in Japan, All Illustrated Taxonomic Guide*. Uchida Rokakuho Publishing, Tokyo, 1–407.

GAQSIQ (2007b). *The specification for marine monitoring–Part 7: Ecological survey for offshore pollution and biological monitoring (GB 17378.7–2007)* (Beijing: China Standard Press).

Gao, Y., Jiang, Z., Chen, Y., Liu, J., Zhu, Y., Liu, X., et al. (2022). Spatial variability of phytoplankton and environmental drivers in the turbid Sanmen bay (East China Sea). *Estuaries and Coasts* 45, 2519–2533. doi: 10.1007/s12237-022-01104-7

Garmendia, M., Revilla, M. I., Bald, J., Franco, J., Martinez, J. L., Orive, E., et al. (2011). Phytoplankton communities and biomass size structure (fractionated chlorophylla), along trophic gradients of the Basque coast (northern Spain). *Biogeochemistry* 106 (2), 243–263. doi: 10.1007/s10533-010-9445-2

General Administration of Quality Supervision, Inspection and Quarantine (GAQSIQ) (2007a). *The specification for marine monitoring–Part 4: Seawater analysis (GB 17378.4–2007)* (Beijing: China Standard Press).

Glibert, P. M., Allen, J. I., Bouwman, A. F., Brown, C. W., Flynn, K. J., Lewitus, A. J., et al. (2010). Modeling of HABs and eutrophication: status, advances, challenges. *J. Mar. Syst.* 83, 262–275. doi: 10.1016/j.jmarsys.2010.05.004

Glibert, P. M., and Burkholder, J. A. M. (2011). Harmful algal blooms and eutrophication: "strategies" for nutrient uptake and growth outside the redfield comfort zone. *Chin. J. Oceanology Limnology* 29 (4), 724–738. doi: 10.1007/s00343-011-0502-z

Hart, J. A., Phlips, E. J., Badylak, S., Dix, N., Petrinec, K., Mathews, A. L., et al. (2015). Phytoplankton biomass and composition in a well-flushed, sub-tropical estuary: the contrasting effects of hydrology, nutrient loads and allochthonous influences. *Mar. Environ. Res.* 112, 9–20. doi: 10.1016/j.marenvres.2015.08.010

Hu, J. H. (2004). The coastal currents offshore the nuclear power plants at northern Taiwan. *J. Mar. Sci. Technol.* 12 (5), 355–363. doi: 10.51400/2709-6998.2256

Irwin, A. J., Finkel, Z. V., Schofield, O. M. E., and Falkowski, P. G. (2006). Scaling-up from nutrient physiology to the size-structure of phytoplankton communities. *J. Plankton Res.* 28 (5), 459–471. doi: 10.1093/plankt/fbi148

Jiang, Z., Chen, Q., Zeng, J., Liao, Y., and Liu, J. (2012). Phytoplankton community distribution in relation to environmental parameters in three aquaculture systems in a Chinese subtropical eutrophic bay. *Mar. Ecol. Prog. Ser.* 446, 73–89. doi: 10.3354/meps09499

Jiang, Z., Du, P., Liu, J., Chen, Y., Zhu, Y., Shou, L., et al. (2019a). Phytoplankton biomass and size structure in Xiangshan Bay, China: current state and historical comparison under accelerated eutrophication and warming. *Mar. Pollut. Bull.* 142, 119–128. doi: 10.1016/j.marpolbul.2019.03.013

Jiang, Z., Gao, Y., Chen, Y., Du, P., Zhu, X., Liao, Y., et al. (2019b). Spatial heterogeneity of phytoplankton community shaped by a combination of anthropogenic and natural forcings in a long narrow bay in the East China Sea. *Estuar. Coast. Shelf Sci.* 217, 250–261. doi: 10.1016/j.ecss.2018.11.028

Jiang, Z. B., Liu, J. J., Chen, J. F., Chen, Q. Z., Yan, X. J., Xuan, J. L., et al. (2014). Responses of summer phytoplankton community to drastic environmental changes in the Changjiang (Yangtze River) estuary during the past 50 years. *Water Res.* 54, 1–11. doi: 10.1016/j.watres.2014.01.032

Jiang, Z. B., Liu, J. J., Zhu, X. Y., Chen, Y., Chen, Q. Z., and Chen, J. F. (2020). Quantitative comparison of phytoplankton community sampled using net and water collection methods in the southern Yellow Sea. *Regional Stud. Mar. Sci.* 35, 2352–4855. doi: 10.1016/j.rsma.2020.101250

Kim, H., Kang, D., Jung, S. W., and Kim, M. (2019). High-frequency acoustic backscattering characteristics for acoustic detection of the red tide species akashiwo sanGuinea and Alexandrium affine. *J. Oceanol. Limnol.* 37, 1268–1276. doi: 10.1007/s00343-019-8113-1

Krishnakumar, V., Sastry, J., and Swamy, G. N. (1991). Implication of thermal discharges into the sea-a review. *Indian J. Environ. Protect.* 11, 525–527. doi: AIX-24-026508

Langford, T. (1990). *Ecological effects of thermal discharges* (London: Elsevier Applied Science Publishers), 28–103.

Laurent, A., Fennel, K., Ko, D. S., and Lehrter, J. (2018). Climate change projected to exacerbate impacts of coastal eutrophication in the northern Gulf of Mexico. *J. Geophys. Res. Oceans* 123 (5), 3408–3426. doi: 10.1002/2017JC013583

Lee, K. H., Jeong, H. J., Lee, K., Franks, P. J., Seong, K. A., Lee, S. Y., et al. (2019). Effects of warming and eutrophication on coastal phytoplankton production. *Harmful Algae* 81, 106–118. doi: 10.1016/j.hal.2018.11.017

Lee, M., Ro, H., Kim, Y. B., Park, C. H., and Baek, S. H. (2021). Relationship of spatial phytoplankton variability during spring with eutrophic inshore and oligotrophic offshore waters in the East Sea, including Dokdo, Korea. *J. Mar. Sci. Eng.* 9 (12), 1455. doi: 10.3390/jmse9121455

Liang, J., Zhou, Y., and Wang, Z. (2021). Environmental quality assessment of the Sanmen Bay and its annual changes. *J. Zhejiang Ocean. Univ. (Nat. Sci.)* 40, 121–127. doi: 10.3969/j.issn.1008-830X.2021.02.004

Liang, J. X., Zhou, Y. D., Wang, Z. M., Zhang, Y. Z., Jin, H. W., and Xu, K. D. (2020). Community structure of macrozoobenthos and its relationship with environmental factors in Sanmen Bay, Zhejiang, China. *Chin. J. Appl. Ecol.* 31 (9), 3187–3193. doi: 10.13287/j.1001-9332.202009.037

Lin, C., Su, J., Xu, B., and Tang, Q. (2001). Long-term variations of temperature and salinity of the Bohai Sea and their influence on its ecosystem. *Prog. Oceanogr.* 49, 7–19. doi: 10.1016/S0079-6611(01)00013-1

Liu, X., Duan, X., Tian, Y., Gao, K., Gao, F., Yin, P., et al. (2021). Variation of nutrients in Sanmen Bay and its response to human activities. *Mar. Geology Front.* 37 (5), 46–56. doi: 10.16028/j.1009-2722.2020.052

Liu, J. J., Jiang, Z. B., Chen, Y., Zeng, J. N., Huang, W., Peng, L., et al. (2015). Community characteristics of net-phytoplankton in spring in Sanmen Bay, China. *J. Mar. Sci.* 33 (1), 74–80. doi: 10.11693/hyhz20160700153

Liu, S., Lou, S., Kuang, C., Huang, W., Chen, W., Zhang, J., et al. (2011). Water quality assessment by pollution-index method in the coastal waters of Hebei Province in western Bohai Sea, China. *Mar. Pollut. Bull.* 62 (10), 2220–2229. doi: 10.1016/j.marpolbul.2011.06.021

Liu, S. M., Hong, G. H., Zhang, J., Ye, X. W., and Jiang, X. L. (2009). Nutrient budgets for large Chinese estuaries. *Biogeosciences* 6, 2245–2263. doi: 10.5194/BG-6-2245-2009

Lo, W. T., Hwang, J. J., Hsu, P. K., Hsieh, H. Y., Tu, Y. Y., Fang, T. H., et al. (2004). Seasonal and spatial distribution of phytoplankton in the waters off nuclear power plants, north of Taiwan. *J. Mar. Sci. Technol.* 12 (5), 372–379. doi: 10.51400/2709-6998.2258

Marcus, N. (2004). An overview of the impacts of eutrophication and chemical pollutants on copepods of the coastal zone. *Zool. Stud.* 43, 211–217. Available at: https://www.sinica.edu.tw/zool/zoolstud/43.2/211.

Martínez, M. L., Intralawan, A., Vázquez, G., Pérez-Maqueo, O., Sutton, P., and Landgrave, R. (2007). The coasts of our world: ecological, economic and social importance. *Ecol. Econ.* 63, 254–272. doi: 10.1016/j.ecolecon.2006.10.022

Matsubara, T., Nagasoe, S., Yamasaki, Y., Shikata, T., Shimasaki, Y., Oshima, Y., et al. (2008). Inhibitory effects of centric diatoms on the growth of the dinoflagellate akashiwo sanGuinea. *Nippon Suisan Gakkai Shi* 74, 598–606. doi: 10.2331/suisan.74.598

Meng, Z., Wei, Y. J., Wang, X. B., and Han, X. Q. (2022). Niche and interspecies association of major epifauna in Sanmen Bay of Zhangjiang Province. *Oceanologia Et Limnologia Sin.* 53 (5), 1269–1278. doi: 10.31497/zrzyxb.20220414

Meyer-Reil, L. A., and Köster, M. (2000). Eutrophication of marine waters: effects on benthic microbial communities. *Mar. Pollut. Bull.* 41, 255–263. doi: 10.1016/S0025-326X(00)00114-4

Miyamoto, Y., Nakano, T., Yamada, K., Hatakeyama, K., and Hamaguchi, M. (2019). Combined effects of drift macroalgal bloom and warming on occurrence and intensity of diel-cycling hypoxia in a eutrophic coastal lagoon. *Estuar. Coasts* 42, 494–503. doi: 10.1007/s12237-018-0484-6

Ning, X. R. (2005). "Environmental quality assessment of the Sanmen Bay and its annual changes," in *Research and evaluation on aquaculture ecology and aquaculture capacity in Leqing Bay and Sanmen Bay*. Ed. X. R. Ning (Beijing: Ocean Press), 120–160.

Novak, T., Godrijan, J., Pfannkuchen, D. M., Djakovac, T., Medic, N., Ivancic, I., et al. (2019). Global warming and oligotrophication lead to increased lipid production in marine phytoplankton. *Sci. Total Environ.* 668, 171–183. doi: 10.1016/j.scitotenv.2019.02.372

Philippart, C. J. M., Cadee, G. C., van Raaphorst, W., and Riegman, R. (2000). Long-term phytoplankton-nutrient interactions in a shallow coastal sea: algal community structure, nutrient budgets, and denitrification potential. *Limnology Oceanography* 45 (1), 131–144. doi: 10.4319/lo.2000.45.1.0131

Poornima, E. H., Rajadurai, M., Rao, V. N. R., Narasimhan, S. V., and Venugopalan, V. P. (2006). Use of coastal waters as condenser coolant in electric power plants: impact on phytoplankton and primary productivity. *J. Therm. Biol.* 31 (7), 556–564. doi: 10.1016/j.jtherbio.2006.05.009

Qiu, K. C., Zhang, R. L., Chao, M., Cheng, F. P., Zeng, J. N., Peng, X., et al. (2022). Spatiotemporal variations in cluster structure of fish eggs, larvae, and juveniles in the Sanmen Bay, Zheejiang, East China Sea. *Oceanologia Et Limnologia Sin.* 53, 684–696. doi: 10.11693/hyhz20211100285

Redfield, A. C. (1958). The biological control of chemical factors in the environment. *Am. Scientist* 46, 205–221. doi: 10.2307/27827150

Rice, E., Dam, H. G., and Stewart, G. (2015). Impact of climate change on estuarine zooplankton: surface water warming in long island sound is associated with changes in copepod size and community structure. *Estuar. Coasts* 38, 13–23. doi: 10.1007/s12237-014-9770-0

Shi, X. (2013). Distribution characters of nitrogen, phosphorus and other factors in surface water of Sanmen Bay in spring and autumn. *J. Appl. Oceanography* 32 (4), 461–467. doi: 10.3969/J.ISSN.2095-4972.2013.04.003

Shou, L., and Zeng, J. (2015). *Coastal ecological environment and environmental capacity of bays in Zhejiang Province* (Beijing: Ocean Press), 154–209.

Song, Y., Guo, Y., Liu, H., Zhang, G., Zhang, X., Thangaraj, S., et al. (2022). Water quality shifts the dominant phytoplankton group from diatoms to dinoflagellates in the coastal ecosystem of the Bohai Bay. *Mar. pollut. Bull.* 183, 114078. doi: 10.1016/j.marpolbul.2022.114078

Song, N. Q., Wang, N., Lu, Y., and Zhang, J. R. (2016). Temporal and spatial characteristics of harmful algal blooms in the Bohai Sea during 1952–2014. *Cont. Shelf Res.* 122, 77–84. doi: 10.1016/j.csr.2016.04.006

Strickland, J. D. H., and Parsons, T. R. (1968). Determination of dissolved oxygen. In A Practical Handbook of Seawater Analysis. *Fisheries Res. Board Canada Bull.* 167, 71–75. doi: 10.1002/iroh.19700550118

Sun, J., and Liu, D. (2002). The preliminary notion on nomenclature of common phytoplankton in China Sea waters. *Oceanologia Limnol. Sin.* 33, 271–286. doi: 10.1088/1009-1963/11/5/313

Tagliani, P. R. A., Landazuri, H., Reis, E. G., Tagliani, C. R., Asmus, M. L., and Sanchez-Arcilla, A. (2003). Integrated coastal zone management in the Patos Lagoon estuary: Perspectives in context of developing country. *Ocean Coast. Manage.* 46 (9), 807–822. doi: 10.1016/S0964-5691(03)00063-2

Tang, Y., Liu, Q., Cheng, C., Yang, M., Meng, Q., and Zhao, S. (2018). Characteristics of phytoplankton community structure in dongji sea area of zhoushan. *Southwest China J. Agric. Sci.* 31, 2715–2722. doi: 10.16213/j.cnki.scjas.2018.12.042

Tomas, C. R. (1997). *Identifying marine phytoplankton* (Academic Press, San Diego).

Tsirtsis, G., and Karydis, M. (1998). Evaluation of phytoplankton community indices for detecting eutrophic trends in the marine environment. *Environ. Monit. Assess.* 50 (3), 255–269. doi: 10.1023/A:1005883015373

Utermöhl, H. (1958). Zur vervollkommung der quantitativen phytoplankton-methodik. *Limnology* 9, 263–272. doi: 10.1080/05384680.1958.11904091

Wang, Q., Li, H., Zhang, Y., Wang, X., Zhang, C., Xiao, K., et al. (2019). Evaluations of submarine groundwater discharge and associated heavy metal fluxes in Bohai Bay, China. *Sci. Total Environ.* 695, 133873. doi: 10.1016/j.scitotenv.2019.133873

Wang, W., Lin, C., Jiang, R., Liu, Y., Sun, X., Lin., H., et al. (2022). Distribution, source identification and environmental risk assessment of potentially toxic elements (PTEs) in the surface sediment of Sanmen Bay, Zhejiang Province, China. *Mar. Pollut. Bull.* 174, 113237. doi: 10.1016/j.marpolbul.2021.113237

Wang, B., Xin, M., Wei, Q., and Xie, L. (2018). A historical overview of coastal eutrophication in the China seas. *Mar. Pollut. Bull.* 136, 394–400. doi: 10.1016/j.marpolbul.2018.09.044

Wei, Y., Ding, D., Gu, T., Jiang, T., Qu, K., Sun, J., et al. (2022). Different responses of phytoplankton and zooplankton communities to current changing coastal environments. *Environ. Res.* 215, 114426. doi: 10.1016/j.envres.2022.114426

Wells, M. L., Trainer, V. L., Smayda, T. J., Karlson, B. S. O., Trick, C. G., Kudela, R. M., et al. (2015). Harmful algal blooms and climate change: learning from the past and present to forecast the future. *Harmful Algae* 49, 68–93. doi: 10.1016/j.hal.2015.07.009

Winder, M., and Sommer, U. (2012). Phytoplankton response to a changing climate. *Hydrobiologia* 698 (1), 5–16. doi: 10.1007/s10750-012-1149-2

Wu, X., Liu, H., Ru, Z., Tu, G., and Ding, Y. (2021). Meta-analysis of the response of marine phytoplankton to nutrient addition and seawater warming. *Mar. Environ. Res.* 168, 105294. doi: 10.1016/j.marenvres.2021.105294

Wu, M., Wang, Y., Wang, Y., Yin, J., Dong, J., Jiang, Z., et al. (2017). Scenarios of nutrient alterations and responses of phytoplankton in a changing Daya Bay, South China Sea. *J. Mar. Syst.* 165, 1–12. doi: 10.1016/j.jmarsys.2016.09.004

Xia, R., Zhang, Y., Critto, A., Wu, J., Fan, J., Zheng, Z., et al. (2016). The potential impacts of climate change factors on freshwater eutrophication: implications for research and countermeasures of water management in China. *Sustainability* 8, 229. doi: 10.3390/su8030229

Xiao, W., Liu, X., Irwin, A. J., Laws, E. A., Wang, L., Chen, B., et al. (2018). Warming and eutrophication combine to restructure diatoms and dinoflagellates. *Water Res.* 128, 206–216. doi: 10.1016/j.watres.2017.10.051

Xie, C. Q., Ai, W. M., Peng, X., Chen, S. B., and Xie, Q. L. (2015). Diversity and seasonal variation of phytoplankton in the sea near Sanmen Nuclear Power Station. *Bull. Sci. Technol.* 31 (7), 222–228. doi: 10.13774/j.cnki.kjtb.2015.07.055

Xin, M., Wang, B., Xie, L., Sun, X., Wei, Q., Liang, S., et al. (2019). Long-term changes in nutrient regimes and their ecological effects in the Bohai Sea, China. *Mar. Pollut. Bull.* 146, 562–573. doi: 10.1016/j.marpolbul.2019.07.011

Yan, R. X., Han, Q. X., and Wang, X. B. (2020). Community composition and diversity of macrobenthos trawled in Hangzxhou Bay and Sanmen Bay. *Oceanologia Et Limnologia Sin.* 51, 484–493. doi: 10.11693/hyhz20191200272

Yang, H., Zhao, Y., Zhang, H. R., Dai, G. X., Ding, J., and Chen, J. (2013). Study on the impact of water environmental factors on dominant species of phytoplankton around the power plant in xiangshan bay. *Advanced Materials Res.* 610-613, 3371–3374. doi: 10.4028/www.scientific.net/AMR.610-613.3371

Ye, R., Liu, L., Wang, Q., Ye, X., Cao, W., He, Q., et al. (2017). Identification of coastal water quality by multivariate statistical techniques in two typical bays of northern Zhejiang Province, East China Sea. *Acta Oceanologica Sin.* 36 (2), 1–10. doi: 10.1007/s13131-017-0981-7

Yu, J., Tang, D. L., Oh, I. S., and Yao, L. J. (2007). Response of harmful algal blooms to environmental changes in Daya Bay, China. *Terr. Atmos. Ocean Sci.* 18 (5), 1011–1027. doi: 10.3319/TAO.2007.18.5.1011(Oc)

Zhang, J., Wang, Y., Ottmann, D., Cao, P., Yang, J., Yu, J., et al. (2023). Seasonal variability of phytoplankton community response to thermal discharge from nuclear power plant in temperate coastal area. *Environ. pollut.* 318, 120898. doi: 10.1016/j.envpol.2022.120898

Zhang, L., Xiong, L., Li, J., and Huang, X. (2021). Long-term changes of nutrients and biocenoses indicating the anthropogenic influences on ecosystem in Jiaozhou Bay and Daya Bay. *China. Mar. Pollut. Bull.* 168, 112406. doi: 10.1016/j.marpolbul.2021.112406

Zhang, Y. X., Yu, J., Jiang, Z. B., Wang, Q., and Wang, H. (2015). Variations of summer phytoplankton community related to environmental factors in a macro-tidal estuarine embayment, Hangzhou Bay, China. *J. Ocean Univ. China* 14 (6), 1025–1033. doi: 10.1007/s11802-015-2483-6

Zhao, S. J., Jiao, N. Z., Wu, C. W., Liang, B., and Zhang, S. Y. (2005). Evolution of nutrient structure and phytoplankton composition in the Jiaozhou Bay ecosystem. *Chin. J. Environ. Sci.* 17 (1), 95–102. doi: 10.3321/j.issn:1001-0742.2005.01.019

Zhou, M. J., Shen, Z. L., and Yu, R. C. (2008). Responses of a coastal phytoplankton community to increased nutrient input from the Changjiang (Yangtze) River. *Continental Shelf Res.* 28 (12), 1483–1489. doi: 10.1016/j.csr.2007.02.009

Zhu, G., Noman, M. A., Narale, D. D., Feng, W., Pujari, L., and Sun, J. (2020). Evaluation of ecosystem health and potential human health hazards in the Hangzhou Bay and Qiantang Estuary region through multiple assessment approaches. *Environ. Pollut.* 264, 114791. doi: 10.1016/j.envpol.2020.114791

Zhu, G. H., Qian, J., and Chen, L. H. (2012). Studies on the community structure of phytoplankton in the sea near Sanmen Bay. *Advanced Materials Res.* 518–523, 502–508. doi: 10.4028/www.scientific.net/AMR.518-523.502

frontiers | Frontiers in Marine Science

TYPE Original Research
PUBLISHED 08 January 2024
DOI 10.3389/fmars.2023.1280821

OPEN ACCESS

EDITED BY
Ganesh Thiruchitrambalam,
Pondicherry University, India

REVIEWED BY
Solomon Dan,
Beibu Gulf University, China
Peng Zhang,
Guangdong Ocean University, China
Padmakumar Kb,
Cochin University of Science and Technology, India

*CORRESPONDENCE
You-Shao Wang
yswang@scsio.ac.cn

RECEIVED 21 August 2023
ACCEPTED 14 December 2023
PUBLISHED 08 January 2024

CITATION
Zhou J and Wang Y-S (2024) A comprehensive approach to assessing eutrophication for the Guangdong coastal waters in China.
Front. Mar. Sci. 10:1280821.
doi: 10.3389/fmars.2023.1280821

A comprehensive approach to assessing eutrophication for the Guangdong coastal waters in China

Jing Zhou[1,2,3] and You-Shao Wang[1,2,4]*

[1]State Key Laboratory of Tropical Oceanography, South China Sea Institute of Oceanology, Chinese Academy of Sciences, Guangzhou, China, [2]Innovation Academy of South China Sea Ecology and Environmental Engineering, Chinese Academy of Sciences, Guangzhou, China, [3]University of Chinese Academy of Sciences, Beijing, China, [4]Daya Bay Marine Biology Research Station, Chinese Academy of Sciences, Shenzhen, China

Eutrophication is a global issue associated with increasing anthropogenic activities. Previous studies have mainly focused on nutrients and phytoplankton biomass in some typical estuaries and bays along the Guangdong coast, while integrated evaluations of eutrophication status based on ecological symptoms is still rare in this area. To better understand the health of the Guangdong coastal waters, two comprehensive methods including the Assessment of Estuarine Trophic Status (ASSETS) and the Northwest Pacific Action Plan Common Procedure (NOWPAP CP) were employed with slight modifications. The study area was divided into eight coastal zones (Z1~Z8) based on multiple criteria including salinity, catchment range, and administrative division. The results of the modified NOWPAP CP method demonstrated a generally increasing trend in the degree and effects of nutrient enrichment along the Guangdong coast in the past 30 years mainly due to the increasing nutrients and chlorophyll *a* (Chl-*a*). The results of the modified ASSETS method revealed that the water quality was between moderate and high for most coastal zones during 2015-2018, with the highest score (0.83) in the northern part of the Pearl River Estuary (PRE). However, the ecological symptoms showed inconsistent spatial patterns with the water quality, being high or moderate high in Z2 (including Zhanjiang Harbor and Leizhou Bay), Z4~Z5 (representing the northern and southern parts of the PRE, respectively), and Z6 (containing Mirs Bay and Daya Bay) for severe ecological symptoms, such as high levels of Chl-*a*, frequent harmful algal blooms (HABs). Moreover, eutrophication in Z4~Z6 may further deteriorate due to the increasing nutrient loads driven by growing economy and population. Synthetically, Z2, Z4~Z6 were graded between poor and bad for the overall eutrophication conditions (OEC), while Z1 (including the western and southern parts of the Leizhou Peninsula) and Z7 (consisting of Honghai Bay and Jieshi Bay) had a good OEC. The application of the modified ASSETS method effectively identified areas of severe eutrophication problems and the prospect of nutrient load along the Guangdong coast. The assessment results revealed the spatiotemporal variations and potential trends in the eutrophication status, providing scientific basis for the coastal management related to nutrient problems.

KEYWORDS

eutrophication, coastal ecosystem, nutrient, assessment method, South China Sea

1 Introduction

Coastal eutrophication has been considered one of the greatest threats to coastal ecosystem health in recent decades, as various anthropogenic activities have substantially increased nutrient inputs to coastal areas and caused undesirable effects, such as algal blooms, depleted dissolved oxygen (DO), coastal acidification, and loss of submerged aquatic vegetation and benthic fauna, thereby exacerbating coastal ecosystem degradation (Diaz and Rosenberg, 2001; Breitburg et al., 2018; Wang et al., 2018; Malone and Newton, 2020). The evaluation of eutrophication status is an important tool for effective management concerned with nutrient enrichment issues. Early studies mainly paid attention to nutrient concentrations and compositions in water bodies. Methods based on the nutrients have been widely used in Chinese coastal waters, including the eutrophication index (EI) method (Zou et al., 1983; Niu et al., 2020), the nutrient quality index (NQI) method (Peng and Wang, 1991), the potential eutrophication assessment (PEA) method (Guo et al., 1998) and the fuzzy evaluation method (Xiong and Chen, 1993; He and Yuan, 2007). However, it has recently been agreed upon that nutrient concentrations may not accurately reflect the eutrophication conditions of water bodies. Because coastal ecosystems are also influenced by other factors, such as light limitation due to turbidity, hydrodynamic conditions, runoff input, and precipitation (Cloern, 2001; Bricker et al., 2003; Sinha et al., 2017; Xu et al., 2019). As a result, the magnitude of ecological impact on nutrient enrichment varies widely across different coastal ecosystems. A comprehensive approach based on multiple indicators is therefore essential to understand the extent and ecological effects of nutrient enrichment.

Several integrated assessment methodologies based on ecological symptoms have been developed and successfully applied worldwide in recent years, including the ASSETS (Bricker et al., 2003), the OSPAR comprehensive procedure (OSPAR COMP) (OSPAR Commission, 2003), the HELCOM eutrophication assessment tool (HEAT) (Andersen et al., 2011), and NOWPAP CP (NOWPAP CEARAC, 2011). These methods are different in definitions and application, but all use key indicators for evaluating eutrophication status, such as phytoplankton biomass, DO, frequency of HABs and fish kills incident, and changes in aquatic community structure (Devlin et al., 2011). The ASSETS method has been proven to be a scientific and practical method for eutrophication assessment and has been applied in 141 US water bodies and many other countries (Bricker et al., 2003; Borja et al., 2008; Devlin et al., 2011). In China, it has been applied in the Yangtze River estuary, the Bohai Sea, Jiaozhou Bay, and Xiamen Bay with some methodology modifications according to the regional coastal environments (Wu et al., 2013; Wu et al., 2019; Luo et al., 2022). The NOWPAP CP method has advantages in providing more details of ecological symptoms and showing long-term changes of the indicators, which has been used in the Jiaozhou Bay assessment (Wu et al., 2019).

The Guangdong coastal area is one of the most developed regions in China, which has received a lot of nutrients due to massive economic growth, urban development, and population aggregation in recent decades (Liu et al., 2009; Qu and Kroeze, 2010; Strokal et al., 2014; Wang et al., 2018). Eutrophication problems have been reported in many estuaries and bays along the Guangdong coast (Huang et al., 2003; Han et al., 2012; Wang et al., 2018). Algal blooms have occurred about 10 times per year along the Guangdong coast (DOF (Department of Ocean and Fisheries of Guangdong Province), 2015-2017). The increasing eutrophication and associated seasonal hypoxia problems in the PRE and adjacent areas have attracted widespread attention from academics and the public (Huang et al., 2003; Qi et al., 2004; Wang et al., 2007; Yin and Harrison, 2007; Wang et al., 2008; Wang et al., 2011; Han et al., 2012; Li et al., 2014). Nevertheless, previous studies have mainly focused on the characterization of nutrient and phytoplankton biomass, with a lack of comprehensive evaluations based on different ecological effects of nutrient enrichment. Knowledge about the overall eutrophication condition of the study area, containing the major pressure, state and future perspective, remains indeterminate.

To fill this gap, this study employed two comprehensive methods, including the ASSETS and NOWPAP CP methods, to assess the eutrophication status of the Guangdong coastal waters. The indicators and their thresholds used in the assessment were modified to accommodate the relative sensitivity of local systems to nutrient-related degradation. Trends of nutrient load, which was based on the major drivers in watersheds, were considered in the ASSETS assessment to provide a view on the future outlook of nutrient pressures and potential impacts. The present study aimed to: (1) explore an appropriate technique to comprehensively illustrate the impacts of nutrient enrichment on the Guangdong coastal waters; (2) investigate the variations in eutrophication status and causative factors between different coastal zones; (3) anticipate the future outlook of eutrophication and provide implications for targeted management.

2 Materials and methods

2.1 Study area

The Guangdong coast is located in the north of the South China Sea (Figure 1). The Pearl River, the largest river discharging into the northern part of the South China Sea, transports a large amount of freshwater (~3.1×10^{11} m^3/a) and sediment (~6.4×10^7 t/a). Nearly 80% of the river discharge occurs during the wet season from April to September. Previous studies have shown that the diluted waters of the Pearl River play an important role in carrying nutrients to the Guangdong coast (Huang et al., 2003; Lu et al., 2009). The complicated hydrodynamic conditions also contribute to nutrient transportation, which are controlled by coastal currents, seasonally reversed winds, and upwelling (Niino and Emery, 1961; Bao et al., 2005; Gu et al., 2012; Shu et al., 2018; Lao et al., 2019). According to the differences in geography, environment, and socioeconomic conditions, the Guangdong coast is usually divided into three

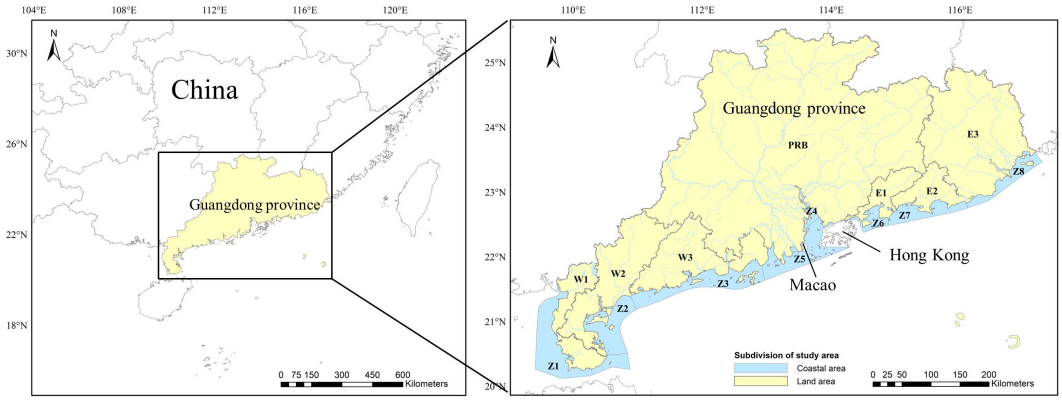

FIGURE 1
Geographical location and subdivisions of the study area along the Guangdong coast.

regions: the PRE, the western and eastern parts of Guangdong Province. In this study, it was divided into eight coastal zones (Z1~Z8) to better understand the spatial variations in water quality and their potential influencing factors (Figure 1). A coastal zone, which was mainly identified by the catchment range and administrative borders of relevant counties, usually consisted of several adjacent estuaries and bays. Moreover, the PRE was divided into two subdivisions (Z4~Z5) based on salinity and depth to distinguish the characteristics between the upper and lower reaches of the estuary. Accordingly, the land area of Guangdong Province was divided into seven subregions (W1~W3, PRB, and E1~E3). There are significant differences in salinity, runoff, population and economy between different zones (Table 1). The Pearl River Basin has a large land area and dense population, which encompass major population centers including Guangzhou City, Shenzhen City, Dongguan City, Foshan City and Zhuhai City. Besides, these areas are industrial, economic and cultural centers of Guangdong Province. The watersheds in the western and eastern coastal zones were characterized by intensified agricultural activities.

2.2 Data description

Water quality and ecological data was collected from the estuarine and marine environment monitoring network to assess the eutrophication status of the Guangdong coastal waters between 2015 and 2018 (Figure 2). The monitoring data was obtained from the routine monitoring program of water quality in Guangdong Province, which was conducted by the Department of Ocean and Fisheries of Guangdong Province (DOF) and the Department of Ecology and Environment of Guangdong Province (DEE). Water samples of dissolved inorganic nitrogen (DIN), dissolved inorganic phosphorus (DIP), chemical oxygen demand (COD), Chl-*a*, and dissolved oxygen (DO) were obtained from more than 300 sampling sites along the Guangdong coast. The majority of sampling stations had a depth less than 20 m, and sampling stations in estuaries and bays were more intensive than those in the open sea. The survey was usually taken during spring (March to May), summer (July to August), and autumn (September to November), with a survey frequency of three to four times annually. The collection, storage,

TABLE 1 Characteristics of the subdivisions of the Guangdong coast.

Coastal zone		Coastal area/ km^2	Salinity/ PSU	Annual average runoff/ $\times10^8$ m^3	Land area/km^2	Population/ $\times10^4$ persons	GDP/ $\times10^8$ yuan	Major estuaries and bays
Western coast	Z1	6645	29.1	48.99	W1/6701	270.4	749.4	Anpu Harbor, Liusha Bay
	Z2	4025	25.1	119.7	W2/15759	881.3	4333	Zhanjiang Harbor, Leizhou Bay
	Z3	4973	24.9	106.5	W3/13474	498.3	2208	Shuidong Harbor, Hailing Bay
PRE	Z4	548	4.29	3132	PRB/108178	8 330	79148	Northern part of the PRE
	Z5	4328	18.0					Southern part of the PRE
Eastern coast	Z6	1120	31.5	0.18	E1/4191	173.3	2092	Mirs Bay, Daya Bay
	Z7	2460	31.0	56.51	E2/4865	271.8	983.2	Honghai Bay, Jieshi Bay
	Z8	2277	28.8	383.5	E3/26476	1773	6390	Shantou Harbor, Zhelin Bay

The salinity for each zone was averaged during 2015-2018. Population and GDP for each zone were averaged during 2015-2020.

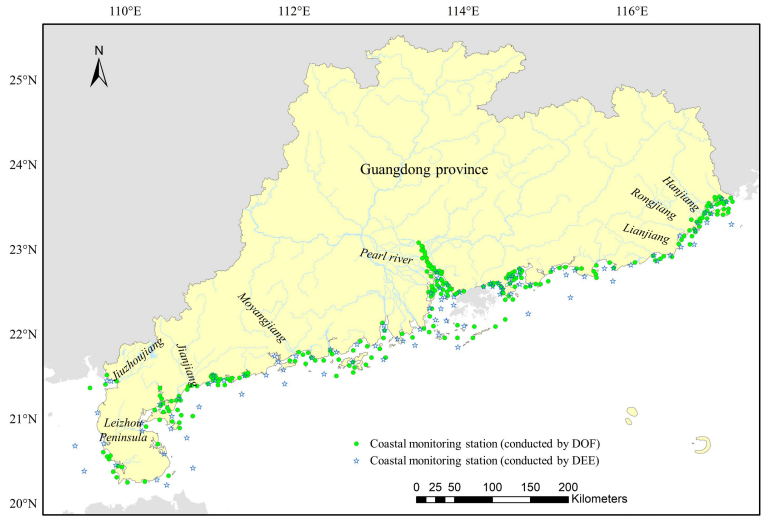

FIGURE 2
Map of the Guangdong coast and the sampling stations in this study.

and analysis of water samples had complied with China's national standard specifications for marine monitoring (SAQSIQ (State Administration of Quality Supervision, Inspection and Quarantine, China), and SSA (State Standardization Administration, China), 2007a; SAQSIQ (State Administration of Quality Supervision, Inspection and Quarantine, China), and SSA (State Standardization Administration, China), 2007b; SAQSIQ (State Administration of Quality Supervision, Inspection and Quarantine, China), and SSA (State Standardization Administration, China), 2007c). Finally, between 2015 and 2018, over 4700 data points for nutrients, COD, and DO, and more than 3600 data points for Chl-*a* were collected. The spatial and temporal variations of the monitoring data are shown in Figures S1 , S2. The annual average and standard deviation of the main parameters are shown in Table S1.

Data of HABs was obtained from the Bulletin of Marine Environmental Quality of Guangdong Province (http://gdee.gd.gov.cn/hjzkgb/index.html), Bulletin of Guangdong Marine Disaster (http://nr.gd.gov.cn/zwgknew/sjfb/tjsj/), and China Ocean Yearbook (http://cnki.nbsti.net/csydmirror). The socioeconomic statistics data was collected from the Guangdong Statistical Yearbook (http://stats.gd.gov.cn/gdtjnj). The annual runoff and precipitation data was collected from the Guangdong Water Resources Bulletin (http://slt.gd.gov.cn/szygb). The main sources of the data used in this study are shown in Table S2.

2.3 Methods

2.3.1 Modified ASSETS method

The ASSETS method is derived from the National Estuarine Eutrophication Assessment (NEEA) conducted by the U.S. National Oceanic and Atmospheric Administration (NOAA) for evaluating both current eutrophic conditions and the effectiveness of management actions aimed at reducing eutrophic conditions (Bricker et al., 2003; Scavia and Bricker, 2006; Bricker et al., 2008). It has been developed and applied in coastal waters of the US, Europe, Australia, and China. This study adapted the pressure-state-response framework derived from the original ASSETS application (Bricker et al., 2003), and learned from the recent modifications described in the eutrophication assessment of the southwest Bohai Sea (Wu et al., 2013). The overall eutrophication condition (OEC) was determined by three component parts: water quality (WQ, pressure), ecological symptoms (ES, state), and future outlook of nutrient load (FO, response). The indicators and thresholds were modified to accommodate the relative sensitivity of local areas to nutrient-related degradation.

2.3.1.1 Indicators and thresholds of WQ and ES

The WQ indicators included DIN, DIP, and COD, with thresholds designed according to China's national seawater quality standard (SAEP (State Administration of Environmental Protection, China), 1997) and previous studies (Zou et al., 1983; Guo et al., 1998). High Chl-*a* concentration and phytoplankton abundance were considered the primary ecological symptoms, while low DO and occurrence of HABs were considered the secondary symptoms. Their thresholds were determined based on previous studies and relevant technological standards (Zou et al., 1983; SAEP (State Administration of Environmental Protection, China), 1997; CEC (Council of European Communities), 2000; Bricker et al., 2003; OSPAR Commission, 2003; Wu et al., 2013). Details of the classification and thresholds are shown in Table 2.

2.3.1.2 Evaluation of FO

Changes in the main drivers of coastal eutrophication were used to access FO. Previous studies revealed that riverine discharge and atmospheric deposition contributed significantly to coastal eutrophication (Howarth, 2008; Liu et al., 2009; Jickells et al.,

TABLE 2 Classifications and thresholds of indicators for the two methods.

Indicator	Modified ASSETS method					Modified NOWPAP CP method		Reference
	1	2	3	4	5	1	2	
	Low	Moderately low	Moderate	Moderately high	High	Low	High	
DIN/mg·L^{-1}	≤0.2	>0.2, ≤0.3	>0.3, ≤0.4	>0.4, ≤0.5	>0.5	≤0.3	>0.3	(SAEP (State Administration of Environmental Protection, China), 1997)
DIP/mg·L^{-1}	≤0.015	>0.015, ≤0.03	>0.003, ≤0.045	>0.045		≤0.03	>0.03	
COD/mg·L^{-1}	≤2	>2, ≤3	>3, ≤4	>4, ≤5		≤3	>3	
DIN/DIP	NC					≤16	>16	(Redfield, 1963)
Chl-*a*/μg·L^{-1}	≤5	>5, ≤10	>10, ≤20	>20		Maximum ≤ 20; Average ≤ 10	Maximum>20; Average>10	(Bricker et al., 2003)
Phytoplankton abundance/ cells·L^{-1}	≤10^3	>10^3, ≤10^4	>10^4, ≤10^6	>10^6		NC		(Zou et al., 1983; CEC (Council of European Communities), 2000; Bricker et al., 2003)
DO/mg·L^{-1}	>6	>5, ≤6	>4, ≤5	>2, ≤4	≤2	Mean>5; Bottom>2	Mean ≤ 5; Bottom ≤ 2	(SAEP (State Administration of Environmental Protection, China) 1997; Bricker et al., 2003; OSPAR Commission, 2003)
Diatom/ dinoflagellate and other species bloom	Determined by the affected area, number of incident and duration in a logical matrix					≤1 (per 3 years)	>1(per 3 years)	(NOWPAP CEARAC, 2011; NSA (National Standardization Administration, China), 2014)
Noctiluca species bloom						≤3 (per 3 years)	>3(per 3 years)	
fish kill/ shellfish poisoning incident	NC					≤1 (per 3 years)	>1(per 3 years)	
Future outlook of nutrient load	Improve high	Improve low	No change	Worsen low	Worsen high	Decrease	Increase	(Bricker et al., 2003; NOWPAP CEARAC, 2011)

NC indicates that the indicator was not considered as part of the assessment.

2017). According to the Bulletin of the Second National Census on the Sources of Pollution of Guangdong (http://gdee.gd.gov.cn/wrygzdt/content/post_3100417.html), population and agriculture accounted for approximately 97.8% of total nitrogen (TN) discharge from water pollutants (Figure S3), while mobile (including automobile and non-road mobile sources) pollution and industrial pollution were the major sources of nitrogen oxides from air pollutants. Agricultural non-point source pollution of TN was mainly attributed to chemical fertilizers and livestock farming, while livestock farming and aquaculture were the main sources of TP pollution (Ge et al., 2022). To capture trends of the major drivers that might significantly impact nutrient inputs, five indicators were selected for evaluation, including population (PO), value-added of industry (IN), consumption of chemical fertilizer (CF), output of meat (OM), and aquatic products (AP). The Spearman correlation coefficient was used to analyze the trends of the main drivers during 2015-2020. The final assessment was based on the synthetic analysis of the historical presentation and prospects of the five indicators according to statistics and relevant development planning.

2.3.1.3 Evaluation procedure and calculation method

To provide a consistent spatial framework for information collection, a physical subdivision of the water body was made using salinity (Bricker et al., 2003). In this study, the Guangdong coast was divided into eight zones based on the multiple criteria, including salinity, depth, catchment range, administrative division, and sampling sites. No further subdivisions were made as most sampling sites in the PRE were in the mixing zone (salinity between 0.5-25 PSU) and the majority of other coastal zones were in the seawater zone (salinity above 25 PSU). The concentration for assessment was calculated through a percentile-based approach (10^{th} percentile for DO and 90^{th} percentile for the other indicators) to avoid extremely high or low values. The indicator scores were determined by combining concentration, spatial

coverage, frequency of occurrence, affected area, and duration (for HABs) through a logical decision process. In order to fully reflect the severity of HABs, algal blooms had been sorted into nuisance blooms and toxic blooms due to their relative ecological effects (Shen, 2001; Bricker et al., 2003; NSA (National Standardization Administration, China), 2014). Problem conditions for toxic blooms resulted from the production of toxin by the organism, causing mortality or shellfish-vectored poisoning of humans. Problem conditions for nuisance blooms referred to other adverse impacts including physiological damage to marine organisms, and die-offs of farmed fish and cultivated shellfish which could lead to financial losses in aquaculture. Moreover, each category of algal blooms was divided into several classifications according to the scope of affected area (NSA (National Standardization Administration, China), 2014). The WQ ratings and primary ecological symptoms ratings were averaged, while the worst secondary symptoms rating was selected in a precautionary approach. The WQ expression was classified into five levels. The ES rating was determined by combining the primary and secondary symptoms in a matrix, giving more weight to the secondary symptoms. Detailed calculation procedures were shown in the application of the Bohai Sea (Wu et al., 2013). The modifications in the Chl-*a* and DO evaluation processes are shown in Tables S3, S4. The OEC rating was determined by combining WQ, ES, and FO through 125 possible combinations (Table 3) that fell into one of five grades: 1 (excellent), 2 (good), 3 (moderate), 4 (poor), and 5 (bad).

2.3.2 Modified NOWPAP CP method

The NOWPAP CP method was developed to assess the eutrophication status in the NOWPAP region (NOWPAP CEARAC, 2011). It was separated into two steps, the same as OSPAR CP: the screening procedure was used to preliminarily assess eutrophication by detecting symptoms of eutrophication within minimum parameters (nutrients inputs, red tide event frequencies, and Chl-*a*), and the comprehensive procedure was used to assess the status and possible causes of eutrophication. The comprehensive procedure required the collection of information and data in line with the following four categories of parameters considering the degree and effects of nutrient enrichment: (I) degree, including DIN and DIP concentrations and their molar mass proportion; (II) direct effects, including Chl-*a* concentration and HABs, except for Noctiluca species blooms; (III) indirect effects, including DO and COD concentrations and fish kill events; and (IV) other possible effects, including Noctiluca species blooms and shellfish poisoning incidents. The indicators were assessed by classification (high or low) and trends (increasing, decreasing, or no change). The eutrophication status was classified into one of six categories: High-Increase (HI); High-No Trend (HN); High-Decrease (HD); Low-Increase (LI); Low-No Trend (LN); and Low-Decrease (LD). The eutrophication level of DO was determined in reverse to other parameters. For example, it was rated as "LD" when the DO values were above the reference value and showed an increasing trend and "HI" when they were below the reference value and had a decreasing trend.

In this study, most indicators and reference values conformed to those used in the Jiaozhou Bay assessment (Wu et al., 2019). In addition, slight modifications were made to accommodate local environmental characteristics and facilitate comparison with the ASSETS method as follows: (1) the riverine nutrient load based on the major drivers in the watershed was used instead of the riverine DIN concentration; (2) the surface DO concentration was replaced by the mean DO concentration; and (3) the threshold of the mean Chl-*a* concentration was increased from 5 μg/L to 10 μg/L. Details are shown in Table 2. The three-year moving average method was

TABLE 3 Aggregation of pressure (WQ), state (ES) and response (FO) components into an overall eutrophication condition category.

Grade	1 Excellent	2 Good	3 Moderate	4 Poor	5 Bad
Pressure (WQ)	Low	Moderately low	Moderate	Moderately high	High
State (ES)	Low	Moderately low	Moderate	Moderately high	High
Response (FO)	Improve high	Improve low	No change	Worsen low	Worsen high
Metric	Combination matrix				Class
P S R	1 1 1 2 2 2 1 1 1 1 1 1 1 2 3 1 2 3				1 Excellent
P S R	1 1 1 1 1 1 1 2 2 2 2 2 3 3 3 3 3 4 4 4 1 1 2 2 2 2 2 1 1 2 2 2 1 1 1 2 2 2 1 1 1 4 5 1 2 3 4 5 4 5 1 2 3 1 2 3 1 2 3 1 2 3				2 Good
P S R	1 1 1 1 1 1 1 1 1 1 2 2 2 2 2 2 2 3 3 3 3 3 3 3 4 4 4 4 4 4 4 4 4 4 5 5 5 5 5 5 5 5 5 5 3 3 3 3 3 4 4 4 4 4 2 2 2 3 3 3 3 3 1 1 2 2 3 3 3 3 1 1 1 2 2 2 2 2 3 3 3 4 1 1 1 1 1 2 2 2 3 3 1 2 3 4 5 1 2 3 4 5 4 5 1 2 3 4 5 4 5 4 5 1 2 3 4 5 4 5 1 2 3 4 5 1 2 3 4 5 1 2 3 1 1 2 3 4 5 1 2 3 1 2				3 Moderate
P S R	1 1 1 1 1 2 2 2 2 2 2 2 2 2 2 3 3 3 3 3 3 3 4 4 4 4 4 4 4 5 5 5 5 5 5 5 5 5 5 5 5 5 4 4 4 4 4 5 5 5 5 5 3 3 4 4 4 4 4 3 3 4 4 4 4 4 2 2 3 3 3 4 4 1 2 3 4 5 1 2 3 4 5 1 2 3 4 5 4 5 1 2 3 4 5 4 5 2 3 4 5 4 5 3 4 5 1 2				4 Poor
P S R	3 3 3 3 3 4 4 4 4 4 5 5 5 5 5 5 5 5 5 5 5 5 5 5 5 5 5 5 4 4 4 5 5 5 5 5 5 1 2 3 4 5 1 2 3 4 5 3 4 5 1 2 3 4 5				5 Bad

used to calculate algal bloom incidences. In addition, changes in typical estuaries and bays were used to represent the trends of coastal zones due to insufficient long-term monitoring data for all sampling sites. The long-term trends of HABs were identified using the nonparametric Mann–Kendall test (Salmi et al., 2002) with long-term observation from 2001 to 2020. Changes in the other indicators were analyzed by comparison with reference conditions in the 1990s obtained from related reports and previous studies (Editorial Board of China Bay Survey, 1998a; Editorial Board of China Bay Survey, 1998b; Editorial Board of China Bay Survey, 1999; Du et al., 2003; He and Yuan, 2007; Huang et al., 2010; EPD (Environmental Protection Department of the Hong Kong Special Administrative Region), 2020; Hu et al., 2021; Zhang et al., 2022). A deviation greater than 50% from the reference value was considered an upward or downward trend. The assessment rating for each category was determined by selecting the most representative status of indicators.

3 Results

3.1 Results of the modified ASSETS method

3.1.1 Expression of water quality and ecological symptoms

The relative proportions of WQ (Figure 3) classification as good, moderate, poor, and bad were as follows: 4%, 35%, 59%, and 2%, respectively. High or moderately high levels of WQ were widespread along the Guangdong coast due to high concentrations of DIN and DIP, showing the highest score (0.83) in Z4. A moderately low level (graded good) of WQ appeared in Z6 with the lowest score of 0.25. The annual variation in WQ showed an improvement in the study area from 2015 to 2018 (Figures 4, 5) because the relative proportions of water bodies as excellent and good increased from 4% to 39%.

The ES ratings for the Guangdong coast are shown in Figure 3, of which 53% had a moderately low ES, 9% were moderate, 32% were moderately high, and 6% had a high ES. The scores of the eight zones for the primary symptoms were between moderate and high, revealing high levels of Chl-*a* biomass. High levels of secondary symptoms were mostly confined to Z4 and Z6 due to the distinct low-oxygen conditions in the bottom waters. Z2 and Z5 had a moderate rating for secondary symptoms mainly because of the periodic occurrence of nuisance algal blooms. As a result, the final ES ratings were graded bad for Z4 and Z6, followed by Z2 and Z5, which had a poor grade. The annual variation in ES (Figures 4, 5) showed opposite trends in the study area during 2015-2018, as the relative proportions of excellent and good increased from 43% to 59%, while that of bad increased from 6% to 23%. Notable enhancements in ES were seen in the western part of Guangdong Province, such as Z1 and Z3, whereas degradation was seen in the eastern part.

The application of the percentile-based approach for ES assessment was illustrated for Chl-*a* and DO (Figure 6) using data from the PRE between 2015 and 2018. The 90th percentile Chl-*a* in the northern part of the PRE (Z4) was more than twice as high as that in the southern part of the PRE (Z5), both exceeding the threshold

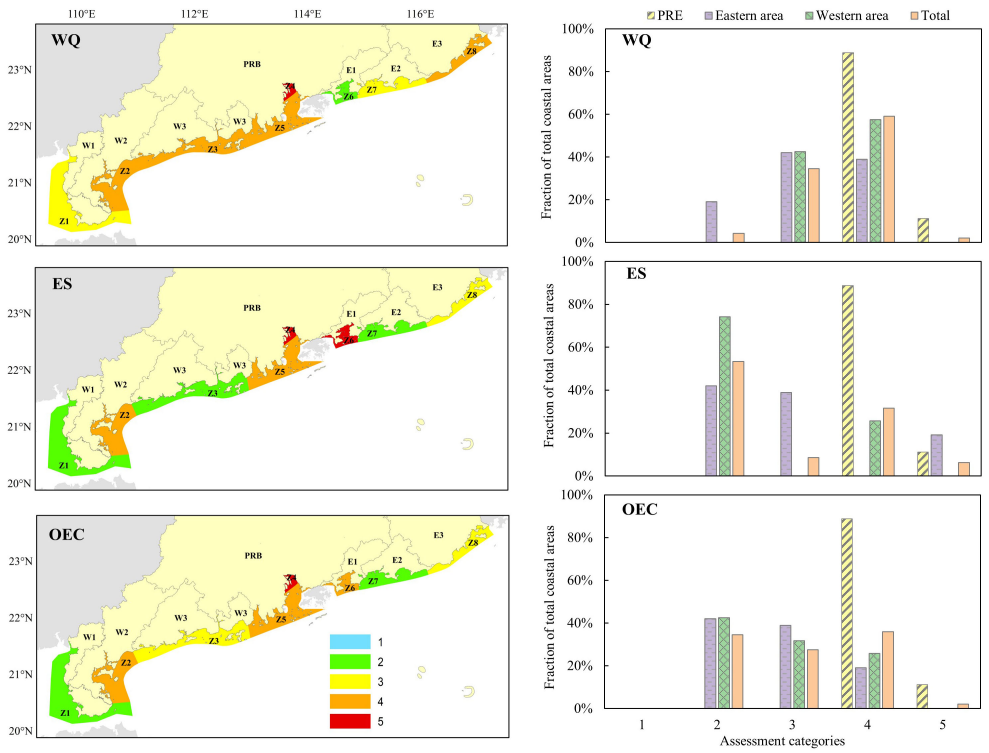

FIGURE 3
The WQ, ES, and OEC gradings for coastal zones on the Guangdong seaboard in the comprehensive assessment (2015-2018) by the modified ASSETS method. Grades 1 to 5 represent excellent, good, moderate, poor, and bad, respectively.

(10 μg/L). The 10th percentile DO was lower than 3 mg/L with a coverage rate of 100% for Z4, while it was periodically close to 4 mg/L with a coverage rate of 55% for Z5, indicating more severe hypoxic conditions for Z4. HABs occurred twice a year in the PRE, with an affected area of less than 100 km^2 and durations between 4 and 13 days. These symptoms resulted in a poor ecological condition in the PRE, rating moderately high in the south and high in the north.

3.1.2 Trends of nutrient load

Spearman correlation coefficient analysis revealed that PO and IN increased significantly (p<0.01) in the study area, while CF showed a decreasing trend (p<0.01). Moreover, OM and AP showed no obvious change. Significant spatial variations in these indicators (Figure S4) existed among different coastal areas due to the regional imbalance of development. The final FO grade based on the trend analysis of the five major drivers for each zone is shown in Table S5. The results demonstrated that nutrient loads for Z4~Z6 might continue to increase due to the growing economy and population. The nutrient loads for Z8 might decrease due to the distinct declines in PO, CF and OM. The other coastal zones might have no obvious changes in nutrient discharge.

3.1.3 Synthesis of the overall eutrophication condition

The OEC ratings for the eight coastal zones were between good and bad (Figure 3), showing higher ratings in Z2, Z4, Z5 and Z6 (graded bad for Z4 and poor for the other zones). Lower ratings of OEC were shown in Z1 and Z7 (both graded good). The relative proportions of OEC classification as good, moderate, poor, and bad were as follows: 35%, 27%, 36%, and 2%, respectively. The results indicated the most severe eutrophication problems were in the PRE, showing high OEC in the north and moderately high OEC in the south. The eastern and western parts of Guangdong Province presented a similar proportion of OEC, placing most zones in the good and moderate categories.

3.2 Results of the modified NOWPAP method

3.2.1 Status ratings for each category

The degree of nutrient enrichment (Category I) between 2015 and 2018 was at a high level, as determined by high concentrations of DIN for most coastal zones except Z1, Z6, and Z7 (Table 4). Coastal zones with high ratings for Category I also presented a high level of direct effects (Category II), mainly because their annual maximum Chl-*a* concentrations exceeded the threshold. In addition, the direct effects were graded high for Z6 and Z7 due to the high level of dinoflagellate and other species blooms. The DO and COD concentrations were at low levels for the study area, while a high rating of Noctiluca species blooms was confined only in Z6. Fish kills and shellfish poisoning incidents have rarely been

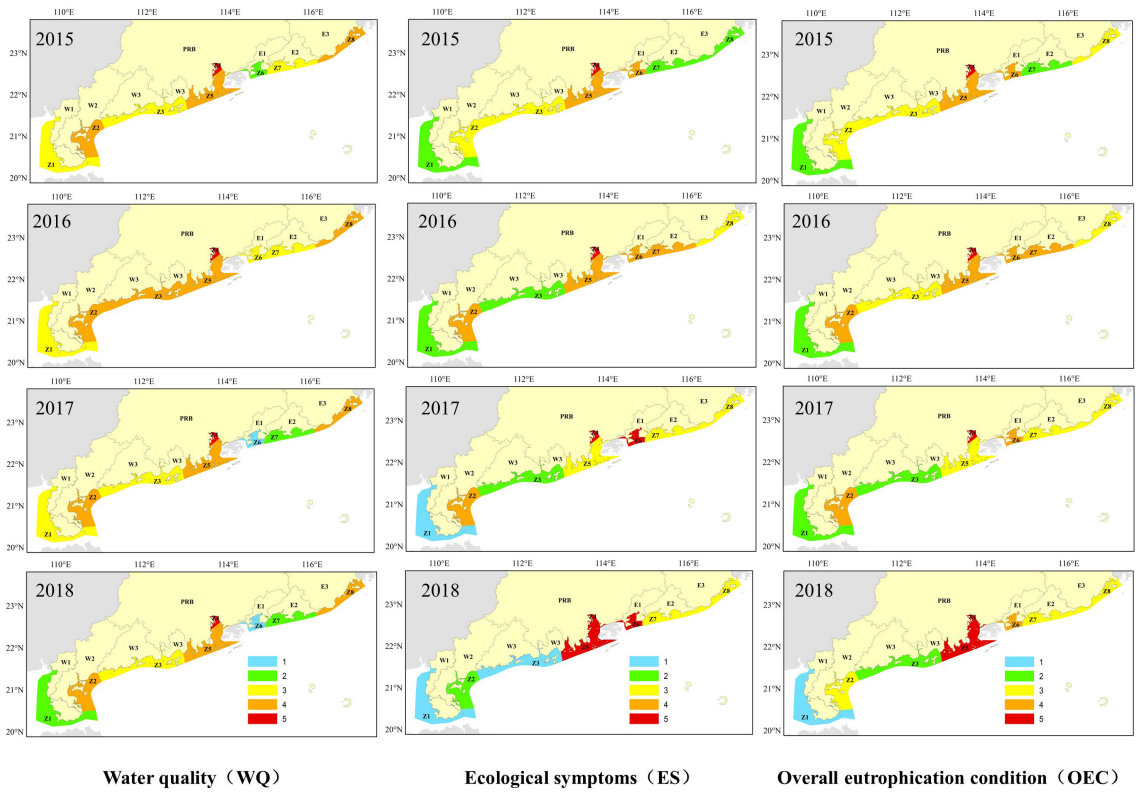

FIGURE 4
The WQ, ES and OEC gradings for coastal zones on the Guangdong seaboard in the annual assessment by the modified ASSETS method. Grades 1 to 5 represent excellent, good, moderate, poor, and bad, respectively.

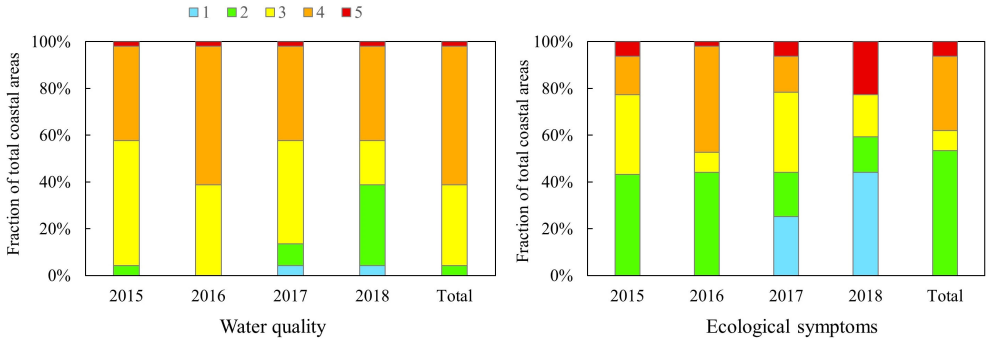

FIGURE 5
Comparison of the annual variation in the relative proportion of the WQ and ES classifications. Grades 1 to 5 represent excellent, good, moderate, poor, and bad, respectively.

reported in the study area in recent years, thereby gaining a low rating in the assessment. As a result, the indirect effects (Category III) and other possible effects (Category IV) were graded low for all zones except Z6, which had a high Category IV rating. In summary, most coastal zones were considered eutrophication problem areas with a high rating for at least one category except Z1, which was the only zone graded low for all four categories.

3.2.2 Long-term trends analysis

Increasing DIN and DIP were observed in many estuaries and bays along the Guangdong coast since the 1990s Figures 7A, C and D. As a result, most zones were classified as increase in Category I except Z8, which had no apparent change in DIN concentration. Category II also demonstrated an increasing trend in the PRE and eastern areas (including Z6, Z7 and Z8) mainly due to the enhancement of Chl-*a* in these areas over the past 30 years. Low-oxygen problems in the PRE and Mirs Bay have become increasingly severe as identified through long-term observations, resulting in an increasing trend in Category III for Z4, Z5 and Z6. Nevertheless, changes in Chl-*a* and DO on the west coast of Guangdong Province remained unclear due to insufficient data. Only a few studies provided the evidence of increasing COD in some typical bays, contributing to a rise in Category III for the western zones (including Z1, Z2 and Z3).

The incidence and affected area of algal blooms had decreased significantly ($p<0.05$) during 2001-2020 based on the Mann–

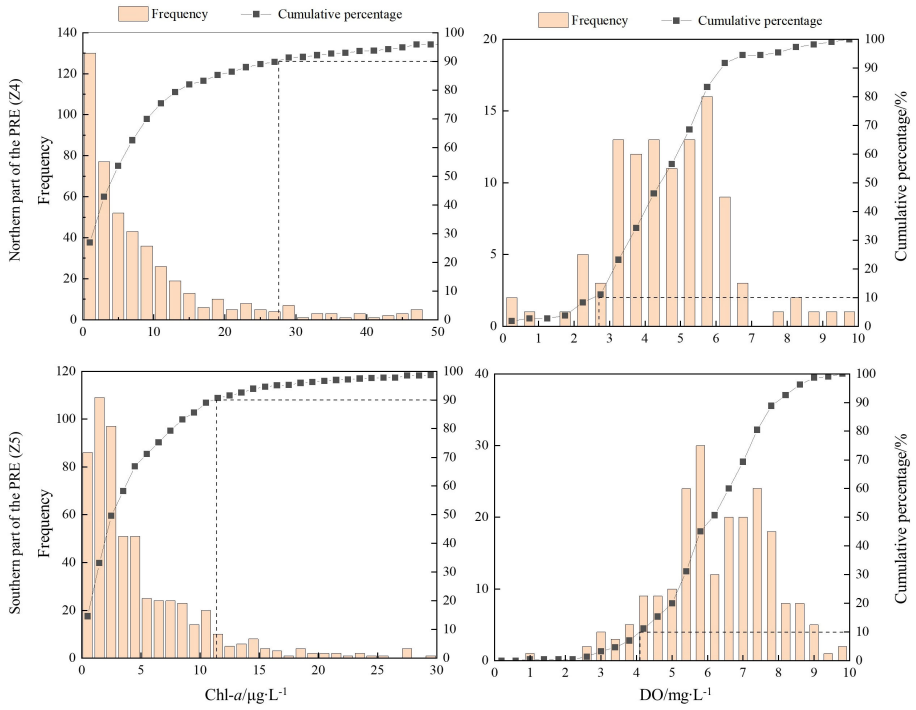

FIGURE 6
Example diagrams showing the 90th percentile for Chl-*a* and the 10th percentile for DO in the subdivisions of the PRE.

TABLE 4 Eutrophication status for coastal zones by different methods.

Coastal zone		Grade of modified ASSEST method				Grade of modified NOWPAP CP method			
		WQ	ES	FO	OEC	I	II	III	IV
Western part of Guangdong Province	Z1	3/M	2/ML	3/N	2/Good	LI	LN	LI	LN
	Z2	4/MH	4/MH	3/N	4/Poor	HI	HN	LI	LN
	Z3	4/MH	2/ML	3/N	3/Moderate	HI	HN	LI	LN
PRE	Z4	5/H	5/H	4/WL	5/Bad	HI	HI	LI	LN
	Z5	4/MH	4/MH	4/WL	4/Poor	HI	HI	LI	LI
Eastern part of Guangdong Province	Z6	2/ML	5/H	4/WL	4/Poor	LI	HI	LI	HN
	Z7	3/M	2/ML	3/N	2/Good	LI	HI	LN	LN
	Z8	4/MH	3/M	2/IL	3/Moderate	HN	HI	LN	LN

WQ, Water quality; ES, Ecological symptoms; FO, Future outlook of nutrient loads; OEC, Overall eutrophication condition; H, High; M, Moderate; MH, Moderately high; ML, Moderately low; N, No change; IL, Improve low; WL, Worsen low; HI, High and increase; HD, High and decrease; HN, High and no change; LI, Low and increase; LD, Low and decrease; LN, Low and no change.

Kendall test (Table S6). The decline was mainly due to reductions in the occurrence of diatom and chromophyta species blooms. Significant increases were observed in Z7 (diatom species) and Z5 (Noctiluca species), while noticeable decreases were identified in Z5 (diatom species), Z6 (dinoflagellate and other species) and Z8 (dinoflagellate and other species). In addition, noticeable increases were observed in the affected area and duration of HABs for Z3, despite the incidence of HABs had no statistically significant change. Besides, incidences of fish kills and shellfish poisoning were uncommon during the last 20 years. Therefore, there was no obvious change in Category IV for most zones in the long-term analysis, with the exception of Z5.

The results for the four categories are shown in Table 4.

4 Discussion

4.1 Comparison of the overall eutrophication status between the two methods

Despite differences in methodologies, both the ASSETS and the NOWPAP CP methods showed a consistently low rating for Z1, indicating good status was achieved in this area. In addition, both approaches identified the poor situation for Z2, Z4, Z5 and Z6, indicating the emergence of strong management intervention in these areas. However, the assessment results for the other coastal zones were quite different between the two methods. Z7 was assessed as good by the ASSETS method, while it was identified as a problem area with a high level of dinoflagellate and other species bloom incidence using the NOWPAP CP method. Moreover, Z3 and Z8 were graded as moderate by the ASSETS method, whereas they were both high in categories I and II using the NOWPAP CP method. The findings of Z3, Z7 and Z8 revealed that despite high levels of nutrients and Chl-*a* were detected, there was no evidence of significant secondary ecological symptoms (indirect effects) in these areas. Nevertheless, suggestions were made to reduce land-based nutrient inputs and develop environmental monitoring plans in order to improve the eutrophication status of these areas. The comparisons of the two assessment results are shown in Table 4.

Detailed information from the application of the two methods is shown for Z5 (Table 5) to illustrate the differences in the assessment outputs. Both approaches indicated high levels of nutrient concentrations in this zone, however, significant differences mainly came from the evaluation of ecological effects. The 90th percentile Chl-*a* concentration with a spatial coverage greater than 50% and a periodic occurrence by the ASSETS method resulted in a high score (0.75) for the assessment of primary ecological symptoms. In comparison, the maximum and average concentrations of Chl-*a* were classified as high and low, respectively, by the NOWPAP CP method. Similar results were reported by previous studies (Huang et al., 2004; Qiu et al., 2010; Lu and Gan, 2015) in which Chl-*a* maxima occurred distinctly in particular places and changed seasonally instead of a persistent phytoplankton bloom occurring over the entire estuary. The 10th percentile DO concentration was lower than 5 mg/L periodically, with a coverage rate of 55% using the ASSETS method, indicating the presence of low-oxygen conditions. In contrast, the NOWPAP CP result showed a low DO level using the average value; however, this approach might underestimate the severity of hypoxia in this area (Yin et al., 2004; Zhang and Li, 2010; Qian et al., 2018; Hu et al., 2021). The periodic occurrence of small-scale nuisance algal blooms resulted in a moderate rating for HABs by the ASSETS method. The ratings of diatom species blooms, Noctiluca species blooms, and other species blooms for the NOWPAP CP method were classified as LD, LI, and HN, respectively, revealing the high risk of chromophyta species blooms and an early warning of increasing Noctiluca species blooms. In summary, the combination of high nutrients, high Chl-*a* biomass, periodic occurrence of HABs, and the presence of hypoxia contributed to a moderately high (poor) rating of OEC in Z5 based on the ASSETS approach. In contrast, the degree and direct effects of nutrient enrichment were classified as high, while the indirect and other effects were recognized as low, and all categories showed an increasing trend using the NOWPAP CP method.

TABLE 5 Final outcomes for the southern part of the PRE (Z5) from application of two methods to data during 2015-2018.

Element	Indicator	ASSETS				NOWPAP CP			
		Val.	Spa.	Freq.	Score/ Rating	Val.	Status	Trend	Rating
Physicochemistry	Nutrient loads	N/A			Worsen low	N/A		I	I
	DIN	2.17 mg/L	95%	PS	1/High	1.13 mg/L	High	I	HI
	DIP	0.106 mg/L	59%	PS	1/High	0.065 mg/L	High	N	HN
	DIN/DIP	NC				102	High	I	HI
	COD	2.38 mg/L	50%	PS	0.25/ Moderately low	1.54 mg/L	Low	I	LI
Phytoplankton	Chl-*a*	11.41 μg/L	59%	PD	0.75/High	Maximum: 57.0 mg/L; Average: 5.32 mg/L	Maximum: High; Average: Low	I	HI
	Phytoplankton cell abundance	NA				NC			
	HABs	2 times per year	<500km^2	PD	0.5/ Moderate	NC			
	Diatom species blooms	NC				0.8 times per 3 years	Low	D	LD
	Noctiluca species blooms	NC				2.3 times per 3 years	Low	I	LI
	Other species blooms	NC				3.8 times per 3 years	High	N	HN
Other	Zoobenthos kills/ Fish kills	NC				None reported	Low	N	LN
	DO	4.16 mg/L	55%	PD	0.5/ Moderate	Mean: 6.83 mg·L^{-1}; Bottom: 4.69 mg·L^{-1}	Low	I	LI
Rating of causative factors		WQ: 4 Moderately high				Category I: HI			
Rating of ecological symptoms/effects		PES: High; SES: Moderate; ES: 4 Moderately high				Category II: HI; Category III: LI; Category IV: LI			
Final assessment of Eutrophication condition		OEC: 4 Poor				No final integration			

Val., Value; Spa., Spatial coverage; Freq., Frequency; PES, Primary ecological symptoms; SES, Secondary ecological symptoms; PS, Persistent; PD, Periodic; I, Increasing; D, Decreasing; N, No change; HI, High and increase; HN, High and no change; LI, Low and increase; LD, Low and decrease; LN, Low and no change; NC, Not considered as part of the assessment; NA, Not applicable.

By comparing the results between the two approaches, the modified ASSETS method is recommended as a scientific and practical approach to more accurately and comprehensively reveal the status and regional distribution of eutrophication in the Guangdong coastal waters. In addition, the long-term trend analysis by the NOWPAP CP method helps to better understand the changes in coastal zones and their main drivers.

4.2 Spatial variations and possible causes of eutrophication

4.2.1 Water quality and the main drivers

This study revealed high levels of water quality for most coastal areas (Figure 3), such as the PRE, Zhanjiang Harbor, Leizhou Bay, Shantou Harbor, which agreed with previous studies (Yin and Harrison, 2008; Lu et al., 2009; Zhang et al., 2016; Lao et al., 2019). The poor water quality of the PRE was due to the large amount of riverine nutrient inputs and sewage discharge from dense population and intensive industry (Huang et al., 2003; Yin and Harrison, 2008; Lu et al., 2009). Intensive agricultural in watersheds (Figure S4) was the major pressure on water quality for Z2 and Z3 (both classified as moderately high). In addition, the western coastal currents, which were greatly affected by the Pearl River plume, might also bring in abundant nutrients (Shu et al., 2018; Lao et al., 2019). Shantou Harbor and adjacent areas (Z8) was another hotspot with high nutrient loads, receiving lots of nutrients from large rivers including the Hanjiang, Rongjiang and Lianjiang. These rivers were all characterized by dense population and intensive agricultural activities in their catchments.

The annual comparison of water quality between 2015 and 2018 (Figure 4) revealed an improvement in Z1 and Z7. The declines in population (Table S5) and precipitation (Figure 7A), which had reduced nutrient inputs from sewage and agriculture non-point source pollution (Carpenter et al., 1998; Lao et al., 2019), might be the main causes. Particularly in Z7, despite not statistically significant, CF, OM and AP in this area had decreased during 2015-2018, contributing to the reduction of agricultural pollutants. In comparison, there were no apparent changes in areas with high or moderately high WQ ratings, indicating heavy nutrient stress from anthropogenic inputs in these areas, although in some areas (such as the PRE) a noticeable decreasing trend in CF was observed.

4.2.2 Ecological symptoms and potential influencing factors

The results of the ASSETS assessment revealed significant temporal and spatial variations in the ecological response to nutrient enrichment for different zones (Figure 3, Table 4). For Z2, Z4 and Z5, the ES ratings were as high as the WQ ratings, indicating that excess nutrients were the key causative factors of eutrophication. Z1, Z3, Z7, and Z8 showed lower ES ratings compared to their WQ ratings, revealing their lower sensitivity to nutrient enrichment. A sharp contrast between the low rating of WQ and the high rating of ES was observed in Z6, indicating that the hydrological conditions and biochemical processes might play a more important role in determining the health of coastal ecosystems (Cloern, 2001; Ferreira et al., 2005). In the case of Z6, the combination of a high Chl-*a* concentration, low bottom DO concentration, and periodic occurrence of HABs led to a high ES rating. Previous studies have demonstrated that the high primary production and frequent algal blooms in this area were probably due to the suitable temperature conditions, highly efficient nutrient circulation, and nutrient supplementation from upwelling (Sun et al., 2011; Wu et al., 2016; Wu et al., 2017). In addition, seasonal hypoxia observed in Mirs Bay and its adjacent waters was driven by coupled physical and biochemical processes (Li et al., 2014; Zhang et al., 2018). Therefore, it is needed for further tests to gain insight into the magnitude of ecological sensitivity to nutrient enrichment for different coastal systems.

The results revealed that more severe ecological symptoms occurred in the northern part of the PRE than in the southern part. The high rating in the north was determined by the high Chl-*a* and severe hypoxic conditions (Figure 6), which were rarely noticed in previous studies (Zhang and Li, 2010; Lu and Gan, 2015). The research areas in previous studies were often confined to the middle and lower parts of the estuary with a salinity higher than 10 PSU; however, those areas were recognized as the southern part of the PRE in this study. Lu and Gan (2015) found that the high Chl-*a* in the upper reach was likely induced by the inactive phytoplankton from the river discharge rather than by cells generated locally, and this result was supported by the low DO concentration at the same location. In addition, the persistent low-oxygen waters in the north observed in this study confirmed that the hypoxic conditions in the upper part were mainly due to the large amounts of pollutants and low-oxygen waters from upstream reaches (Qian et al., 2018; Hu et al., 2021). Unlike the upper reach (northern part), the high biomass and the seasonal low-oxygen condition in the southern part resulted from the combination of physical and biochemical effects associated with variable riverine discharge and stratification during summer (Zhang and Li, 2010; Lu and Gan, 2015; Hu et al., 2021).

The annual analysis of the ecological response to nutrient enrichment revealed a remarkable shift in the southern part of the PRE, showing a moderate ES rating in 2017 and dropping to a low rating in 2018. The 10th percentile DO concentration decreased

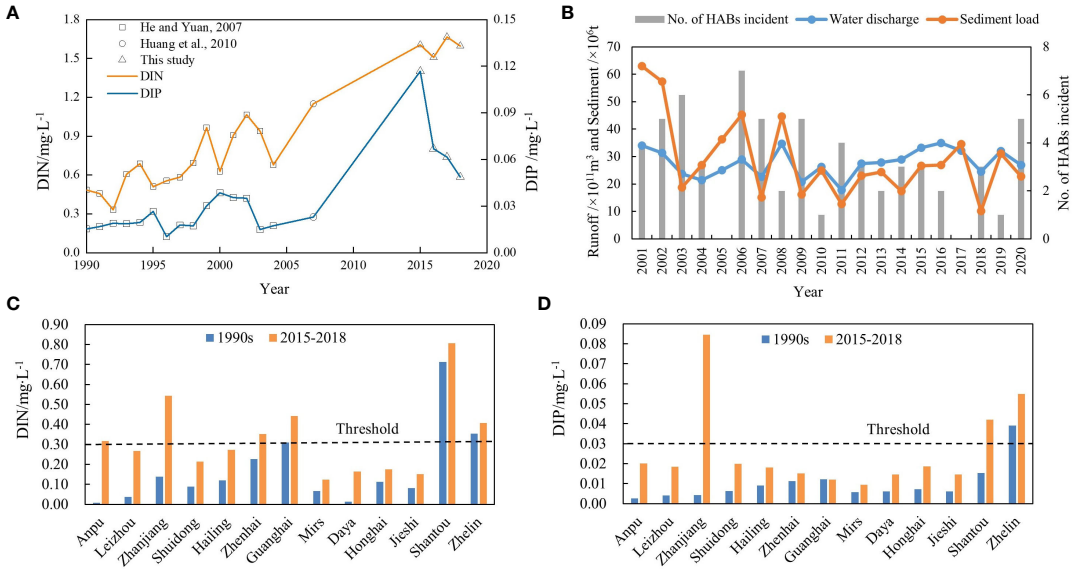

FIGURE 7
Long-term trends of the indicators. **(A)** Variations in nutrient concentrations in the PRE. **(B)** Comparison of the temporal variations in water and sediment discharge and the frequency of HABs in the PRE. **(C, D)** Comparisons of the nutrient concentrations of the major bays along the Guangdong coast between different periods.

from 4.9 mg/L to 3.1 mg/L, and the number of algal bloom events increased from zero to three during 2017-2018. Various factors may have contributed to this abrupt change due to the complex physical and biochemical interactions in the PRE (Yin et al., 2000; Huang et al., 2003; Zhang and Li, 2010). Researchers have noticed that changes in the riverine sediment loads might be essential in controlling biological processes by regulating the turbidity distribution, which significantly influenced phytoplankton growth in estuaries (Cloern, 1987; Tian et al., 2009; Horemans et al., 2020). The reduction in sediment supply and subsequent decline in turbidity for large estuaries, such as the Yangtze River estuary and the PRE, could strengthen oxygen depletion and increase the risk of HABs, as the light-shading effect of suspended sediments on primary production was greatly weakened (Wang et al., 2016; Hu et al., 2021). In this study, a remarkable decline in sediment loads of the PRE (measured at the Gaoyao, Shijiao, and Boluo stations) was observed between 2017 and 2018 (Figure 8B), decreasing from 34.52 Mt/a to 10.11 Mt/a. This might be the critical factor leading to the dramatic deterioration of ecological conditions in the southern part of the PRE. It is required for future work to investigate the roles and contributions of the changes with long-term observations.

4.3 Advantages and limitations of the assessment methods

Compared with previous applications of the ASSETS method, there were still great differences in the selection and estimation of key indicators for the pressure and response components. The pressure was characterized by influencing factors including nitrogen load and the estuary's susceptibility to nitrogen (dilution and flushing rates) in the US ASSETS applications (Bricker et al., 2008). Because the system's susceptibility (largely determined by the residence time of water within a system), as well as land-based nutrient sources, had played an important role in the development of eutrophication. Previous studies have shown higher ratings of Chl-*a* and HABs problems in systems with slower flushing or longer residence time (Ferreira et al., 2005). Unlike the US, the pressure was estimated by water quality indicators (such as DIN, DIP, and COD) in the Chinese applications. The selection of water quality indicators, which conformed to the widely used EI method (Zou et al., 1983), had the advantage of reflecting the degree of nutrient enrichment in the coastal waters and helped to establish a link to the coastal management in China. However, it failed to identify the natural influencing factors that might have remarkable contributions in the development of eutrophication. Despite certain hydrographic characteristics and nutrient inputs were available from previous studies for some typical estuaries and bays along the Guangdong coast, information was very limited for some other coastal areas, especially in less developed areas. Therefore, there was still a lack of data to support the evaluation of susceptibility in the eight coastal zones.

The estimation of the response (future outlook of nutrient load) was one of the significant differences between these applications using the ASSETS method. In the US ASSETS applications, the response of eutrophication was based on demographic projections which were complemented by expert knowledge. In comparison, the response was ignored or replaced by simplified calculations in previous Chinese applications. For example, some researchers (Wang et al., 2012; Luo et al., 2022) selected the annual rate of change in future nutrient emissions as the response indicator, which could lead to a misunderstanding of the future outlook. Because in many systems, nutrient inputs were also influenced by the environmental changes

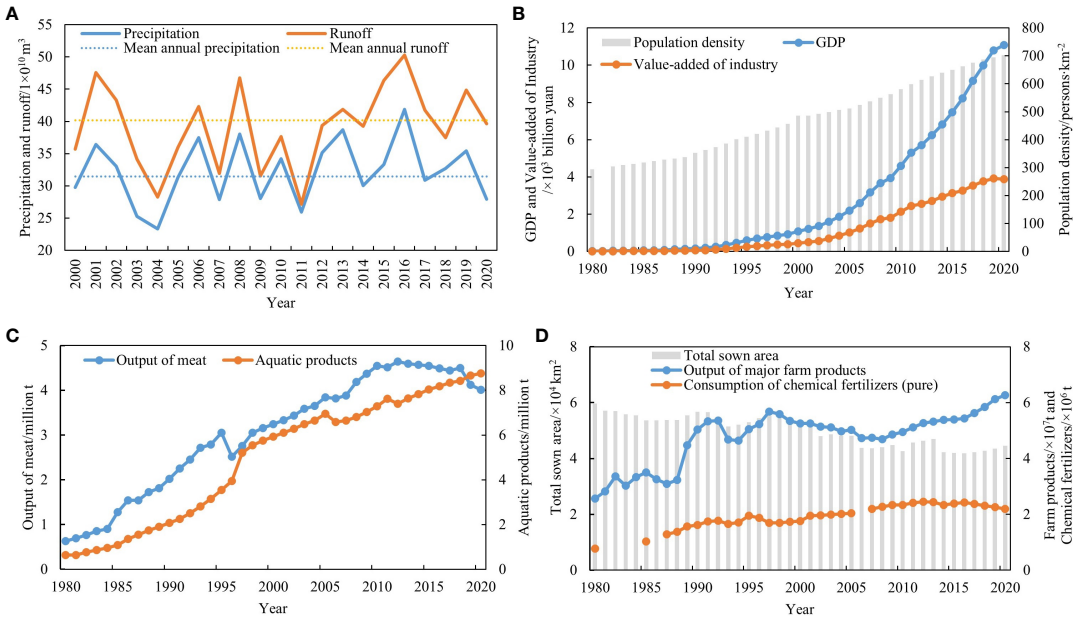

FIGURE 8
Long-term variations in the major drivers of Guangdong Province. **(A)** Precipitation and runoff. **(B)** Population density, GDP, and value-added of industry. **(C)** Aquatic products and output of meat. **(D)** Consumption of chemical fertilizers.

such as runoff and precipitation. In the applications of the Bohai sea (Wu et al., 2013) and Jiaozhou Bay (Wu et al., 2019), the response variable was ignored, resulting in an incomplete assessment of eutrophication condition. To fill in this gap, this study employed a semi-quantitative approach to analyze the future outlook of nutrient load. It was determined by a synthetic analysis of the historical presentation and prospects of the main drivers in watersheds, including population, industry and agriculture. The integrated evaluation of the response in the present study provided a more scientific and reliable result than that based on expert experience or used an unsuitable variable. Nevertheless, quantitative methods are still required to obtain robust assessment results.

In addition, compared to the indicators used in the US and EU countries, information on aquatic communities and changes in food webs caused by nutrient enrichment were not considered in this study due to insufficient data. Because large-scale marine ecological surveys had been carried out at low frequency (perhaps every few years) and the data cannot usually be obtained from open access. The comparison of the key indicators of eutrophication assessment used in this study and the other applications is shown in Table S7. Further improvements should make efforts in using more hydrographic and biological indicators to identify the susceptibility of coastal ecosystems, and combining multisource data to investigate the cumulative effects of eutrophication.

4.4 Future outlook of eutrophication

The long-term statistics revealed significant increases in the growth of economy and population in Guangdong Province since 1980 (Figure 7B). The annual gross domestic product (GDP) in 2020 was approximately 440 times higher than that in 1980, and the population increased 1.4 times. IN, AP, OM, and CF also increased dramatically during this period (Figures 7B–D). There is an overall anticipation about the socioeconomic development of the study area in the future based on the 14th Five-Year Plans of Guangdong Province (http://www.gd.gov.cn/zwgk/jhgh/content/post_3268882.html): Increasing trends in economy and population are likely to continue even though the pace of growth may slow, and the gap in regional development may widen. Moreover, it is also needed for stable agricultural production outputs and improved agricultural pollution management. However, some researchers were less optimistic and anticipated increased riverine nutrient inputs due to more intensive agricultural practices and industrial activities in the coming decades (Rabalais et al., 2009; Statham, 2012; Strokal et al., 2014; Laurent et al., 2018).

Although anthropogenic nutrient inputs are responsible for coastal eutrophication, climate change also plays an important role by modifying temperature, wind patterns, precipitation, the hydrological cycle, and sea level rise (Statham, 2012; Strokal et al., 2014). Increasing temperatures have been anticipated to lead to major changes in the functioning and structure of ecosystems by changing biodiversity and interactions between trophic levels (Brierley and Kingsford, 2009). The changes in precipitation are especially likely to experience significant increases in nutrient flux, thereby exacerbating eutrophication in China (Sinha et al., 2017). The rising surface ocean temperatures, freshwater and nutrient inputs, and atmospheric CO_2 will further exacerbate eutrophication-driven acidification and low-oxygen conditions in the PRE (Luo et al., 2014; Zhao et al., 2020; Liang et al., 2021).

Based on the trend analysis of the major drivers, it is suggested that the nutrient loads will increase due to growing economy and population in Z4~Z6. Z2 is another hot spot requiring attention because of the high nutrient loads and poor eutrophic conditions. The combination of climate change and continuing high nutrient loads through human activity is anticipated to lead to enhanced eutrophication in the future in these areas.

5 Conclusion

This study applied the ASSETS and NOWPAP CP methods to assess the Guangdong coastal waters using the same temporal-scale data (2015-2018). The results revealed the changes of water quality for most coastal zones, indicating that there was an overloading nutrient pressure mainly from the terrestrial input. The results of the ASSETS assessment revealed the temporal and spatial variations in the ecological response to nutrient enrichment for different zones. More severe eutrophication conditions were detected in Z2, Z4~Z6 mainly due to the HABs and low-oxygen problems. The eutrophication conditions in Z4~Z6 may further deteriorate due to the increasing nutrient loads driven by the growing economy and population. Targeted management interventions are required to reduce the effects of nutrient enrichment, considering the changes in nutrient loads and the major drivers in watersheds. The modified ASSETS method was suggested to more accurately and comprehensively reveal the eutrophication conditions in the Guangdong coastal waters, while the NOWPAP CP method helped to know about the long-term changes in ecological effects of nutrient enrichment. Further work for evaluation efforts should aim to investigate the susceptibility of coastal ecosystems and the cumulative effects of eutrophication.

Data availability statement

The original contributions presented in the study are included in the article/Supplementary Material. Further inquiries can be directed to the corresponding author.

Author contributions

YW: Conceptualization, Supervision, Writing – review & editing. JZ: Data curation, Investigation, Writing – original draft.

Funding

The author(s) declare financial support was received for the research, authorship, and/or publication of this article. This research was supported by the International Partnership Program of Chinese Academy of Sciences (No.133244KYSB20180012), the National Natural Science Foundation of China (No. U1901211 and

No. 41876126), the Strategic Priority Research Program of the Chinese Academy of Sciences (No. XDA23050200 and XDA19060201), the National Key Research and Development Program of China (Science & Technology Basic Resources Investigation Program of China) (No. 2017FY100700), and the Innovation Team of Nansha District High-Level Talents: Innovation Team of Mangrove Wetland for Blue Carbon Enhancement Technology.

Conflict of interest

The authors declare that the research was conducted in the absence of any commercial or financial relationships that could be construed as a potential conflict of interest.

Publisher's note

Supplementary material

The Supplementary Material for this article can be found online at: https://www.frontiersin.org/articles/10.3389/fmars.2023.1280821/full#supplementary-material

References

Andersen, J. H., Axe, P., Backer, H., Carstensen, J., Claussen, U., Fleming-Lehtinen, V., et al. (2011). Getting the measure of eutrophication in the Baltic Sea: towards improved assessment principles and methods. *Biogeochemistry* 106 (2), 137–156. doi: 10.1007/s10533-010-9508-4

Bao, X. W., Hou, Y. J., Chen, C. S., Chen, F., and Shi, M. C. (2005). Analysis of characteristics and mechanism of current system on the west coast of Guangdong of China in summer. *Acta Oceanologica Sin.* 4), 1–9.

Borja, A., Bricker, S. B., Dauer, D. M., Demetriades, N. T., Ferreira, J. G., Forbes, A. T., et al. (2008). Overview of integrative tools and methods in assessing ecological integrity in estuarine and coastal systems worldwide. *Mar. pollut. Bull.* 56 (9), 1519–1537. doi: 10.1016/j.marpolbul.2008.07.005

Breitburg, D., Levin, L. A., Oschlies, A., Gregoire, M., Chavez, F. P., Conley, D. J., et al. (2018). Declining oxygen in the global ocean and coastal waters. *Science* 359 (6371), 46–4+. doi: 10.1126/science.aam7240

Bricker, S. B., Ferreira, J. G., and Simas, T. (2003). An integrated methodology for assessment of estuarine trophic status. *Ecol. Model.* 169 (1), 39–60. doi: 10.1016/S0304-3800(03)00199-6

Bricker, S. B., Longstaff, B., Dennison, W., Jones, A., Boicourt, K., Wicks, C., et al. (2008). Effects of nutrient enrichment in the nation's estuaries: A decade of change. *Harmful Algae* 8 (1), 21–32. doi: 10.1016/j.hal.2008.08.028

Brierley, A. S., and Kingsford, M. J. (2009). Impacts of climate change on marine organisms and ecosystems. *Curr. Biol.* 19 (14), R602–R614. doi: 10.1016/j.cub.2009.05.046

Carpenter, S. R., Caraco, N. F., Correll, D. L., Howarth, R. W., Sharpley, A. N., and Smith, V. H. (1998). Nonpoint pollution of surface waters with phosphorus and nitrogen. *Ecol. Appl.* 8 (3), 559–568. doi: 10.1890/1051-0761(1998)008[0559:Nposww]2.0.Co;2

CEC (Council of European Communities) (2000). Directive 2000/60/EC of the european parliament and of the council of 23 october 2000 establishing a framework for community action in the field of water policy. *Off. J. Eur. Communities* 327, 1–73.

Cloern, J. E. (1987). Turbidity as a control on phytoplankton biomass and productivity in estuaries. *Continental Shelf Res.* 7 (11-12), 1367–1381. doi: 10.1016/0278-4343(87)90042-2

Cloern, J. E. (2001). Our evolving conceptual model of the coastal eutrophication problem. *Mar. Ecol. Prog. Ser.* 210, 223–253. doi: 10.3354/meps210223

Devlin, M., Bricker, S., and Painting, S. (2011). Comparison of five methods for assessing impacts of nutrient enrichment using estuarine case studies. *Biogeochemistry* 106 (2), 177–205. doi: 10.1007/s10533-011-9588-9

Diaz, R. J., and Rosenberg, R. (2001). Overview of anthropogenically-induced hypoxic effects on marine benthic fauna. *Coast. Estuar. Sci.* 58, 129–145. doi: 10.1029/CE058p0129

DOF (Department of Ocean and Fisheries of Guangdong Province) (2015-2017) *Bulletin of Marine Environmental Quality of Guangdong Province*. Available at: http://gdee.gd.gov.cn/hjzkgb/index.html.

Du, H., Huang, C., Chen, S., He, X., and Zhu, L. (2003). Assessment and analysis of eutrophication in Zhelin Bay. *Ecologic Sci. (In Chinese)* 22, 13–17.

Editorial Board of China Bay Survey (1998a). *Survey of China Bays Volume 9: Eastern Bays of Guangdong Province (In Chinese)* (Beijing: Ocean Press).

Editorial Board of China Bay Survey (1998b). *Survey of China Bays Volume 14: Important Estuaries (In Chinese)* (Beijing: Ocean Press).

Editorial Board of China Bay Survey (1999). *Survey of China Bays Volume 10: Western Bays of Guangdong Province (In Chinese)* (Beijing: Ocean Press).

EPD (Environmental Protection Department of the Hong Kong Special Administrative Region) (2020) *Marine Water Quality in Hong Kong in 2020*. Available at: https://www.epd.gov.hk/epd/english/environmentinhk/water/hkwqrc/waterquality/marine-2.html.

Ferreira, J. G., Wolff, W. J., Simas, T. C., and Bricker, S. B. (2005). Does biodiversity of estuarine phytoplankton depend on hydrology? *Ecol. Model.* 187 (4), 513–523. doi: 10.1016/j.ecolmodel.2005.03.013

Ge, X. J., Huang, B., Yuan, Z. J., Wang, D. D., Wang, Q. Q., Chen, J. C., et al. (2022). Temporal and spatial variation characteristics and source analysis of agricultural non-point source pollution load in guangdong during the past 20 years. *Environ. Sci. (In Chinese)* 43 (6), 3118–3127. doi: 10.13227 /j.hjkx.202108071

Gu, Y., Pan, J., and Lin, H. (2012). Remote sensing observation and numerical modeling of an upwelling jet in Guangdong coastal water. *J. Geophysical Research-Oceans* 117, C08019. doi: 10.1029/2012JC007922

Guo, W., Zhang, X., Yang, Y., and Hu, M. (1998). Potential eutrophication assessment for Chinese coastal waters. *J. Oceanography Taiwan Strait (In Chinese)* 17 (1), 64–70.

Han, Q., Huang, X., Xing, Q., and Shi, P. (2012). A review of environment problems in the coastal sea of South China. *Aquat. Ecosystem Health Manage.* 15 (2), 108–117. doi: 10.1080/14634988.2012.687611

He, G., and Yuan, G. (2007). Assessment of the water quality by fuzzy mathematics for last 20 years in Zhujiang Estuary. *Mar. Environ. Sci. (In Chinese)* 26 (1), 53–57.

Horemans, D. M. L., Meire, P., and Cox, T. J. S. (2020). The impact of temporal variability in light-climate on time-averaged primary production and a phytoplankton bloom in a well-mixed estuary. *Ecol. Model.* 436, 109287. doi: 10.1016/j.ecolmodel.2020.109287

Howarth, R. W. (2008). Coastal nitrogen pollution: A review of sources and trends globally and regionally. *Harmful Algae* 8 (1), 14–20. doi: 10.1016/j.hal.2008.08.015

Hu, J. T., Zhang, Z. R., Wang, B., and Huang, J. (2021). Long-term spatiotemporal variations in and expansion of low-oxygen conditions in the Pearl River estuary: a study synthesizing observations during 1976-2017. *Biogeosciences* 18 (18), 5247–5264. doi: 10.5194/bg-18-5247-2021

Huang, X. P., Huang, L. M., and Yue, W. Z. (2003). The characteristics of nutrients and eutrophication in the Pearl River estuary, South China. *Mar. pollut. Bull.* 47, 30–36. doi: 10.1016/s0025-326x(02)00474-5

Huang, L. M., Jian, W. J., Song, X. Y., Huang, X. P., Liu, S., Qian, P. Y., et al. (2004). Species diversity and distribution for phytoplankton of the Pearl River estuary during rainy and dry seasons. *Mar. pollut. Bull.* 49, 588–596. doi: 10.1016/j.marpolbul.2004.03.015

Huang, X. P., Tian, L., Peng, B., and Zhang, D. W. (2010). Environmental pollution in the Pearl River Estuary: a review. *J. Trop. Oceanography (In Chinese)* 29 (1), 1–7.

Jickells, T. D., Buitenhuis, E., Altieri, K., Baker, A. R., Capone, D., Duce, R. A., et al. (2017). A reevaluation of the magnitude and impacts of anthropogenic atmospheric nitrogen inputs on the ocean. *Global Biogeochemical Cycles* 31 (2), 289–305. doi: 10.1002/2016gb005586

Lao, Q., Chen, F., Liu, G., Chen, C., Jin, G., Zhu, Q., et al. (2019). Isotopic evidence for the shift of nitrate sources and active biological transformation on the western coast of Guangdong Province, South China. *Mar. pollut. Bull.* 142, 603–612. doi: 10.1016/j.marpolbul.2019.04.026

Laurent, A., Fennel, K., Ko, D. S., and Lehrter, J. (2018). Climate change projected to exacerbate impacts of coastal eutrophication in the northern gulf of Mexico. *J. Geophysical Research: Oceans* 123 (5), 3408–3426. doi: 10.1002/2017jc013583

Li, X. L., Shi, H. M., Xia, H. Y., Zhou, Y. P., and Qiu, (2014). Seasonal hypoxia and its potential forming mechanisms in the Mirs Bay, the northern South China Sea. *Continental Shelf Res.* 80, 1–7. doi: 10.1016/j.csr.2014.03.003

Liang, B., Xiu, P., Hu, J., and Li, S. (2021). Seasonal and spatial controls on the eutrophication-induced acidification in the Pearl River Estuary. *J. Geophysical Research: Oceans* 126 (5), 1–18. doi: 10.1029/2020jc017107

Liu, S. M., Hong, G. H., Zhang, J., Ye, X. W., and Jiang, X. L. (2009). Nutrient budgets for large Chinese estuaries. *Biogeosciences* 6 (10), 2245–2263. doi: 10.5194/bg-6-2245-2009

Lu, Z. M., and Gan, J. P. (2015). Controls of seasonal variability of phytoplankton blooms in the Pearl River Estuary. *Deep-Sea Res. II* 117, 86–96. doi: 10.1016/j.dsr2.2013.12.011

Lu, F. H., Ni, H. G., Liu, F., and Zeng, E. Y. (2009). Occurrence of nutrients in riverine runoff of the Pearl River Delta, South China. *J. Hydrology* 376, 107–115. doi: 10.1016/j.jhydrol.2009.07.018

Luo, Y., Liu, J. W., Wu, J. W., Yuan, Z., Zhang, J. W., Gao, C., et al. (2022). Comprehensive assessment of eutrophication in Xiamen Bay and its implications for management strategy in Southeast China. *Int. J. Environ. Res. Public Health* 19, 13055. doi: 10.3390/ijerph192013055

Luo, X. S., Tang, A. H., Shi, K., Wu, L. H., Li, W. Q., Shi, W. Q., et al. (2014). Chinese coastal seas are facing heavy atmospheric nitrogen deposition. *Environ. Res. Lett.* 9, 95007. doi: 10.1088/1748-9326/9/9/095007

Malone, T. C., and Newton, A. (2020). The globalization of cultural eutrophication in the coastal ocean: causes and consequences. *Front. Mar. Sci.* 7. doi: 10.3389/fmars.2020.00670

Niino, H., and Emery, K. O. (1961). Sediments of shallow portions of East China Sea and South China Sea. *Geological Soc. America Bull.* 72, 731–762. doi: 10.1130/0016-7606(1961)72[731:Sospoe]2.0.Co;2

Niu, L. X., van Gelder, P., Luo, X. X., Cai, H. Y., Zhang, T., Yang, Q. S., et al. (2020). Implications of nutrient enrichment and related environmental impacts in the Pearl River Estuary, China: characterizing the seasonal influence of riverine input. *Water* 12, 1–12. doi: 10.3390/w12113245

NOWPAP CEARAC. (2011). *Integrated Report on Eutrophication Status Including Evaluation of Land-Based Sources of Nutrients for the NOWPAP Common Procedure* (Toyama: NOWPAP CEARAC). Available at: http://www.cearac-project.org/cearac-project/integrated-report/eut_2011.pdf.

NSA (National Standardization Administration, China). (2014). *Technical Guidelines for Treatment with Red Tide Disaster (GB/T 30743-2014)* (Beijing: Standards Press of China).

OSPAR Commission. (2003). *OSPAR Integrated Report 2003 on the Eutrophication Status of the OSPAR Maritime Area Based Upon the First Application of the Comprehensive Procedure* (London: OSPAR Commission). Available at: https://www.ospar.org/about/publications?q=Eutrophication%20Status%20of%20the%20OSPAR%20Maritime%20Area.

Peng, Y., and Wang, Z. (1991). Eutrophication level evaluation of the Pearl River Estuary. *Mar. Environ. Sci. (In Chinese)* 10 (3), 7–13.

Qi, Y. Z., Chen, J. F., Wang, Z. H., Xu, N., Wang, Y., Shen, P. P., et al. (2004). Some observations on harmful algal bloom (HAB) events along the coast of Guangdong, southern China in 1998. *Hydrobiologia* 512, 209–214. doi: 10.1023/B:HYDR.0000020329.06666.8c

Qian, W., Gan, J. P., Liu, J. W., He, B. Y., Lu, Z. M., Guo, X. H., et al. (2018). Current status of emerging hypoxia in a eutrophic estuary: The lower reach of the Pearl River Estuary, China. *Estuar. Coast. Shelf Sci.* 205, 58–67. doi: 10.1016/j.ecss.2018.03.004

Qiu, D., Huang, L., Zhang, J., and Lin, S. (2010). Phytoplankton dynamics in and near the highly eutrophic Pearl River Estuary, South China Sea. *Continental Shelf Res.* 30 (2), 177–186. doi: 10.1016/j.csr.2009.10.015

Qu, H. J., and Kroeze, C. (2010). Past and future trends in nutrients export by rivers to the coastal waters of China. *Sci. Total Environ.* 408, 2075–2086. doi: 10.1016/j.scitotenv.2009.12.015

Rabalais, N. N., Turner, R. E., Diaz, R. J., and Justic, D. (2009). Global change and eutrophication of coastal waters. *Ices J. Mar. Sci.* 66 (7), 1528–1537. doi: 10.1093/icesjms/fsp047

Redfield, A. C. (1963). The influence of organisms on the composition of seawater. *Sea* 2, 26–77.

SAEP (State Administration of Environmental Protection, China). (1997). *Seawater Quality Standard (GB 3097-1997)*. Beijing: SAEP.

Salmi, T., Mtt, A., Anttila, P., Ruoho-Airola, T., and Amnell, T. (2002). *Detecting Trends of Annual Values of Atmospheric Pollutants by the Mann-Kendall Test and Sen's Solpe Estimates the Excel Template Application MAKESENS. Helsinki* (Finland: Finnish Meteorological Institute).

SAQSIQ (State Administration of Quality Supervision, Inspection and Quarantine, China), and SSA (State Standardization Administration, China). (2007a). *The Specification for Marine Monitoring—Part 4: Seawater Analysis (GB 17378.4-2007)* (Beijing: Standards Press of China).

SAQSIQ (State Administration of Quality Supervision, Inspection and Quarantine, China), and SSA (State Standardization Administration, China). (2007b). *The Specification for Marine Monitoring—Part 7: Ecological Survey for Offshore Pollution and Biological Monitoring (GB 17378.7-2007)* (Beijing: Standards Press of China).

SAQSIQ (State Administration of Quality Supervision, Inspection and Quarantine, China), and SSA (State Standardization Administration, China). (2007c). *Specifications for Oceanographic Survey—Part 4: Survey of Chemical Parameters in Sea Water (GB/T 12763.4-2007)* (Beijing: Standards Press of China).

Scavia, D., and Bricker, S. B. (2006). Coastal eutrophication assessment in the United States. *Biogeochemistry* 79, 187–208. doi: 10.1007/s10533-006-9011-0

Shen, Z. L. (2001). Historical changes in nutrient structure and its influences on phytoplantkon composition in Jiaozhou Bay. *Estuar. Coast. Shelf Sci.* 52 (2), 211–224. doi: 10.1006/ecss.2000.0736

Shu, Y., Wang, Q., and Zu, T. (2018). Progress on shelf and slope circulation in the northern South China Sea. *Sci. China Earth Sci.* 61 (5), 560–571. doi: 10.1007/s11430-017-9152-y

Sinha, E., Michalak, A. M., and Balaji, V. (2017). Eutrophication will increase during the 21st century as a result of precipitation changes. *Science* 357, 405–408. doi: 10.1126/science.aan2409

Statham, P. J. (2012). Nutrients in estuaries - An overview and the potential impacts of climate change. *Sci. Total Environ.* 434, 213–227. doi: 10.1016/j.scitotenv.2011.09.088

Strokal, M., Yang, H., Zhang, Y., Kroeze, C., Li, L., Luan, S., et al. (2014). Increasing eutrophication in the coastal seas of China from 1970 to 2050. *Mar. pollut. Bull.* 85, 123–140. doi: 10.1016/j.marpolbul.2014.06.011

Sun, C. C., Wang, Y. S., Wu, M. L., Dong, J. D., Wang, Y. T., Sun, F. L., et al. (2011). Seasonal variation of water quality and phytoplankton response patterns in daya bay, China. *Int. J. Environ. Res. Public Health* 8, 2951–2966. doi: 10.3390/ijerph8072951

Tian, T., Merico, A., Su, J., Staneva, J., Wiltshire, K., and Wirtz, K. (2009). Importance of resuspended sediment dynamics for the phytoplankton spring bloom in a coastal marine ecosystem. *J. Sea Res.* 62 (4), 214–228. doi: 10.1016/j.seares.2009.04.001

Wang, Y. S., Lou, Z. P., Sun, C. C., and Sun, S. (2008). Ecological environment changes in Daya Bay, China, from 1982 to 2004. *Mar. pollut. Bull.* 56 (11), 1871–1879. doi: 10.1016/j.marpolbul.2008.07.017

Wang, Y. S., Lou, Z. P., Sun, C. C., Wang, H., Greg Mitchell, B., Wu, M. L., et al. (2011). Identification of water quality and zooplankton characteristics in Daya Bay, China, from 2001 to 2004. *Environ. Earth Sci.* 66 (2), 655–671. doi: 10.1007/s12665-011-1274-7

Wang, B. D., Sun, X., Wei, Q. S., and Xie, L. P. (2012). A new method for assessment of eutrophication status in estuarine and coastal waters of China and its application. *Acta Oceanologica Sin. (In Chinese)* 34 (4), 61–66.

Wang, S., Tang, D., He, F., Fukuyo, Y., and Azanza, R. V. (2007). Occurrences of harmful algal blooms (HABs) associated with ocean environments in the South China Sea. *Hydrobiologia* 596 (1), 79–93. doi: 10.1007/s10750-007-9059-4

Wang, B. D., Xin, M., Sun, X., Wei, Q. S., and Zhang, X. L. (2016). Does reduced sediment load contribute to increased outbreaks of harmful algal blooms off the Changjiang Estuary? *Acta Oceanologica Sin.* 35 (8), 16–21. doi: 10.1007/s13131-016-0846-5

Wang, B. D., Xin, M., Wei, Q. S., and Xie, L. P. (2018). A historical overview of coastal eutrophication in the China Seas. *Mar. pollut. Bull.* 136, 394–400. doi: 10.1016/j.marpolbul.2018.09.044

Wu, M. L., Wang, Y. S., Wang, Y. T., Sun, F. L., Sun, C. C., Cheng, H., et al. (2016). Seasonal and spatial variations of water quality and trophic status in Daya Bay, South China Sea. *Mar. pollut. Bull.* 112 (1-2), 341–348. doi: 10.1016/j.marpolbul.2016.07.042

Wu, M. L., Wang, Y. S., Wang, Y. T., Yin, J. P., Dong, J. D., Jiang, Z. Y., et al. (2017). Scenarios of nutrient alterations and responses of phytoplankton in a changing Daya Bay, South China Sea. *J. Mar. Syst.* 165, 1–12. doi: 10.1016/j.jmarsys.2016.09.004

Wu, Z. X., Yu, Z. M., Song, X. X., Cao, X. H., and Yuan, Y. Q. (2019). Application and comparison of two symptom-based eutrophication-assessment methods in Jiaozhou Bay, China. *J. Oceanology Limnology* 37 (5), 1582–1594. doi: 10.1007/s00343-019-8099-8

Wu, Z. X., Yu, Z. M., Song, X. X., Yuan, Y. Q., Cao, X. H., and Liang, Y. B. (2013). Application of an integrated methodology for eutrophication assessment: a case study in the Bohai Sea. *Chin. J. Oceanology Limnology* 31 (5), 1064–1078. doi: 10.1007/s00343-013-2286-9

Xiong, D. Q., and Chen, S. Y. (1993). Fuzzy evaluation theory model of seawater eutrophication. *Mar. Environ. Sci. (In Chinese)* 12 (3-4), 104–110.

Xu, H. L., Zhang, Y., Zhu, X. Z., and Zheng, M. F. (2019). Effects of rainfall-runoff pollution on eutrophication in coastal zone: a case study in Shenzhen Bay, southern China. *Hydrology Res.* 50 (4), 1062–1075. doi: 10.2166/nh.2019.012

Yin, K., and Harrison, P. J. (2007). Influence of the Pearl River estuary and vertical mixing in Victoria Harboron water quality in relation to eutrophication impacts in

Hong Kong waters. *Mar. pollut. Bull.* 54 (6), 646–656. doi: 10.1016/j.marpolbul.2007.03.001

Yin, K. D., and Harrison, P. J. (2008). Nitrogen over enrichment in subtropical Pearl River estuarine coastal waters: Possible causes and consequences. *Continental Shelf Res.* 28 (12), 1435–1442. doi: 10.1016/j.csr.2007.07.010

Yin, K., Lin, Z., and Ke, Z. (2004). Temporal and spatial distribution of dissolved oxygen in the Pearl River Estuary and adjacent coastal waters. *Continental Shelf Res.* 24 (16), 1935–1948. doi: 10.1016/j.csr.2004.06.017

Yin, K. D., Qian, P. Y., Chen, J. C., Hsieh, D. P. H., and Harrison, P. J. (2000). Dynamics of nutrients and phytoplankton biomass in the Pearl River estuary and adjacent waters of Hong Kong during summer: preliminary evidence for phosphorus and silicon limitation. *Mar. Ecol. Prog. Ser.* 194, 295–305. doi: 10.3354/meps194295

Zhang, H., Cheng, W., Chen, Y., Yu, L., and Gong, W. (2018). Controls on the interannual variability of hypoxia in a subtropical embayment and its adjacent waters in the Guangdong coastal upwelling system, northern South China Sea. *Ocean Dynamics* 68 (8), 923–938. doi: 10.1007/s10236-018-1168-2

Zhang, H., and Li, S. (2010). Effects of physical and biochemical processes on the dissolved oxygen budget for the Pearl River Estuary during summer. *J. Mar. Syst.* 79 (1-2), 65–88. doi: 10.1016/j.jmarsys.2009.07.002

Zhang, P., Peng, C. H., Zhang, J. B., Zhang, J. X., Chen, J. Y., and Zhao, H. (2022). Long-term harmful algal blooms and nutrients patterns affected by climate change and anthropogenic pressures in the zhanjiang bay, China. *Front. Mar. Sci.* 9. doi: 10.3389/fmars.2022.849819

Zhang, L., Shi, Z., Zhang, J. P., Jiang, Z. J., Huang, L. M., and Huang, X. P. (2016). Characteristics of nutrients and phytoplankton productivity in Guangdong coastal regions, South China. *Mar. pollut. Bull.* 113 (1-2), 572–578. doi: 10.1016/j.marpolbul.2016.08.081

Zhao, Y. Y., Liu, J., Uthaipan, K., Song, X., Xu, Y., He, B. Y., et al. (2020). Dynamics of inorganic carbon and pH in a large subtropical continental shelf system: Interaction between eutrophication, hypoxia, and ocean acidification. *Limnology Oceanography* 65 (6), 1359–1379. doi: 10.1002/lno.11393

Zou, J., Dong, L., and Qin, B. (1983). The preliminary discussion of eutrophication and red tide in Bohai Sea of China. *Mar. Environ. Sci. (In Chinese)* 2 (2), 41–54.

frontiers | Frontiers in Marine Science

TYPE Original Research
PUBLISHED 08 January 2024
DOI 10.3389/fmars.2023.1308953

OPEN ACCESS

EDITED BY
Ganesh Thiruchitrambalam,
Port Blair Campus, India

REVIEWED BY
Gopalakrishnan Thilagam,
Pachaiyappa's College for Men, India
Satheeswaran Thangaraj,
China University of Geosciences Wuhan, China
Nithyanandam Marimuthu,
Zoological Survey of India, India

*CORRESPONDENCE
Pankaj Verma
vermabios@gmail.com
Gopal Dharani
dhara@niot.res.in

RECEIVED 07 October 2023
ACCEPTED 29 November 2023
PUBLISHED 08 January 2024

CITATION
Verma P, Pandey V, Seleyi SC, Alagarsamy A and Dharani G (2024) Exploring the hidden treasures: Deep-sea bacterial community structure in the Bay of Bengal and their metabolic profile.
Front. Mar. Sci. 10:1308953.
doi: 10.3389/fmars.2023.1308953

Exploring the hidden treasures: Deep-sea bacterial community structure in the Bay of Bengal and their metabolic profile

Pankaj Verma[1*], Vikas Pandey[2], Seyieleno C. Seleyi[1], Abirami Alagarsamy[1] and Gopal Dharani[1*]

[1]Marine Biotechnology Group, National Institute of Ocean Technology, Ministry of Earth Sciences, Government of India, Chennai, India, [2]Biological Oceanography Division, Council of Scientific and Industrial Research - National Institute of Oceanography (CSIR-NIO), Dona Paula, Goa, India

Deep sea bacterial communities demonstrate remarkable adaptability to high-pressure environments coupled with low temperatures which has sparked curiosity about their diversity and exceptional metabolic pathways. Additionally, bacteria in the deep sea exert a substantial influence over various biogeochemical processes. To date, we have relatively very little information about the deep-sea bacterial communities and, they remain largely unexplored. We investigated the variability in the physicochemical conditions, heavy metals and their influence on deep-sea bacterial community structure across three different depths in the Bay of Bengal. The structural and metabolic diversity of deep-sea sediment microbial communities were examined through culture-based sequencing of 16S rRNA genes, ecto-enzymatic studies, and community-level physiological profiling. Bacillota was the most dominant phylum representing 61% of the cultured bacterial isolates, while the remaining belonged to Actinomycetota and Pseudomonodata. Five potential novel species belonging to the genera *Fictibacillus*, *Lysinibacillus*, *Salinicola*, *Robertmurraya* and *Blastococcus* were identified. The extracellular enzymatic activity was positive for >50% of the bacterial isolates, wherein the genera *Bacillus* and *Micromonospora* exhibited versatile profiles. High metabolic diversity was recorded through the carbon substrate utilization profiles indicating that microbial communities are active participants in biogeochemical cycles in the deep sea. The most prominently utilized carbon substrates were α-cyclodextrin, glucose-1-phosphate, D-xylose, glycogen, and 2-hydroxy benzoic acid which serve as organic substrates for microbial metabolism, facilitating the decomposition of organic matter and, recycling carbon in deep-sea ecosystems. Multivariate statistical analyses confirmed that the environmental variables had a profound influence on the bacterial community. The findings shed light on spatial variability in the bacterial community structure, enzyme activity and metabolic profiles, and enhance our understanding of Bay of Bengal deep-sea sedimentary microbial ecology.

KEYWORDS

deep-sea sediment, microbial community, benthos, spatial variation, heavy metals, ecto-enzyme activity, metabolic profile

Introduction

Earth is often referred to as the "blue planet", owing to the fact that ~71% of the planet is covered by the oceans. It is estimated that ~95% of the total ocean volume comprises of the deep sea (Nemergut et al., 2011) lying below 200m depth (Rogers, 2015) with predominantly high hydrostatic pressures; low temperatures (2-4°C) and lack of sunlight (Nogi, 2017). The deep sea plays a notable role in carbon sequestration helping to mitigate the impact of anthropogenic carbon emissions on the climate (Thurber et al., 2014). The microbial oxidation of methane in the deep sea prevents the release of potent greenhouse gases in the atmosphere (Jiang et al., 2022). Additionally, the role of the deep sea in nutrient regeneration and driving global biogeochemical cycles is essential for the sustenance of primary and secondary production in the oceans (Danovaro, 2018). Furthermore, the deep sea is also a reservoir of huge fish stocks, mineral resources, oil and gas, offering enormous potential for bioprospecting (Kato et al., 2011; Thurber et al., 2014; Sweetman et al., 2017).

The prevalence of extremities in the deep-sea environment supports unique habitats and biota (Sogin et al., 2006; Ramirez-Llodra et al., 2010). The deep-sea microorganisms, in particular, exhibit remarkable metabolic adaptations that enable them to thrive in extreme and often harsh environments (Padmanaban et al., 2017; Garel et al., 2021). Due to the absence of sunlight in the deep ocean, these microbes rely on chemosynthesis rather than photosynthesis for energy production. They harness chemical compounds such as hydrogen sulfide, methane, and dissolved iron as energy sources, deriving metabolic energy from the oxidation of these compounds (McCollom, 2000; Jørgensen and Boetius, 2007). These microorganisms are essentially heterotrophs that play a pivotal role in carbon and nutrient cycling by breaking down organic matter (OM), recycling essential elements, and contributing to the overall resilience and stability of the deep-sea ecosystem (Falkowski et al., 2008; Zehr and Kudela, 2011; Acinas et al., 2021).

The bacterial diversity of the deep sea has gained global attention in recent years encompassing the world oceans. Studies have shown that the deep sea sediments harbour a rich diversity of bacteria including, Pseudomonodata, Planctomycetota, Bacteroidota, Acidobacteriota, Actinomycetota, Chloroflexota, Nitrospirota, Gemmatimonadota and Bacillota (Sogin et al., 2006; Jørgensen and Boetius, 2007; Lauro and Bartlett, 2008; Zinger et al., 2011; Corinaldesi, 2015; Walsh et al., 2016; Gawas et al., 2019). However, a significant proportion of microbes in the deep-sea sediments remain taxonomically unidentified, implying that a sizable fraction of the global microbial diversity is undiscovered (Scheckenbach et al., 2010; Zinger et al., 2011; Danovaro et al., 2016). Moreover, the paucity of cultured representatives from the deep-sea sediments poses a significant challenge in studying biodiversity and hinders our ability to accurately assess their role in ecological processes (Dong et al., 2019).

The Bay of Bengal (BOB) forming the northeastern part of the Indian Ocean is the largest triangular basin in the world, that is approximately 2090 kilometres long, 1600 kilometres wide and has an average depth of approximately 2600 metres (Jasna et al., 2020). Multiple riverine influxes (1.6×10^{12} m^3 yr^{-1}; UNESCO, 1979) from the Indian subcontinent and Himalayan range, such as the Ganges, Brahmaputra, Irrawaddy, and Salween on the north and Mahanadi, Godavari, Krishna, and Kaveri on the west, deposit sediments in BOB, supporting a complex marine microbiome (Varkey et al., 1996; Padmanaban et al., 2017; Angelova et al., 2019). Studies in the BOB focussing on benthic bacterial diversity remain underrepresented and have gained impetus only in recent years (Verma et al., 2017; Rajpathak et al., 2018; Angelova et al., 2019; Padmanaban et al., 2019; Lincy and Manohar, 2020; Parvathi et al., 2020; Gu et al., 2022; Guo et al., 2022; Marimuthu et al., 2022). Despite the critical importance of deep-sea microbenthos, our knowledge is limited and lags significantly behind that of coastal ecosystems due to several factors, including the logistical challenges of accessing deep-sea environments. Additionally, the extreme conditions of the deep sea pose unique challenges for studying these organisms. Therefore, efforts to bridge this knowledge gap and understand the biodiversity and ecological processes of deep-sea ecosystems are crucial for a comprehensive understanding of microbial interactions in the deep sea.

The present study focuses on a comparative analysis of the prevailing environmental conditions and resultant bacterial diversity across three different depths of the BOB. Community-level physiological profiling based on sole carbon substrates was carried out to investigate the metabolic capacities of the deep-sea microbial communities. Additionally, distinct preferences of the bacterial communities for different culture media and ecto-enzyme activity were studied. Understanding these preferences can provide valuable information for studying the microbial ecology and biogeochemical processes in the BOB. The results of this study can have implications for various fields, including biotechnology and environmental conservation, as deep-sea bacteria hold enormous untapped potential for novel enzymes and bioremediation strategies.

Methods

Sample collection and analysis of sediment characteristics

Sediment samples were collected on-board the ocean research vessel Sagar Nidhi (Cruise No. SN142), from three different locations in the northern Bay of Bengal (BOB) during June 2019 (Figure 1). The sampling was carried out using the gravity corer from the depths of 2725m, 2191m, and 955m for the stations BOB16N, BOB17N, and BOB20N, respectively. Physical properties were measured using Ocean Seven 320Plus CTD equipped with Idronaut sensors. The detection limits for temperature, salinity, pH, and pressure were 0.001°C, 0.001 PSU (calculated), 0.001, and 0.05 dbar, respectively.

To estimate the concentration of heavy metals, sediment samples were initially dried, ground using an agate pestle and mortar, and subsequently sieved through a 2 mm sieve following standard procedures (USEPA, 2001). Analytical-grade chemicals were utilized, and Milli-Q water (Millipore, USA) was used to make the solutions. The Teflon and polypropylene containers were soaked in 5% HNO_3 for 24 hours, followed by rinsing with Milli-Q water and drying. In a microwave digestion system (Anton Paar),

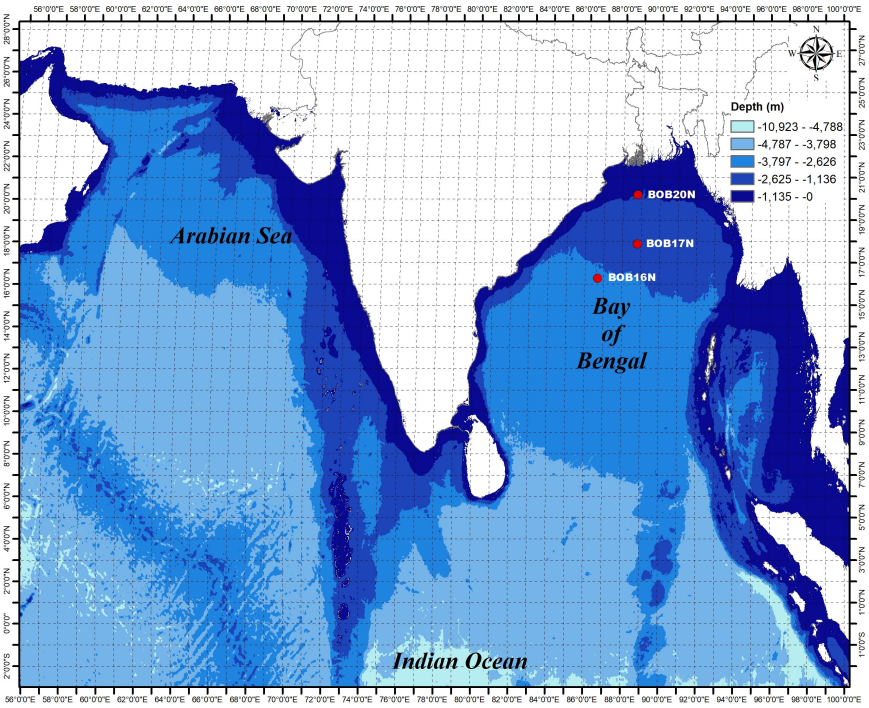

FIGURE 1
Study area of three deep-sea sampling sites in the Bay of Bengal.

one gram of dried sediment was digested at 140°C with 5 ml HNO_3 (Suprapur, Merck) as per APHA, 2005. The digested, clear solution was transferred to centrifuge tubes, and 10 ml of Milli-Q water (Millipore, resistivity: 18.2 MΩ/cm) was added to make up the volume (Cortada and Collins, 2013). The concentrations of metals were determined using Inductively Coupled Plasma Mass Spectrometry (ICP-MS) (Agilent-7500). Replicate analytical blanks were analyzed alongside certified reference materials to check for potential contamination, by following protocol adopted by Jha et al. (2019). The total organic carbon (TOC) in sediment was determined using the modified Walkley-Black wet oxidation method (Gaudette et al., 1974), and OM was calculated by multiplying the TOC by a factor of 1.724 (Trask, 1939). The sediment texture was analysed by wet sieve and pipette method to classify it into sand, silt, and clay (Buchanan, 1984).

Isolation of bacteria

Sterile 15ml polypropylene conical tubes were used to collect three replicate sediment sub-samples of 5cm layer from each core. For the isolation of heterotrophic bacteria, on-board processing of samples was done by addition of 2g of sediment to 18ml sterile seawater. The slurry was vigorously vortexed three times for 1 minute each with an intermittent gap of 30 seconds and kept at a shaker (200rpm) for 20 minutes. The particles were allowed to settle for 5 minutes and diluted at four gradients from 10^0 to 10^{-4}. 100µL of each dilution was spread plated in triplicate on different media (HiMedia, India), ZoBell marine agar 2216 (ZMA), starch casein agar (SCA), ISP7, and Streptomyces agar (SMA), and incubated at 20°C in the dark for 3-14 days. Considering low-nutrient deep-sea conditions, growth medium were used at 1/5 of their original strength in sterile seawater. Morphologically unique bacterial colonies were counted and individually chosen from each culture plate through visual examination using a stereomicroscope (Nikon SMZ 800).

Axenic strains were achieved through three quadrant streaking cycles on specific media. Pure isolates were preserved in 30% (v/v) glycerol with 50% (v/v) culture media broth at -80°C and maintained on media slants at 4°C for further analysis. Strains were grouped based on the colony characteristics like morphology, pigment production, and Gram-staining, and a representative from each phenotype was subjected to molecular identification and extracellular enzyme screening.

DNA extraction and 16S rDNA amplification

The phenol-chloroform-isoamyl alcohol (25:24:1) extraction method with proteinase K treatment was used to extract the genomic DNA from the axenic cultures (Sambrook and Russell, 2001). The bacterial cells were initially lysed by bead-beating with ceramic beads to break open and release the DNA physically. To eliminate any remaining salt or impurities, the extracted DNA pellet was washed twice with 70% ethanol, air-dried, and dissolved in TE buffer. The primers, 27F (5′-AGRGTTTGATCMTGGCTCAG-3′) and 1525R (5′-AAGGAGGTGWTCCARCC-3′) or 1492R (5′-TACGGYTACCTTGTTACGACTT-3′) were used for 16S

rDNA amplification of bacteria. The 50µl PCR reaction mixture contains 1.2µl (~ 60 ng) of template DNA, 0.5pmol/µl of each primer, 10% BSA of concentration 10mg/ml, and Emerald AMP GT PCR Master Mix (Takara, Japan) at 1X final concentration. Reactions without templates were used as negative control. The PCR conditions were as follows: a 5-minute initial denaturation at 95°C, 35 cycles of 1 minute at 94°C, 1 minute at 55°C, and 1.2 minutes at 72°C, and a 10-minute final extension at 72°C. After ethidium bromide staining, the reaction products were observed on an agarose gel (1%) under UV illumination and purified using the QIAquick gel extraction kit (Qiagen) according to the manufacturer's instructions.

Sequencing and taxonomic assignment

The purified PCR products were sequenced after setting sequencing reactions with BigDye Terminator Kit v. 3.1 (Applied Biosystems). The initial PCR primers along with additional internal primers 704F (5′-GTAGCGGTGAAATGCGTAGA-3′) and 907R (5′-CCGTCAATTCCTTTGAGTTT-3′) were used for setting up the sequencing reactions individually and after purification the run was carried out in Applied Biosystems 3730 Genetic Analyzer. ChromasPro version 1.5 software (www.technelysium.com.au/ChromasPro) was used to manually assemble and edit the partial 16S rDNA sequences of each strain to produce near full-length sequences. The taxonomic assessment of sequences was carried out using the BLASTN (Altschul et al., 1997) program against the EzBioCloud database containing type strains with validly published prokaryotic names (http://www.ezbiocloud.net; Yoon et al., 2017). The top three sequences with the highest similarity were downloaded for each strain and the multi-sequence alignment of nucleotide sequences was carried out using ClustalW in MEGA11 alignment explorer (Kumar et al., 2018). The Neighbor-Joining method in MEGA11 was used to infer the evolutionary history, the evolutionary distances were computed using the Maximum Composite Likelihood method and are in the units of the number of base substitutions per site. The final dataset contained 1621 positions and all ambiguous positions were removed for each sequence pair. The robustness of the topology of phylogenetic trees was evaluated by using bootstrap analysis with 1000 resamplings.

Ectoenzymatic hydrolytic activity

Screening for the production of extracellular hydrolytic enzymes was carried out by spotting bacterial isolates onto respective agar medium. A solid medium containing marine agar 2216 supplemented with 2% (w/v) of sterile skim milk, extra pure gelatin, and soluble starch, respectively, was used to assess the generation of extracellular hydrolases like caseinase, gelatinase, and amylase, respectively (Bjerga et al., 2014). The hydrolytic zone formations were monitored on the plates for up to two weeks while they were incubated at 20°C. The plates were flooded with acidic mercuric chloride (Balan et al., 2012) and Lugol's iodine solution to determine gelatinase and amylase activity respectively.

Metabolic diversity of microbial communities

The community-level physiological profiling (CLPP) of the deep-sea sediment samples in triplicates was performed using BIOLOG® EcoPlates™ to assess the ability of heterotrophic microbial communities to utilize different carbon substrates. The Ecoplates contain 31 single carbon sources and tetrazolium dye. The utilization of any carbon source by the microbial community results in the respiration-dependent reduction of the dye and purple colour formation that can be quantified and monitored over time (Garland, 1997). For CLPP, 2 g of sediment was mixed with 18 ml sterile 50% artificial seawater and kept on the shaker for 30 min. After settling for 5 minutes,150 µL of suspension was inoculated in each well, and the plates were incubated at 20°C for 144 h. Every 24 h, optical density (OD) at 590 nm was measured using a microplate reader to monitor the carbon source utilization by microbial communities. Each Ecoplate contains the control well in triplicate, which is devoid of any carbon sources. The average well-color development (AWCD) was measured to represent the metabolic proficiency of microbes. The AWCD was calculated as:

$$AWCD = \sum_{i=1}^{n}(C_i - R)/n$$

where C_i is the absorbance value of each well at 590 nm, R is the absorbance value of the blank control well, and n is representative of the number of wells. When plotted over time, the AWCD of EcoPlate represented the activity or overall carbon substrate utilization potential of heterotrophic microbial communities (Garland and Mills, 1991).

Data analysis

To assess the structural properties of the bacterial community, the most broadly utilized univariate diversity indices such as number of taxa (S), species richness (Margalef's d), Shannon-Wiener diversity index (H′, $\log_e$), Simpson's index (1- Lambda′), and Pielou's evenness (J′) were estimated using PRIMER v 6.1 (Clarke and Gorley, 2006). A two-way ANOVA was conducted to investigate the differences in microbial diversity indices between different stations and the culture media used. In case of significant interaction between the stations and media used, an analysis of simple main effects for media was performed with statistical significance receiving a Bonferroni adjustment for multiple pairwise comparisons between media at each station. Prior to conducting the two-way ANOVA, all the assumptions were checked for the data. The data had no outliers, normality was assessed using Shapiro-Wilk's test, and homogeneity of variances was assessed using Levene's test. The microbial community's metabolic diversity (Shannon index H′) and substrate richness (number of carbon substrates utilized, R) were calculated using BIOLOG® with a threshold AWCD value of ≥0.35 (OD 590nm). To identify carbon sources which were driving the variability in the metabolic patterns of bacterial communities, Principal Component Analysis (PCA) was carried out on standardized OD 590nm values

for each substrate using the PASW Statistics 18 software. A correlation matrix based on the Kaiser-Meyer-Olkin measure of sampling adequacy and Bartlett's test of Sphericity was used for factor analysis. The microbial abundance data was transformed to log(x+1) values to smooth the extremes in data and allow less represented taxa to exert same influence while simultaneously reducing the potentially overwhelming impact of the most exorbitant taxa. The Bray-Curtis resemblance matrix was created using the transformed data, and non-metric multi-dimensional scaling (nMDS) was used to observe the bacterial taxa assemblage pattern (Clarke and Warwick, 1994). Whereas, the relationship between taxa and the environmental parameters within the sites was assessed by a direct gradient analysis of the multivariate linear regression ordination technique (canonical correspondence analysis, CCA).

Data availability

The 16S rDNA sequence data generated for all the deep-sea bacterial strains obtained in the study was submitted in the NCBI GenBank database (http://www.ncbi.nlm.nih.gov/GenBank/index.html) under the accession numbers OR623173 – OR623227 and are included in the Supplementary Table 1.

Results and discussion

Environmental factors and heavy metal distribution in deep-sea

It is well-established that microbes inhabiting deep-sea sediments represent a significant proportion of the biosphere (Danovaro et al., 2016). Their abundance and diversity are largely dependent on environmental conditions such as OM content and sediment texture (Parkes et al., 2014). Table 1A, summarizes the spatial variation of environmental characteristics of deep-sea in the three study locations. The water temperature showed an inverse relationship with the depth, the lowest recorded temperature (1.90 °C) was at the depth of 2725m in BOB16N, and <1 °C rise in temperature (2.41 °C) was observed at a depth of 2191m in BOB17N. The maximum temperature (7.18 °C) was recorded in BOB20N at a depth of 955m. In the case of salinity (34.77 to 34.99 PSU) and pH (7.95 to 8.13), minimum variations were noted across the three locations. OM varied between 0.68% to 2.45% with the highest concentration in BOB20N and the least in BOB17N. The study observed lower concentrations of OM at increasing depths in the deep-sea or in the middle region of Bengal Fan in comparison to the upper region. The Northeastern Indian Ocean is intensely influenced by one of the largest fluvial systems on Earth comprising of the Ganga-Brahmaputra-Meghna rivers (Contreras-Rosales et al., 2016). Transporting substantial sediment and nutrient loads, these rivers significantly elevate the OM concentration, particularly noticeable in the study location BOB20N, as compared to BOB16N and BOB17N (Figure 1). The sediment texture analyses revealed that BOB16N was mostly clayey, BOB17N possessed a mixture of silt and clay and lastly, BOB20N was silty. The obtained results revealed a clear demarcation in sediment texture between the three different depths among the study locations in the BOB. Recent studies have suggested that sediment provenance in the BOB is mostly composed of terrestrial detrital matter with minor contributions of marine autogenous OM, and wind dust (Weber et al., 2003; Tripathy et al., 2014). The variation in sediment textures may be attributed to a combination of factors such as sediment sources, transportation processes and depositional environments which change as we go deeper into the seafloor (Ye et al., 2022). Closer to the coast, sediments tend to be coarser and more variable due to proximity to terrestrial sources, wave action, and river input resulting in a good proportion of sand, gravel and mud (Gunaratna et al., 2019). In contrast, deep-sea sediments are typically composed of fine-grained particles such as silt and clay which accumulate slowly over time and are influenced by factors such as ocean currents, nutrient availability, and the presence of OM (Liu et al., 2023).

The concentration of metals in the sea is regulated by natural processes such as biological uptake, particulate matter scavenging, advection of water masses and Aeolian transport of terrestrial materials (Jones and Murray, 1984; Wangersky, 1986). While some heavy metals, including Al, Fe, and Mn, have a lithogenic origin, human activity is largely responsible for mobilising heavy metals like Pb, Cd, Zn, Cr, Cu, and Ni. (Serrano et al., 2011). In addition to this, factors like ocean circulation patterns, temperature and water chemistry can affect the transport, dispersion and precipitation of heavy metals (Tuohy et al., 2015). Majority of the heavy metal concentrations in all three locations retained a trend in the following order: Fe>Al>Mn>Zn>Ni (Table 1B). Among all the heavy metals determined, significantly high concentrations were observed for Fe (avg. 25584.43 ppm) and Al (avg. 14920.37 ppm). The OM and sediment grain size in the coastal environment are important controllers of metal bioavailability in the coastal environment (Jha et al., 2021). As the proportion of mud (silt and clay) increased at greater depths i.e., BOB16N and BOB17N a corresponding elevation in the concentrations of Fe, Co, Pb, and Ni was observed indicating that these metals may be adsorbed by fine sediment particles and such pattern has also been documented in coastal regions where muddy sediment due to the smaller size, represents a higher adsorption capacity for metals (Pandey et al., 2021).

Table 1B provides a comparison of the average range of trace metal concentrations found in the sediments of the present study with those found in other deep-sea sediments. The cumulative data shows that the concentrations of Fe and Al were the highest in comparison to the other metals indicating that they are abundant in marine sediments. Additionally, the abundance of Fe and Al in the study locations can be explained by their status as the third and fourth most abundant elements on Earth, primarily originating from lithogenic sources (Serrano et al., 2011). This suggests that the high concentrations of Fe and Al in deep-sea ecosystems are likely derived from natural geological processes rather than human activities. Inconsistencies in the concentration of Mn within the current study locations as well as in the reported studies could be attributed to variability in the reductive dissolution of Mn in the sediment (Pakhomova et al., 2007). The sampling sites are also under the influence of riverine discharge in the Bengal Fan region, which is the largest submarine fan on Earth. Additionally, the

geological and tectonic forces can lead to variations in the underlying rock composition and mineral deposits, affecting the availability of heavy metals (Cheng et al., 2022). Conversely, the concentrations of Pb, Cd, Zn, Cr, Cu, and Ni remained well within the average crustal abundance concentration. Overall, the concentrations of heavy metals exhibit significant spatial variation in different deep-sea regions as a result of complex interactions between natural geological processes, local environmental conditions and the unique characteristics of each marine region (Budianto and Lestari, 2018; Sattarova and Aksentov, 2021; Marimuthu et al., 2022).

Deep-sea bacterial community identification and taxonomy

The deep-sea sediments host the largest fraction of microbenthos on Earth which play a vital role in ocean productivity (Corinaldesi, 2015; Danovaro et al., 2016). The average number of heterotrophic bacteria (colony-forming units, CFUs) obtained in the deep-sea sediment samples was highest at station BOB20N (1.67×10^5 CFU/g), followed by BOB16N (6.06×10^4 CFU/g) and BOB17N (5.65×10^4 CFU/g). A total of 76 morphologically distinct bacterial strains were isolated from the BOB16N, BOB17N, and BOB20N sediment samples on different growth media, and based on standard colony morphological characteristics these strains were classified into 55 groups cumulatively for all three stations. The growth medium Streptomyces agar and Zobell Marine agar showed major population of heterotrophic bacteria, 1.49×10^5 and 1.21×10^5 CFU/g, respectively in comparison to other media such as ISP7 (6.99×10^4 CFU/g), and Starch casein agar (5.75×10^4 CFU/g). The 16S rRNA gene sequence has overwhelmingly emerged as the most frequently employed genetic marker for bacterial phylogenetics and taxonomy, serving as a standard housekeeping gene. By utilizing a variety of sequencing primers, we achieved successful sequencing of more than 1350 base pairs of the 16S rRNA gene for all the bacterial groups obtained in this study (Supplementary Table 1). The strains were identified by comparing the 16S rRNA gene sequence to nucleotide sequences within the NCBI database (http://www.ncbi.nlm.nih.gov/) using the Basic Local Alignment Search Tool (BLAST) and EzBioCloud database containing type strains sequences. We obtained a total of 55 bacterial strains which belonged to 39 species and 24 genera. The majority of the bacterial isolates clustered with the phyla Bacillota (61.54%), while the remaining belonged to Actinomycetota (20.51%), and Pseudomonodata (17.95%). Padmanaban et al. (2019) also reported that the majority of isolated microorganisms from deep-sea sediments in the Bay of Bengal and the Andaman Sea belonged to Bacillota. It was found to be the second dominating phylum in deep-sea sediments from the Bay of Bengal and volcanic Barren Island in the Andaman Sea, according to a culture independent study by Verma et al. (2017). Among the 14 families obtained, *Bacillaceae*, had the highest representation with 21 different species (53.84%) (Figure 2). *Bacillus* was the dominant genus discovered within this phylum and formed four distinct clades in the phylogenetic tree (Figure 2), its members are known for their remarkable metabolic versatility and capacity to flourish under extreme conditions. While the wide distribution of the genus *Bacillus* is known, this study reaffirmed its presence in deep-sea sediments.

The dominance of Actinomycetota in deep-sea sediment has been reported from the Southwest Indian Ridge, CIOB (Chen et al., 2016) , BOB (Verma et al. 2017) and the Southern Okinawa trough, China Sea (Dang et al., 2009). Several investigations from other marine environments, like the CIOB (Gawas et al., 2019), the Atlantic Ocean (da Silva et al., 2013), and the Mariana Trench (Ma et al., 2022), also report the isolation of Actinomycetota from deep-sea sediment. Moreover, microbial diversity studies done through culture-independent metagenomes from the sediments of the Arabian Sea (Nair et al., 2017; Vipindas et al., 2020) and the Pacific Ocean (Hongxiang et al., 2008) revealed the presence of Actinomycetota. In the present study, the dominant genus found within the Actinomycetota phylum is *Micromonospora*. Species of this genus are reported from deep-sea sediment in the Mediterranean Sea, Mariana Trench in the Pacific Ocean, and other marine regions. Its members have well-developed pathways for the biosynthesis of secondary metabolites for non-ribosomal peptides and polyketides, (Gärtner et al., 2016). In a previous study on the cultured biodiversity of deep-sea sediment samples from the Atlantic Ocean (da Silva et al., 2013), and the Mariana Trench (Ma et al., 2022), the prevalence of Pseudomonodata were found as major groups. Moreover, culture-independent approaches revealed the presence of bacterial communities belonging to Pseudomonodata in sediments from the central Mediterranean Sea (Mahmoudi et al., 2020), Arabian Sea (Nair et al., 2017; Vipindas et al., 2020), Pacific Ocean (Hongxiang et al., 2008), and China sea (Chen et al., 2023). In this study, within Pseudomonodata, the class Gammaproteobacteria showed the highest representation (71.42%). The genus *Halomonas* of this class was most frequently isolated from our study locations which can be attributed to the vast range of salinity, temperature, and pressure that *Halomonas* can thrive in as a result of its physiological and metabolic adaptability (da Silva et al., 2013).

Regarding the specific study locations, we observed variations in the number of identified bacterial species. The highest number of bacterial species, 24 in total, were found at BOB20N. This count decreased significantly to 13 species at BOB17N and further reduced to the lowest count of 11 species at BOB16N. A similar trend was observed in the distribution of bacterial genera. In BOB20N, the bacterial species were diverse and represented 16 different genera. In contrast, at BOB17N, the number of genera reduced to 10, and at BOB16N, it decreased further to only 8 genera (Supplementary Table 1). This pattern indicates a decreasing trend in both species and genera diversity as we move from BOB20N to BOB17N and then to BOB16N. Furthermore, the bacterial species from BOB20N could be further categorized into 3 phyla, 4 classes, 9 orders, and 10 families. BOB17N bacterial species belonged to 3 phyla, 4 classes, 5 orders, and 6 families. Lastly, BOB16N bacterial species belonged to 3 phyla, 4 classes, 4 orders, and 5 families. Out of 24 bacterial species observed in BOB20N, 16 which were exclusively present are, *Arthrobacter subterraneus*, *Bacillus cabrielesii*, *B. cereus*, *B. tequilensis*, *Blastococcus saxobsidens*,

TABLE 1 (A) Geographical details and environmental characteristics (mean ± SD) of the Bay of Bengal deep-sea samples; (B) Trace metals concentration (ppm) in the deep-sea sediment samples in the present study, average crustal abundances, and other deep sea locations; (C) Diversity and richness estimate indices for the samples and growth media.

(A)

Sl. No.	Sample ID	Depth (m)	Latitude	Longitude	Temperature (°C)	Salinity (PSU)	pH	OM (%)	Sand%	Silt%	Clay%
1.	BOB16N	2725	16° 15.650′N	86° 42.102′E	1.90	34.77	8.13	1.03 ± 0.07	2.45 ± 0.35	28.59 ± 0.18	68.97 ± 0.18
2.	BOB17N	2191	17° 52.492′N	88° 48.018′E	2.41	34.80	8.10	0.68 ± 0.01	0.65 ± 0.07	54.82 ± 0.79	44.53 ± 0.86
3.	BOB20N	955	20° 11.720′N	88° 48.058′E	7.18	34.99	7.95	2.45 ± 0.23	3.43 ± 0.26	67.39 ± 0.83	29.19 ± 0.56

(B)

Heavy metal	Present study			Taylor (1964)	Marimuthu et al. (2022)	Sattarova and Aksentov (2021)	Sattarova and Aksentov (2021)	Budianto and Lestari (2015)
	BOB20N	BOB17N	BOB16N	Average crustal abundance	Off Chennai, Bay of Bengal	Kuril Basin	Kuril-Kamchatka Trench and abyssal plain	Makassar Strait
Al	16073.50	14587.20	14100.40	82300	–	46137.50	59395.83	–
Fe	24552.45	25169.85	27031.00	56300	32170.30	31125.00	34750.00	47038.00
Zn	89.51	80.80	83.39	70	58.10	104.55	85.51	101.00
Co	13.22	16.55	24.10	25	22.90	–	–	–
Cu	46.34	38.20	39.36	55	41.06	51.66	99.53	65.20
Pb	13.63	16.44	21.07	12.50	4.11	18.75	19.46	12.50
Mn	331.23	2531.78	1216.59	950	903.48	17412.5	3804.17	–
Ni	47.55	50.96	59.68	75	30.66	46.09	40.30	144.80
Cr	36.99	39.23	35.20	100	37.01	35.24	30.91	–

(C)

Station-wise diversity indices					
	S	d	J′	H′(log_e)	1-Lambda′
BOB20N	24	1.91	0.85	2.70	0.89

(Continued)

10.3389/fmars.2023.1308953

10.3389/fmars.2023.1308953

Continued

Station-wise diversity indices						Media-wise diversity indices					
	S	d	J'	H'(log$_e$)	1-Lambda'		S	d	J'	H'(log$_e$)	1-Lambda'
BOB17N	13	1.10	0.77	1.98	0.77	ISP7	12	0.99	0.78	1.94	0.78
BOB16N	11	0.91	0.87	2.08	0.86	ZMA	21	1.71	0.89	2.72	0.92
						SMA	20	1.60	0.82	2.46	0.88
						SCA	9	0.73	0.82	1.80	0.79

Brachybacterium paraconglomeratum, *Brevibacterium casei*, *Cytobacillus oceanisediminis*, *Fictibacillus barbaricus*, *Halomonas meridiania*, *Metabacillus indicus*, *Micromonospora marina*, *M. tulbaghiae*, *Paenibacillus lautus*, *Robertmurraya beringensis* and *Rossellomorea marisflavi*. The bacterial species unique to BOB17N were *Alkalihalobacillus hwajinpoensis*, *Alteromonas macleodii*, *Fictibacillus aquaticus*, *Micromonospora fluminis*, *Priestia filamentosa* and *Staphylococcus arlettae*. Moreover, the bacterial species encountered only in BOB16N were *Bacillus fengqiuensis*, *B. safensis*, *Domibacillus indicus*, *Halobacillus trueperi*, *Limimaricola soesokkakensis*, *Lysinibacillus capsica* and *Salinicola salarius*.

The role of the 16S rRNA gene sequence similarity threshold has been pivotal in the classification of prokaryotes, particularly in recognizing new species. Initially, the suggested threshold value was 97%, as proposed by Stackebrandt and Goebel, (1994). However, this value has faced challenges from various research groups. Kim et al. (2014), proposed a revised threshold of 98.65% based on an extensive analysis of over a million comparisons between genome sequences and complete 16S rRNA gene sequences. In light of this criterion, our study has yielded noteworthy results. Specifically, we identified five potential novel isolates with 16S rRNA gene sequence similarity values below the established threshold. Strain B1TS8, with a 98% bootstrap-supported cluster in the phylogenetic tree, was found as a potential novel species closely related to *Fictibacillus aquaticus*, sharing 98.4% similarity (Figure 2). Strain B2TS8H formed a divergent node in the genus *Lysinibacillus* clade and shared 98.2% similarity with *L. capsici*. Strain B2TS2H, showed 98.3-98.4% similarity of 16S rDNA with multiple species of genus *Salinicola* and formed a tight cluster with *S. halophyticus*, *S. halimionae* and *S. salarius*. Strains of *S. salarius* are reported as piezophilic bacterium that requires pressures of 102 MPa to grow and bacteria belonging to this genus have been reported earlier from the deep-sea sediments. Strains B0TS14 and B0TS14H showed 98.7 and 98.6% similarity with *Robertmurraya beringensis* and formed a distinct group in the genus *Robertmurraya* clade. Strain B0TS39, showed 98.6% similarity of 16S rDNA with *Blastococcus saxobsidens*. It formed a moderate bootstrap-supported (64%) cluster in a phylogenetic tree reflecting similarity with multiple species. Members of this genus have been isolated from sandstone monuments, sea, soil, plant, and snow samples.

Bacterial diversity and abundance in deep-sea

The diversity indices offer a comprehensive view of the distribution of the bacterial population in the sediment samples of the BOB (Table 1C). The diversity indices indicate that BOB20N had the highest values for number of species, S; species richness, d; Shannon diversity, H′; and Simpson' estimate, 1- Lambda' except for evenness, J'. However, it was noted that J' had the highest value in BOB16N. The obtained values suggest that BOB20N harbours a rich and diverse bacterial community, with a high probability of encountering distinct genotypes within the population. The distribution of bacterial species further indicates a balanced ecological niche, potentially contributing to the overall stability

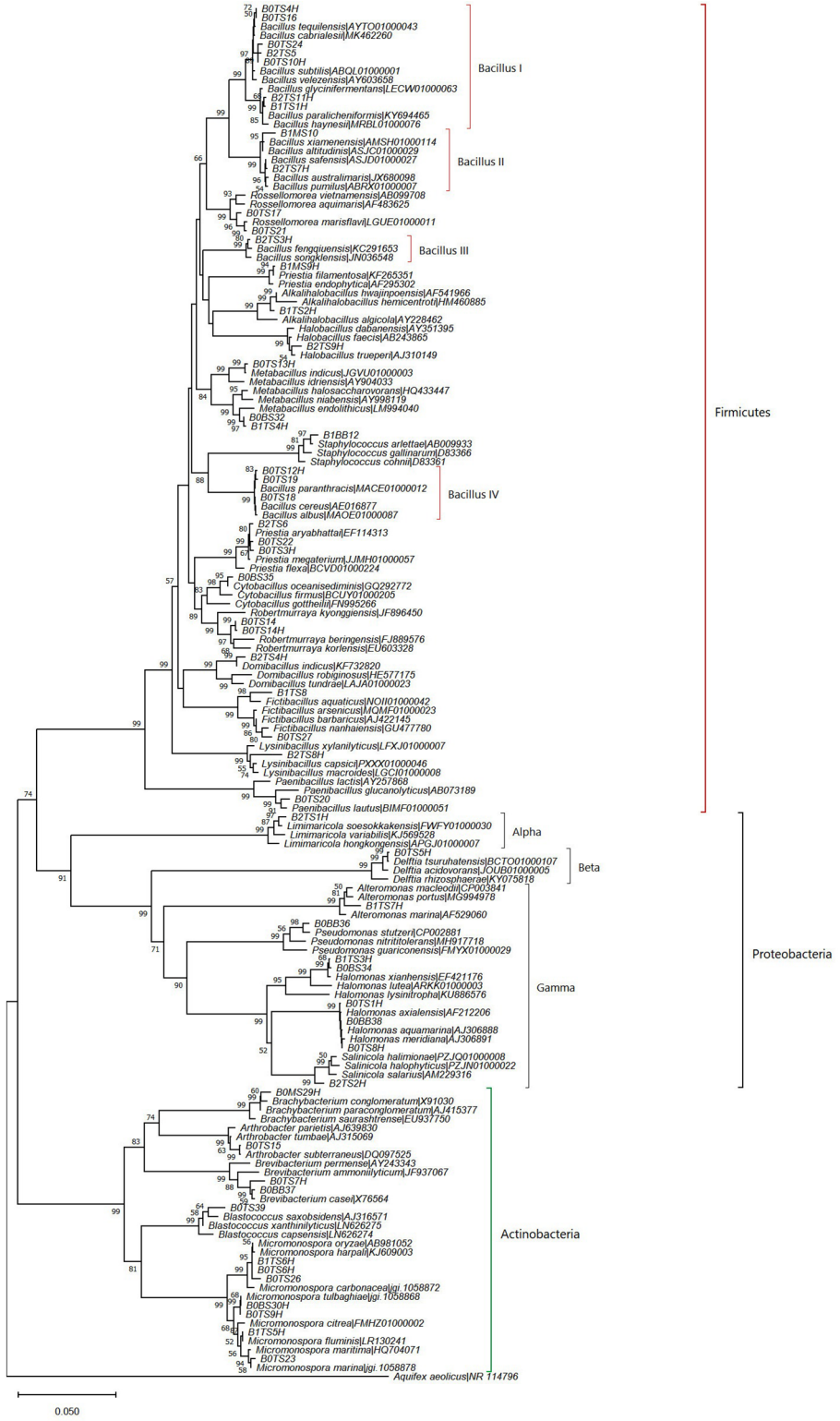

FIGURE 2
Neighbor-joining phylogenetic tree based on nearly complete and aligned 16S rDNA sequences of isolated bacteria and their nearest type strains. Bootstrap values (≥50%) of 1000 resamplings are shown at branch points. *Aquifex aeolicus* (NR 114796) was used as an outgroup.

and resilience of the ecosystem in BOB20N. Considering all the samples together, the results suggest that ZMA was the most favourable culture medium for obtaining different bacteria species, as it showed the highest values for S, d, J', H', and 1-Lambda'. On the other hand, SMA was found to be the most suitable medium for promoting bacterial growth, as it recorded the peak density among all the media used. Regarding the optimal growth medium for specific study locations, it was observed that

ZMA displayed the highest values for S, d, J', H' and 1- Lambda'. Conversely, in the case of BOB20N, SMA medium exhibited the highest population density among all the tested growth media (Supplementary Figure 1). In BOB17N, the SMA medium exhibited highest values for density, S, d, H' and 1-Lambda', however, the highest value for J' was observed with the ISP7 medium. Conversely, in BOB16N, the ZMA medium displayed the highest values for density, S, d, H' and 1-Lambda' and maximum in ISP7 and SMA for J'.

It is noteworthy that the SCA medium recorded the lowest values across majority of the diversity indices, indicating that it was the least favourable medium for bacterial diversity and abundance in the BOB deep-sea sediment samples examined in this study. These findings indicate that among the culture media tested, ZMA exhibited the most favourable conditions for bacterial growth, as it yielded the highest counts of species, evenness, richness, and genotypic diversity. Meanwhile, SMA demonstrated the highest abundance. The combination of ZMA's high species diversity and SMA's peak abundance suggests that different media can provide complementary insights into the microbial community composition and dynamics in BOB20N.

The two-way ANOVA confirmed significant spatial variation between the study locations and the media for the diversity indices ($p<0.05$) (Supplementary Table 2). The simple main effect of "media" on the station's diversity indices was statistically significant for each station ($p< 0.0001$), except for J' in BOB20N and 1-Lambda' in BOB17N. Moreover, there is a statistically significant difference in density at BOB16N bacteria cultured in ISP7, ZMA, SMA or SCA, $F_{(3, 24)} = 4.09$, $p = 0.018$. The same holds true for BOB17N, $F_{(3, 24)} = 39.1$, $p< 0.0001$ and BOB20N, $F_{(3, 24)} = 74.4$, $p< 0.0001$. The pairwise comparisons for species richness, evenness, Shannon index, Simpson index and density showed a combination of significant as well as insignificant values for every media in the different sampling stations (Supplementary Figure 1). The obtained results of two-way ANOVA and pairwise comparisons confirmed that the choice of media significantly affects the diversity indices of bacteria at each station. These findings suggest that the bacterial communities in the BOB sediments have distinct preferences for different media, which may be indicative of specific ecological niches or resource availability.

Ecto-enzymatic activities of deep-sea sedimentary bacteria and nutrient cycling

The microbial communities of deep-sea sediment meet their substrate needs by breaking down organic components deposited at the bottom of the sea (Mahmoudi et al., 2020). The primary step in the breakdown of OM is the production of extracellular enzymes that make high molecular weight compounds easily accessible for bacterial consumption (Polymenakou et al., 2008). The polymer mineralization and regeneration of deep-sea nutrients are indicated by the production of these enzymes from marine bacteria (Raghukumar et al., 2001). Thus, the production of extracellular hydrolytic enzymes by deep-sea sedimentary bacteria plays a significant role in the biogeochemical processes through decomposition of OM (Dang et al., 2009). In our study, we investigated the enzymatic activities of 55 bacterial strains. Among these strains, 28 exhibited positive activity for caseinase, indicating their capacity to hydrolyze protein polymer. Additionally, 31 strains displayed positive gelatinase activity, suggesting their ability to break down gelatin, a protein derived from collagen (Supplementary Table 1). These findings have important implications for deep-sea environments, as they highlight the potential role of these bacteria in protein degradation, leading to an increase in free amino acid availability, as previously discussed in the works of Dang et al. (2009) and Saunders et al. (2022).

In the case of amylolytic activity, 28 bacterial isolates were positive indicating their role in carbohydrate polymer degradation (Supplementary Table 1). Complex polysaccharide degradation is particularly pertinent to the study of microbial metabolism since they are the major elements of phytoplankton, marine particles, and sediments (Raghukumar et al., 2001; Arnosti et al., 2005). Notably, sedimentary bacteria of genus *Bacillus* and *Micromonospora* exhibited all three enzyme activities, indicating their versatility in enzymatic degradation and crucial roles in nutrient cycling in the deep-sea environment. *Limimaricola, Brevibacterium, Robertmurraya, Blastococcus*, and some cultures of *Metabacillus* were negative for all enzyme activities (Supplementary Table 1).

Assemblage pattern of bacterial community and relationship with environmental factors

The 2D nMDS (stress 0.01) ordination plot showed the assemblage pattern of bacteria from three deep-sea stations cultured using different growth media (Figure 3). Specifically, for BOB20N, it was observed that the bacterial species grown in SMA, ZMA and ISP7 formed a cluster in the plot, indicating their similarity in terms of community composition. However, SCA appeared as a separate point on the plot, suggesting that it had a distinct bacterial community composition compared to the other three media. Similarly, for BOB17N, SMA, ZMA and SCA were clustered closely together, whereas, ISP7 appeared as a separate point in the plot. Lastly, in the case of BOB16N, ZMA, SMA and SCA were grouped and ISP7 was positioned far away in the plot indicating that the latter had a distinct bacterial community composition compared to the other media and study locations.

The nMDS analysis visually highlighted the distinct clustering patterns among bacterial species cultured on different growth media. These distinct clustering patterns indicate that the composition and abundance of bacterial species can vary significantly depending on the growth media used. Based on the obtained results, ZMA, SMA and SCA promote more similar communities, while ISP7 support the growth of distinct bacterial communities.

The CCA ordination plotted for bacterial families against the environmental variables and heavy metals revealed the influence of variables on bacterial families. The CCA plot suggests that both the environmental variables and heavy metals have a parallel influence on

the spatial variability of the bacterial community in the study locations. (Figure 4). A clear demarcation was observed on axis-2 between the bacterial families related to BOB20N and much deeper stations BOB16N & BOB17N. Bacterial families related to BOB20N i.e., *Halomonadaceae*, *Paenibacillaceae*, *Dermabacteraceae*, *Geodermatophilaceae*, *Pseudomonadaceae* and *Bacillaceae* were primarily influenced by the sandy texture of the sediment, OM, temperature, and salinity. In addition, Zn and Cu were two metals that were also important in structuring the bacterial community in the sediment samples of BOB20N. Sediment with distinct textures exhibit differences in their surface area available for bacterial attachment and growth including its ability to retain oxygen, leading to changes in the composition of the bacterial community (Wang et al., 2013; Zheng et al., 2014). *Comamonadaceae*, *Micrococcaceae* and *Micromonosporaceae* were positively correlated to silt, Cr and Al. *Rhodobacteraceae*, *Brevibacteraceae* and *Planococcaceae* were dominant in BOB16N and related to depth, clay, Co, Fe, Ni and Pb whereas in BOB17N, *Alteromonadaceae* and *Staphylococcaceae* were dominant and showed correlation mainly with silty sediment, Cu and Mn on the first axis on CCA plot. The higher diversity in BOB20N may be attributed to the availability of high OM content that supports the growth of bacteria. The prevalence of both positive and negative correlations between the bacterial community, physical and chemical parameters indicate a complex and dynamic relationship between microbial communities and the ambient environment. Positive correlations suggest the existence of bacterial species that thrive in metal-rich conditions, possibly due to their specialized metal resistance or metabolism (Yin et al., 2015). These bacteria might play essential roles in metal cycling, accumulation, or transformation within the ecosystem. Conversely, negative correlations could signify the sensitivity or inhibition of certain bacterial taxa in the presence of high metal concentrations, potentially reflecting their vulnerability to metal toxicity.

Carbon metabolic characteristics of bacterial communities

Biolog plates have served as valuable tools for evaluating the functional diversity of microorganisms in various environments ever since their initial proposal by Garland and Mills (1991). Biolog Ecoplates, which are particularly well-suited for ecological investigations, were subsequently introduced by Insam (1997). These Ecoplates are designed with a selection of carbon sources that are highly pertinent to environmental contexts. The fundamental principle behind Biolog plates is to undertake miniaturized enrichment experiments wherein bacterial growth on a single carbon source is concurrently assessed across 31 different carbon sources, and the analysis is carried out in triplicate. While it's important to acknowledge that the methodology of Biolog Ecoplates does have its limitations, which have been thoughtfully examined in the work of Preston-Mafham et al. (2002). It is worth noting that these Ecoplates have been effectively employed for assessing the utilization of carbon sources in various environmental settings, such as freshwater (Christian and Lind, 2006; Comte and Del Giorgio, 2009), brackish water (Behera et al., 2018) and marine environments (Sinha et al., 2019; Wang et al., 2022).

The EcoPlateTM analysis of carbon metabolism in the deep-sea communities of the BOB unveiled significant metabolic diversity. Over a 6-day incubation period, the bacterial community demonstrated the utilization of 28 out of the 31 different carbon sources tested in at least one of the sediment samples. Notably, 10 carbon substrates (β-methyl-D-glucoside, α-D-lactose, α-cyclodextrin, N-acetyl-D-glucosamine, tween 80, glucose-1-phosphate, D-xylose, pyruvic acid methyl ester, glycogen, and 2-hydroxy benzoic acid) were consistently utilized across all sediment samples, with an average well color development (AWCD) of ≥ 0.2 OD at 590nm for each substrate.

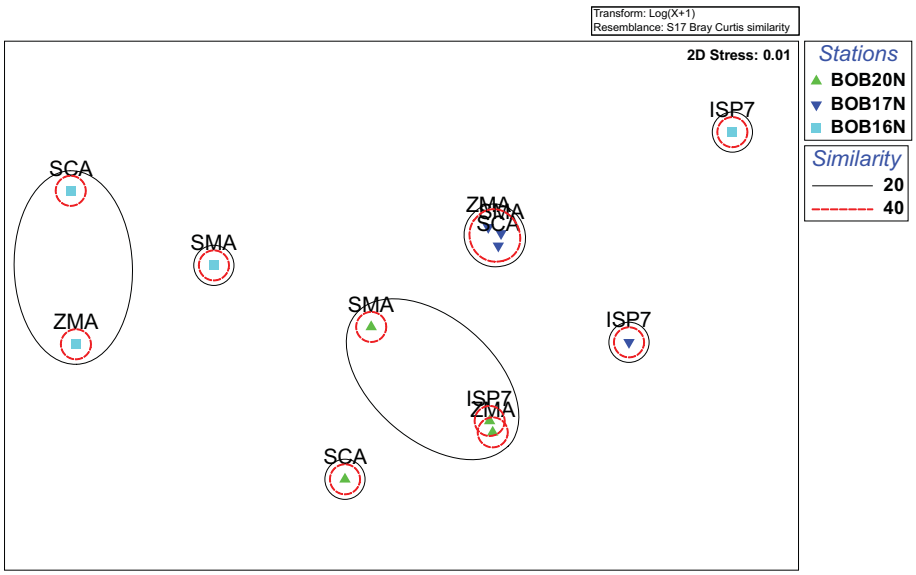

FIGURE 3
nMDS plot highlighting the distinct clustering patterns of bacterial strains isolated on different growth media from deep sea samples.

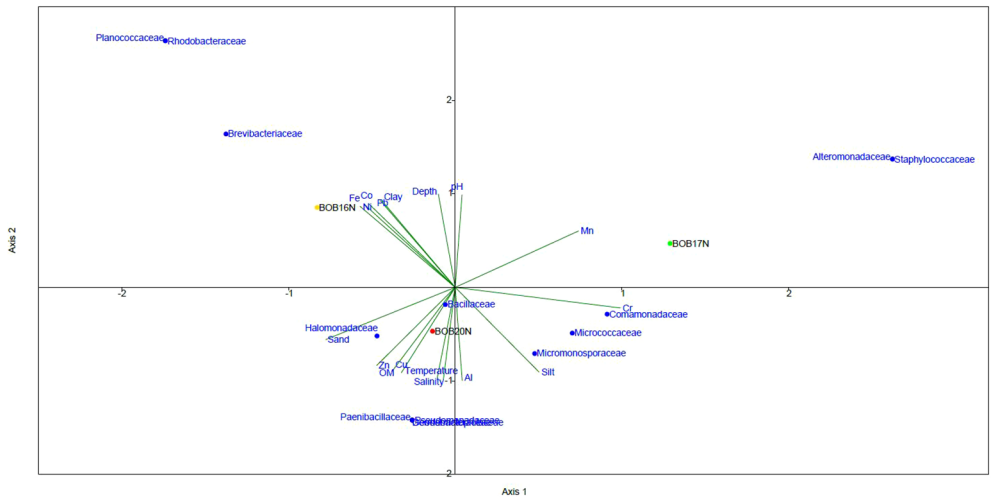

FIGURE 4
The CCA relationship between bacterial families, deep-sea sediment characteristics and environmental variables.

The increase in net AWCD (Absorbance at 590nm) over time provides insight into the metabolic activity of heterotrophic bacterial communities in different samples. Within 24 hours, BOB20N's bacterial community achieved an AWCD of 0.35 OD, indicating a high rate of carbon substrate utilization. In contrast, BOB17N reached the 0.35 OD threshold after 72 hours, and the bacterial communities in the BOB16N sample couldn't reach this threshold even after 6 days of incubation (Figure 5A). This suggests that the deeper samples in BOB16N exhibited lower and more selective utilization of substrates. The functional diversity as reflected by mean H′ was 2.9 (range 2.7–3.1) indicating a high metabolic diversity in the heterotrophic bacterial communities. R ranged from 20 to 28 (average 24) for all samples, which indicates that the deep-sea sediment communities utilized a substantial number of carbon substrates. The richness of substrate utilization was 1.4 and 1.17-fold higher in BOB20N as compared to BOB16N and BOB17N samples, respectively (Figure 5B).

The higher carbon substrate utilization rate along with higher metabolic diversity and carbon substrate richness in the Northern Bay of Bengal sediment sample indicated these bacterial communities were more active and better adapted to quickly metabolize diverse carbon substrates than the BOB16N and BOB17N sediments. The higher rate of carbon substrate utilization in BOB20N sediment could also be attributed to higher bacterial abundances than the BOB16N and BOB17N sediments.

According to their biochemical properties and molecular composition, the 31 carbon sources in the EcoPlate were divided into six categories, including amines (AM), amino acids (AA), carbohydrates (CH), carboxylic acids (CA), phenolic compounds (PC), and polymers (PO). The average substrate utilization of CH, and CA groups were closely related in all the deep-sea sediment samples studied, while substrates of PO group showed fairly increasing trend of utilization from BOB16N< BOB17N< BOB20N. The mean utilization of carbon substrates groups, amine (AM), amino acid (AA) and phenolic compounds (PC) was higher (1.3 to 1.4-fold) in the BOB20N sediment compared to the deeper depth southern samples, indicating that shallow heterotrophic microbial communities have a preference for these specific carbon substrate groups (Figure 6A). When we analyzed the average colour development of all the sediment samples collectively, we found that the wells containing the substrates, α-cyclodextrin (polymer), glucose-1-phosphate (carbohydrate), D-xylose (carbohydrate), glycogen (polymer), D-galacturonic acid (carboxylic acid), and 2-hydroxy benzoic acid (phenols) had the highest AWCD (> 0.3 OD) at 590nm among the 31 carbon sources tested which presents preferential utilisation of these carbon substrates by the deep-sea bacterial communities.

PCA was applied to investigate relationships among different deep-sea sediment samples based on their carbon substrate utilization profiles. PCA revealed that the two principal components (PC1 and PC2) together accounted for 58.02% of the variation in the carbon metabolic profiles of the deep-sea bacterial communities. To determine the most significant carbon sources that were driving the differences in metabolic profiles, loading analysis was carried out by analyzing the correlations between original variables (31 carbon sources) to the PC axes values (Garland and Mills, 1991) (Figure 6B, Supplementary Table 3). The results of the correlation matrix showed that the KMO measure of sampling adequacy was 0.72 and Bartlett's test of sphericity was 2317.06 (P< 0.0001), presenting an adequate sample size for the factor analysis. The carbon sources which were significantly correlated with PC2 are shown in the PCA Figure 6B. Carbon sources namely, Tween 80, Phenylethyl-amine, Tween 40, D-mannitol, α-ketobutyric acid, and L-asparagine showed significant positive correlation. Whereas, α-cyclodextrin, L-arginine and Putrescine were negatively correlated with PC2 axis suggesting

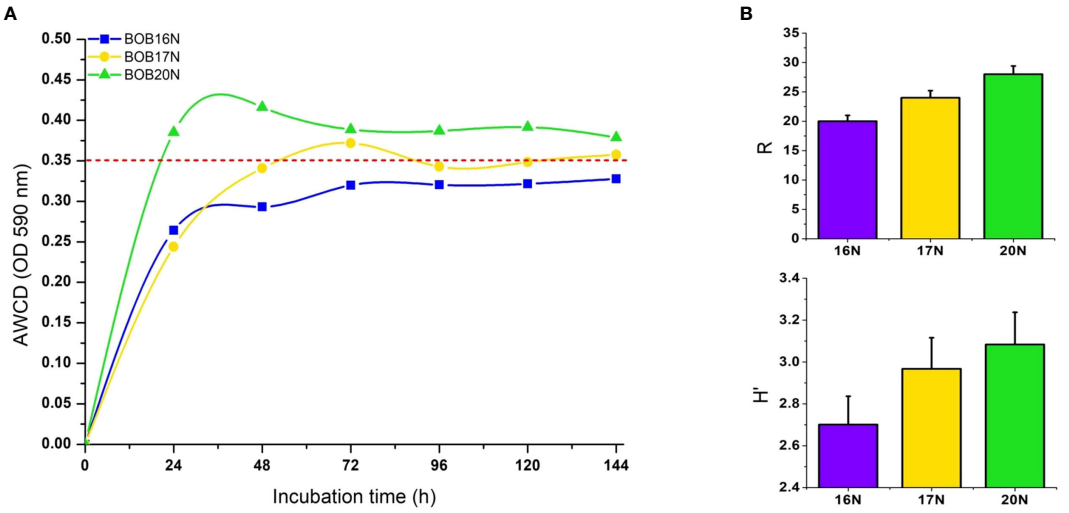

FIGURE 5
(A) AWCD by heterotrophic deep-sea bacterial communities in Biolog EcoPlates, red dashed line indicates the threshold value ($OD_{590nm} \geq 0.35$). **(B)** Richness (R), and Shannon diversity index (H') of deep-sea sediment bacterial communities carbon substrates utilization. Errors bars indicate the standard error.

that separation of samples in PCA plot can be attributed to the differences in the utilization of these important carbon sources by the deep-sea bacterial communities.

In summary, our study revealed notable differences in microbial metabolism both within individual samples and among different samples, underscoring the existence of microbial metabolic diversity. Specifically, across all deep-sea sediment samples, the prominent carbon substrates that exhibited consistent utilization included α-cyclodextrin, glucose-1-phosphate, D-xylose, glycogen, and 2-hydroxy benzoic acid. In this study, we found that the deep-sea bacterial community utilized 28 carbon substrates, displaying significant functional diversity that is essential to effectively decompose the heterogeneous organic carbon pool that accumulates in benthic sediments. Since, the heterotrophic bacteria breakdown complex OM; they can regulate the availability of carbon in benthic sediments (Säwström et al., 2016). Consequently, the higher OM content observed in BOB20N sediments, in comparison to BOB16N and BOB17N, can be linked to the elevated metabolic rates and greater diversity of heterotrophic bacterial communities.

Conclusion

The knowledge of the deep-sea microbiota holds the key to understanding the intricate complexities and ecological interactions as they can have significant impacts on ecosystem functioning and resilience. However, the limited literature on the deep-sea microbial biota emphasizes the expansive need for exploration of their unknown diversity, their ecological roles and untapped potential.

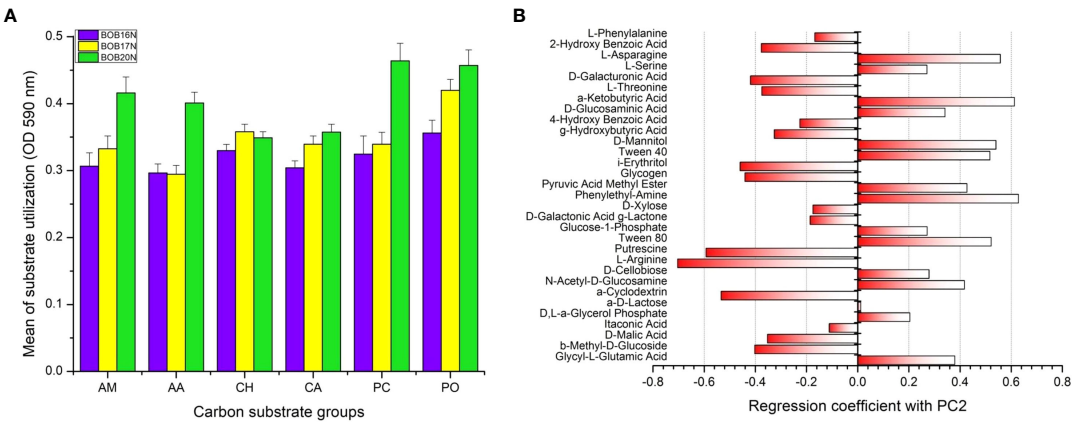

FIGURE 6
(A) Carbon substrate utilization of different substrate groups by the deep-sea bacterial communities. Errors bars indicate the standard error. AM, amines; AA, amino acids; CH, carbohydrates; CA, carboxylic acids; PC, phenolic compounds, PO, polymers. **(B)** PCA loading plot showing positive and negative correlation of carbon substrates with PC2.

The present study revealed a strong correlation between the physicochemical parameters and the bacterial community in the deep sea indicating that the ambient environment exerts a significant influence over the benthic bacterial community structure and composition. The bacterial groups encountered in this study were Bacilli, Actinomycetia, Alphaproteobacteria, Betaproteobacteria and Gammaproteobacteria. Distinct spatial variations observed in the bacterial diversity and retrievable heterotrophic counts may be indicative of environmental gradients, where bacterial composition shifts in response to varying metal levels, and these changes might be influenced by ecological factors, including, OM, sediment texture or competing microbial species. The carbon substrates primarily utilized across all the deep-sea sediment samples were α-cyclodextrin (polymer), glucose-1-phosphate (carbohydrate), D-xylose (carbohydrate), glycogen (polymer), and 2-hydroxy benzoic acid (phenols) presenting widespread presence of related pathways. The utilisation of >90% of the carbon substrates tested by the deep-sea microbenthos in at least one of the sediment samples indicates highly efficient metabolic activity which is essential to maintain the overall functioning and productivity of the ecosystem. Besides, the production of extracellular enzymes is also indicative of the role of deep-sea bacteria in the breakdown of complex OM and nutrient regeneration that is crucial for metabolic activity. The findings of this study provide insights into the adaptations and interactions of bacteria in extreme conditions, contributing to our understanding of complex web of life in deep-sea ecosystems.

Data availability statement

The datasets presented in this study can be found in online repositories. The names of the repository/repositories and accession number(s) can be found in the article/Supplementary Material.

Author contributions

PV: Conceptualization, Formal analysis, Investigation, Methodology, Writing – original draft, Writing – review & editing. VP: Formal analysis, Investigation, Software, Writing – review & editing. SS: Formal analysis, Investigation, Writing – original draft, Writing – review & editing. AA: Investigation, Methodology, Writing – original draft. GD: Project administration, Resources, Writing – review & editing.

Funding

The author(s) declare financial support was received for the research, authorship, and/or publication of this article. The authors thank the Ministry of Earth Sciences, Govt. of India, Deep Ocean Mission (DOM)- Technological innovations for exploration and conservation of deep-sea biodiversity program for the funding support.

Acknowledgments

The authors are grateful to the Ministry of Earth Sciences, Govt. of India, for providing support to carry out the present study. We are thankful to the Director, NIOT, Chennai, for his constant encouragement, support, and guidance. We are thankful to the former group head, Dr. R. Kirubagaran, for his constant support and guidance. The NIOT Vessel Management Cell and crew members of the ORV Sagar Nidhi (SN142) are acknowledged for their support. We thank the scientific and supporting staff of NIOT, Chennai, India, for their support in the field and in the laboratory during this study.

Conflict of interest

The authors declare that the research was conducted in the absence of any commercial or financial relationships that could be construed as a potential conflict of interest.

Publisher's note

Supplementary material

The Supplementary Material for this article can be found online at: https://www.frontiersin.org/articles/10.3389/fmars.2023.1308953/full#supplementary-material

References

Acinas, S. G., Sánchez, P., Salazar, G., Cornejo-Castillo, F. M., Sebastián, M., Logares, R., et al. (2021). Deep ocean metagenomes provide insight into the metabolic architecture of bathypelagic microbial communities. *Commun. Biol.* 4 (1), 604. doi: 10.1038/s42003-021-02112-2

Altschul, S. F., Madden, T. L., Schäffer, A. A., Zhang, J., Zhang, Z., Miller, W., et al. (1997). Gapped BLAST and PSI-BLAST: a new generation of protein database search programs. *Nucleic Acids Res.* 25 (17), 3389–3402. doi: 10.1093/nar/25.17.3389

Angelova, A. G., Ellis, G. A., Wijesekera, H. W., and Vora, G. J. (2019). Microbial composition and variability of natural marine planktonic and biofouling communities from the Bay of Bengal. *Front. Microbiol.* 10, 2738. doi: 10.3389/fmicb.2019.02738

APHA (2005). *Standard methods of water and wastewater. 21st Edn* (Washington, DC.: American Public Health Association), 2–61, ISBN: .

Arnosti, C., Durkin, S., and Jeffrey, W. H. (2005). Patterns of extracellular enzyme activities among pelagic marine microbial communities: implications for cycling of dissolved organic carbon. *Aquat. Microb. Ecol.* 38, 135–145. doi: 10.3354/ame038135

Balan, S. S., Nethaji, R., Sankar, S., and Jayalakshmi, S. (2012). Production of gelatinase enzyme from Bacillus spp isolated from the sediment sample of Porto Novo Coastal sites. *Asian Pacific J. Trop. Biomedicine* 2 (3), S1811–S1816. doi: 10.1016/S2221-1691(12)60500-0

Behera, P., Mohapatra, M., Adhya, T. K., Suar, M., Pattnaik, A. K., and Rastogi, G. (2018). Structural and metabolic diversity of rhizosphere microbial communities of Phragmites karka in a tropical coastal lagoon. *Appl. Soil Ecol.* 125, 202–212. doi: 10.1016/j.apsoil.2017.12.023

Bjerga, G. E. K., Hjerde, E., De Santi, C., Williamson, A. K., Smalås, A. O., Willassen, N. P., et al. (2014). High-quality draft genome sequence of Streptomyces sp. *strain AW19M42 isolated sea squirt Northern Norway. Standards Genomic Sci.* 9 (3), 676–686. doi: 10.4056/sigs.5038901

Buchanan, J. B. (1984). "Sediment analysis," in *Methods for the study of marine benthos* (UK: Wiley Blackwell), 41–65.

Budianto, F., and Lestari, (2018). Trace metal in sediment from a deep-sea floor of Makassar Strait. *IOP Conf. Series: Earth Environ. Sci.* 118, 012057. doi: 10.1088/1755-1315/118/1/012057

Chen, X., Cai, R., Zhuo, X., Chen, Q., He, C., Sun, J., et al. (2023). Niche differentiation of microbial community shapes vertical distribution of recalcitrant dissolved organic matter in deep-sea sediments. *Environ. Int.* 178, 108080. doi: 10.1016/j.envint.2023.108080

Chen, P., Zhang, L., Guo, X., Dai, X., Liu, L., Xi, L., et al. (2016). Diversity, biogeography, and biodegradation potential of actinobacteria in the deep-sea sediments along the southwest Indian ridge. *Front. Microbiol.* 7, 1340. doi: 10.3389/fmicb.2016.01340

Cheng, N., Shi, M., Hou, Q., Wang, J., and Pan, J. (2022). The impact of tectonic stress chemistry on mineralization processes: A review. *Solid Earth Sci.* 7 (2), 151–166. doi: 10.1016/j.sesci.2021.11.002

Christian, B. W., and Lind, O. T. (2006). Key issues concerning Biolog use for aerobic and anaerobic freshwater bacterial community-level physiological profiling. *Int. Rev. hydrobiology* 91 (3), 257–268. doi: 10.1002/iroh.200510838

Clarke, K. R., and Gorley, R. N. (2006). *Primer* (Plymouth: PRIMER-e), 866.

Clarke, K. R., and Warwick, R. M. (1994). Similarity-based testing for community pattern: the two-way layout with no replication. *Mar. Biol.* 118, 167–176. doi: 10.1007/BF00699231

Comte, J., and Del Giorgio, P. A. (2009). Links between resources, C metabolism and the major components of bacterioplankton community structure across a range of freshwater ecosystems. *Environ. Microbiol.* 11 (7), 1704–1716. doi: 10.1111/j.1462-2920.2009.01897.x

Contreras-Rosales, L. A., Schefuß, E., Meyer, V., Palamenghi, L., Lückge, A., and Jennerjahn, T. C. (2016). Origin and fate of sedimentary organic matter in the northern Bay of Bengal during the last 18 ka. *Global Planetary Change* 146, 53–66. doi: 10.1016/j.gloplacha.2016.09.008

Corinaldesi, C. (2015). New perspectives in benthic deep-sea microbial ecology. *Front. Mar. Sci.* 2, 17. doi: 10.3389/fmars.2015.00017

Cortada, U., and Collins, M. (2013). The nature and contamination of sediments in the Plentzia estuary (Biscay province, Spain). *Geogaceta* 54, 147–150.

Dang, H., Zhu, H., Wang, J., and Li, T. (2009). Extracellular hydrolytic enzyme screening of culturable heterotrophic bacteria from deep-sea sediments of the Southern Okinawa Trough. *World J. Microbiol. Biotechnol.* 25, 71–79. doi: 10.1007/s11274-008-9865-5

Danovaro, R. (2018). Climate change impacts on the biota and on vulnerable habitats of the deep Mediterranean Sea. *Rendiconti Lincei. Sci. Fisiche e Naturali* 29 (3), 525–541. doi: 10.1007/s12210-018-0725-4

Danovaro, R., Molari, M., Corinaldesi, C., and Dell'Anno, A. (2016). Macroecological drivers of archaea and bacteria in benthic deep-sea ecosystems. *Sci. Adv.* 2 (4), e1500961. doi: 10.1126/sciadv.1500961

da Silva, M. A. C., Cavalett, A., Spinner, A., Rosa, D. C., Jasper, R. B., Quecine, M. C., et al. (2013). Phylogenetic identification of marine bacteria isolated from deep-sea sediments of the eastern South Atlantic Ocean. *SpringerPlus* 2 (1), 1–10. doi: 10.1186/2193-1801-2-127

Dong, X., Greening, C., Rattray, J. E., Chakraborty, A., ChuvoChina, M., Mayumi, D., et al. (2019). Metabolic potential of uncultured bacteria and archaea associated with petroleum seepage in deep-sea sediments. *Nat. Commun.* 10 (1), 1816. doi: 10.1038/s41467-019-09747-0

Falkowski, P. G., Fenchel, T., and Delong, E. F. (2008). The microbial engines that drive Earth's biogeochemical cycles. *science* 320 (5879), 1034–1039. doi: 10.1126/science.1153213

Garel, M., Panagiotopoulos, C., Boutrif, M., Repeta, D., Sempere, R., Santinelli, C., et al. (2021). Contrasting degradation rates of natural dissolved organic carbon by deep-sea prokaryotes under stratified water masses and deep-water convection conditions in the NW Mediterranean Sea. *Mar. Chem.* 231, 103932. doi: 10.1016/j.marchem.2021.103932

Garland, J. L. (1997). Analysis and interpretation of community-level physiological profiles in microbial ecology. *FEMS Microbiol. Ecol.* 24, 289–300. doi: 10.1111/j.1574-6941.1997.tb00446.x

Garland, J. L., and Mills, A. L. (1991). Classification and characterization of heterotrophic microbial communities on the basis of patterns of community-level sole-carbon-source utilization. *Appl. Environ. Microbiol.* 57, 2351–2359. doi: 10.1128/aem.57.8.2351-2359.1991

Gärtner, A., Wiese, J., and Imhoff, J. F. (2016). Diversity of Micromonospora strains from the deep Mediterranean Sea and their potential to produce bioactive compounds [J]. *AIMS Microbiol.* 2 (2), 205–221. doi: 10.3934/microbiol.2016.2.205

Gaudette, H. E., Flight, W. R., Toner, L., and Folger, D. W. (1974). An inexpensive titration method for the determination of organic carbon in recent sediments. *J. Sedimentary Res.* 44 (1), 249–253. doi: 10.1306/74D729D7-2B21-11D7-8648000102C1865D

Gawas, V. S., Shivaramu, M. S., Damare, S. R., Pujitha, D., Meena, R. M., and Shenoy, B. D. (2019). Diversity and extracellular enzyme activities of heterotrophic bacteria from sediments of the Central Indian Ocean Basin. *Sci. Rep.* 9 (1), 9403.

Gu, B., Liu, J., Cheung, S., Ho, N. H. E., Tan, Y., and Xia, X. (2022). Insights into prokaryotic community and its potential functions in nitrogen metabolism in the Bay of Bengal, a pronounced Oxygen Minimum Zone. *Microbiol. Spectr.* 10 (3), e00892–e00821. doi: 10.1128/spectrum.00892-21

Gunaratna, T., Suzuki, T., and Yanagishima, S. (2019). Cross-shore grain size and sorting patterns for the bed profile variation at a dissipative beach: Hasaki Coast, Japan. *Mar. Geology* 407, 111–120. doi: 10.1016/j.margeo.2018.10.008

Guo, R., Ma, X., Zhang, J., Liu, C., Thu, C. A., Win, T. N., et al. (2022). Microbial community structures and important taxa across oxygen gradients in the Andaman Sea and eastern Bay of Bengal epipelagic waters. *Front. Microbiol.* 13, 1041521. doi: 10.3389/fmicb.2022.1041521

Hongxiang, X., Min, W., Xiaogu, W., Junyi, Y., and Chunsheng, W. (2008). Bacterial diversity in deep-sea sediment from northeastern Pacific Ocean. *Acta Ecologica Sin.* 28 (2), 479–485. doi: 10.1016/S1872-2032(08)60026-8

Insam, H. (1997). *Microbial communities: functional versus structural approaches*. Eds. H. Insam and A. Rangger (Germany: Springer Science and Business Media), 259–260.

Jasna, V., Nathan, V. K., and Parvathi, A. (2020). Comparison of bacterial community structure in coastal and offshore waters of the Bay of Bengal, India. *Regional Stud. Mar. Sci.* 39, 101414. doi: 10.1016/j.rsma.2020.101414

Jha, D. K., Dharani, G., Verma, P., Ratnam, K., Kumar, R. S., and Rajaguru, S. (2021). Evaluation of factors influencing the trace metals in Puducherry and Diu coasts of India through multivariate techniques. *Mar. pollut. Bull.* 167, 112342. doi: 10.1016/j.marpolbul.2021.112342

Jha, D. K., Ratnam, K., Rajaguru, S., Dharani, G., Devi, M. P., and Kirubagaran, R. (2019). Evaluation of trace metals in seawater, sediments, and bivalves of Nellore, southeast coast of India, by using multivariate and ecological tool. *Mar. pollut. Bull.* 146, 1–10. doi: 10.1016/j.marpolbul.2019.05.044

Jiang, Q., Jing, H., Liu, H., and Du, M. (2022). Biogeographic distributions of microbial communities associated with anaerobic methane oxidation in the surface sediments of deep-sea cold seeps in the South China Sea. *Front. Microbiol.* 13, 1060206. doi: 10.3389/fmicb.2022.1060206

Jones, C. J., and Murray, J. W. (1984). Nickel, cadmium, and copper in the northeast Pacific off the coast of Washington 1, 2. *Limnology Oceanography* 29 (4), 711–720. doi: 10.4319/lo.1984.29.4.0711

Jørgensen, B. B., and Boetius, A. (2007). Feast and famine—microbial life in the deep-sea bed. *Nat. Rev. Microbiol.* 5 (10), 770–781. doi: 10.1038/nrmicro1745

Kato, Y., Fujinaga, K., Nakamura, K., Takaya, Y., Kitamura, K., Ohta, J., et al. (2011). Deep-sea mud in the Pacific Ocean as a potential resource for rare-earth elements. *Nat. Geosci.* 4 (8), 535–539. doi: 10.1038/ngeo1185

Kim, M., Oh, H. S., Park, S. C., and Chun, J. (2014). Towards a taxonomic coherence between average nucleotide identity and 16S rRNA gene sequence similarity for species demarcation of prokaryotes. *Int. J. Systematic Evolutionary Microbiol.* 64 (Pt_2), 346–351. doi: 10.1099/ijs.0.059774-0

Kumar, S., Stecher, G., Li, M., Knyaz, C., and Tamura, K. (2018). MEGA X: molecular evolutionary genetics analysis across computing platforms. *Mol. Biol. Evol.* 35 (6), 1547. doi: 10.1093/molbev/msy096

Lauro, F. M., and Bartlett, D. H. (2008). Prokaryotic lifestyles in deep sea habitats. *Extremophiles* 12, 15–25. doi: 10.1007/s00792-006-0059-5

Lincy, J., and Manohar, C. S. (2020). A comparison of bacterial communities from OMZ sediments in the Arabian Sea and the Bay of Bengal reveals major differences in nitrogen turnover and carbon recycling potential. *Mar. Biol. Res.* 16 (8-9), 656–673. doi: 10.1080/17451000.2020.1840593

Liu, S., Ye, W., Zhang, H., Cao, P., Li, J., Sun, X., et al. (2023). Sediment provenances shift driven by sea level and Indian monsoon in the southern Bay of Bengal since the last glacial maximum. *Front. Mar. Sci.* 10, 1106663. doi: 10.3389/fmars.2023.1106663

Ma, Y., Ding, W., Wang, Y., Chen, P., Zhou, H., Li, X., et al. (2022). Environmental factors shape the culturable bacterial diversity in deep-sea water and surface sediments from the Mariana Trench. *bioRxiv*. doi: 10.1101/2022.01.13.476188

Mahmoudi, N., Hagen, S. M., Hazen, T. C., and Steen, A. D. (2020). Patterns in extracellular enzyme activity and microbial diversity in deep-sea Mediterranean sediments. *Deep Sea Res. Part I: Oceanographic Res. Papers* 158, 103231.

Marimuthu, J., Rangamaran, V. R., Subramanian, S. H. S., Balachandran, K. R. S., Kulasekaran, N. T., Vasudevan, D., et al. (2022). Deep-sea sediment metagenome from Bay of Bengal reveals distinct microbial diversity and functional significance. *Genomics* 114 (6), 110524. doi: 10.1016/j.ygeno.2022.110524

McCollom, T. M. (2000). Geochemical constraints on primary productivity in submarine hydrothermal vent plumes. *Deep Sea Res. Part I: Oceanographic Res. Papers* 47 (1), 85–101. doi: 10.1016/S0967-0637(99)00048-5

Nair, H. P., Puthusseri, R. M., Vincent, H., and Bhat, S. G. (2017). 16S rDNA-based bacterial diversity analysis of Arabian Sea sediments: A metagenomic approach. *Ecol. Genet. Genomics* 3, 47–51. doi: 10.1016/j.egg.2017.09.001

Nemergut, D. R., Costello, E. K., Hamady, M., Lozupone, C., Jiang, L., Schmidt, S. K., et al. (2011). Global patterns in the biogeography of bacterial taxa. *Environ. Microbiol.* 13 (1), 135–144. doi: 10.1111/j.1462-2920.2010.02315.x

Nogi, Y. (2017). "Microbial life in the deep sea: Psychropiezophiles," in *Psychrophiles: from biodiversity to biotechnology* (Cham: Springer), 133–152.

Padmanaban, V. P., Verma, P., Gopal, D., Sekar, A. K., and Ramalingam, K. (2019). Phylogenetic identification and metabolic potential of bacteria isolated from deep sea sediments of Bay of Bengal and Andaman Sea. *Indian J. Exp. Biol.* 57, 561-572.

Padmanaban, V. P., Verma, P., Venkatabaskaran, S., Keppayan, T., Gopal, D., Sekar, A. K., et al. (2017). Antimicrobial potential and taxonomic investigation of piezotolerant Streptomyces sp. NIOT-Ch-40 isolated from deep-sea sediment. *World J. Microbiol. Biotechnol.* 33, 1–11. doi: 10.1007/s11274-016-2193-2

Pakhomova, S. V., Hall, P. O., Kononets, M. Y., Rozanov, A. G., Tengberg, A., and Vershinin, A. V. (2007). Fluxes of iron and manganese across the sediment–water interface under various redox conditions. *Mar. Chem.* 107 (3), 319–331. doi: 10.1016/j.marpolbul.2021.112031

Pandey, V., Venkatnarayanan, S., Kumar, P. S., Ratnam, K., Jha, D. K., Rajaguru, S., et al. (2021). Assessment of ecological health of Swarnamukhi river estuary, southeast coast of India, through AMBI indices and multivariate tools. *Mar. Pollut. Bull.* 164, 112031. doi: 10.1016/j.marpolbul.2021.112031

Parkes, R. J., Cragg, B., Roussel, E., Webster, G., Weightman, A., and Sass, H. (2014). A review of prokaryotic populations and processes in sub-seafloor sediments, including biosphere: geosphere interactions. *Mar. Geol.* 352, 409–425. doi: 10.1016/j.marpolbul.2021.112031

Parvathi, A., Jasna, V., Aswathy, V. K., Aparna, S., Nathan, V. K., and Jyothibabu, R. (2020). Dominance of Wolbachia sp. in the deep-sea sediment bacterial metataxonomic sequencing analysis in the Bay of Bengal, Indian Ocean. *Genomics* 112 (1), 1030–1041. doi: 10.1016/j.ygeno.2019.06.019

Polymenakou, P. N., Lampadariou, N., and Tselepides, A. (2008). Exo-enzymatic activities and organic matter properties in deep-sea canyon and slope systems off the southern Cretan margin. *Deep Sea Res. Part I: Oceanographic Res. Papers* 55 (10), 1318–1329. doi: 10.1016/j.dsr.2008.05.010

Preston-Mafham, J., Boddy, L., and Randerson, P. F. (2002). Analysis of microbial community functional diversity using sole-carbon-source utilisation profiles–a critique. *FEMS Microbiol. Ecol.* 42 (1), 1–14. doi: 10.1111/j.1574-6941.2002.tb00990.x

Raghukumar, C., Sheelu, G., Loka Bharathi, P. A., Nair, S., and Mohandass, C. (2001). Microbial biomass and organic nutrients in the deep-sea sediments of the Central Indian Ocean Basin. *Mar. Georesources Geotechnol.* 19 (1), 1–16.

Rajpathak, S. N., Banerjee, R., Mishra, P. G., Khedkar, A. M., Patil, Y. M., Joshi, S. R., et al. (2018). An exploration of microbial and associated functional diversity in the OMZ and non-OMZ areas in the Bay of Bengal. *J. Biosci.* 43, 635–648. doi: 10.1007/s12038-018-9781-2

Ramirez-Llodra, E., Brandt, A., Danovaro, R., De Mol, B., Escobar, E., German, C. R., et al. (2010). Deep, diverse and definitely different: unique attributes of the world's largest ecosystem. *Biogeosciences* 7 (9), 2851–2899. doi: 10.5194/bg-7-2851-2010

Rogers, A. D. (2015). Environmental change in the deep ocean. *Annu. Rev. Environ. Resour.* 40, 1–38. doi: 10.1146/annurev-environ-102014-021415

Sambrook, J., and Russell, D. W. (2001). *Molecular cloning-sambrook & Russel-vol. 1, 2, 3* (Long Island, NY, USA: Cold Springs Harbor Lab Press).

Sattarova, V. V., and Aksentov, K. I. (2021). Trace metals in deep-sea sediments collected from Kuril Basin (Sea of Okhotsk) and Kuril-Kamchatka Trench area. *Mar. pollut. Bull.* 164, 112055. doi: 10.1016/j.marpolbul.2021.112055

Saunders, J. K., McIlvin, M. R., Dupont, C. L., Kaul, D., Moran, D. M., Horner, T., et al. (2022). Microbial functional diversity across biogeochemical provinces in the central Pacific Ocean. *Proc. Natl. Acad. Sci.* 119 (37), e2200014119. doi: 10.1073/pnas.2200014119

Säwström, C., Serrano, O., Rozaimi, M., and Lavery, P. S. (2016). Utilization of carbon substrates by heterotrophic bacteria through vertical sediment profiles in coastal and estuarine seagrass meadows. *Environ. Microbiol. Rep.* 8 (5), 582–589. doi: 10.1111/1758-2229.12406

Scheckenbach, F., Hausmann, K., Wylezich, C., Weitere, M., and Arndt, H. (2010). Large-scale patterns in biodiversity of microbial eukaryotes from the abyssal sea floor. *Proc. Natl. Acad. Sci.* 107 (1), 115–120. doi: 10.1073/pnas.0908816106

Serrano, O., Mateo, M. A., Dueñas-Bohórquez, A., Renom, P., López-Sáez, J. A., and Cortizas, A. M. (2011). The Posidonia oceanica marine sedimentary record: A Holocene archive of heavy metal pollution. *Sci. Total Environ.* 409 (22), 4831–4840. doi: 10.1016/j.scitotenv.2011.08.001

Sinha, R. K., Krishnan, K. P., Thomas, F. A., Binish, M. B., Mohan, M., and Kurian, P. J. (2019). Polyphasic approach revealed complex bacterial community structure and function in deep sea sediment of ultra-slow spreading Southwest Indian Ridge. *Ecol. Indic.* 96, 40–51. doi: 10.1016/j.ecolind.2018.08.063

Sogin, M. L., Morrison, H. G., Huber, J. A., Welch, D. M., Huse, S. M., Neal, P. R., et al. (2006). Microbial diversity in the deep sea and the underexplored "rare biosphere". *Proc. Natl. Acad. Sci.* 103 (32), 12115–12120. doi: 10.1073/pnas.0605127103

Stackebrandt, E., and Goebel, B. M. (1994). Taxonomic note: a place for DNA-DNA reassociation and 16S rRNA sequence analysis in the present species definition in bacteriology. . *Int. J. Syst. Bacteriol* 44, 846–849. doi: 10.1099/00207713-44-4-846

Sweetman, A. K., Thurber, A. R., Smith, C. R., Levin, L. A., Mora, C., Wei, C.-L., et al. (2017). Major impacts of climate change on deep-sea benthic ecosystems. *Elem Sci. Anth* 5, 4. doi: 10.1525/elementa.203

Taylor, S. R. (1964). Abundance of chemical elements in the continental crust: a new table. *Geochimica cosmochimica Acta* 28 (8), 1273–1285. doi: 10.1016/0016-7037(64)90129-2

Thurber, A. R., Sweetman, A. K., Narayanaswamy, B. E., Jones, D. O., Ingels, J., and Hansman, R. L. (2014). Ecosystem function and services provided by the deep sea. *Biogeosciences* 11 (14), 3941–3963. doi: 10.5194/bg-11-3941-2014

Trask, P. D. (1939). Organic content of recent marine sediments: part 6. Special features of sediments. *Amer. Assoc. Petrol. Geologists, Tulsa.* 428-453

Tripathy, G. R., Singh, S. K., and Ramaswamy, V. (2014). Major and trace element geochemistry of Bay of Bengal sediments: Implications to provenances and their controlling factors. *Palaeogeography Palaeoclimatology Palaeoecol.* 397, 20–30. doi: 10.1016/j.palaeo.2013.04.012

Tuohy, A., Bertler, N., Neff, P., Edwards, R., Emanuelsson, D., Beers, T., et al. (2015). Transport and deposition of heavy metals in the Ross Sea Region, Antarctica. *J. Geophysical Research: Atmospheres* 120 (20), 10–996. doi: 10.1002/2015JD023293

UNESCO (1979). *Discharge of selected rivers of the world: A contribution to the international hydrological decade* (Paris: UNESCO), 104.

USEPA (2001). *Supplemental guidance for developing soil screening levels for superfund sites* (Office of Soild Waste and Emergency Response). OSWER USEPA, 9355.4-24.

Varkey, M. J., Murty, V. S. N., and Suryanarayana, A. (1996). Physical oceanography of the bay of Bengal and Andaman sea. *Oceanogr. Mar. Biol. Annu. Rev.* 34, 1-70.

Verma, P., Raghavan, R. V., Jeon, C. O., Lee, H. J., Priya, P. V., Dharani, G., et al. (2017). Complex bacterial communities in the deep-sea sediments of the Bay of Bengal and volcanic Barren Island in the Andaman Sea. *Mar. Genomics* 31, 33–41. doi: 10.1016/j.margen.2016.08.003

Vipindas, P. V., Mujeeb, R. K. M., Jabir, T., Thasneem, T. R., and Hatha, A. M. (2020). Diversity of sediment bacterial communities in the South Eastern Arabian Sea. *Regional Stud. Mar. Sci.* 35, 101153. doi: 10.1016/j.rsma.2020.101153

Walsh, E. A., Kirkpatrick, J. B., Rutherford, S. D., Smith, D. C., Sogin, M., and D'Hondt, S. (2016). Bacterial diversity and community composition from seasurface to subseafloor. *ISME J.* 10 (4), 979–989. doi: 10.1038/ismej.2015.175

Wang, L., Liu, L., Zheng, B., Zhu, Y., and Wang, X. (2013). Analysis of the bacterial community in the two typical intertidal sediments of Bohai Bay, China by pyrosequencing. *Mar. Pollut. Bull.* 72 (1), 181–187. doi: 10.1016/j.marpolbul.2013.04.005

Wang, F., Zhang, Y., Jing, H., and Liu, H. (2022). Spatial variation and metabolic diversity of microbial communities in the surface sediments of the Mariana Trench. *Front. Microbiol.* 13, 1051999. doi: 10.3389/fmicb.2022.1051999

Wangersky, P. J. (1986). Biological control of trace metal residence time and speciation: a review and synthesis. *Mar. Chem.* 18 (2-4), 269–297. doi: 10.1016/0304-4203(86)90013-7

Weber, M. E., Wiedicke-Hom, M., Kudrass, H. R., and Erlenkeuser, H. (2003). Bengal Fan sediment transport activity and response to climate forcing inferred from sediment physical properties. *Sedimentary Geology* 155 (3-4), 361–381. doi: 10.1016/S0037-0738(02)00187-2

Ye, W., Liu, S., Fan, D., Zhang, H., Cao, P., Pan, H. J., et al. (2022). Evolution of sediment provenances and transport processes in the central Bay of Bengal since the Last Glacial Maximum. *Quaternary Int.* 629, 27–35. doi: 10.1016/j.quaint.2020.12.007

Yin, H., Niu, J., Ren, Y., Cong, J., Zhang, X., Fan, F., et al. (2015). An integrated insight into the response of sedimentary microbial communities to heavy metal contamination. *Sci. Rep.* 5 (1), 14266. doi: 10.1038/srep14266

Yoon, S. H., Ha, S. M., Kwon, S., Lim, J., Kim, Y., Seo, H., et al. (2017). Introducing EzBioCloud: a taxonomically united database of 16S rRNA gene sequences and whole-genome assemblies. *Int. J. Syst. Evol. Microbiol.* 67 (5), 1613–1617. doi: 10.1099/ijsem.0.001755

Zehr, J. P., and Kudela, R. M. (2011). Nitrogen cycle of the open ocean: from genes to ecosystems. *Annu. Rev. Mar. Sci.* 3, 197–225. doi: 10.1146/annurev-marine-120709-142819

Zheng, B., Wang, L., and Liu, L. (2014). Bacterial community structure and its regulating factors in the intertidal sediment along the Liaodong Bay of Bohai Sea, China. *Microbiological Res.* 169 (7-8), 585–592. doi: 10.1016/j.micres.2013.09.019

Zinger, L., Amaral-Zettler, L. A., Fuhrman, J. A., Horner-Devine, M. C., Huse, S. M., Welch, D. B. M., et al. (2011). Global patterns of bacterial beta-diversity in seafloor and seawater ecosystems. *PloS One* 6 (9), e24570. doi: 10.1371/journal.pone.0024570

Frontiers in Marine Science

Explores ocean-based solutions for emerging global challenges

The third most-cited marine and freshwater biology journal, advancing our understanding of marine systems and addressing global challenges including overfishing, pollution, and climate change.

Discover the latest Research Topics

See more →

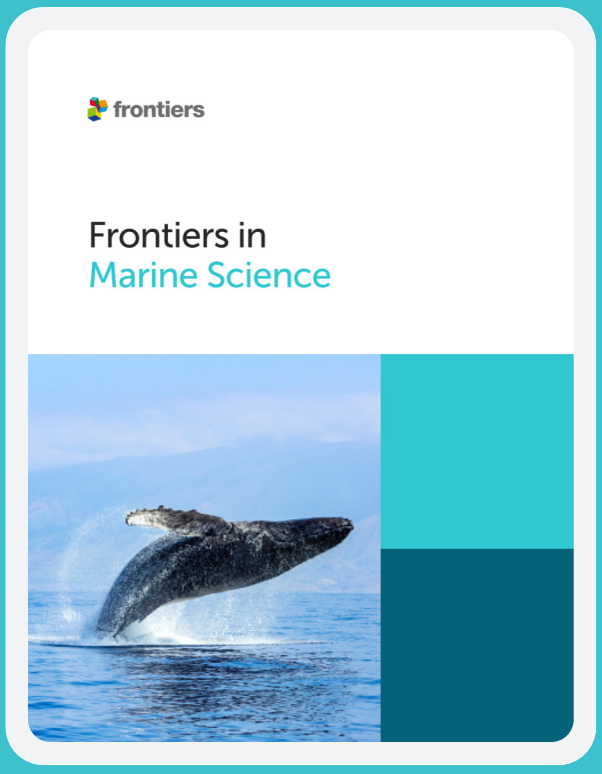

Frontiers

Avenue du Tribunal-Fédéral 34
1005 Lausanne, Switzerland
frontiersin.org

Contact us

+41 (0)21 510 17 00
frontiersin.org/about/contact